# EPI International Journal of Engineering
## Editorial Board

# Foreword

We are pleased to present the EPI International Journal of Engineering (EPI-IJE) Volume 4 Number 2 August 2021. In order to shorten the publication time, there is a slight change in this edition where each manuscript is arranged not based on the topic similarity but on the manuscript acceptance date. By doing this, we hope the accepted manuscript can be uploaded earlier on the journal website.

This edition consists of 13 (thirteen) manuscripts. The first 2 (two) manuscripts are related to mechanical engineering which are about the simulation of aluminum alloy flange reducer cast and about the investigation of LED bulb light as photon energy on a photovoltaic panel installed inside buildings. The third manuscript is about the study of environmental carrying capacity on the development of formal housing in Moncongloe district, Maros regency.

The next 2 (two) manuscripts are related to monitoring and control systems. They are about a prototype of a self-adaptive traffic light control system using cameras and the development of an earthquake simulator. They are followed by other 2 (two) manuscripts related to urban development and architecture. They studied the effectiveness of utilizing non-green public space in fishermen's settlements and analysis of the floodlight lighting effect on the visual quality of the tower building facade.

The eighth manuscript evaluated the achievement of the production target using the fishbone diagram method at a site in South Sumatera province. It is followed by a manuscript that conducted a feasibility analysis of the runway, taxiway, and apron dimensions of an airport in Fakfak Regency, Papua. There are again 2 (two) next manuscripts related to architecture. They are studying the characteristics of the traditional house of the Tolaki tribe and about the impact of local wisdom on the coastal settlement spatial configuration in the city of Parepare. The last two manuscripts investigated the free vibration characteristics of thin spherical shells and free vibration of doubly curved shallow shells of rectangular planform.

We are thankful to all authors who have contributed manuscripts to this edition. We also really appreciate all other people and institutions for their ongoing support for the EPI journal publication. We hope the published manuscripts will have a positive contribution to the future development of science and technology.


Warm regards,


**Prof. Baharuddin Hamzah**
Editor-in-Chief of EPI-IJE

# TABLE OF CONTENTS

# Calculation and Simulation of Aluminium Alloy Flange Reducer Cast using Resin Sand Mold

Andi Ari Putra[a,*], Muhammad Syahid[b], Andi Amijoyo Mochtar[c]

[a]Department of Mechanical Engineering, Faculty of Engineering, Hasanuddin University, Makassar, Indonesia. Email : aariputra1@gmail.com
[b]Department of Mechanical Engineering, Faculty of Engineering, Hasanuddin University, Makassar, Indonesia. Email : syahid@unhas.ac.id
[c]Department of Mechanical Engineering, Faculty of Engineering, Hasanuddin University, Makassar, Indonesia. Email : andijoyo@unhas.ac.id

**Abstract**

One of the causes of defects in casting is due to poor gating system design. In conventional casting methods, the gating system design process is carried out by trial and error to find the best design results. Computer modeling and simulation offer process design in a much faster time, and at much less cost, compared to conventional methods. The gating system design approach with a combination of well calibrated simulation software can avoid defect before casting. Casting simulation helps to visualize the phenomena of filling, molten metal solidification, and shrinkage porosity. The resulting casting simulation can be displayed in graph variants at specific nodes with line graphs or numerical numbers manually. This study discusses the simulation of casting a flange reducer from aluminum alloy material using a resin sand mold. The initial dimensions of the gating system used are sprue of 14.5 x 8.4 x 180 mm, runner 147 x 10 x 5.5 mm, ingate 80 x 10 x 5.5 mm with a bottom gate channel system. Total of dominant porosity that occurs using the initial gating system is 65.31 % and show the undirectional solidificiation behavior. After modifying the gating system and increasing the riser size, the simulation results show directional solidification behavior starting from the thinnest part to the thickest part and ending at the riser. The shrinkage porosity can compensate with the total of porosity is 57.60 % at the riser. Modification of the channel system is required to obtain a sound casting or porosity free.

*Keywords: Casting simulation; flange reducer; gating system; resin sand; shrinkage porosity*

## 1. Introduction

Sand casting is a manufacturing process for making complex shapes from metal materials in mass production. There are two successive main stages, the filling process, and the compaction process, in foundry production. In the filling process, a gating system was designed consisting of a pouring cup, runner, sprue, sprue well, and in-gate to guide the filling of molten metal. The riser system is used to compensate for the shrinkage caused by the solidification of the casting [1]–[3].

The flange is the most important component in the piping system. Flange reducers are used to make reductions in pipe diameter. Flange reducers are most often used in installations with limited space [4]. In general, aluminum is widely used in foundry because it is relatively low cost and easy to form. When casting aluminum, several factors affect its quality. It is undeniable that many types of defects occur in the sand casting process, such as porosity and incomplete filling. Shrinkage porosity is probably the most common phenomenon in the foundry, and it is difficult to eliminate it [5, 6].

In conventional methods only use the identified experience to design the gating system or by trial and error. Whereby doing manual calculations and directly apply them. If a defect occurs with this system, then the gating system is modified according to the position and level of the defect. This trial method is continuously until the defects in the casting are reduced. This trial and error method is considered to be ineffective and efficient so that it can cause the relationship between the dealer and the customer to be damaged because it requires and consumes more time and effort [7].

The use of calculation and simulations in sand casting has become a powerful tool for analyzing mold filling, compaction, and cooling, as well as for imagining the location and type of internal defects. Casting simulation helps optimize casting process design and improve casting yield. This simulation plays an important role in overcoming casting defects that occur during the casting

*Corresponding author. Tel.: +62-823-4350-2572
*Jalan Poros Malino km. 6, Bontomarannu*
*Gowa, Indonesia 92171*
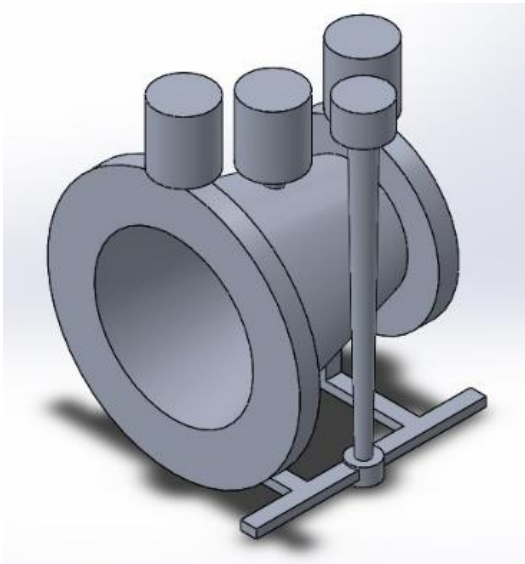
Figure 1. 3D Model gating system

process [8]–[11]. The calculation carried out in the casting process is then simulated using Procast software to optimize the results of the casting to be carried out.

## 2. Research Methodology

The method used in this study is an experimental method, which is a method used to predict the mechanism of compaction of aluminum alloys, analyze the results, and optimize casting parameters to achieve good properties of a material by experimentation using software simulations.

3d modeling of flange reducer is done with the help of Solidwork software. The 3D geometry of the flange reducer with a gating system using Solidwork is shown in Fig. 1. The material chosen for the flange reducer is A 356.0 with dimensions 101.60 mm x 50.80 mm x 127 mm The modeling consists of determining the bottom gating system.

In performing the calculation of the channel system, initial data is needed which will be used to determine the dimensions of the channel system. Mathematically the calculation of the channel system is as follows [12, 13]:

- Determine volume of cast object ($V$)
- Determine dominant thickness of cast ($t$)
- Determine depth of metal in pouring basin ($b$)
- Calculation mass of object cast, the equation is shown as:

$$W = V \, x \, \rho \qquad (1)$$

where:
  $W$  = Mass of cast object (gr)
  $V$  = Volume of cast object (cm$^3$)
  $\rho$  = Density of aluminium (gr/cm$^3$)

- Calculation of pouring volume, $Qp$ (m$^3$) is shown as:

$$Qp = \frac{Wp}{\rho} \qquad (2)$$

where:
  $Qp$  = Pouring volume (m$^3$)
  $Wp$  = Pouring weight (kg)
  $\rho$  = Material density (kg/m$^3$)

- Calculation of pouring time, $tp$ (s) according by Nielsen as follows:

$$tp = 0.32 \; x \, t \; x \, Wp^{0.4} \qquad (3)$$

where:
  $tp$  = Pouring time(s)
  $t$  = Dominant thickness of cast (mm)
  $Wp$  = Mass of cast object (gr)

- Effective sprue height $H$ (mm) use bottom gate as:

$$\textit{Effective sprue height} = h - \frac{p}{2} \qquad (4)$$

where:
  $ESH$ = Effective sprue height (mm)
  $h$  = Height of sprue (mm)
  $p$  = Cast height (mm)

- Determine the area of the bottom sprue (choke area) as:

$$As = \frac{W}{\rho \cdot tp \cdot c \sqrt{2 \cdot g \cdot H}} \qquad (5)$$

where:
  $A_B$  = Area of the bottom sprue (mm$^2$)
  $W$  = Mass of cast object (kg)
  $\rho$  = Liquid metal density (kg/m$^3$)
  $tp$  = Pouring time (s)
  $H$  = Effective height of descending channel (m)
  $g$  = gravitational acceleration (9.81 m/s$^2$)
  $c$  = Efficiency factor of channel down (0.88)

- Determine the diameter of the bottom sprue (choke area) as:

$$D_B = \sqrt{\frac{4 \, x \, A_B}{\pi}} \qquad (6)$$

where:
  $D_B$  = Diameter of the bottom sprue (mm)
  $A_B$  = Area of the bottom sprue (mm$^2$)

- Determine the area of the top sprue, as:

$$A_A = A_B \sqrt{\frac{h}{b}} \qquad (7)$$

where:

$A_A$ = Area of the top sprue (mm$^2$)
$A_B$ = Area of the bottom sprue (mm$^2$)
$h$ = Height of sprue (mm)
$b$ = Depth of pouring basin (mm)

- Determine the diameter of the bottom sprue, show:

$$D_A = \sqrt{\frac{4 \, x A_A}{\pi}} \qquad (8)$$

where:

$D_A$ = Diameter of the top sprue (mm)
$A_A$ = Area of the top sprue (mm$^2$)

- Determine of ingate use the ratio of American AFS horizontal gating system between choke area : runner area : gate area = 1:4:4, then the runner is equal to four times the choke area and the gate area is equal to four times the choke area.

- Determine *well base area* (mm$^2$), the equation is shown as:

$$well\ base\ area = 5\ x\ A_B \qquad (9)$$

- Determine well base diameter (mm), the equation is shown as:

$$d = \sqrt{\frac{4\ x\ well\ area}{\pi}} \qquad (10)$$

- Determine *well base depth* (mm) is shown as:

$$Well\ base\ depth\ = 2\ x\ runner\ depth \qquad (11)$$

Generally casting simulation software has three main parts, namely:
- Visual Mesh: the program reads the geometry and generates a mesh.
- Visual Cast: addition of boundary conditions and material data, filling, and temperature calculation.
- Visual Viewer: show simulation result data.

During the casting simulation process, compaction and porosity are checked and the gravity sand casting process is optimized by modifying the gating system. The elements that are taken into account in the flange reducer casting process are pouring cup, sprue and sprue base, in gate, riser, which are designed using solidworks software. The initial dimensions of the duct system used are sprue of 14.5 x 8.4 x 180 mm, runner 147 x 10 x 5.5 mm, in gate 80 x 10 x 5.5 mm. and the location of their respective molds. From the dimension size data, it will be used to build a 3D simulation model using computer simulation software.

## 3. Results and Discussion

### 3.1. Channel System Planning

#### 3.1.1. Cast Material

- Material type = A356.0
- Densty = 2,685 kg/m$^3$
- Liquidus = 613°C
- Solidus = 548°C

#### 3.1.2. Specimen

- Volume of cast object ($V$) = 537,949.92 mm$^3$
- Dominant thickness ($t$) = 20 mm
- Depth of metal pouring basin ($b$) = 20 mm
- Mass of cast object

The equation of cast object mass is shown as:

$$W = V \times \rho$$
$$= 537.949 \times 2,685$$
$$= 1,444.39\ gr = 1.444\ kg$$

- Calculation pouring volume, $Qp$ (m$^3$) is shown as:

$$Qp = \frac{Wp}{\rho}$$
$$= \frac{1.442}{2,685}$$
$$= 0.000537\ m^3$$

- Calculation pouring time, $tp$ (s). according by Nielsen as follows:

$$tp = 0.32 \times t \times Wp^{0.4}$$
$$= 0.32 \times 20 \times 1.157$$
$$= 7.4\ sec$$

- Determine *effective sprue height*, $H$ (mm) use bottom gate

$$Effective\ sprue\ height = h - \frac{p}{2}$$
$$= 180 - \frac{161,6}{2}$$
$$= 99.2\ mm = 0.0992\ m$$

- Determine area of the bottom sprue, $A_B$ (mm$^2$)

$$As = \frac{w}{\rho \cdot tp \cdot c\sqrt{2 \cdot g \cdot H}}$$
$$= \frac{1.444}{2,685 \cdot 7.4 \cdot 0.88\sqrt{2 \cdot 9.81 \cdot 0.0992}}$$
$$= \frac{1.444}{17,484.72 \cdot 1.395}$$
$$= 5.92 \times 10^{-5}\ m^2 = 59.2\ mm^2$$

- Determining the diameter of the bottom sprue:

$$\frac{1}{4}\pi d^2 = 59.2$$

$$D_B = \sqrt{\frac{4 \times A_B}{\pi}}$$

$$= \sqrt{\frac{4 \times 59.2}{\pi}}$$

$$= \sqrt{\frac{236.8}{3.14}} = 8.7 \; mm$$

- Area of the top sprue $A_A$ ($mm^2$):

$$A_A = A_B \sqrt{\frac{h}{b}}$$

$$= 59.2 \sqrt{\frac{180}{20}} = 177.6 \; mm^2$$

- Determining the diameter of the top sprue:

$$\frac{1}{4}\pi d^2 = 177.6$$

$$D_A = \sqrt{\frac{4 \times A_A}{\pi}}$$

$$= \sqrt{\frac{4 \times 177.6}{\pi}}$$

$$= \sqrt{\frac{710.4}{3.14}}$$

$$= 15.04 \; mm$$

- Determining ingate

The ratio of AFS horizontal gating system 1:4:4 can be obtained as:

$$Area \; ingate = 4 \times A_B$$

$$= 4 \times 59.2$$

$$= 236.8 \; mm^2$$

$$Then \; size \; ingate = L \times T$$

$$= 20 \times 11.84$$

$$= 236.8 \; mm^2$$

- For a channel system that uses two ingates then:

$$R1 = R2 = runner \; area;$$

$$2 = 118.4 : 2 = 59.2 \; mm^2$$

$$Then \; size \; ingate = L \times T$$

$$= 10 \times 5.92$$

$$= 59.2 \; mm^2$$

- Determining *Well base area* :

$$Well \; base \; area = 5 \times A_B$$

$$= 5 \times 59.2$$

$$= 296 \; mm^2$$

Table 1. Result of dimension of calculation the gating system

| Part of gating system | Dimensions |
| --- | --- |
| Volume of cast | 537,949.92 mm³ |
| Dominant thicknest | 20 mm |
| Depth of metal pouring basin | 20 mm |
| Pouring volume | 537,000 mm³ |
| Pouring time | 7.4 second |
| Effective sprue height | 99.2 mm |
| Area of the bottom sprue | 59.2 mm² |
| Diameter of the bottom sprue | 8.7 mm |
| Part of gating system | Dimensions |
| Area of the top sprue | 177.6 mm² |
| Diameter of the top sprue | 15.04 mm |
| Area ingate | 236.8 mm² |
| Size ingate | 20 mm x 11.84 mm |
| Well base area | 296 mm² |
| Well base diameter | 19.4 mm |
| Well base depth | 11.84 mm |

- Well base diameter*:*

$$d = \sqrt{\frac{4 \times well \; area}{\pi}}$$

$$= \sqrt{\frac{4 \times 296}{3.14}} = 19.4 \; mm$$

- Determining *Well base depth*:

$$well \; base \; depth = 2 \times runner \; depth$$

$$= 2 \times 5.92 = 11.84 \; mm$$

### 3.2. Simulation Result and Analysis

#### 3.2.1. Solidification

Solidification is the time in every second the reducer flange becomes completely solid, from the time of the end of pouring to the point of solidification. Solidification time is proportional to the ratio of volume to the surface area [14, 15]. After the molten metal is poured into the mold cavity, the compaction of the flange reducer begins. Solidification in the casting process is generally complex, where physical, thermal, and metallurgical phenomena occur simultaneously.

To obtain good casting quality, directional compaction is required. Solidification is the result of heat transfer from the internal casting to the external environment [9]. The actual solidification of the metal begins at a liquidus temperature of 613 °C. Metal solidification ends at a solidus temperature of 548 °C.

Figure 2 shows that the solidification times at different time stages have been displayed in various colors, which helps to locate the isolated areas of molten metal in the casting and gives an overview of the directional compaction in the various areas of the flange reducer.
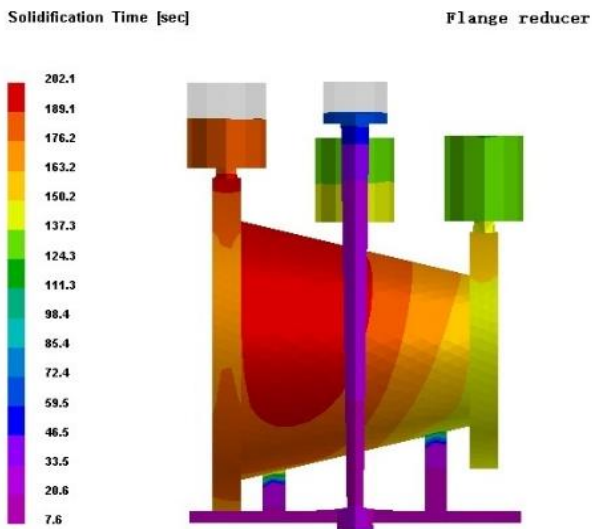
Figure 2. Initial gating system solidification time
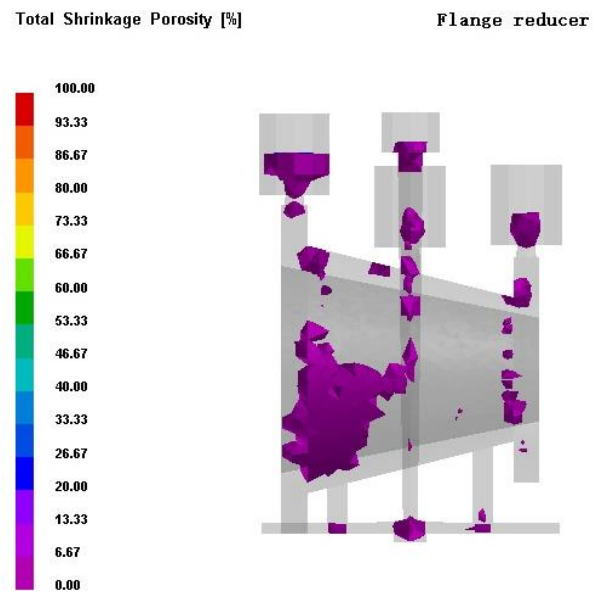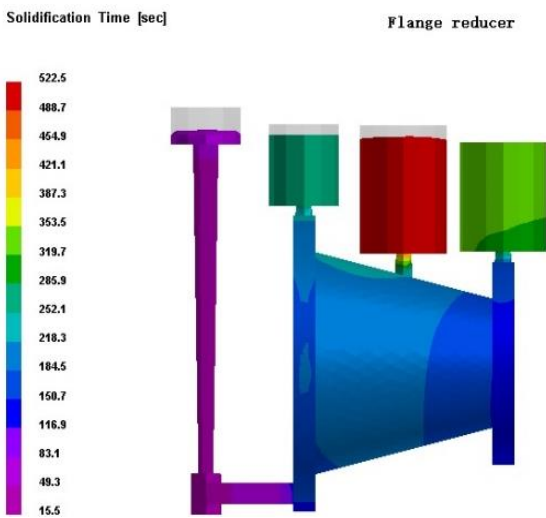


Figure 3. Gating system solidification time after modification



(a)
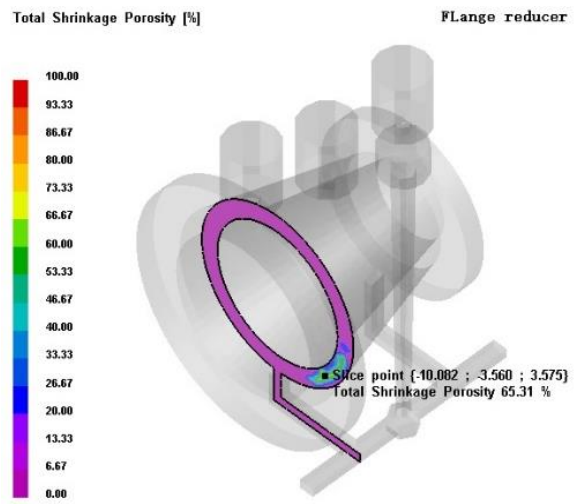


(b)

Figure 4. (a) Total shrinkage porosity (b) Slice point major shrinkage porosity on initial gating system

Figure 2 shows a plot of the initial gating system compaction time where the compaction results are less than perfect, the red gradient shows the last part of the compaction process. Figure 3 shows the compaction of the flange reducer with a modified gating system where the compaction takes place in a directed manner, starting from the thinnest part to the thickest part and ending at the riser.

### 3.2.2. Porosity

Shrinkage porosity defects are voids within components that can cause the material to weaken and if placed on the surface can deteriorate its aesthetic qualities and corrosion resistance. Porosity shrinkage occurs during the solidification phase of the material, which begins with the mold filling phase and ends when each part of the material is completely compacted. The cause of porosity is material shrinkage [9], [16].

Shrinkage porosity was predicted by computer simulation of the filling and compaction processes. Molten metal becomes solid when the heat in it is released and a phase change occurs from liquid to solid. As a result, porosity shrinkage occurs in the casting process. A shrinkage defect occurs when the feed metal is not available to compensate for shrinkage as the metal hardens. If the shrinkage porosity is small in diameter and confined to the center of a very thick section, it usually will not cause any problems [9]. Figure 4a shows the shrinkage porosity present in the simulation with the initial gating system. It has been observed that the shrinkage porosity is in the riser and flange reducer components with total porosity of 65.31% as shown in Figure 4b.

(a)



(b)
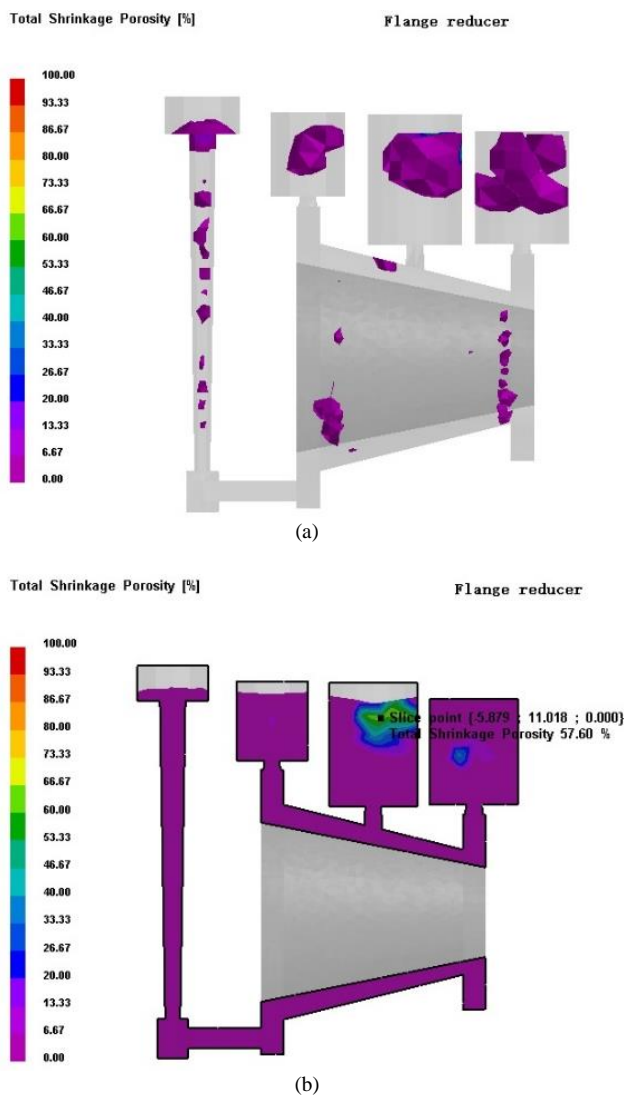
Figure 5. (a) Total shrinkage porosity (b) Slice point major shrinkage porosity on modified gating system

After the gating system is modified, the shrinkage porosity can be reduced in the flange reducer by providing the appropriate gate, the riser in the right location, and increasing the riser height as shown in Figure 5a The largest number of porosities is in Figure 5b Indicated on the riser of 57.60%.

## 4. Conclusions

a. The simulation software in foundry creates opportunities to prevent wastage of material, energy, cost, and time associated with casting trials to get good quality.

b. The gating system design approach with a combination of well calibrated simulation software can avoid defects before casting.

c. Casting simulation helps to visualize the phenomena of filling, molten metal solidification, and shrinkage porosity.

d. The resulting casting simulations can be displayed in graph variants at specific nodes with line graphs or numerical numbers manually.

e. Modifying the gating system can compensate for the shrinkage porosity.

## References

[1] C. M. Choudharia, B. E. Narkhedeb, and S. K. Mahajanc, "Methoding and Simulation of LM 6 Sand Casting for Defect Minimization with its Experimental Validation," in *Procedia Engineering 97*, 2014, pp. 1145 – 1154.

[2] M. Iqbal, S. Patel, and G. Vidyarthee, "Simulation of casting and its validation by experiments," *Int J Eng Sci Res Technol*, vol. 3, no. 8, pp. 55–56, 2014.

[3] V. M. Vasava and D. R. Joshi, "Identification of casting defects by computer simulation," *Int J Eng Res Technol*, vol. 2, no. 8, pp. 2550–2555, 2013.

[4] R. A. Parisher and R. A. Rhea, "Pipe Drafting and Design," in *Flange Basics*, 2012, pp. 56–78.

[5] J. Campbell, *Castings*. Oxford: Elsevier Science Ltd, 2003.

[6] F. Liu, "Optimized design of gating/riser system in casting based on CAD and simulation technology," Worcester polytechnic institute, 2008.

[7] Ravi, "Casting method optimization driven by simulation," *Indian Foundry Cong.*, vol. 57, pp. 70–74, 2009.

[8] K. S. Reddy, "Casting Simulation of Cast Iron Rotor-Disc using ProCAST," *Int. J. Curr. Eng. Technol.*, vol. 4, no. 6, pp. 4091–4094, 2014.

[9] T. H. Hirigo and B. Singh, "Design and analysis of sand casting process of mill roller," *Int. J. Adv. Manuf. Technol.*, vol. 105, no. 5–6, pp. 2183–2214, 2019.

[10] J. Jezierski, R. Dojka, and K. Janerka, "Optimizing the gating system for steel castings," *Metals (Basel).*, vol. 8, no. 66, pp. 1–13, 2018.

[11] T. Roy, "Analysis of Casting Defects in Foundry by Computerised Simulations (CAE) - A New Approach along with Some Industrial Case Studies," 2013.

[12] American Foundrymen's Society Training & Research Institute, "Basic Principle of Gating and Risering, Golf & Wolf Roads Des Plainers Illinois," 1972.

[13] J. R Brown, *Foseco Ferrous Foundryman's Handbook*, 11th ed. Oxford: ButterworthHeinemann, 1994.

[14] M. C. Flemings, "Solidification processing," *Metall. Mater. Trans. B*, vol. 5, no. 10, pp. 2121–2134, 1974.

[15] M. Mc Guinness and A. J. Roberts, "Efficient design of tall tapered feeders," New Zealand, 2001.

[16] J. P. Anson and J. E. Gruzleski, "Effect of Hydrogen Content on Relative Shrinkage and Gas Micro-porosity in Al-7% Si Casting," McGill University Canada, 2000.

# Optimum Investigation of LED Bulbs Light as Photon Energy on Photovoltaic Panel Installed Inside Buildings

Mustofa[a,*], Anjar Asmara[b], Yuli Asmi Rahman[c], Tutang Muhtar Kamaludin[d], Hariyanto Hariyanto[e], Zuryati Djafar[f], Wahyu H. Piarah[g]

[a]Department of Mechanical Engineering, Universitas Tadulako, Palu, Indonesia. Email: mustofauntad@gmail.com
[b]Department of Mechanical Engineering, Universitas Tadulako, Palu, Indonesia. Email: anjarhasann@gmail.com
[c]Department of Electrical Engineering, Universitas Tadulako, Palu, Indonesia. Email: yuliasmi.rahman81@gmail.com
[d]Department of Civil Engineering, Universitas Tadulako, Palu, Indonesia. Email: tmuhtar_teknikuntad@yahoo.co.id
[e]Department of Mechanical Engineering, Musamus University, Merauke, Indonesia. Email: hariyanto_ft@unmus.ac.id
[f]Department of Mechanical Engineering, Universitas Hasanuddin, Gowa, Indonesia. Email: zuryatidjafar@unhas.ac.id
[g]Department of Mechanical Engineering, Universitas Hasanuddin, Gowa, Indonesia. Email: wahyupiarah@unhas.ac.id

### Abstract

This study was conducted to obtain the angle of elevation of solar panels (PV) to harvest photon light energy sources from LED bulbs that are often used in residential homes or buildings. The PV tilt angles tested are 0, 15, 30 and 90º by placing a constant bulb in its position. The results of the observations show that a slope of 0º produces the highest PV electrical power, although it is not significant compared to the other 3 slope angles. The decrease in PV output power occurs when the slope angle increases. Optimum power of 16.93 Watt is obtained by using a Hannochs bulb at a power of 15 Watt with an angle of elevation of 0º. Furthermore, the power decreased to 16.33, 12.92, and 12.91 Watts at angles of 15, 30 and 90º, respectively. Further research is still needed by increasing the variation of bulb power above 15 Watts to validate the position of the PV panels on the walls of the building according to light source.

*Keywords: light energy, photovoltaic panel, interior building, LED energy*

## 1. Introduction

The sun is a source of energy that is very important for the benefit of mankind and the natural surroundings. The sun is a source of renewable energy that is pollution-free, environmentally friendly, quiet and free. However, technology is needed to harvest the energy optimally. The technology that is widely known to the millennial community is photovoltaic or photovoltaic (PV) panels. This panel is made up of arranged and bonded semiconductor crystals that can absorb photon light and solar thermal energy at the same time. However, what the panel needs is only photon light that is able to excite electrons to the holes, so that there is a difference in voltage and electric current flow in the junction (+) and negative (-).

The sun is not the only source of energy that PV can use to generate electricity. Other energies such as LED light bulbs in buildings or domestic and office buildings are alternative photon light that can be obtained free of charge at night. So the bulb becomes a source of lighting as well as a new source of energy for PV whose electrical output can be used for charging electronic devices such as mobile phones, power banks and laptops. This process will help save electricity usage of PLN per month. The

problem with PV panels is determining the right angle between the light from the bulb and the PV surface on the walls of the building. Therefore, this study aims to investigate several angles of PV panel elevation by assuming the position of a static LED bulb on the ceiling of the house under review. After knowing the elevation angle, the aesthetic value of the panel position in the interior of the building becomes a separate x factor.

Several studies related to the use of the bulb as photon energy have been carried out. Mustofa et al., [1] investigated the radiation of Halogen, Incandescent and Xenon bulbs as energy sources in a mini-hybrid photovoltaic and thermoelectric generator (TEG) using a hot mirror as a photon and thermal bulb separator. The test results displayed focus more on the size of the light spectrum that goes to the PV and TEG without displaying the output power. This research was continued in the following year by Piarah et al., [2]. They compared the spectrum splitters of hot and cold mirrors by using only 50 Watt Halogen bulb as the energy source to be splitted by the mirror. The difference lies in the PV and TEG positions. The results indicate in total that the cold mirror splitter is larger in terms of PV and TEG output power. Simultaneously, research related to the same topic was also carried out in [3], [4], [5] and [6]. The simulation results show that the PV module provides good output power characteristics according to the dimensions of the

*Corresponding author. Tel.: +62-813-4107-4257
*Palu, Sulawesi Tengah, Indonesia, 94118*

PV with the type of bulb as a photon energy source, while the output power (voltage and electrical current) produced by the TEG module is very small and can be ignored.

However, from the reference sources above, no one has tested the type of LED bulb as an energy source that aims to excite electrons to holes in the conductive polycrystalline crystals of the PV panel surface. This LED is a type of bulb that is currently widely used in home and office buildings. Kamaludin et al., [7] have used a TEG module with an LED bulb as a source of thermal radiation which results are still small. Although the electrical power is still small, the application of the LED bulb as a thermal energy source has provided an overview of the TEG output power characteristics that are in accordance with the theoretical basis of the module. Need to test for PV module as well. In this study, the test has directly used monocrystalline type commercial solar panel (60 Wh), so the results can be directly applied.

Regarding the PV panel elevation angle, with 4 poly silicon crystalline panels arranged in series-parallel, Wardy et al., [8] placing the angle of elevation around 122° with an average power of 21 Watts. They concluded that weather conditions affect the magnitude of the voltage, while the surface temperature affects the magnitude of the PV output current. Temperature rises, PV amperage goes down. Lysbetti et al., [9] using PV panel tilt angles of 45, 60, 90, 120 and 130°. The angle of 60° which shows a more stable and optimal PV output voltage. Tira et al., [10] in the test using a 10 Wp PV panel, comparing solar radiation with a sun simulator using a 500 W Halogen bulb that can be adjusted its voltage with a dimmer. The tilt angle that is set is the position of the bulb, not the panel PV. The optimal PV slope is 10°.

The slope of PV affects its output power as described in the studies above by utilizing radiation from both the sun irradiation and the sun simulator of a high-power Halogen bulb of 500 Watt. The high power bulb is not used commercially by the public, so its application is limited, suitable only for experiment in the laboratory. In this study, we will use low-power LED bulbs that are widely used by people in residential homes.

## 2. Materials and Methods

In this study, the bulb was placed at the top position which was installed statically and ensured that the light that radiated shone on the entire surface of the PV. Different study from Tira et al., [10], where the position of the bulb can be tilted and forms an angle with a constant PV panel, this study places a static bulb like [11]. The position of the PV at a distance of 25 cm from the bulb with elevation angles of 0, 15, 30 and 90°. The tilt angle of 0° means the panel is perpendicular to the direction of the light, while 90° the PV panel gets light from the side of the bulb. The PV panel used is a monocrystalline type with dimensions of 70 x 54 cm with a maximum of 60 W as specified in Table 1.

Table 1. Specification of monocrystalline photovoltaic

| Technical Data | |
|---|---|
| Peak Power (Pmax) | 0 W |
| Production Tolerance | 3% |
| Maximum Power Current (Imp) | .33 A |
| Maximum Power Voltage (Vmp) | 8 V |
| Short Circuit Current (Isc) | .67 A |
| Open Circuit Voltage (Voc) | 50 VDC |



Figure 1. Type of bulbs on PV testing

Meanwhile, the type of bulb used there are 3 trademarks; Hannochs 15 Watt, Camus 20 Watt, and Philips 20 Watt (Figure 1). Hannochs is different from the others because it doesn't get the same power as the other two brands, so it's only close to the chosen one. The 3 types of bulbs are widely used by consumers at home. However, to prove the validity of the bulbs another study should be conducted.

Furthermore, experimental set-up was carried out by installing a light steel frame. This frame is a support for PV panel and the bulb poles. as shown in Figure 2.2. The measuring instruments used during the test were a digital multimeter, digital infrared thermometer, and a watt meter with a rechargeable sealed lead-acid battery for energy storage. The PV output power measurement is recorded every minute with 60 minutes each slope of PV panel and one single bulb type. The bulb is left Switch-On for 10 minutes before measuring the voltage and current to adjust to ambient temperature and power stability.
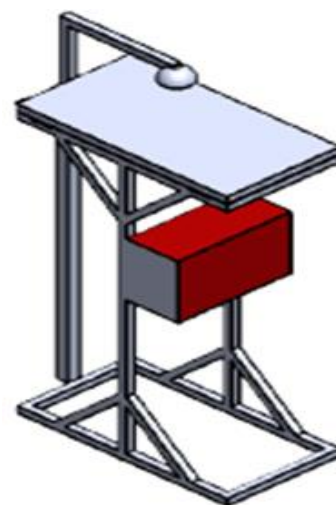


Figure 2. Experimental set-up of PV elevation

## 3. Results and Discussion

### 3.1 LED bulb 15 Watt Hannochs as source of irradiance at PV elevation on 0, 15, 30 and 90º

From the 4 graphs below show that the greater the PV elevation angle to the Hannochs LED bulb irradiation source, the lower the output power. 0º PV angle is the best, but the PV slope angle is not the main factor for installing interior room building. The aesthetic value of the room is a factor that also needs to be considered.
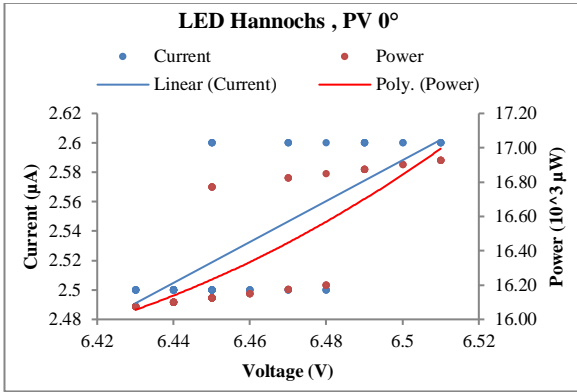
Figure 3. Power of monocrystalline PV panel at 0º elevation angle with 15 Watt Hannochs LED bulb radiations
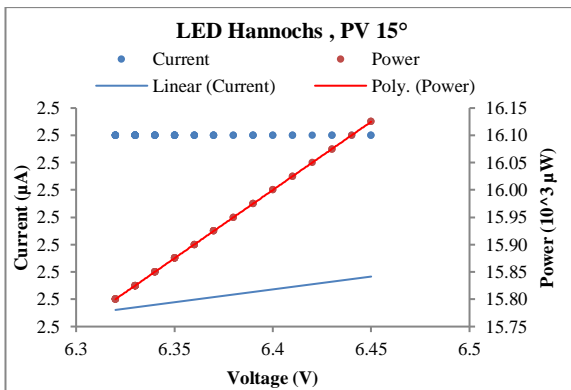
Figure 4. Power of monocrystalline PV panel at angle of 15º with 15 Watt Hannochs LED bulb radiations
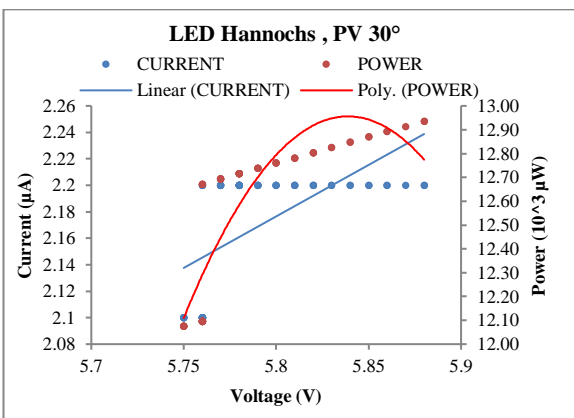
Figure 5. Power of monocrystalline PV panel at angle of 15º with 15 Watt Hannochs LED bulb radiations
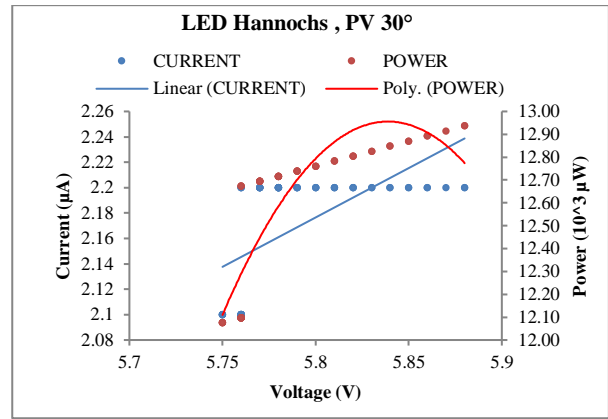
Figure 6. Power of monocrystalline PV panel at angle of 90º with 15 Watt Hannochs LED bulb radiations

### 3.2 LED bulb 20 Watt Camus as source of irradiance at PV elevation on 0, 15, 30 and 90º

The below figures describe power of 20 Watt of Camus LED bulb in which it has same trend as the 15 Watt Hannocs bulb light. Interestingly, 15 Watt contributes more PV output power than that of 20 Watt. One of the possible causes is the unequal surface geometry of the bulb, which affects the area and intensity of the light beam to the PV. In addition, changes in the light irradiation angle affect the PV output power which has been simulated in the study [12].
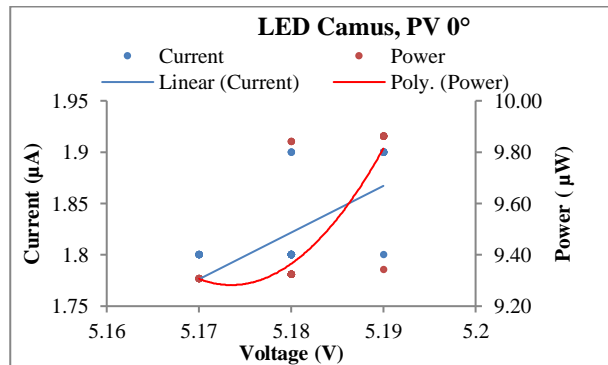
Figure 7. Power of monocrystalline PV panel at angle of 0º with 20 Watt Philips LED bulb radiation
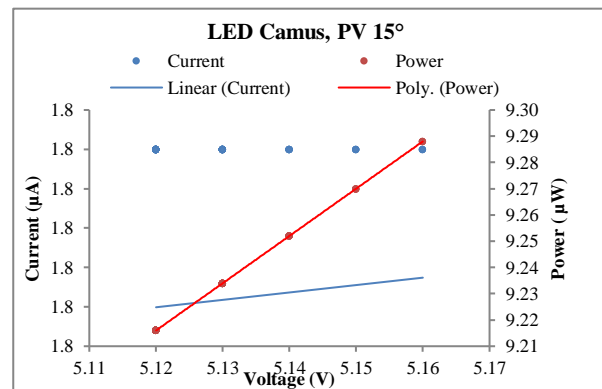
Figure 8. Power of monocrystalline PV panel at angle of 15º with 20 Watt Camus LED bulb radiation bulb radiations
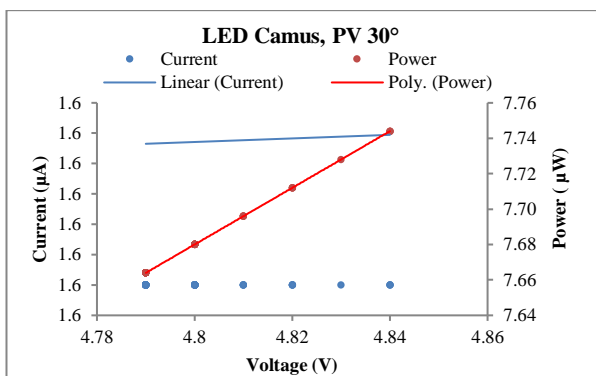
Figure 9. Power of monocrystalline PV panel at angle of 30º with 20 Watt Camus LED bulb radiation



Figure 10. Power of monocrystalline PV panel at angle of 90º with 20 Watt Camus LED bulb radiations

### 3.3 LED bulb 20 Watt Philips as source of irradiance at PV elevation on 0, 15, 30 and 90º

The power of Philips bulb to generate electricity through PV is still less than Hannocs. The best type of domestic bulb light in this study is Hannochs even though it's only 15 Watts. It is important to do further research on the characterization of this type of bulb by adding the higher and more varieties bulb power. In general, the angle of inclination of solar panel does not provide a significant difference in output power by using light bulbs as a photon energy source. This means that the installation of solar panels on the interior room walls of buildings has the potential to provide electrical energy conservation for the use of small DC-powered electronic devices, such as computer/notebook and power bank.
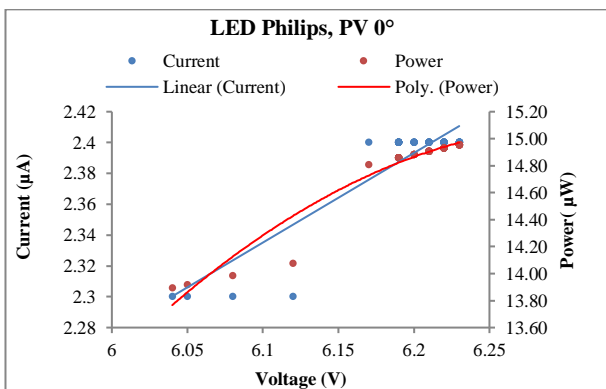


Figure 11. Power of monocrystalline PV panel at angle of 0º with 20 Watt Camus LED bulb radiation



Figure 12. Power of monocrystalline PV panel at angle of 15º with 20 Watt Camus LED bulb radiations



Figure 13. Power of monocrystalline PV panel at angle of 30º with 20 Watt Camus LED bulb radiation
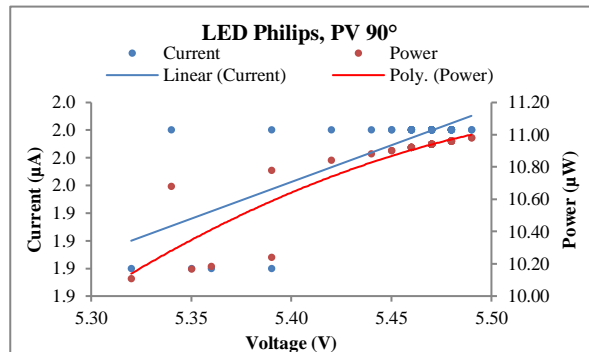


Figure 14. Power of monocrystalline PV panel at angle of 90º with 20 Watt Camus LED bulb radiations

The results of research using light bulbs as a source of constant irradiation of energy are certainly different from using solar energy that changes irradiance, and its air mass every time as well as the height factor at the observation location [13].

The results of this study indicate that the PV output power is still relatively small for the needs of electronic devices sourced from AC electricity (the State Electricity Company), but it is only sufficient for charging small power devices, such as charging mobile phones and fans. The way to fix this is by using a rather bigger bulb and PV power. It is also important to add more variative LED colors to provide much light intensity and spectrums [14]. Besides that, combining the light of the bulb in the night and sunlight on the day will generate more output PV power and can be store in a battery, too. Sunlight can be let into the interior of the building by applying room construction management [15].

## 4. Conclusions

In conclusion, research on the angle of inclination of solar cells at angles of 0, 15, 30 and 90° to the light source of an LED bulb provides clues about optimizing the electrical power generated by PV at night. From this study, Hannochs brand provides an optimum output power, although at a lower power commercially compared to Camus and Philips brands. Of course, to obtain a more valid study, a higher and more varied Hannochs power variation is needed.

## Acknowledgment

## References

[1] Mustofa, Z. Djafar, Syafaruddin, and W. H. Piarah, "A New Hybrid of Photovoltaic-thermoelectric Generator with Hot Mirror as Spectrum Splitter," *J. Phys. Sci.*, vol. 29, no. Supp. 2, pp. 63–75, Aug. 2018.

[2] W. H. Piarah, Z. Djafar, Syafaruddin, and . Mustofa, "The Characterization of a Spectrum Splitter of TechSpec AOI 50.0mm Square Hot and Cold Mirrors Using a Halogen Light for a Photovoltaic-Thermoelectric Generator Hybrid," *Energies*, Jan. 2019.

[3] W. H. Piarah, Z. Djafar, Hariyanto, and Mustofa, "A New Simulation of Photovoltaic and Thermoelectric Generator Hybrid System with a Beam Splitter Cold and Hot Mirror for Low Intensity," *Int. Rev. Mech. Eng.*, vol. 13, no. 9, 2019.

[4] D. Neupane, H. Yasuhara, H. Putra, and N. Kinoshita, "Inorganically Precipitated Phosphates and Carbonates to Improve Porous Material Properties," *EPI Int. J. Eng.*, vol. 1, no. 1, pp. 1–6, 2018.

[5] Mustofa *et al.*, "Low Sun Spectrum on Simulation of a Thin Film Photovoltaic, Heat Absorber, and Thermoelectric Generator System," *Nihon Enerugi Gakkaishi/Journal Japan Inst. Energy*, vol. 99, no. 8, 2020.

[6] Z. Djafar, A. Z. Salsabila, and W. H. Piarah, "Performance Comparison Between Hot Mirror and Cold Mirror as a Beam Splitter on Photovoltaic-Thermoelectric Generator Hybrid using Labview Simulator," *Int. J. Heat Technol.*, vol. 39, no. 5, pp. 1609–1617, 2021.

[7] T. Muhtar Kamaludin, S. Awal Syahrani, W. Danny Syamsu, Basri, and Mustofa, "Experimental Study of Cascaded Thermoelectric Generators with Differences in Focal Length using LED Lights Energy Radiation," in *IOP Conference Series: Materials Science and Engineering*, 2020, vol. 909, no. 1.

[8] R. R. Wardy and C. B. Nugroho, "Crystalline Silicon in Riau University Area With Series-Parallel Series," *JOM FMIPA*, vol. 1, no. 2, pp. 70–76.

[9] N. Lysbetti, E. Ervianto, and R. Amri, "Effect of Tilt Angle on Solar Module Output Voltage," *Prosiding Seminar Nasional Teknik Elektro*, pp. 237–240, 1876. [in Bahasa]

[10] H. S. Tira, A. Natsir, and M. S. Anwar, "Experimental Study on Solar Emulators Based on the Intensity of the Sun on the Performance of 10 Wp Polycristalline Solar Cells," *Rotasi*, vol. 19, no. 4, p. 237, 2017, doi: 10.14710/rotasi.19.4.237-242. [in Bahasa]

[11] R. K. Demak, R. Hatib, and Asrul, "Comparison of Solar Energy with Halogen Lamps on the Efficiency of a Muticrystalline Photopoltaic Module," *Jurnal Mekanikal*, vol. 7, no. 1, pp. 625–633, 2016. [in Bahasa]

[12] S. Harika, R. Seyezhai, and A. Jawahar, "Simulation Study of Shading Effects in PV Array," *Lect. Notes Mech. Eng.*, no. January, pp. 655–663, 2021.

[13] A. M. Shakir, S. M. Yousif, and A. L. Mahmood, "An Optimum Location of On-Grid Bifacial Based Photovoltaic System in Iraq," *Int. J. Electr. Comput. Eng.*, vol. 12, no. 1, pp. 250–261, 2022.

[14] A. Wijayanto, K. Karim, and S. Pradana, "Design and Build a Photovoltaic Use Practicum Module," *PoliGrid*, vol. 1, no. 2, p. 39, 2020. [in Bahasa]

[15] S. Darula, J. Christoffersen, and M. Malikova, "Sunlight and Insolation Of Building Interiors.," in *Energy Procedia*, 2015, vol. 78, pp. 1245–1250.

# Study of Environmental Carrying Capacity on the Development of Formal Housing in Moncongloe District, Maros Regency

Samsuddin Amin[a,*], Nurmaida Amri[b], Abdul Rachman Rasyid[c], Muhammad Faathir Nugraditama[d], Syifa Beby Alisha[e]

[a]Department of Architecture, Engineering Faculty, Hasanuddin University. Email: samsuddin@unhas.ac.id
[b]Department of Architecture, Engineering Faculty, Hasanuddin University. Email: nurmaidaamri@unhas.ac.id
[c]Department of Urban and Regional Planning, Engineering Faculty, Hasanuddin University. Email: rahmanrasyid@eng.unhas.ac.id
[d]Department of Urban and Regional Planning, Engineering Faculty, Hasanuddin University. Email: tyo.nugraditama@gmail.com
[e]Department of Urban and Regional Planning, Engineering Faculty, Hasanuddin University. Email: syivabebyalisha91@gmail.com

**Abstract**

Moncongloe District is an area with a relatively high population growth rate and distribution of housing, especially formal housing. This condition has implications for the tendency of increasing problems related to the carrying capacity of the environment and the suitability of land functions in the area. Therefore, it is necessary to harmonize the development of formal housing with the carrying capacity of the environment so that the negative impact of the phenomenon of formal housing development in this area can be avoided. The purpose of this study is to analyze the environmental carrying capacity of the development of formal housing for the prediction of the next 20 years. The analytical method used is a combined method of qualitative and quantitative analysis with a focus on the study of population projections, land availability and needs, and the carrying capacity of residential land. The results showed that the population in Moncongloe District in 2021 was 23,738 people, while the projected population in 2041 was 46,779 people, which means an increase of 97.06%. The results of the analysis of land availability show that 50% of the area of Moncongloe District is recommended for the development of residential land, including formal housing. The value of the carrying capacity of residential land (DDPm) in Moncongloe District in 2021 is 20.7 while in 2041 it is 20 so it can be concluded that the environmental carrying capacity in Moncongloe District can still accommodate the development of settlements for the next 20 years.

*Keywords: Environmental carrying capacity, land availability, land requirement*

## 1. Introduction

Utilization of land is a human renewal of the environment to regulate their lives. Humans need land to live which is a rare natural resource because the amount is limited and does not increase, but the need for land continues to increase. According to Law Number 32 of 2009 concerning Environmental Processing (Undang-undang No. 32 tahun 2009 tentang Pengolahan Lingkungan Hidup), the carrying capacity of the environment is defined as the ability of the environment to support human life and living creatures. One of the factors that can be used as a measure of environmental carrying capacity is the availability of land which describes the area's capacity to support population growth. The importance of analyzing population development in relation to the ability of the area to accommodate it is based on the fact that human activities have a significant

impact on environmental conditions. This is because human activities will take advantage of the natural resources around them. Therefore, human activities must be in accordance with the natural carrying capacity they occupy. Furthermore, this human activity can generally be seen from population growth and economic development [1].

The concept of carrying capacity has been written in Indonesia's spatial planning law which mostly deals with environmental issues. The carrying capacity of the environment is divided into two, namely carrying capacity and carrying capacity. Carrying capacity means the ability of the environment to support human life and other organisms, carrying capacity is the capacity of the environment to absorb objects, energy or other components that are discharged into the environment by themselves or through human intervention. The purpose of Indonesia's spatial planning is to make effective and efficient use of space, which in essence is towards sustainable environmental management, prevention of space wastage and prevention of space quality degradation. Spatial planning based on area characteristics

---

*Corresponding author. Tel.: +81-355-585-193
*Kompleks Unhas Antang Blok B138 Makassar
Indonesia, 90235*

or carrying capacity and supported by adequate technology [2].

Carrying capacity and containment capacity of the environment is an instrument that describes the process/method of scientific studies to determine/know the ability of an area to support the needs of human life and other living creatures. Therefore, the determination of the carrying capacity and carrying capacity of the environment is carried out through an indicative approach based on the unit of analysis, parameters, indicators and benchmarks in each of these units of analysis. Bearing in mind that the carrying capacity and containment capacity are dynamic and complex and highly dependent on the geographical characteristics of an area, the number of inhabitants and the existing conditions of natural resources in their respective regions.

The definition of environmental carrying capacity according to the regulation of the state minister of the environment regarding guidelines for determining environmental carrying capacity in regional spatial planning is the ability of the environment to support the lives of humans and other living creatures. The definition of environmental carrying capacity (carrying capacity) in an ecological context is the number of populations or communities that can be supported by the resources and services available in the ecosystem. Factors that affect the limitations of ecosystems to support livelihoods are the number of available resources, population numbers and consumption patterns. The concept of environmental carrying capacity in this ecological context is closely related to natural capital. However, in the context of sustainable development, a community does not only have natural capital, but also human capital, social capital and artificial environmental capital. Therefore, in the context of the continuity of a city, the carrying capacity of the urban environment is the number of populations or communities that can be supported by available resources and services because of the natural, human, social and artificial environmental capital it has.

In its later development, the concept of environmental carrying capacity was applied as a calculation method to determine the number of living organisms that can be continuously supported by an ecosystem, without destroying the balance in the ecosystem. The decline in quality and damage to the ecosystem is then defined as an indication that the carrying capacity of the environment has been exceeded [3].

Land use by any development activity must be in line with the principles of sustainable development, namely balanced economic, socio-cultural, and environmental development as pillars that are interdependent and mutually reinforcing one another. Development that aims to improve the welfare of the community cannot be avoided from excessive use of natural resources or exploitation that threatens its sustainability, this will result in a decrease in the ability of the environment to support human survival in the future [4]. The carrying capacity of land is highly correlated with the availability of land, the economic value of the land, and the high demand housing. In relation to efforts to provide housing in relation to the carrying capacity of land, every effort to provide settlements must consider the stability of the foundation, drainage, availability of ground water, and aspects of disaster vulnerability [5].

The construction of housing and settlements as one of the mandates of the law is an aspect that is directly correlated with the availability of land and the carrying capacity of the environment. Housing is a group of houses that function as a residential or residential environment that is equipped with environmental infrastructure, namely the basic physical features of the environment, such as the provision of drinking water, waste disposal, availability of electricity, telephone, roads, which allow the residential environment to function properly [6].

Settlement is part of a residential environment consisting of more than one housing unit that has infrastructure, facilities, public utilities, and has supporting telephone activities, roads, which allow the residential environment to function as it should other functions in urban areas or rural areas [7]. Housing and settlements are multi-sectoral activities, the results of which directly touch one of the basic needs of the community. The problems faced cannot be separated from aspects that develop in the dynamics of people's lives and government policies in managing existing problems. In order for the implementation of housing and settlement development to run optimally, orderly and well organized, the process is carried out in stages through the stages of preparation, planning, implementation, management, maintenance and development [8].

There are five elements in settlement planning that must be considered, including: (1) the shell/environment, namely the place where humans live starting from the micro scale such as space, buildings to the macro scale such as villages, cities or regional agglomerations; (2) Network, or a network that includes infrastructure where humans communicate and interact; (3) Nature, or nature as a natural environment consisting of non-biotic and biotic elements and the habitats of creatures that occupy them. These natural elements are also in natural processing conditions such as landscaping, agriculture, forestry; (4) Man, or humans as individual beings with all their personalities and identities; and (5) Society, or society/human group from family, neighborhood to the world with all its complex relationships in social, economic, cultural and political life [9].

In the 1980s, low-cost housing and home improvement programs remained the two main policies in Indonesia in both rural and urban areas. However, Indonesia still faces serious housing problems related to high population growth rates, high rates of urbanization, resource scarcity, inefficient housing production, economic crisis, rampant corruption, lack of control over land prices, land speculation, misdirected subsidies and etc [10]. Ideally, when housing development has become a national work, the perspective on housing must become one unit. There are five perspectives on housing that must be considered, namely: (1) Houses as an economic commodity that directs their perspective on the fact that all housing is financed, produced and distributed by the private market;

(2) House as Home which directs perspective to the fact that the house is inhabited together by the people who live in it. There they create life and families. Therefore, these residential spaces must be protected and are expected to receive legal recognition. On a broad scale, laws and policies should benefit householders; (3) Housing as a human right that directs the perspective that equality, security and affordability of housing is very important for human development. Homes enable humans to be healthy, benefit from educational opportunities, be productive members of working groups and to care for families. Because the house is important as the basis of human development, all humans have the right to a house that is protected by law; (4) The house provides a social order that directs the perspective that wherever the location of the house is, the type of house, and who lives in it, the housing pattern creates a social order, in which we live and become part of a life. Therefore, housing laws and policies must respect and promote good community, including by respecting people who interact socially in residential areas; and (5) The house as a function of the land use system that directs the perspective of the fact that housing is one of the many land uses that are important for a healthy city. Housing also has positive and negative aspects. Therefore laws and policies must be planned with regard to financing, provision, design and management in relation to other land uses as a geographical area [11].

Sustainable settlement development in Indonesia has a dualism in terms of formal and informal aspects. The resolution of this dualism is a new phenomenon in several urban areas in Indonesia [12]. Housing and settlement development policies and programs tend to adopt it as one-step regularization, meaning regularization of the housing supply system in one step [13]. Housing and settlement development policies and programs tend to adopt it as one-step regularization, meaning regularization of the housing supply system in one step [13]. The one-step regularization policy is driven by an obsession to provide housing 'only' through 'formal' development mechanisms through organized control of both technical requirements and formal development procedures. In the following, many excerpts from the policy obsession with one-step regularization, such as various 'informal' resettlement programmes, follow. However, one step The regularization policy in Indonesia ignores harmonization in the provision of housing and the settlement system in Indonesia is very dynamic and complex with a cross between 'formal' and 'informal' as a dualism in the housing mechanism [14].

To overcome housing and settlement problems, several ideas that can support housing and settlement policies in Indonesia are: (1) Development management by formulating a comprehensive and integrated housing policy by considering functional environmental aspects, potential funds and resources, economic improvement, governance space and land use; (2) an ethical approach to development by considering the principle of affordability, differentiation of subsidies, differentiation of programs so that it can cover various problems in all circles of society

and the principle of equitable distribution of housing; (3) a technical approach, housing development in stages, continuously with appropriate and targeted technology; (4) Sociological approach with consideration of social aspects that have a culture that should be considered in making site planning [15]. From the aspect of development management, there is the term property management which is the process of managing financial, physical conditions in terms of administration in the process of operating a property. The term property management is usually used for office buildings, hotels and shopping centers, while for residential property the term estate management is used. The function of estate management is not only managing the physical environment but also managing the psychological environment such as a sense of security, comfort and order. Developers must always maintain the quality of the residential environment by establishing estate management because it can attract consumers and have a better image in the eyes of consumers [16].

Maros Regency is one of the administrative regions of South Sulawesi Province with an area of 1,619 km2 consisting of fourteen sub-districts. Maros Regency is an area directly adjacent to Makassar City, therefore this area plays an important role in the development of Makassar City because it is a crossing area which is also the gateway to the Mamminasata Region in the north which in itself provides a very large opportunity for the development of the Mamminasata Area. . Likewise, the largest air transportation facility in Eastern Indonesia, which is located in Maros Regency, makes it the entry and exit point for the South Sulawesi Province. This condition is strategically very beneficial for the Maros economy as a whole.

Moncongloe District is one of the 14 sub-districts in Maros Regency. The total area of all villages in Moncongloe District is 46.87 km2. Geographical conditions, in the west it borders with Makassar City, in the east it borders with Tanranlili District, in the north it borders Mandai District and in the south it borders Gowa Regency.

## 2. Methodology

This type of research is a descriptive type of research with quantitative and qualitative approaches. This study aims to provide an overview of the suitability of land use for formal housing in Moncongloe District, Maros Regency. The quantitative approach is an approach that in research efforts, processes, hypotheses, goes to the field, analyzes data and concludes data until the writing uses aspects of measurement, calculation, formula and certainty of numerical data. On the other hand, a qualitative approach is an approach that in research proposals, processes, hypotheses, goes to the field, analyzes data and concludes data until the writing uses aspects of tendencies, non-numeric calculations, situational descriptive, and in-depth interviews, content analysis, snowballing, and stories [17].

Table 1. Projection of the population of Moncongloe District in 2021-2041

| No. | Village | R(Growth rate) | Projection Year | | | | |
|---|---|---|---|---|---|---|---|
| | | | 2021 | 2026 | 2031 | 2036 | 2041 |
| 1 | Moncongloe Lappara | 1.39 | 8,957 | 9,667 | 10,376 | 11,086 | 11,795 |
| 2 | Moncongloe Bulu | 2.92 | 4,971 | 5,936 | 6,902 | 7,867 | 8,833 |
| 3 | Moncongloe | 4.96 | 6,448 | 9,084 | 11,719 | 14,355 | 16,900 |
| 4 | Bonto Bunga | 3.76 | 2,010 | 2,558 | 3,106 | 3,654 | 4,202 |
| 5 | Bonto Marannu | 2.49 | 3,035 | 3,516 | 3,997 | 4,478 | 4,959 |
| | Total | 3.10 | 25,421 | 30,761 | 36,100 | 41,440 | 46,779 |

The data collection method is based on the needs of primary and secondary data. Primary data is data taken directly in the field, while secondary data is data taken from other parties as primary data takers, or data obtained through studies and analysis of literature studies or documents related to the carrying capacity of the environment. In the analysis of the environmental carrying capacity study in the formal housing of Moncongloe District, Maros Regency, primary data collection includes observation, documentation, and interviews using a questionnaire that aims to determine the physical condition of the area, the general condition of settlements in Moncongloe District, and documentation of formal/informal housing. Secondary data used include data on land use, soil type, slope, rainfall, disaster vulnerability, border areas, data related to housing investment, review of spatial plans, and population data.

The data analysis method used is a combination of qualitative and quantitative methods. Qualitative and quantitative descriptive analysis methods are used to analyze research questions regarding the physical characteristics of housing that display data in the form of an explanatory description of the data obtained from both the RTRW thematic data, image interpretation and observation results, while quantitative data for research questions concerns projected needs that analyze population projections. , the availability and need of land, and the carrying capacity of residential land. Spatial analysis methods (scoring, overlay, and buffer) were used to research and explore data from a spatial perspective with the help of ArcGIS software. Spatial analysis is carried out to determine the function of the area with predetermined parameters according to the criteria for suitability of residential land.

## 3. Results and Discussion

### 3.1. Projection and Population Growth

The calculation and population growth of Moncongloe District was calculated using the least square method because this method has the smallest standard deviation value. Population growth projection data in Moncongloe District can be seen in the Table 1.

### 3.2. Land Availability Analysis

Calculation of land availability aims to determine the total area of land that still has the potential to be built and can be used for residential functions. Land availability is assessed based on the results of the spread between existing land use, physical conditions such as slope and soil type, as well as the spatial pattern plan contained in the RTRW of Maros Regency.

Other aspects to be considered are protected areas in the form of protected forests that have been established and the proposed Sustainable Food Agricultural Land, in which areas that have been designated as part of these two aspects may not be developed into built-up areas. The results of the spread of several variables to measure land availability can be seen in Fig. 1.
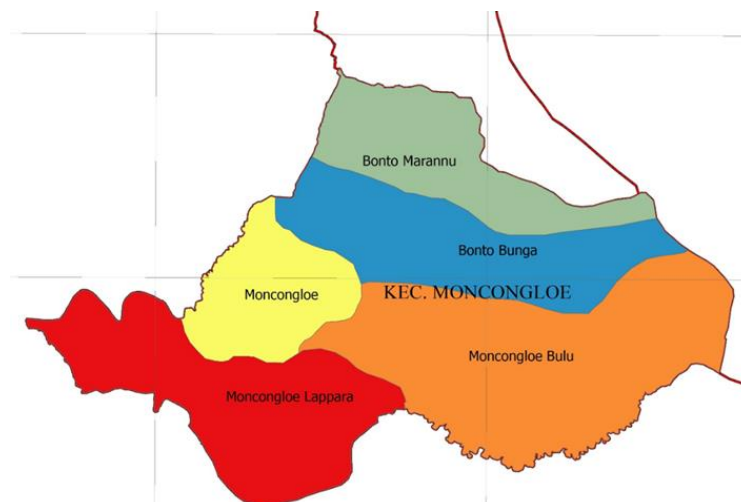


Figure 1. Maros district administration map
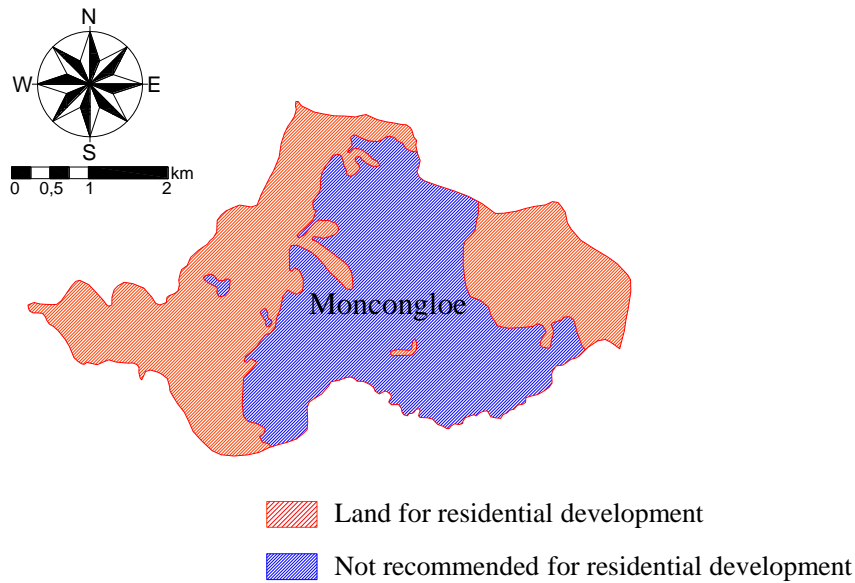
Figure 2. Land map for settlement development

Table 2. Availability of land for residential areas

| No | Description | Area (Ha) |
|----|-------------|-----------|
| 1 | Recomended | 2,417.99 |
| 2 | Not recomended | 2,417.17 |
| | Total | 4,835.17 |

Based on Fig. 2, there are two land classifications that can indicate land availability. Land for development is an area that is recommended and directed for development settlement. What is not recommended is an area that has been built and has other aspects, such as having been designated as sustainable food agricultural land or physically not meeting the criteria for settlement development. The area available for development is in the middle of the Moncongloe District, where this is in line with the Maros Regency spatial pattern plan that directs residential areas in the area. In the region the eastern and western parts, there are Sustainable Food Lands and the land use is mostly in the form of rice fields. The area of each classification on the map is described in Table 2.

Based on the data presented in Table 2, it can be explained that the recommended and non-recommended land areas have almost the same area. This shows that around 50% of the area can still be developed as a residential area.

### 3.3. Land Requirements Analysis

The need for land for housing development in Moncongloe District based on data from the Maros Regency Housing and Settlement Service is presented in Table 3. The data presented in this table shows that population growth from 2021 shows a significant increase until the projected year 2041 which has direct implications for land needs in Moncongloe District of 854,209 $m^2$.

### 3.4. Analysis of the Environmental Carrying Capacity of Formal Housing

The carrying capacity of residential land is obtained through data on the vastness of the area, the vastness of protected areas, and the vastness of disaster prone areas where the area is obtained from satellite imagery using the digitized method of land use which is then overlaid. The area of Moncongloe District is 48,408,400 $m^2$, the protected area is 24,171,700 $m^2$, and the disaster-prone area is 7,363,700 $m^2$.

Table 3. Projected land requirements in Moncongloe District in 2021-2041

| No. | Years | Total population | Amount KK | Home Supplies (Unit) | | | House Area Needs (m2) | | | Total Area Requirement (m²) |
|-----|-------|------------------|-----------|---------------------|---------------------|----------------|-----------|-------------|-----------|------------------------------|
| | | | | Big (10%) | Currently (30%) | Small (60%) | Big | Cuurrently | Small | |
| 1 | 2021 | 25,421 | 6,219 | 622 | 1,866 | 3,731 | 186,570 | 279,855 | 358,214 | 824,639 |
| 2 | 2026 | 30,761 | 6,236 | 624 | 1,871 | 3,742 | 187,080 | 280,620 | 359,194 | 826,894 |
| 3 | 2031 | 36,100 | 6,247 | 625 | 1,874 | 3,748 | 187,410 | 281,115 | 359,827 | 828,352 |
| 4 | 2036 | 41,440 | 6,258 | 626 | 1,877 | 3,755 | 187,740 | 281,610 | 360,461 | 829,811 |
| 5 | 2041 | 46,779 | 6,442 | 644 | 1,933 | 3,865 | 193,260 | 289,890 | 371,059 | 854,209 |

The area of residential land can be calculated using the formula [18]:

$$LPm = LW - (LKL + LKRB) \qquad (1)$$

where:
LPm      = Residential Land
LW      = An area ($m^2$)
LKL      = Protected Area ($m^2$)
LKRB      = Area of Disaster Prone Area ($m^2$)

After value *LPm* is found, the carrying capacity of settlements can be calculated using the formula [18]:

$$DDPm = \frac{LPM/JP}{\alpha} \qquad (2)$$

where:
DDPm      = Residential Carrying Capacity
LPm      = Area of Settlement ($m^2$)
JP      = Total population (jiwa)
$\alpha$      = Coefficient of Land Area Requirement ($m^2$/kapita)

The limits of the feasibility of carrying capacity of land for settlements are formulated as follows [18]:
a. $DDPm > 1$ : Able to accommodate balance residents to live;
b. $DDPm = 1$ : There is a balance between the population and those who live wit the existing area;
c. $DDPm < 1$ : Unable to accommodate residents to live in the area.

Furthermore, the carrying capacity of residential land in Moncongloe District for 2021 based on the calculation results can be seen in Table 4.

Based on the calculation results of the formula for carrying capacity of residential land in 2021, accumulatively obtained the final result of *DDPm* in Moncongloe District is 20.7. Bonto Bunga Village has the highest *DDPm* of 262.4, and the lowest *DDPm* of 58.9 is in Moncongloe Lappara Village. Thus, it can be concluded that based on the calculation results, in 2021 the Moncongloe District can accommodate residents to live.

Table 4. Carrying capacity of residential land in Moncongloe District in 2021

| No | Village | *DDPm* | Description |
|----|---------|--------|-------------|
| 1 | Moncongloe Lappara | 58.9 | Able to accommodate residents to live |
| 2 | Moncongloe Bulu | 106.1 | Able to accommodate residents to live |
| 3 | Moncongloe | 81.8 | Able to accommodate residents to live |
| 4 | Bonto Bunga | 262.4 | Able to accommodate residents to live |
| 5 | Bonto Marannu | 173.7 | Able to accommodate residents to live |
| Moncong district | | 20.7 | Able to accommodate residents to live |

Table 5. Carrying capacity of residential land in Moncongloe District in 2041

| No | Village | DDPm | Description |
|----|---------|------|-------------|
| 1 | Moncongloe Lappara | 79.5 | Able to accommodate residents to live |
| 2 | Moncongloe Bulu | 106.1 | Able to accommodate residents to live |
| 3 | Moncongloe | 55.2 | Able to accommodate residents to live |
| 4 | Bonto Bunga | 223.1 | Able to accommodate residents to live |
| 5 | Bonto Marannu | 189.0 | Able to accommodate residents to live |
| Moncong district | | 20 | Able to accommodate residents to live |

Furthermore, the carrying capacity of residential land in Moncongloe District for 2041 based on the calculation results can be seen in Table 5.

Based on the calculation of the carrying capacity formula for residential land in 2041, accumulatively obtained the final *DDPm* of Moncongloe District is 20. Bonto Bunga Village has the highest *DDPm* of 223.1, and the lowest *DDPm* of 55.2 is in Moncongloe Village. Thus, it can be concluded that based on the calculation results, in 2041 the Moncongloe District can accommodate residents to live.

## 4. Conclusion

Moncongloe District is an area with a relatively high population growth rate and distribution of housing, especially formal housing. Therefore, a study is needed that can be a guideline for controlling formal housing growth based on an analysis of the environmental carrying capacity which includes population analysis, land needs analysis, and housing needs analysis. From the results of a study of environmental carrying capacity indicators using the calculation formulation of environmental carrying capacity, it was found that the limit for the feasibility of environmental carrying capacity in 2021 and the projected year 2041 is above number 1, both calculations based on urban areas, as well as cumulative calculations in the Moncongloe District area. Thus, it can be concluded that the Moncongloe District area can accommodate community living activities until the projected year 2041.

## Referensi

[1] Z. Sheng, W. Changwen, H. Huasheng, and Z. Luoping, "Linking the Concept of Ecological Footprint and Valuation of Ecosystem Services-A Case Study of Economic Growth and Natural Carrying Capacity," *Int. J. Sustain. Dev. World Ecol.*, vol. 16, no. 2, pp. 137–142, 2008.
[2] S. Henning, et al., "Carrying Capacity: An Approach to Local Spatial Planning in Indonesia," *J. Transdiscipl. Environ. Stud.*, vol. 11, no. 1, pp. 27–39, 2012.
[3] Ruwayari, et al., "Analysis of the Carrying Capacity and Capacity of Land on Bunaken Island," *J. Spasial*, vol. 7, no. 1, 2020. [in Bahasa]
[4] Lahamendu, "Analysis of the Suitability of Sustainable Land Use on Bunaken Island, Manado," *J. Sabua*, vol. 7, no. 1, pp. 383–388, 2015. [in Bahasa]
[5] A. Prilia, "The Effect of Land Suitability for Settlements on the Carrying Capacity of Land," *J. Univ. Taruma Negara*, vol. 5, no.

5, pp. 1–10, 2012. [in Bahasa]

[6] Nasution, "Problems and Settlements in Medan City," *J. Archit. Urban. Res.*, vol. 3, no. 1, pp. 27–46, 2019. [in Bahasa]

[7] Republic of Indonesia, "Regulation No. 1 of 2011 concerning Housing and Settlement Areas", Jakarta, 2011. [in Bahasa]

[8] Ernamaiyanti, "Analysis of the Carrying Capacity and Capacity of Land for Housing and Settlement Development in Banten Province," *J. Tek. Sipil UNPAL*, vol. 9, no. 1, 2019. [in Bahasa]

[9] C. A. Doxiadis, *Ekistic: An Introduction to the Science of Human Settlement*. London: Hutchinson and Co, 1968.

[10] N. P. Sueca, "Home transformation: Prospects for improving housing conditions in Indonesia (A Preliminary Study)," *J. Permukim. Natah*, vol. 2, no. 1, pp. 1–55, 2004. [in Bahasa]

[11] N. M. Davidson and R. P. Malloy, *Affordable Housing and Public-Private Partnership*. Burlington USA: Ashgate Publishing Company, 2009.

[12] M. Baiquni, "Social-Economics Integration of Dualistic Settlement Environment at Urban Areas in Indonesia (Case Study in Yogyakarta City)," *Forum Geogr.*, vol. 14, no. 1, 2000.

[13] G. Lim, "Housing Policies for the Urban Poor in Developing Countries," *APA Journal, Spring*, 1987.

[14] W. A. Doebelle, "The Evolution of Concepts of Urban Land Tenure in Developing Countries in Habitat International," *1987*, vol. 11, no. 1.

[15] A. T. Sulistiyani, "Urban Housing Problems and Policies," *J. Ilmu Sos. dan Ilmu Polit.*, vol. 5, no. 3, pp. 327–344, 2002. [in Bahasa]

[16] Anastasia, Njo, Handayani, Yunita, and C. Emmanuelle, "Developer Accountability in the Maintenance of Housing Areas in Surabaya (Case Study on Housing in West Surabaya and East Surabaya)," *J. Manaj. Kewirausahaan*, vol. 4, no. 1, pp. 26–35, 2002. [in Bahasa]

[17] Musianto, "The difference between the Quantitative Approach and the Qualitative Approach in research methods," *J. Manaj. Kewirausahaan*, vol. 4, no. 2, pp. 123–13, 2002. [in Bahasa]

[18] Republic of Indonesia, "Regulation No. 17 of 2009 concerning Guidelines for Environmental Carrying Capacity in Regional Spatial Planning", Ministry of Environment , Jakarta, 2009. [in Bahasa]

# Prototype Self-Adaptive Traffic Light Control System using Cameras

Channareth Srun[a,*], Saran Meas[b], Sok Oeun Un[c], Saokun Khim[d], Virbora Ny[e]

[a]Faculty of Electronics, National Polytechnic Institute of Cambodia. Email: nareth16npic@gmail.com
[b]Faculty of Electronics, National Polytechnic Institute of Cambodia.
[c]Faculty of Electronics, National Polytechnic Institute of Cambodia.
[d]Faculty of Electronics, National Polytechnic Institute of Cambodia.
[e]Faculty of Electronics, National Polytechnic Institute of Cambodia.

## Abstract

Cambodia is a developing country with rapid development. More vehicle usage on the road is increased, this leads to more traffic problems. The traditional traffic light and traffic police officer help solve the problem at a level and limited conditions. For better improvement in this research, the smart traffic light is a better solution that can adapt to the real-world environment. There are four cameras are used for capturing and analyzing the vehicle traffic to control the modes of the traffic light. This method gives the improvement over the limited time of the traditional traffic light. This smart traffic light system comes with three-term mode conditions including normal mode, camera mode, and night mode.

*Keywords: Camera; self-adaptive; smart traffic; traffic light*

## 1. Introduction

Along with the rapid development in Cambodia, traffic has increased rapidly. This led to traffic problems in the country such as traffic jams and traffic accidents. These reasons are due to the traditional timing-based traffic light system that is based on the fixed timed control sequence. Adaptive Traffic Control System (ATCS) is a better technique than the traditional preprogrammed time delay traffic light, this method helps to ensure that the system can adapt to the real traffic situation and reduce the traffic jam by relying on the sensors and cameras [1]. Since the actual traffic volume is not always the same from time to time. According to research, showing that delays during traffic can cause an environmental issue due to the $CO_2$ emission from a vehicle's engine [2]. To reduce the traffic along with the growth of the population in an urban area, the smart city concept is applied. This concept is to use the smart and automatic control system for monitoring and creating an effective control algorithm for the traffic problem [3]. To solve this problem, the camera and computer vision are used to reduce the traffic jam with adaption to the traffic situation [4, 5]. The camera is the main component for capturing the image for vehicle recognition and gives the command to the traffic light controller. This solution helps improve the traffic light's ability to adapt to the traffic condition along with the adjustable mode to different conditions of use. This is a

system designed as a standalone system for monitoring and controlling the traffic condition from the computer software [6, 7]. In our research, there are three terms mode available for the traffic operation control such as normal mode (embedded with sub-mode 1 to 6), camera mode (embedded with 15 conditions), and night mode. Normal mode operates with the duration set by the traffic controller. The camera operates automatically by analyzing and computing the data for generating the traffic sub-mode command. Night mode is enabled during the night-time with fixed conditions, this mode operates the traffic light with yellow color as a warning for the vehicle operator and pedestrian traveling at night.

## 2. Image Processing

Image processing is the method of calculating the image and processing the image into another form of data. This method also allows retrieving the data from the image and using it for other purposes [8]. These methods include:

- *Method of Converting RGB Image to Gray Image*

A Pixel was created with four elements including alpha, red, green, and blue shown in Fig. 1.



Figure 1. Bit of a pixel

---

*Corresponding author. Tel.: +855-17-592-963
Phnom Penh, Cambodia, 12000*
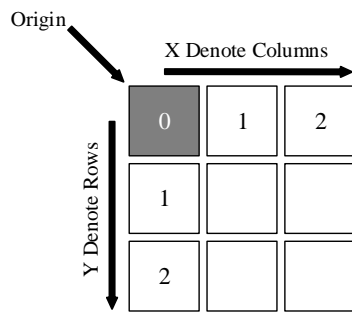
Figure 2. Pixel of an image



Figure 3. Image thresholding

The alpha value set the transparency of the three colors red, green, and blue pixel. These values are known as Alpha-A, Red-R, Green-G, and Blue-B [9, 10]. These elements (A, R, G, and B) have the 8 bits value ranging from 0 to 255, in a total of 32 bits for a pixel.

Figure 2 describes the 2D pixel aligned on the column and row of an image. The first pixel is called the origin (staring pixel) of the image with the coordinate of. X and Y is the coordinate of a pixel with A, R, G and B is the value of a pixel.

An example: $P_{0,0}(255,100,150,200)$ indicate the pixel with the coordinate of has the value of $A = 255, R = 100, G = 150, B = 200$.

To convert the (RGB Image) into the (Grayscale Image) the following step is used:
a) Take the RGB value of a pixel
b) Calculate the average value of RGB pixel
c) Change the RGB value of each pixel to $A_{vg}$ value

A pixel of the coordinate at the pixel, the alpha value stays the same with the R, G, and B value is the same [11].

- *Emgu CV*
Emgu CV is a cross-platform image-processing library related to OpenCV since the Emgu CV is a .NET framework connecting to OpenCV. Emgu CV can be used with programming languages such as C#, VB, Iron Python, and C++ [12]. This library is supported on a desktop platform such as Linux, Windows, and macOS X and a mobile platform such as Android, iPhone, iPod Touch, and iPad. Emgu CV was used for replacement on OpenCV since the .NET is not supported on C and C++.

- *Thresholding Theory*
The intensity of a pixel in the background is the value of outer value limited set to the binary image shown in Fig. 3. The Thresholding process is organizing each pixel value ranging between the value of 0 and 1. Hence, the (Binary image) divided the pixel into two parts:
a) Value 1 is the value of the set boundary
b) Value 0 is the value of the outer boundary

Most digital cameras are designed to operate with the Thresholding process on the hardware layer. The output data is generated as a binary image. Thresholding is a method of converting from a Grayscale image to the binary image of one or more objects separated from the background. This method is efficient for separating the object from the background image [13, 14].
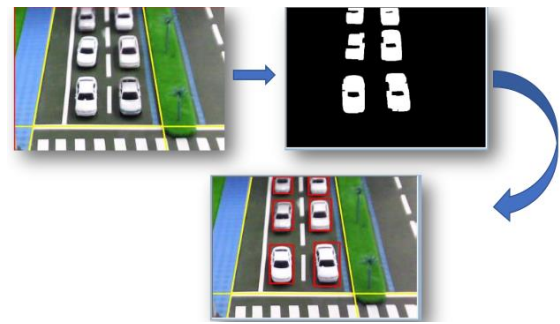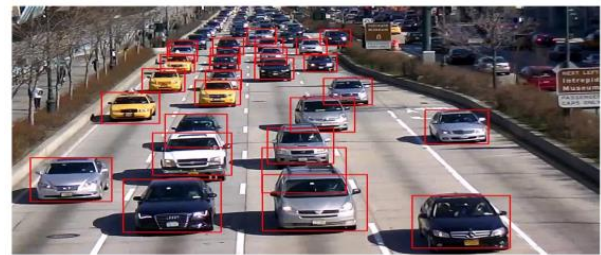


Figure 4. Motion detection principle

- *Motion Detection*
Motion detection is a camera process of detecting an object while the object is moving related to the camera. This technology is divided into two main parts:
a) Motion detection using software-based motion sensor camera
b) Motion detection using the sensor in operation (PIR sensor)

In Fig. 4, the software-based motion sensor camera detects the object comparing the changing pixels during changing frame. In case a human or animal moves in a different pixel the object will be detected by the movement [15, 16].

## 3. Hardware Design and Implementation

Figure 5 is the traffic light model designed as a scale down from the actual traffic light. This model was designed with the dimension of $1 \times 1m$, the height of $370mm$, and the floor thickness of $20mm$. In Fig. 6, the width of each lane is not included in the walking path with the height of the traffic light is $370mm$.

Figure 7 shows the description block diagram of the traffic management system. The input block contains the four cameras as the input to the system. The processor includes the PC as the central processor for image processing and data analysis, Arduino NANO is the embedded controller used for controlling the traffic lights.



(a) Traffic light model top view

(b) Traffic light model side view
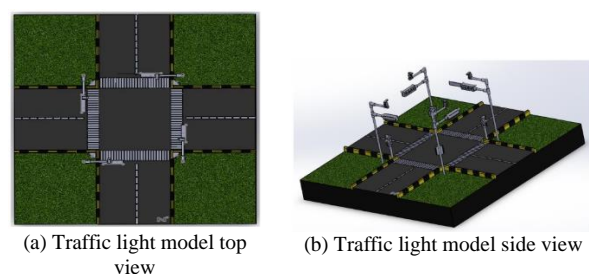
Figure 5. Traffic light model

(a) Traffic lane width     (b) Traffic light height
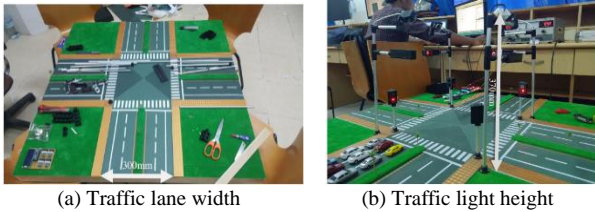
Figure 6. Real-world traffic light model
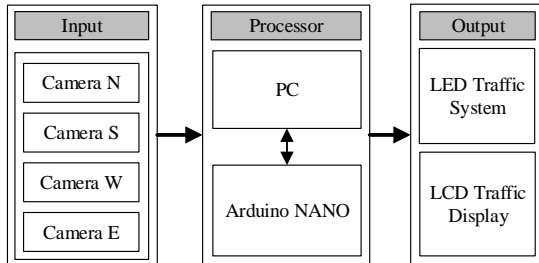


Figure 7. Block diagram of traffic system

The command sent from the computer will activate the operation mode on the traffic light managed by the microcontroller. The serial communication protocol is used for the communication between the computer and the microcontroller. All four cameras are shown in Fig.7 are used as the image capturing sensor communicating with the computer using the USB protocol. These hardware components are assembled as a complete traffic model shown in Fig. 6(b).

## 4. Software Implementation

The user interface was designed using Microsoft Visual Studio. Figure 8 is interface designed using Khmer text with the security feature before login to the system. Figure 9 is the user interface designed with the control menu on the right side and the four-camera monitoring on the left side.

Figure 10 describes the process of the complete traffic light operating process. The images are captured from the camera are processed through the object detection procedure and determine the percentage of road-free areas. The result of the road free is the input for the system for determining the term and mode of the traffic light. The data will later send to the traffic light hardware controller.



Figure 8. Login user interface
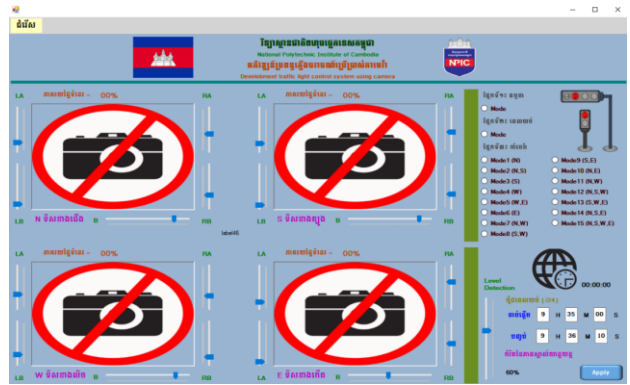


Figure 9. Traffic light management user interface
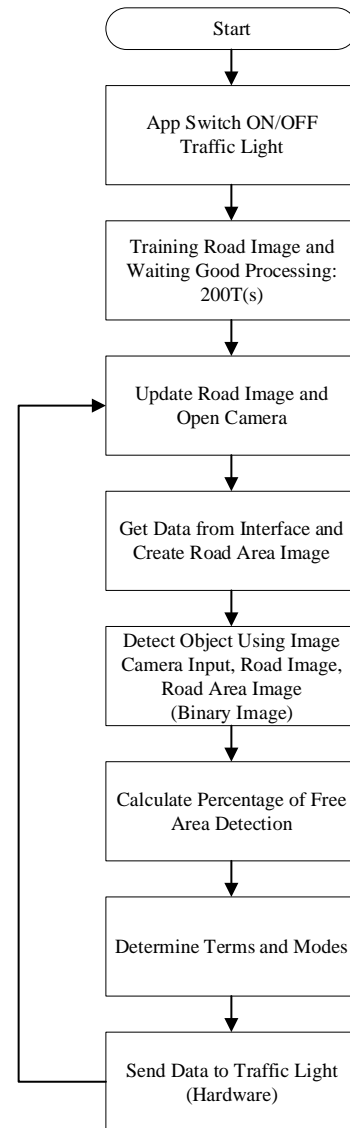


Figure 10. Traffic light system block diagram of a process

The operation modes of the traffic light process are divided into three modes including sub-modes 1 to 6 in normal mode, camera mode, and night mode. Figure 11 shows the detailed decision process made by the traffic light mode through the data from camera image processing.
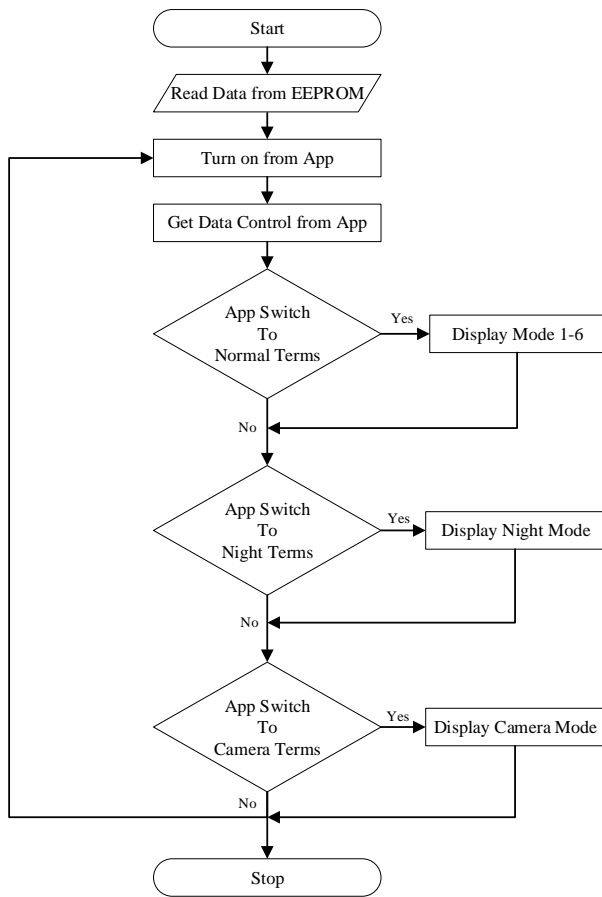
Figure 11. Flowchart of traffic light modes

The system starts the traffic controlling process by the command from the desktop application. The command sent from the desktop application will decide the operation mode of the traffic light. The decision of each operation mode is decided by the data processed from the image processing obtained by the cameras and the traffic control algorithm. The command sent from the traffic management software activates the microcontroller, controlling the colors of the traffic light.

## 5. Experiment Testing

The experiment process of the traffic light system is divided into two parts:
- Testing the control interface and circuitry of the system
- Testing the responds modes of the system

### 5.1. Camera Detection Error Calibration

The process of capturing the image via the camera has an error by the distance to the vehicles. This error occurred the further the vehicle to the camera. The result is the smaller size of the vehicle used for analysis. The error detection of the image processing is determined as follows.

Theoretical:
- Full Image $(F_A)$

$$F_A = 132 \ mm \times 270 \ mm$$
$$= 36828 \ mm^2$$

- Free Detect Area $(F_D)$

$$F_D = F_D - 2(Length \times Width)$$
$$= 36828 \ mm^2 - 3250 \ mm^2$$
$$= 33578 \ mm^2$$

- Percentage $(P)$

$$TP = \frac{33578}{36828} \times 100 = 91.18\%$$

Experimental:
- Full Area $(F_A)$

$$F_A = 137662$$

- Free Detect Area $(F_D)$

$$F_D = F_A - Detected$$
$$= 127622 - 26232$$
$$= 111430$$

- Percentage $(P)$

$$EP = \frac{111430}{137662} \times 100$$
$$= 80.94\%$$

$$\%ERROR = \frac{E_P - T_P}{T_P} \times 100$$
$$= \frac{80.94 - 91.18}{91.18} \times 100$$
$$= 11.23\%$$
$$\%ERROR = \frac{80.94 - 95}{95} \times 100$$
$$= \mp 14.8\%$$

### 5.2. Traffic Mode Testing

The traffic mode testing is divided into three modes. The first mode, Figure 12 is the normal traffic mode. In this mode, the road was detected with 100% empty road. The algorithm sends the command to the traffic light as Green.

In night mode, the time is limited to the set value. In this experiment, the time is set to the range of 00:00 (Midnight) to 6:00 AM. During this mode, the algorithm sends the command to the traffic light as Yellow shown in Fig. 13.
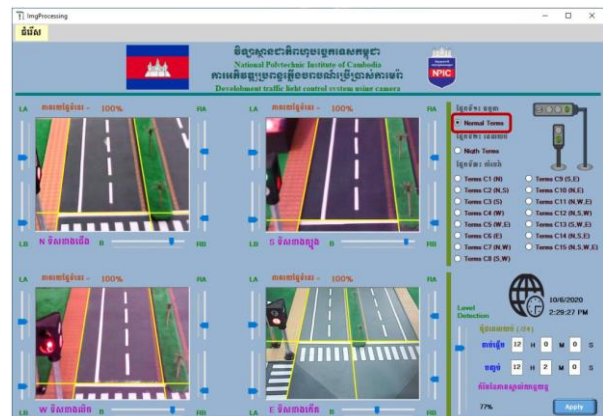


Figure 12. Traffic light "Normal mode" operation

Figure 13. Traffic light "Night mode" operation



Figure 14. Traffic light "Traffic mode" operation

In traffic mode, in testing mode 1. The north side has the detected vehicle on the road. The algorithm is set to at least four cars is defined as a signal to activate the traffic mode algorithm. In Fig 14, the north camera detected 69.40% of free space with five cars detected and the other three lanes available. The algorithm sends the green signal to the other three empty lanes as Green.

### 5.3. Experimental Result

The testing result is shown in Table 1. This table is divided into terms, camera lane detection, and traffic sub-mode selection. Notably, the terms of the traffic may vary due to the traffic conditions. The algorithm decides the selected mode via the information from the camera's detection. The camera lane detection determines the cardinal traffic conditions. The detection results are divided into two blocks with free space and used space on each lane. The algorithm sends the control signal to the traffic light controller based on the sub-mode of the traffic operation shown from Figs. 15 to 20.

For testing purposes, the time of operation in each mode is 15 seconds with green light. After the main mode timer is completed, the traffic light switches back to the yellow light for warning mode with the blink interval of 0.5s.

Table 1. Traffic mode experimental results

| Term Camera | N | | S | | W | | E | | Sub mode |
|---|---|---|---|---|---|---|---|---|---|
| | F/S (%) | U/S (%) | F/S (%) | U/S (%) | F/S (%) | U/S (%) | F/S (%) | U/S (%) | |
| C1 | 69.40 | 30.60 | 100 | 0 | 100 | 0 | 100 | 0 | 1 |
| C2 | 73.46 | 26.54 | 77.49 | 22.49 | 93.20 | 6.80 | 95.43 | 4.57 | 2 |
| C3 | 73.55 | 26.45 | 69.84 | 30.16 | 100 | 0 | 100 | 0 | 3 |
| C4 | 92.54 | 7.46 | 94.51 | 5.49 | 77.72 | 22.28 | 94.48 | 5.52 | 4 |
| C5 | 92.20 | 7.80 | 94.56 | 5.44 | 73.10 | 26.90 | 78.50 | 21.50 | 5 |
| C6 | 94.25 | 5.75 | 95.51 | 4.49 | 90.99 | 9.01 | 73.86 | 26.14 | 6 |
| C7 | 79.10 | 20.90 | 95.25 | 4.75 | 68.05 | 31.95 | 95.26 | 4.74 | 4 |
| | 68.05 | 31.95 | 95.25 | 4.75 | 79.10 | 20.90 | 95.26 | 4.74 | 1 |
| C8 | 94.26 | 5.74 | 82.95 | 17.05 | 71.96 | 28.04 | 94.31 | 5.69 | 4 |
| | 94.26 | 5.74 | 79.10 | 28.04 | 82.95 | 17.05 | 94.31 | 5.69 | 3 |
| C9 | 94.25 | 5.75 | 80.53 | 19.47 | 89.30 | 10.70 | 77.73 | 22.27 | 6 |
| | 94.25 | 5.75 | 77.73 | 22.27 | 89.30 | 10.70 | 80.53 | 19.47 | 3 |
| C10 | 78.78 | 21.22 | 93.78 | 6.22 | 88.75 | 11.25 | 71.88 | 28.12 | 6 |
| | 71.88 | 28.12 | 93.78 | 6.22 | 88.75 | 11.25 | 72.17 | 21.22 | 1 |
| C11 | 68.28 | 31.72 | 100 | 0 | 71.00 | 29.00 | 72.17 | 27.83 | 1 |
| | 71.00 | 29.00 | 100 | 0 | 68.28 | 31.72 | 72.17 | 27.83 | 4 |
| | 71.00 | 29.00 | 100 | 0 | 72.17 | 27.83 | 68.28 | 31.72 | 6 |
| C12 | 69.22 | 30.78 | 63.36 | 36.64 | 72.27 | 27.73 | 96.04 | 3.96 | 3 |
| | 63.36 | 36.64 | 69.22 | 30.78 | 72.27 | 27.73 | 96.04 | 3.96 | 1 |
| | 72.27 | 27.73 | 69.22 | 30.78 | 63.36 | 36.64 | 96.04 | 3.96 | 4 |
| C13 | 93.29 | 6.71 | 72.93 | 27.07 | 69.71 | 30.29 | 74.62 | 25.38 | 4 |
| | 93.29 | 6.71 | 69.71 | 30.29 | 72.93 | 27.07 | 74.62 | 25.38 | 3 |
| | 93.29 | 6.71 | 74.62 | 25.38 | 72.93 | 27.07 | 69.71 | 30.29 | 6 |
| C14 | 71.97 | 28.23 | 72.24 | 27.76 | 86.57 | 13.43 | 73.41 | 26.59 | 1 |
| | 72.24 | 27.76 | 71.97 | 28.23 | 86.57 | 13.43 | 73.41 | 26.59 | 3 |
| | 72.24 | 27.76 | 73.41 | 26.59 | 86.57 | 13.43 | 71.97 | 28.23 | 6 |
| C15 | 72.18 | 27.82 | 72.06 | 27.94 | 70.16 | 29.84 | 72.71 | 27.29 | 4 |
| | 70.16 | 29.84 | 72.06 | 27.94 | 70.16 | 27.82 | 72.71 | 27.29 | 1 |
| | 72.06 | 27.94 | 70.16 | 29.84 | 72.18 | 27.82 | 72.71 | 27.29 | 3 |
| | 72.06 | 27.94 | 70.16 | 29.84 | 72.18 | 27.82 | 70.16 | 29.84 | 6 |

*F/S: Free Space, U/S: Used Space.
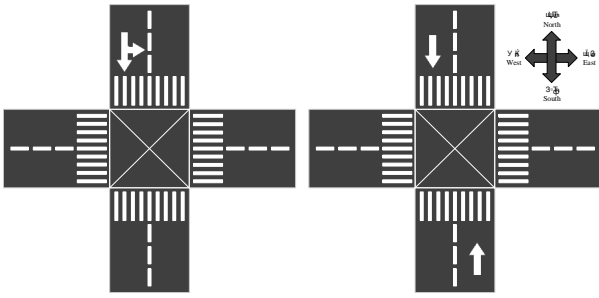
Figure 15. Traffic operation sub-mode 1 and sub-mode 2
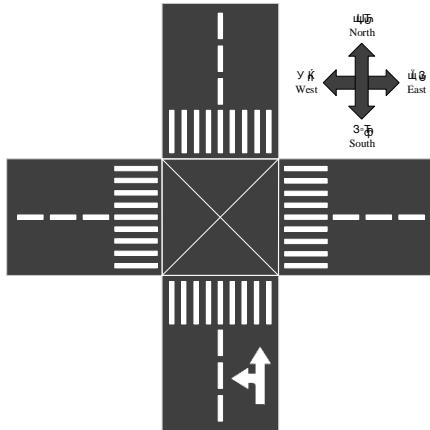


Figure 16. Traffic operation sub-mode 3

Figure 15 describes the operation process of traffic sub-mode 1 and sub-mode 2 of the camera detection sequence.

Sub-mode 1: This mode allows the vehicle to pass from the north lane to the south lane and turn to the left and right.

Sub-mode 2: This mode allows the vehicle to pass from the south lane to the north lane. The operation time is the same as the mode one operation.

Sub-mode 3: This mode allows the vehicle to pass through from the south to the north and able to turn left and right shown in Fig. 16.

Sub-mode 4: This mode allows the vehicle to pass through from the west to the east and able to turn left and right shown in Fig. 17.

Sub-mode 5: this mode allows the vehicle to pass from the east to the west lane, and able to pass from the west to the east lane shown in Fig. 18.
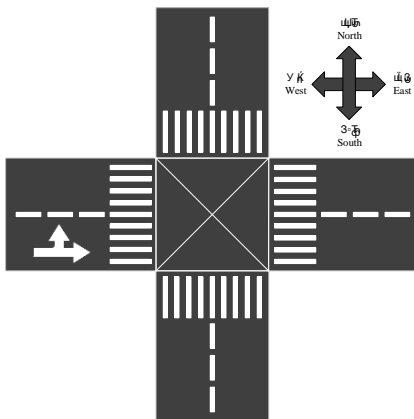


Figure 17. Traffic operation sub-mode 4
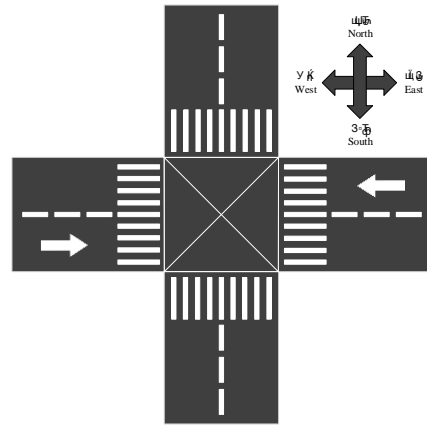


Figure 18. Traffic operation sub-mode 5
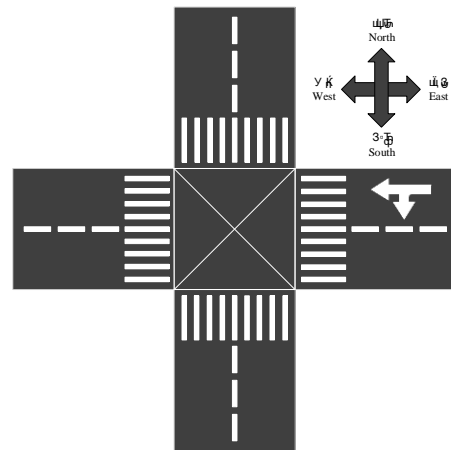


Figure 19. Traffic operation sub-mode 6

Sub-mode 6: this mode allows the vehicle to pass from the east to the west lane, and able to turn to the left and right lane shown in Fig. 19.

Figure 20 shows the possible turns for each lane at night mode. This mode is enabled due to the less traffic at nighttime the night mode activation is set from 11:00 PM to 4:00 AM. In this mode, the camera detections are disabled and only enable for yellow light as a warning for pedestrians.
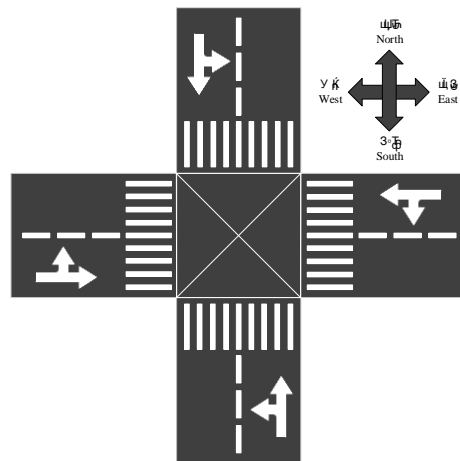


Figure 20. Traffic operation in "Night mode"

## 6. Conclusion

The process of controlling the traffic light conditions can be achieved by analyzing the data from the input cameras. The modes of the traffic operation can be controlled from the desktop application. The user can switch between the modes manually and the command will be processed by the traffic control algorithm controlling the traffic operation. The percentage of vehicle detection is determined as a percentage value. In the experiment, the camera with the vehicle detection, the system has an ±14.8% error rate. The detection error is caused by the shadows of the vehicle due to the small size of the traffic light model and the position of the camera. For further practice, applying this system to the actual traffic application can help reduce the error rate.

## References

[1] S. Shankaran and L. Rajendran, "Real-Time Adaptive Traffic Control System for Smart Cities," in *International Conference on Computer Communication and Informatics (ICCCI-2021)*, 2021, pp. 27–29.

[2] K. Cikhardtova, Z. Belinova, T. Tichy, and J. Ruzicka, "Evaluation of Traffic Control Impact on Smart Cities Environment," in *Smart Cities Symposium Prague*, 2016, pp. 1–4.

[3] L. F. P. de Oliveira, L. T. Manera, and P. D. G. da Luz, "Development of a Smart Traffic Light Control System With Real-Time Monitoring," *IEEE Internet Things J.*, vol. 8, no. 5, pp. 3384–3393, 2021.

[4] M. Razavi, M. Hamidkhani, and R. Sadeghi, "Smart Traffic Light Scheduling in Smart City Using Image and Video Processing," in *2019 3rd International Conference on Internet of Things and Applications (IoT)*, 2019, pp. 1–4.

[5] K. Iwaoka, M. Maruyama, and S. Nukura, "Public Transportation Priority Systems Combined with Multiple Traffic Control Strategies," in *IEEE Intelligent Transportation Systems.*, 2000, pp. 173–177.

[6] M. F. Rachmadi *et al.*, "Adaptive Traffic Signal Control System Using Camera Sensor and Embedded System," in *TENCON 2011 - 2011 IEEE Region 10 Conference*, 2011, pp. 1261–1265.

[7] P. Rizwan, K. Suresh, and M. R. Babu, "Real-time Smart Traffic Management System for Smart Cities by Using Internet of Things and Big Data," in *2016 International Conference on Emerging Technological Trends (ICETT)*, 2016, pp. 1–7.

[8] M. M. Hasan, G. Saha, A. Hoque, and M. B. Majumder, "Smart Traffic Control System with Application of Image Processing Techniques," in *2014 International Conference on Informatics, Electronics Vision (ICIEV)*, 2014, pp. 1–4.

[9] M. Sinecen, *Applications from Engineering with MATLAB Concepts*. 2016.

[10] S. Annadurai, *Fundamentals of Digital Image Processing*. India: Pearson, 2006.

[11] Z. Li, "Introduction to Computer Vision," 2020.

[12] S. Shi, *Emgu CV Essential*. Birmingham: Packt Publishing Ltd, 2012.

[13] M. V. K. S. C. Thavreak, *Machine Vision Inspection System*. Phnom Penh, 2019.

[14] R. Holzer, "OpenCV Tutorial Documentation," pp. 61–68, 2019.

[15] R. Jain, R. Kasturi, and B. G. Schunck, *Machine vision*. McGraw-Hill, 1995.

[16] Z. Yu and Y. Chen, "A Real-Time Motion Detection Algorithm for Traffic Monitoring Systems Based on Consecutive Temporal Difference," in *2009 7th Asian Control Conference*, 2009, pp. 1594–1599.

# The Development of Earthquake Simulator

Nur Azhary Iriawan Eka Putra[a,*], Rafiuddin Syam[b], Ilyas Renreng[c], Tri Harianto[d], Nanang Roni Wibowo[e]

[a]Department of Mechanical Engineering, Faculty of Engineering, University of Hasanuddin. Email: ary.iriawan04@gmail.com
[b]Electronic Engineering Education, Faculty of Engineering, State University of Jakarta. Email: rafiuddin_syam@unj.ac.id
[c]Department of Mechanical Engineering, Faculty of Engineering, University of Hasanuddin. Email: ilyas_renreng@gmail.com
[d]Department of Civil Engineering, Faculty of Engineering, University of Hasanuddin. Email: triharianto@unhas.ac.id@gmail.com
[e]Mechatronic Engineering, Polytechnic of Bosowa. Email: nanangroni80@gmail.com

**Abstract**

An earthquake is an event that vibrates or shakes the earth due to the sudden movement or shift of rock layers on the earth's crust due to the movement of tectonic plates. Earthquakes that occur cause damage to buildings and loss of life and can trigger other natural disasters such as tsunamis and even liquefaction. To anticipate this, it is necessary to study the structure of the building and tools to test the strength of the building, so that it becomes an effective tool and is needed to anticipate the occurrence of large losses. The earthquake simulator was built in the form of a shaking table driven by a hydraulic actuator. The earthquake simulator is equipped with a proximity sensor to determine the cylinder motion distance which is controlled using proportional and integral using the Arduino Mega2560 controller. The results showed that the shaking table can work ideally with a value of P(kc) = 0.066195 and a value of I(ki) = 2.009974 which can produce acceleration data in actual (real-time) which is displayed in graphical form on the LabVIEW front panel.

*Keywords: Arduino; earthquake, electro-hydraulic; simulator*

## 1. Introduction

An earthquake is an event that occurs due to the movement and collision of rock layers on the earth's crust or tectonic plates. These collisions or shifts produce energy that propagates to the earth's surface as seismic waves [1]. Earthquakes can be caused by several factors such as volcanic eruptions, shifting of the earth's plates, and dynamite explosions [2].

Earthquakes for the territory of Indonesia are one of the sources of natural disasters that often appear. The Meteorology, Climatology, and Geophysics Agency (BMKG) recorded 18 significant earthquakes in Indonesia in 2018. Significant earthquakes are earthquakes with a magnitude of M≥6 and earthquakes that cause damage even though the magnitude of the earthquake is M≤6. One of the significant earthquakes recorded was an earthquake that occurred in Central Sulawesi with a magnitude of 7.4 on the Richter Scale which caused a tsunami and liquefaction [3]. This certainly makes earthquakes one of the concerns in the field of research.

In this case, theory, practice, and application are needed so that they need to be supported by practical means to improve learning that is good and can be understood easily and can be practiced directly. Through the learning model, the help of simulation tools will make it easier to find out building structures that are resistant to earthquake loads.

Earthquakes are catastrophic and widespread natural disasters, causing damage and causing casualties [4]. In addition, earthquakes can also trigger other natural disasters, such as tsunamis and liquefaction, which have a very large loss impact [5]. Therefore, every building must be designed so that it can withstand earthquakes that can cause a collapse as a form of anticipation [6].

Anticipation of countermeasures or prevention of victims from disasters makes earthquake test equipment a necessary and effective tool. This tool is indispensable for earthquake-prone areas and areas where earthquakes rarely occur.

Earthquake simulator tool is an experimental method that has an important role in conducting experimental earthquake simulations as well as for evaluating structural performance in earthquake engineering. Earthquake simulator systems provide an effective way of subjecting structural components, substructures, or the entire structural system to dynamic excitation, which is like earthquake induction. In general, an earthquake simulator system consists of mechanical, hydraulic, and electronic components (controllers and sensors) [7].

The earthquake simulator system is given parameters to represent the actual earthquake. The earthquake wave vibration parameters recorded by the seismograph are velocity (cm/s), deviation in units (µm), and deviation (gal or cm/s$^2$). One of the important things in seismological research is knowing the damage caused by earthquakes, where the source of damage is expressed in-ground acceleration so that Peak Ground Acceleration (PGA) due

*Corresponding author. Tel.: +62-822-8338-6540
*Balla Somba Opu Residence*
*Makassar, Indonesia, 92113*

to earthquake vibrations is important to describe the level of risk [8].

Parameter testing is generally modeled in two categories, namely testing under earth acceleration (test with a vibrating table) and testing under conditions above earth acceleration (centrifuge test). In testing the shaking table can be conditioned to different amplitude conditions, one direction or many directions and it is easy to make experimental observations. The shaking table tool works by using the power that comes from the driving motor, which is then converted into a horizontal movement [9].

The shaking table earthquake simulator has an important role in earthquake engineering. This is because the shaking table is the only experimental device that can mimic the nature of an earthquake. The principle is a test plate/table which is driven by an actuator to produce ground acceleration replication [10]. With the earthquake simulator capabilities, it can be used to analyze the influence of earthquake strength on buildings and help develop about the influence of earthquake strength.

Based on these problems, the purpose of this research is to design and build a simulator that can represent earthquakes.

## 2. Research Method

### 2.1. Earthquake simulator (shaking table)

An earthquake simulator is a tool used to replicate or create an acceleration that resembles an earthquake. The acceleration is generated from the actuator which is driven by a controller that gives a command to the valve to reach a certain position so that the platform will follow the target movement that has been determined [11]. Figure 1 is an example of an earthquake simulator.

Figure 1 shows an earthquake simulator that resembles a table commonly called a shaking table. Earthquake simulators are grouped according to their actuator power, frequency range, and the maximum load they can handle. However, it is usually classified within small scale with a load of 0 to 1000 kg, medium scale ranges from 1000 to 5000 kg, and large-scale ranges more than 5000 kg [12].

Earthquake simulator testing is carried out by placing the test object on a table-mounted with binders or compacted artificial soil. The test object will undergo a shaking process at a certain frequency value and time limit.

In this research, an earthquake simulator tool in the form of a shaking table was built using st-37 material. However, in this study, the use of material types and the calculation of material loading were not considered.
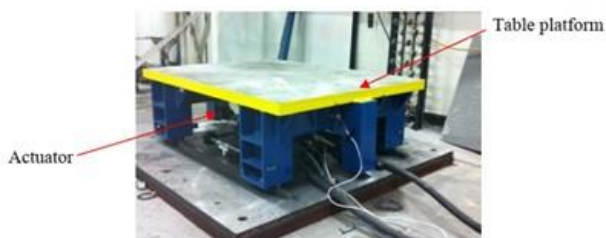


Figure 1. Earthquake simulator



Figure 2. Arduino Mega2560 [13]

### 2.2. Microcontroller

The Microcontroller is a device that functions as an input and output controller on an earthquake simulator. The microcontroller has pins for external connection of input and output, power, time, and control signals. The pins for input and output are grouped in units called input/output ports [14].

In this study, Arduino Mega2560 was used to control the movement of the hydraulic actuator by adjusting the valve opening and closing [15]. Arduino mega2560 is shown in Fig. 2. In this figure, a total of 54 digital pins and 16 analog pins, the Arduino mega2560 is a versatile, inexpensive, and easy to use option. In addition to being open-source, Arduino also has other advantages compared to other microcontroller boards, namely Arduino has its own programming language in the form of C language. Besides that, the Arduino board already has a USB loader, making it easier for us when programming the Arduino microcontroller.

### 2.3. Actuator

An actuator is an element of a mechatronic system that receives a command from a control (in the form of a power supply) and produces changes in the physical system by generating force, motion, flow, etc. [16]. Figure 3 shows a typical actuator unit.

In this research, an actuator or hydraulic drive is used. The hydraulic system functions as a power transfer system or as a control system. Hydraulic actuators are widely applied to large power requirements. So in this study, a hydraulic actuator was used. In Nakata's study, hydraulics were used as actuators for earthquake simulators [17].

### 2.4. Accelerometer

An accelerometer is an instrument used to measure acceleration, detect, and measure vibration, or measure acceleration due to Earth's gravity. This study used the ADXL345 accelerometer. The ADXL345 is a three-axis accelerometer with high-resolution specifications (13 bits), and measurements up to ±16g. This tool will take the acceleration data and then forward it to the microcontroller (Arduino mega2560). The form of the ADXL345 sensor can be seen in Fig. 4.
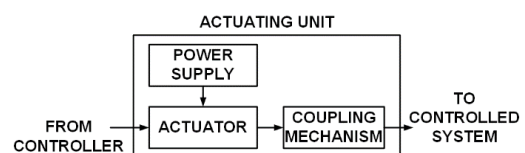


Figure 3. Actuating unit
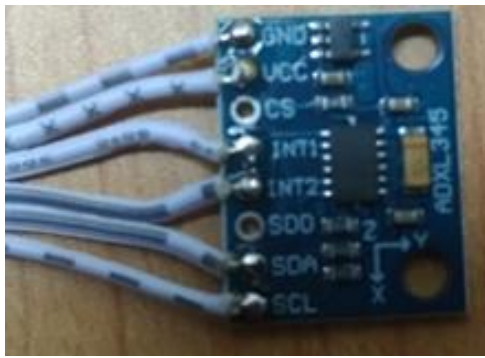
Figure 4. ADXL345

In addition, the adxl345 accelerometer sensor can also be used to measure the frequency of a system [18].

### 2.5. LabVIEW

LabVIEW is software that is used to process and visualize data, control and instrumentation, and automation. LabVIEW stands for Laboratory Virtual Instrument Engineering Workbench [19]. LabVIEW can perform real-time data acquisition and display the results in graphical form [20].

This study uses LabVIEW to control the output, acquire input from the sensor, and regulate the work of the system to the Arduino Mega2560.

### 2.6. Stages of research

The preliminary study includes a literature study that is collecting information, theory, and literature that can assist in the process of making the system. The literature sought is related to earthquake information, the working system of earthquake simulators, testing methods for simulators, measuring instruments, controllers, and propulsion devices.

The design stage includes the design of hardware and software. The hardware design includes the manufacture of mechanical shaking tables and electronic circuits. While the software is making the system work and making an earthquake simulator control program.

The testing phase includes giving the program to the tool that has been made to see the response of the system in the form of step units, sinusoidal waves, and can generate acceleration data. The results of the design of the tool, it is expected to be able to provide solutions to problems and meet or adjust the needs of the users of the tool [21].

Figure 5 is the shaking table simulator design and a block diagram of the working system of the tool.
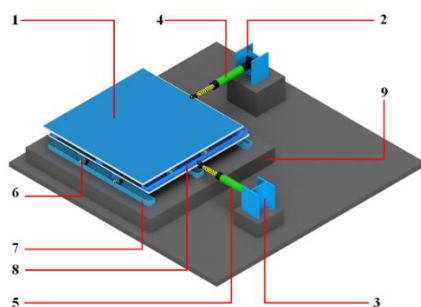


Figure 5. Design of earthquake simulator
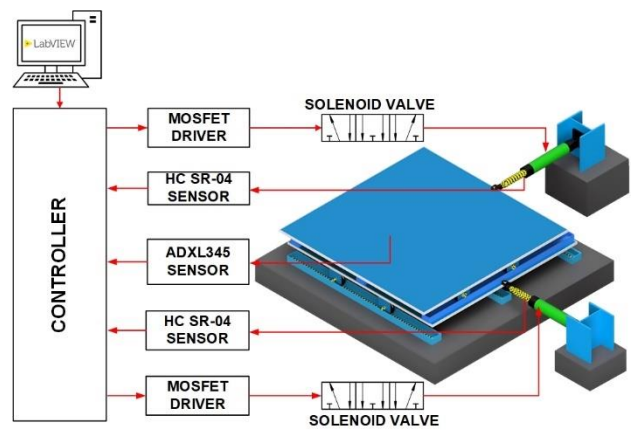


Figure 6. Earthquake simulator block diagram

Figure 5 shows the parts consisting of:
- Testing table (1)
- Y axis cylinder holder (2)
- X axis cylinder holder (3)
- Y-axis cylinder (4)
- X-axis cylinder (5)
- Wheel (6)
- X-axis rail (7)
- Y-axis rail (8)
- Support (9)

Earthquake simulator design was made using Autodesk Inventor software with dimensions of 1.25 m × 1.25 m. The block diagram of the earthquake simulator is shown in Fig. 6.

The test includes the work system of the tool on the simulation software and the hardware system that has been made.

### 2.7. Operation of shaking table

As it is known, the shaking table system is used to produce seismic motion that is like ground motion (in this case acceleration) so that the examiner can place the product on the test table to evaluate the product and improve response and ability to withstand the seismic motion [22].

In Fig. 7, to produce ground acceleration (seismic motion), the testing table must be driven by an actuator. This testing table is mounted on a platform (support) with rails and wheels, thus producing a linear motion. The input signal generated by the microcontroller is then entered into the actuator so that the linear motion of the testing table is as desired.
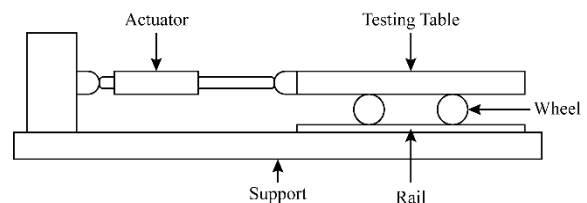


Figure 7. Schematic of an earthquake simulator

136
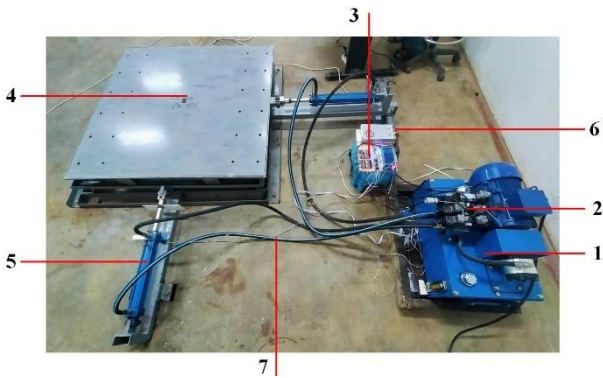
Figure 8. Results of making earthquake simulator

## 3. Results and Discussion

### 3.1. Earthquake Simulator

Figure 8 shows the results of making an earthquake simulator in the form of a shaking table.

Figure 8 is an earthquake simulator that was made consisting of 7 parts, namely:

- Hydraulic Power Pack (1) using a 3 Phase AC motor as the hydraulic power supply.
- Solenoid valve 4/3-way (2) used for regulating the opening and closing of fluid flow in the drive system.
- The controller (3) as a means of controlling input and output on the simulator, is regulating the valve opening and closing on the drive system, reading sensor results, and sending data to be displayed on LabVIEW.
- Test table (4) is used to place the test object. This test table will move according to the frequency and amplitude given to the driving tools.
- Hydraulic cylinder (5) is used to drive the test table.
- Power supply (6) used as a source of electrical energy for earthquake simulators.
- hydraulic hose (7) is used to deliver fluid to the system

In addition, the simulator is also equipped with a cylinder movement distance reading system. Cylinder movement distance readings using the PING HC SR-04 sensor. The distance reading data will be processed on the Arduino Mega2560 microcontroller.

Figure 9 shows the form of the HC SR-04 ping sensor.



Figure 9. HC SR-04 Ping Sensor
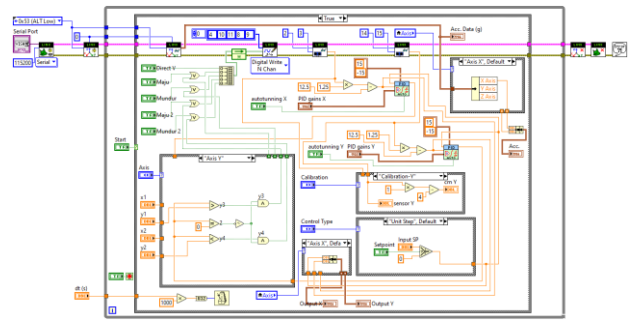


Figure 10. LabVIEW block diagram program display
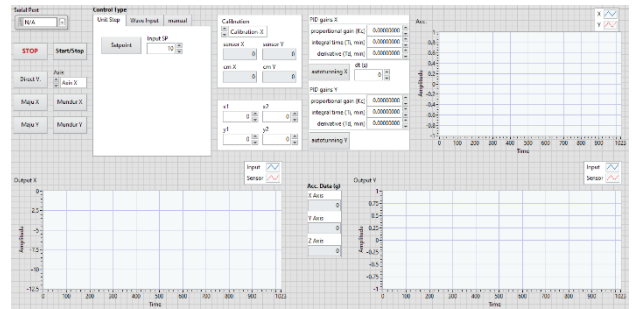


Figure 11. LabVIEW front panel program display results

### 3.2. Cylinder position control programming

The simulator program is made using LabVIEW. LabVIEW consists of two parts, namely the front panel and block diagram. The front panel functions as a user interface while the block diagram functions to build programs using the GUI (Graphical User Interface) programming language. Figure 10 shows the program built in the form of a block diagram. The program built produces a display on the front panel of Fig. 11.

### 3.3. Program implementation

The implementation of the program is by connecting the LabVIEW software which contains programs built with hardware (earthquake simulator) that have been made. In building a system, especially a system that has feedback characteristics, it becomes very prone to imprecision. In the instrumentation and control system, there is a control system that can overcome this, namely PID (Proportional-Integral-Derivative controller). In the simulator system made PID is used to control the valve. In this study, the first step was carried out using only one parameter, namely the proportional parameter (P) to determine whether the system built was ideal and stable or still required parameters I and D.

### 3.3.1. Programming using Proportional (P) controller

The system program using P control begins by giving the gain value. The gain value given is getting bigger until the system reaches a stable condition. Then given a step unit to see the response of the step by giving a gain value = 0.029332.

Figure 12 displays the results of the unit step test performed.
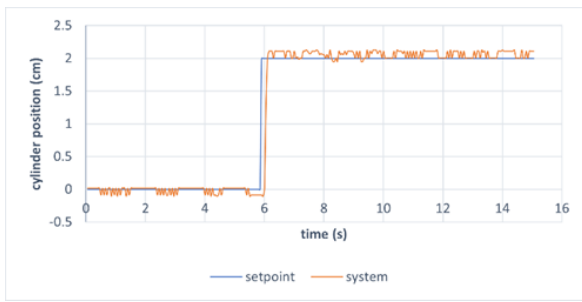
Figure 12. Proportional (P) control test results with a unit step of 2
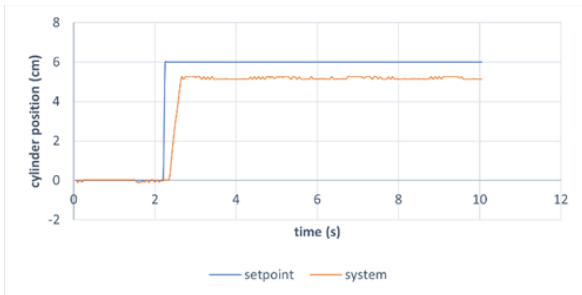


Figure 13. Proportional (P) control test results with a unit step of 6

From the results of the step variation test, when the cylinder position is set to a 2 cm stroke position, the cylinder can reach the setpoint without experiencing overshoot with a settling time of about 0.5 seconds and does not experience a steady-state error as shown in Figure 10. However, when given a setpoint with 6 cm, the hydraulic cylinder moves forward but does not reach the setpoint as shown in Fig. 13. in this case the control system using only proportional parameters (P) does not meet the desired design criteria.

### 3.3.2. Programming using Proportional (P) and Integral (I) controllers

The implementation of programming with PI (proportional-Integral) control begins with increasing the gain value of P (kc) the same as setting the P value (kc), then increasing the value of I (integral time = ki) slowly until the system has reached the setpoint. The value of P (kc) = 0.066195 and the value of I (ki) = 2.009974. The PI value is given a unit step to see the response of each step. Figures 14 and 15 show the results of the step test with PI control.
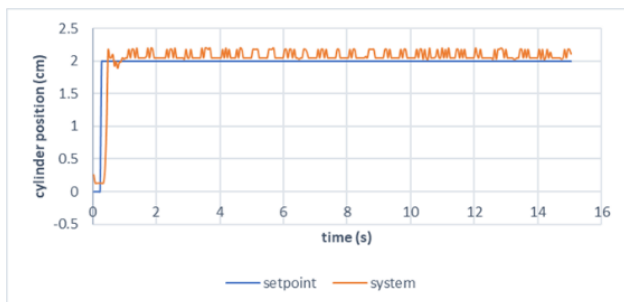


Figure 14. PI control test results with a unit step of 2 cm
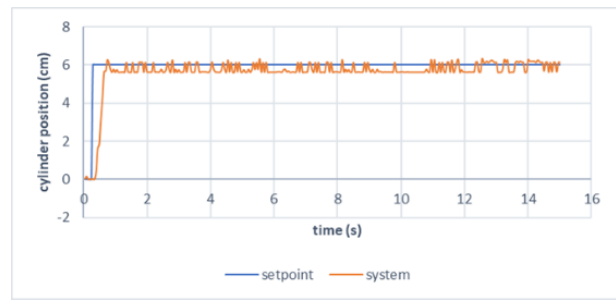


Figure 15. PI control test results with a unit step of 6 cm
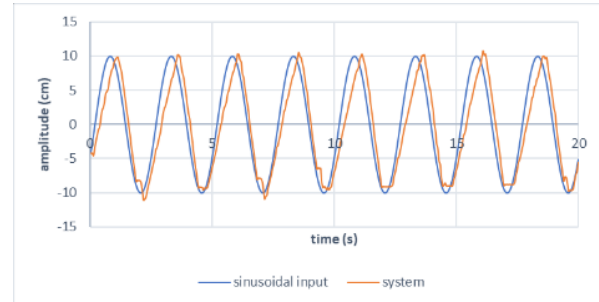


Figure 16. PI control test results with a sinusoidal input

The results above show that when the hydraulic cylinder position is set to reach a stroke position of 2 cm, the hydraulic cylinder can reach the setpoint (2 cm) without experiencing overshoot with a settling time of 0.5 seconds and does not experience a steady-state error (Figure 14). When the position of the hydraulic cylinder is given a unit step variation of 6 cm, the hydraulic cylinder moves forward and successfully reaches the setpoint (Figure 15). In this case, the control system using PI has met the desired system design criteria. This shows that the values of kc and ki used are appropriate and can be used in an earthquake simulator system.

PI parameter data that has been obtained, then tested using a sinusoidal wave to see the response of the system. The input given is a sinusoidal wave with a frequency of 20 mHz and an amplitude of 10.

Based on the Fig. 16, the system is given a sinusoidal wave input with a frequency of 20 mHz and an amplitude of 10 that can follow stably. The cylinder moves forward 10 cm, then back 10 cm according to the given amplitude value.

### 3.3.3. Earthquake simulator acceleration sensor data

Based on the results of earthquake simulator programming using PI control which produces ideal and stable performance, acceleration data is obtained. Acceleration data is generated by giving input values to the LabVIEW front panel in the form of frequency and amplitude data. The following are the results of the experiment by giving frequency and amplitude values which produce acceleration data that is displayed on the LabVIEW front panel in graphic form.

(a)    Frequency and amplitude value input



(b)    Acceleration sensor output
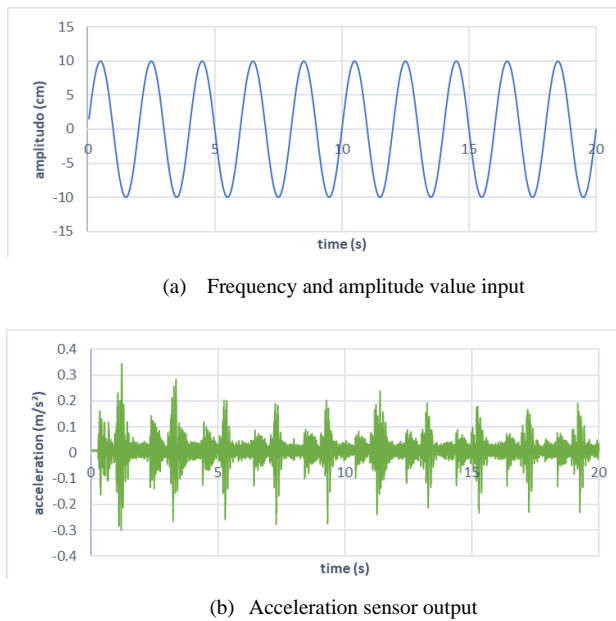
Figure 17. Experimental results the frequency value of 25 mHz and the amplitude of 10 to the acceleration

The experiment above shows that when providing input in the form of a sinusoidal wave with a frequency of 25 mHz and an amplitude of 10 (Fig. 17a), the cylinder can move forward and backward with 10 cm according to the input of the given amplitude. The results of these inputs can be seen in Fig. 17b that the maximum acceleration generated is 0.31 m/s$^2$. Acceleration data is displayed in real-time on the LabVIEW front panel.

## 4.    Conclusion

Earthquake simulator tool built using Arduino Mega2560 microcontroller with PI control, namely P(kc) = 0.066195 and I(ki) = 2.009974. The system response from the given unit step is a settling time of 0.5 s, there is no overshoot, and there is no steady-state error. So that the system complies with the criteria. The earthquake simulator can generate real-time acceleration data that is displayed in the LabVIEW front panel in graphical form.

## References

[1]    K. Kaur, "Earthquake : Its Causes, Types & Measurement," *Int. J. Sci. Res.*, vol. 4, no. 7, pp. 260–261, 2015.

[2]    J. O. Oluwafemi, O. M. Ofuyatan, O. M. Sadiq, S. O. Oyebisi, J. S. Abolarin, and K. O. Babaremu, "Review of World Earthquakes," *Int. J. Civ. Eng. Technol.*, vol. 9, no. 9, pp. 440–464, 2018.

[3]    U. Setiyono *et al.*, *Catalog of Significant and Destructive Earthquakes 1821-2018.* Jakarta: Pusat Gempabumi dan Tsunami Kedeputian Bidang Geofisika Badan Meteorologi Klimatologi dan Geofisika, 2019. [in Bahasa]

[4]    W. Guo, Y. Hu, Y. Li, Z. Zhai, and P. Shao, "Seismic Performance Evaluation of Typical Dampers Designed by Chinese Code Subjected to the Main Shock-Aftershocks," *Soil Dyn. Earthq. Eng.*, vol. 126, no. August 2018, p. 105829, Nov. 2019.

[5]    M. Anda, S. Purwanto, E. Suryani, Husnain, and Muchtar, "Pristine Soil Property and Mineralogy as The Strategic Rehabilitation Basis in Post-Earthquake-Induced Liquefaction, Tsunami and Landslide in Palu, Indonesia," *CATENA*, vol. 203, p. 105345, Aug. 2021.

[6]    Y. Zhou, H. Shao, Y. Cao, and E. M. Lui, "Application of Buckling-Restrained Braces to Earthquake-resistant Design of Buildings: A review," *Eng. Struct.*, vol. 246, no. April 2020, p. 112991, Nov. 2021.

[7]    J. E. Luco, O. Ozcelik, and J. P. Conte, "Acceleration Tracking Performance of the UCSD-NEES Shake Table," *J. Struct. Eng.*, vol. 136, no. 5, pp. 481–490, 2010.

[8]    Sunarjo, M. T. Gunawan, and S. Pribadi, *Earth Quake*, Populer. Jakarta: Badan Meteorologi Klimatologi dan Geofisika, 2012. [in Bahasa]

[9]    M. Giatman, R. Rahmad, and N. Zuwida, "Development of the Shaking Table as an Interactive Learning Media in Earthquake Engineering Lectures (Case Study in the Department of Civil Engineering, Faculty of Engineering, University of Graha Nusantara)," in *Konvensi Nasional Pendidikan Indonesia (KONASPI) VIII*, 2016, pp. 572–579. [in Bahasa]

[10]    R. T. Severn, "The Development of Shaking Tables–A Historical Note," *Earthq. Eng. Struct. Dyn.*, vol. 40, pp. 195–213, 2011.

[11]    G. Maddoni, K. P. Ryu, and A. M. Reinhorn, "Simulation of Floor Response Spectra in Shake Table Experiments," *Earthq. Eng. Struct. Dyn.*, vol. 40, pp. 591–604, 2010.

[12]    K. Bin Ngadimon, "Design and Simulation of Hydraulic Shaking Table," University of Technology Malaysia, 2006.

[13]    "Arduino-Home." .

[14]    W. Bolton, *Mechatronics, Electronic Control Systems in Mechanical and Electrical Engineering*, Sixth. United Kingdom: Pearson Education Limited, 2015.

[15]    E. Damci and Sekerci, "Development of a Low-Cost Single-Axis Shake Table Based on Arduino," *Exp. Tech.*, vol. 43, no. 2, pp. 179–198, 2018.

[16]    R. H. Bishop, *The Mechatronics Handbook*. New York: CRC Press, 2002.

[17]    N. Nakata, "Acceleration Trajectory Tracking Control for Earthquake Simulators," *Eng. Struct.*, vol. 32, no. 8, pp. 2229–2236, 2010.

[18]    M. S. D. P. Rahman, S. Zahara, and M. Nurjanah, "Design and Build of Shaking Table Prototype as Short-period Seismometer Calibrator Based on Microcontroller," *J. Phys. Conf. Ser.*, vol. 1434, no. 1, 2020.

[19]    D. Artanto, *Interaksi Arduino dan LabVIEW*. Jakarta: PT. Elex Media Komputindo, 2012.

[20]    N. R. Wibowo, "Design and Build of a DC Motor Speed Control System as a Control System Practicum Learning Media using Labview," *JST (Jurnal Sains Terapan)*, vol. 6, no. 2, 2020. [in Bahasa]

[21]    H. M. Haines and J. R. Wilson, *Development of a Framework for Participatory Ergonomic*. Nottingham: HSE Books, 1998.

[22]    A. B. K. Teh and C. Venkatratnam, "Design and Development of a Seismic Shaking Table for Evaluation and Analysis of The Performance of Elastomeric Bearing," *2015 IEEE Student Conf. Res. Dev.*, pp. 111–116, Dec. 2015.

# The Effectiveness of Utilizing Non-Green Public Space in Untia Fishermen Settlement

Andi Edy Satar[a],*, Idawarni Asmal[b], Edward Syarif[c]

[a]Housing and Settlement Environment Design Laboratory, Department of Architecture, Faculty of Engineering, Hasanuddin University.
Email: andiedyas@gmail.com
[b]Housing and Settlement Environment Design Laboratory, Department of Architecture, Faculty of Engineering, Hasanuddin University.
Email: idawarniasmal@yahoo.com
[c]Housing and Settlement Environment Design Laboratory, Department of Architecture, Faculty of Engineering, Hasanuddin University.
Email: edosyarif@yahoo.com

**Abstract**

Public space in a settlement will be effective and useful if it has three intrinsic values, namely democratic, meaningful and responsive. Then the existence of people and how they play a role in space is important in reviewing the public nature of a space. The effectiveness of a public space can be assessed from the level of utilization by the community on the types of activities and social interactions of the people in it. Currently, the use of Non-Green Public Space is still not in line with expectations, namely the realization of a comfortable, productive and sustainable space, marked by the lack of community social activities in the Untia Fisherman Settlement Non-Green Public Space (NGPS). The purpose of this study was to evaluate the effectiveness of the use of Non-Green Public Space in the Untia Fisherman Settlement in the form of Delta Playground and Plaza Park. The research method used in this study was descriptive qualitative research because it describes the research location at the time of observation and compares standards and or theories with the facts of the availability of Non-Green Public Space (NGPS) in the settlements using the Good Public Space Index (GPSI) analysis tool. The results show that the existence of the Delta Playground RTNH is still not effectively utilized. Accesibility factors into the RTNH, comfort factors and diversity of activities (comfortable, relaxation, passive and active engagement and discovery), as well as the availability of other supporting facilities and infrastructure are still lacking, both in quantity and quality. Re-effectiveness of the function and nature of the existence of the Non-Green Public Space in the Untia fisherman settlement requires cooperation from various parties.

*Keywords: Effectiveness; Non-Green Public Space; settlement; utilization*

## 1. Introduction

Public space is an important space to meet people's needs for comfort, relaxation, and to carry out active or passive activities outside of the daily activities that people usually do [1]. Meanwhile, environmental parks as part of public spaces that are built and developed in a housing or settlement environment by the developer or local government are actually intended to be used for the general public and are regulated as a shared space for the community. This shared space can be a playground or sports facilities [1]. Sherer [2] shows that environmental parks are public spaces, where people are active in activities, such as sports, chatting and other physical activities, provide space for residents to relax and interact, and will create a sense of community in a residential environment.

The government has determined the rules contained in SNI 03-1733-2004 concerning with Procedures for Planning the Housing Environment in Urban Areas related to the provision of public space in housing to support the social needs of the residents of the housing. However, problems often arise in the process of providing public space because of the gap between the characteristics of the existing space and its use by local residents. Public space planning also seems not to pay attention to the needs and comfort of its users so that public spaces often become neglected. In Law number 26 of 2007, concerning spatial planning, has also mandated the government to provide Green Public Space (RTH) and Non-Green Public Space (RTNH) both macro in urban areas and micro in every residential area, both existing and planned settlements.

An effective and useful public space in a settlement if it has three intrinsic values, namely democratic, meaningful and responsive ([1] in [3]), which can be interpreted on the quality of the attributes of a successful public space, namely comfort and image, access and connectedness, utilization and social activities [3]. The existence of people and how people play a role in space are important things in reviewing the public nature of a space [4].

---

*Corresponding author. Tel.: +6281140028585
*Jl. AP. Pettarani N0.30 Maros, South Sulawesi Indonesia*

Based on these circumstances, a research was conducted on the effectiveness of public space in the Untia fisherman's settlement. Untia Fisherman Settlement is one of the fishing settlements in Makassar City. This settlement was prepared by the Makassar City Government, which at that time was under the leadership of Mayor HA Malik B. Masry, SE., M. Si (1994-1999). The Untia fisherman's settlement, located in Untia Village, Biringkanaya District, Makassar City, is prepared to accommodate fishing communities who were relocated from Lae-Lae Island due to the Makassar City Government's policy to make Lae-Lae Island a tourist area.

As a relocation settlement, the Untia fisherman's settlement has been equipped with more adequate environmental facilities and infrastructure than their place of origin. One of the settlement facilities and infrastructure referred to is the availability of public space. The Untia fisherman's Settlement has three public spaces that are intentionally designed as a place for the community to do daily activities, have recreation and interact. The public spaces are Non-Green Public Spaces in the form Plaza Park, Delta Playground and the other is Child Friendly Public Spaces (RTPRA).

## 2. Literature Review

### 2.1. Utilization effectiveness

Effectiveness is a concept that has a very important meaning, but in reality it is difficult to define with certainty. The reason is that many concepts are related in terms of effectiveness. In general, what is meant by "effectiveness" is a condition that shows the level of success or achievement of a goal as measured by quality, quantity and time as previously planned. Sondang [5] provides the following definition: "Effectiveness is the use of resources, facilities and infrastructure in a certain amount that is consciously determined beforehand to produce a number of goods for the services of the activities it carries out".

Another theory according to Komaruddin [6] in Soetrisno [7] states that effectiveness is a condition that indicates the level of success or failure of activities in achieving the goals that have been set.

### 2.2. Space

Webster [8], explains that space is a 3 (three) dimensional area where objects and events are located. Space has a relative position and direction, especially if a part of the area is designed in such a way for a particular purpose. Space is part of the building in the form of a cavity, between two objects and the open nature that surrounds and surrounds us. Not visible physical and physical objects can only be felt by hearing, smelling and touching.

From the description of the theory about space described above, it can be summarized in one conclusion, namely space is a 3 (three) dimensional area which is a limited or unlimited unit that surrounds us which can be felt by hearing, smelling and touching.

### 2.3. Public space

Webster [8], is a place or area that can accommodate certain human activities, either individually or in groups. Examples of public spaces include roads, parks, pedestrians, plazas, cemeteries, sports fields. Public space is part of the space that has a definition as a container that can accommodate certain activities of the community in an environment that does not have a physical cover [9].

Dewang [10] in Burhanuddin [11] stated that the word "open" in the terminology of public space can be translated into several meanings, namely: free to be entered or used, not closed, not restricted, not prohibited, accessible, not bound, receptionist, and others. Thus, public spaces are parts of the environment that are open to or can be used for spontaneous activities and are freely chosen by the community.

### 2.4. Non-Green Public Space (NGPS)

Types of Green Public Space (GPS) and Non-Green Public Space (NGPS) are part of the public space. Non-Green Public Space is a space that is not physically in the form of a building and is not dominantly overgrown with plants or porous surfaces, can be in the form of pavement, water bodies or other certain conditions (e.g. bodies of mud, sand, desert, rock, and lime) (Minister of Public Works Regulation) [12]. By definition, Non-Green Public Space can be divided into paved public spaces, blue public spaces (bodies of water) and public spaces under certain conditions.

### 2.5. Effectiveness of Non-Green Public Space

The Non-Green Public Space is considered effective if the city community uses it and gets satisfaction after activities in the city park. The management of the city park is said to be successful if the visitors feel satisfied which is indicated by the increasing number of visitors and the frequency of visitors [13] in [14].

### 2.6. Aspects of influence on the effectiveness of Non-Green Public Space

The existence of people (people) and how people (people) play a role in space are important things in reviewing the public nature of a space [4]. Then access and diversity of activities are the main keywords. This is supported by Gehl [15] where the existence of activities in outdoor spaces can be an indicator of the quality of urban public spaces. Logically, it is quite clear, with the assumption that human activities are carried out with random purposes, people tend to prefer activities in outdoor spaces with good quality. Where this quality can be interpreted according to the attributes of a successful public space [3], namely comfort and image, access and connectedness, utilization and social activities.

Carr, et al. [1] in Carmona, et al. [3] argued that public space in a settlement will be effective and useful if it has three intrinsic values, namely democratic, meaningful and responsive. Furthermore, Carmona, et al. [3] and Parkinson [16] described the intrinsic value:

- Democratic, is the availability of good accessibility. With good accessibility, it will encourage the use of public space by various users. This diversity of users can be measured by the diversity of gender, age and several other characteristics.
- Responsive, as a responsive space, public space must be able to provide comfort and flexibility for various uses and activities. In addition to the presence of various activities Shaftoe [17] in Parlindungan [4] user intensity can be used as a benchmark for responsive public spaces.
- Meaning, in the end the existence of social interaction through the formation of space user groups, the intensive use of space and the existence of various activities can explain how public space is meaningful for the community. It can be further explained that the public space provides an attachment for the community which is marked by a sense of concern for the space [1].

From the theoretical description above, we can conclude that the presence of users and user behavior can determine the effectiveness of the utilization of a Non-Green Public Space. This is in line with what is stated by Parlindungan [4] that the presence of users and the behavior of outdoor users can be developed as an approach in the study of public space, especially to assess the response of space users to the quality of public space, especially non-green Public Space.

### 2.7. Factors affecting utilization of Non-Green Public Space

Requirements for the public space [14]:

a. Meet the comfort criteria
   - Protection against sun and weather
   - There is street furniture (seats, street lamps, signposts and information boards)
   - Road conditions
   - Natural lighting
b. Utilization of natural elements
   - Vegetation aspects: vegetation is a fairly important element in a public space, because vegetation has many functions such as forming space, aesthetics and regulating environmental temperature.
   - Water aspect: in this case the water aspect that is intended can be various such as ponds/gardens, rivers.
c. Aspect view
   The aspect of scenery is no less important in planning a public space because it involves psychological comfort for its users for the community as actors. The beautiful and attractive scenery will make the users of the public space feel relaxed and comfortable in the space.
d. Access Achievement (accessibility)
   The factor of access/achievement to the location is also an important thing. An ideal public space is actually easy to reach from anywhere. However, this is also greatly supported by the quality of the road to that location.

e. Various activities/types of activities
   To be able to know that public space in one area meets public demands or not, it can be seen from the types of activities that are there. Although the needs of the community in each area are different, there are some general requirements for an ideal public space.

### 2.8. Non-Green Public Space elements design

According to Rubenstein in [14], the supporting design elements that must be contained in public spaces, especially in this case are Non-Green Public Spaces, include:

a. Pedestrian lights: 4-6 meters high, 10-15 meters placement distance and accommodates a hanger.
b. Street lighting: even lighting, and choosing the type of lamp based on effectiveness.
c. Bus Stop: protected from weather changes, for example, heat and rain, placed on the edge of the main road with heavy traffic, and the minimum length of the bus stop is the same as the length of city buses so that passengers can get on from the front or back doors
d. Direction board: signs are attached to lighting, located in the open, contain information about the location and facilities, not covered by trees, the use of markings must reflect the character of the area, distance and size must be adequate and arranged to ensure visibility, use and presence must be harmonious to architectural buildings, the restriction of large markings that dominate the cityscape.
e. Public phone: characterize as communication facilities, provide convenience for users, are easily visible and protected from the weather, are placed on the edge or middle of pedestrian paths, and each payphone has a width of approximately 1 meter.
f. Trans cans: trash cans are placed at a certain distance, for example every 15-20 meters, easy to transport, and different types of trash cans for dry and wet waste.
g. Vegetation: serves as shade, placed on plant paths (minimum 1.5 meters), branches two meters above the ground, branches do not bend, planted in rows, not only contain aesthetic value, but also as climate control, plants are non-toxic, non-toxic. thorny, the branches are not easily broken, the height of the garden varies, the green color with other color variations is balanced, the types of annual or seasonal plants, the speed of growth is moderate, able to absorb air pollution, and the spacing of the plants is half tight so as to produce optimal shade
h. Air clean/ Bathroom: clean water/bathroom is needed in public spaces.

### 3. Methodology

This research is an evaluative, is a process of evaluating the effectiveness of the results of the design work after the building is completed [18]. This study aims to evaluate the effectiveness of the utilization of the Non-Green Public Space at the Delta Playground in the Untia fisherman's settlement.

This study uses a mixtode approach. Analysis of research data is explained using qualitative descriptive. A qualitative approach is used to observe the social activities and characteristics of Delta Playground users through observation. A qualitative approach is used to interpret the findings from observations.

### 3.1. Method of collecting data

Data collection in the study was carried out by observation. Observations were made on social activities and the characteristics of users of public spaces using the Good Public Space Index (GPSI) form with six variables, namely: Intensity of Use (IU), Intensity of social use in groups (Intensity of Social Use - ISU), Duration of visit (People's Duration). of Stay - PDS), Diversity of activities at one time (Temporal Diversity of Use - TDU), Diversity of use (Variety of Use - VU), Diversity of users (Variety of User - VUr).

### 3.2. Data analysis method

Analysis of the use of public space in the Untia fisherman settlement was carried out using the parameters of the Good Public Space Index (GPSI) [4]. The result of this analysis is an index with numbers 0 – 1 which is directly proportional to the observed variables. From the several levels of the index for the purpose of being more informative, each aspect is categorized into 0 – 0.20 (very low), 0.21 – 0.40 (low), 0.41 – 0.60 (medium), 0.61 – 0.80 (high), 0.81 – 1 (very high). The interpretation of the data is then explained using a qualitative descriptive method, namely accumulating data and explaining phenomena that occur without explaining the relationship between variables, testing hypotheses, making estimates or making meaning implications.

## 4. Overview of Untia Fisherman's Settlement

### 4.1. Geographical situation and population

The Untia fisherman's settlement is located in the Untia village, Biringkanayya sub-district, Makassar City. The Untia Fisherman's Settlement is located on the west coast of Makassar City (Fig. 1).

Administratively, the Untia fisherman's settlement consists of three RWs, namely RW 1,2 and RW 5 and has an area of about 198,863 m² or about 20 ha (Fig. 2).
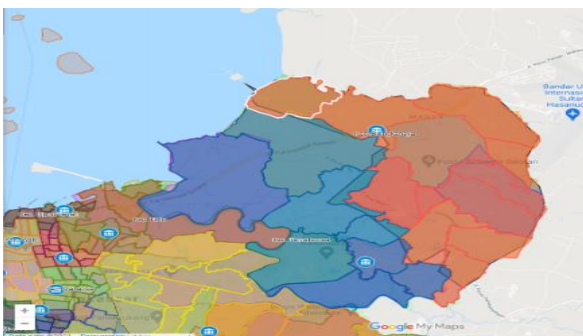


Figure 1. Map of Makassar City which shows the location of the Untia village which is in the Biringkanaya sub-district (Orange color). (Source www.makassar.go.id)
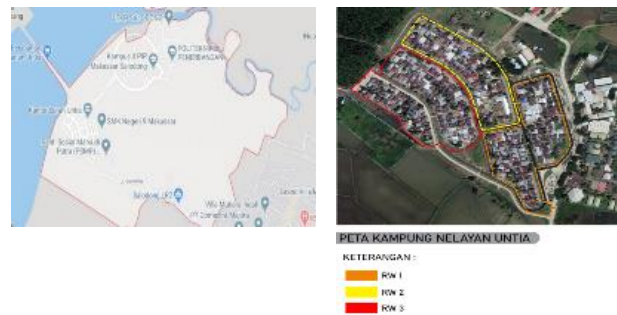


Figure 2. Untia village map (left) and Untia fisherman settlement master plan (Source www.makassar.tribunnews.com/)

Table 1. Population of Untia Fisherman's Settlement

| No | Border area | Population (person) M | F | No of family | No of houses | Area Width (m²) |
|----|-------------|-------|-----|--------------|--------------|------------------|
| 1 | RW 01/ RT 01, 02, 03 | 312 | 282 | 140 | 102 | 23716 |
| 2 | RW 02/ RT 01, 02 | 184 | 171 | 97 | 67 | 19875 |
| 3 | RW 05/ RT 01, 02, 03, 04 | 370 | 306 | 170 | 130 | 27378 |
| | Total | 1625 | | 407 | 299 | 70969 |

The Untia Village community does not only consist of one tribe, but consists of various tribes including the Makassar tribe and the Bugis tribe. Many of these ethnic differences occur because of the urbanization of residents from villages to cities, especially South Sulawesi, namely Untia Village. According to the general data of the Untia Village PKK 2020, the population of the Untia fisherman settlement spread over three RWs that can be seen in Table 1.

### 4.2. Physical condition Non-Green Space of Delta Playground

The Delta Playground is on the inner side of the settlement. The park is in the form of a delta and is surrounded by canals with a width of about 4 m and a depth of about 1-2 m. This park is adjacent to the residential area of RW 03 residents on the north side and RW 01 on the east side with each separated by a canal. Meanwhile, on the south and west sides, they are bordered by residential neighborhood roads which are also separated by canals. With an area of about 1,941 m², and the population of the Untia fisherman's settlement is around 1,625 people. This park can serve the need for Public Space up to the environmental center or RW level (see Table 2).

The existing physical condition of the Delta Playground (see Fig. 3) and the condition of the supporting elements in the Delta Playground can be seen in Table 3.

Table 2. The scope of public space services

| No | Types of Facilities | Number of Supporting Populatiom (Person) | Needs of min. width area (m²) | Standard (m²/prs) | Targeting Radius (m) | Width of open space-OS (m²) | Width of green space-GS (m²) | Width of non-green space-NGS (m²) | Criteria of location & solution |
|---|---|---|---|---|---|---|---|---|---|
| 1 | Park/Playground (RT) | 250 | 250 | 1.0 | 100 | 250 | CGS x 250 | OS - GS | Centre of neighbour hood group |
| 2 | Park/Playground (RW) | 2500 | 1250 | 0.5 | 1.000 | 1250 | CGS x 1.250 | OS - GS | Centre of community activity |
| 3 | Park & Sport area (Subdistrict) | 30000 | 9000 | 0.3 | | 9000 | CGS x 9.000 | OS - GS | It is suggested that to cooperate with education facilities |
| 4 | Park & Sport area (District) | 120000 | 24000 | 0.2 | | 24000 | CGS x 24.000 | OS - GS | Located in the main road. It is suggested to cooperate with education facilities |
| 5 | Green zone | - | - | 15 m | | 9000 | - | - | Located spread |
| 6 | Grave yard/Public grave | 120000 | - | - | | - | - | - | Considering target radius and serviced area |

Table 3. Condition of the supporting elements of Delta Playground

| Facilities | Item | Available | Not Available | Condition | Information |
|---|---|---|---|---|---|
| Accesibilities | - Location of playground | ✓ | | Near settlement, in term of width it is activity for community | |
| | - There is an acces from city centre to Untia Fisherman Settlement | ✓ | | Good condition | |
| | - Acces to the playground | ✓ | | In sufficient of qualities and quantities only one direction acces not supporting for disabilitas | |
| | - Parking area | | ✓ | Temporary | |
| Comfort | - Trees and plants (vegetation) | ✓ | | In sufficient for shady and an astetic | |
| | - Street Furnitures: Seat, gasebo, direction board & spech, lighting | ✓ | | In sufficient quantities, no maintenance | |
| | - View/Natural | ✓ | | Interesting | |
| | - Water/Canal | ✓ | | Good if always maintained | |
| | - Toilet, clean water, recycle bin | | ✓ | Not available | |
| Safety | - Guardrails | | ✓ | Not available | |
| Aktivity | - Child spacecraft | ✓ | | No maintenance | |
| | - Sport area dan Jogging Track | | ✓ | Not available jogging track | |
| Management | Management (hygiene, safety, maintenance and program activity) | | ✓ | Not available | |

Figure 3. Location of NGPS Delta Playground in Untia Fisherman Settlement

## 5. Result and Interpretation

Observations on the use of Non-Green Public Space at research locations based on variables were then analyzed using the Good Public Space Index (GPSI) parameter and the results obtained in Table 4 and Fig. 4.

Based on the results of the GPSI index as shown in the Table 4, it is known that the quality of each public space is based on each variable analyzed. The discussion of the results of the quality index for each of these variables will be explained as follows:

Table 4. Results of the analysis of the effectiveness of the use of Delta Playground

| Public Space/Observable Variables | Variabel Index/Day | | | | | | | Index Average | Variable Category | Total Indx Scoe | GPSI Value | Category |
|---|---|---|---|---|---|---|---|---|---|---|---|---|
| | Mon | Tue | Rab | Wed | Thur | Sat | Sun | | | | | |
| Intensity of Use | - | - | 0.00 | - | - | 0.00 | - | 0.00 | Very Low | | | |
| Intensity of Social Use | - | - | 1.00 | - | - | 1.00 | - | 1.00 | Very High | | | |
| People's Duration of Stay | - | - | 0.54 | - | - | 0.69 | - | 0.62 | High | 3.55 | 0.59 | Standard |
| Temporal Diversity of Use | - | - | - | - | - | 0.53 | - | 0.27 | Low | | | |
| Variety of Use | - | - | 0.89 | - | - | 0.89 | - | 0.89 | Very High | | | |
| Variety of User | - | - | 0.64 | - | - | 0.90 | - | 0.77 | High | | | |
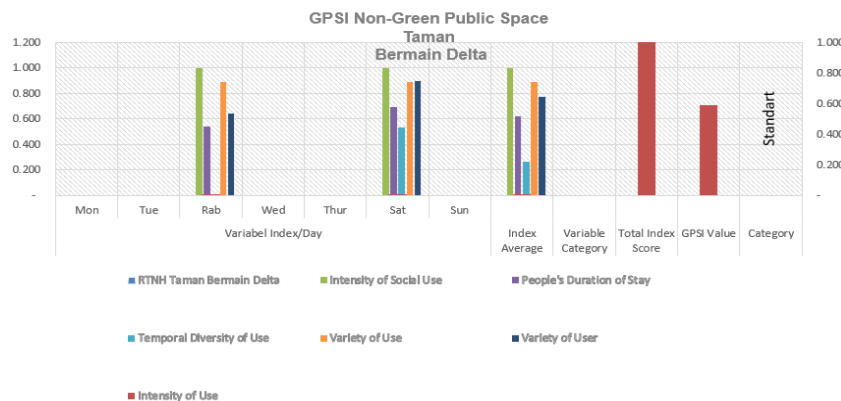


Figure 4. The effectiveness of the utilization of Non-Green Public Space Delta Playground

### 5.1. Intensity of Use (IU)

From the existing data, it can be seen that the intensity of use in the playground is only twice a week while at the Taman Plaza it is still better, namely four times a week. As shown in Table 4, the intensity of the use of these public spaces is still very low.

Carr et al. [1] in Carmona et al. [3] argued that a good public space must have three intrinsic values, namely democratic, meaningful and responsive. Carmona, et al. [3] and Parkinson [16] described that one important aspect in a democratic public sphere is the availability of good accessibility. With good accessibility, it will encourage the use of public space by users.

Existing data shows the condition of access to the playground as shown in Fig. 5, for example, there is only one pedestrian bridge located on the west side of the playground, while residential areas are located in the east and north. Between the playground and residential areas separated by a canal with a width of 2-3 m. So if

residents want to access the park, they have to go around it first. From the results of interviews with the community around the playground and plaza park,.

The problem of access to public spaces has indeed become a complaint of residents of the settlements. Just to accompany the child to play on the swing or slide, the child and his parents must first go around the canal and look for the nearest bridge to enter the playground.



Figure 5. Map of NGPS Delta Playground with access that can only be accessed from one direction (yellow box)

145

Figure 6. Activities that take place in the morning at NGPS Delta Playground and conditions during the day

Based on the results of field observations and the theoretical description presented above, this is one of the reasons why this playground in terms of the intensity of use (IU) is very low. So it is not surprising that access to the location is important. An ideal public space is actually easy to reach from anywhere [14].

### 5.2. Social Intensity of Use (ISU)

One of the functions of public space is as a forum for social activities. So that when the level of social activity that occurs is high, the quality of the public space is getting better [19] which can explain how public space is meaningful to society ([17] in [4]).

The achievement index for the intensity of social use (ISU) variable in both public spaces is in the very high category. This shows that public spaces in fishermen's settlements have been able to accommodate the social activities of their users well. Based on the observations made, there are several activities carried out in groups, such as fishing, children playing slides or gathering, parents bringing their children to play together, chatting or chatting together as shown in Fig. 6. Although in fact this group activity did not continuously take place during the observation period. Figure 7 shows the activities that occur on average users in groups.

### 5.3. People's Duration of Stay (PDS)

Time of visit and duration of visit in a public space can describe whether or not visitors are comfortable in that public space. When visitors feel comfortable to linger in public spaces, it can be said that visitors feel comfortable in that location. The user's duration of activity is shown in the variable of the duration of the visit (people's duration of stay-PDS). Based on the results of the analysis, the quality index of public spaces based on the duration of the visit was included in the high category at the Delta Playground with an average length of activity of more than one hour and very high in Taman Plaza with an average activity duration of less than one hour continuously for almost a week (long observation).



Figure 7. The activities of playground users are more in forming groups in interacting with each other



Figure 8. Natural elements found in Delta Playground as one that makes visitors feel at home for long, although on average it only takes place in the afternoon

The high value of the PDS index in these two public spaces is due to the time distribution of activities when observations are carried out only in the morning and evening, where the hot weather conditions are not scorching hot. Based on the results of observations in these two public spaces in the morning and evening it is quite comfortable, because of the influence of the view of sunrise (sunrise) and sunset (sunset). In addition, there is an element of water in the form of canals that surround and pass through both public spaces which can have a positive psychological impact (see Fig. 8).

### 5.4. Temporal Diversity of Use (TDU)

Good public spaces generally have more to do than less successful spaces [19]. Based on the variable diversity of activities at one time, the quality index of public space is low. Based on the existing conditions, the facilities for supporting activities, both active and passive, in the two open public spaces are still minimal. There are only play facilities for children, while the existing sports fields are in a dilapidated condition and overgrown with weeds as shown in Fig. 9.

### 5.5. Variety of Use (VU)

By looking at the results of field observations for the variety of use variables in two public spaces, the results obtained are in a very high category. This means that the Delta Playground with its current condition as a whole (for each day of observation) can accommodate a variety of users with various kinds of activities.

The activities carried out do not always depend on the facilities provided [19]. Even with the existing conditions where the two public spaces are minimal with playing facilities or passive and active activities, users are still allowed to carry out activities that are physical contact such as chatting, playing or exercising with friends and family and at the same time other users can perform activities that require a long duration of time, such as skateboarding, fishing, swimming or other transitional activities such as sitting, standing, playing, and watching.



Figure 9. The diversity of activities that occur at one time of observation

146

*5.6. Variety of User (VUr)*

With good accessibility, it will encourage the use of public space by various users. This diversity of users can be measured by the diversity of gender, age and several other characteristics. User characteristics also influence the assessment of the quality of public space. A public space that can accommodate various types of users (men, women, children, young adults and old adults) will show a good level of public space quality [19].

Based on the user diversity variable, the VUr index is included in the high category. The quality of a public space based on user characteristics can also be seen from the difference in the number of users based on gender. If the percentage of women in the use of public space is small, then something is wrong with the space, on the contrary if the percentage of women is more, it can be said that the public space is good. This is because women tend to be discriminatory in the selection of public spaces.

## 6. Conclusion and Suggestion

*6.1. Conclusion*

Based on the above discussion, conclusions can be drawn based on the research formulation, as follows:
a. The quality of the results of the analysis of the average value of the effectiveness index for the utilization of the Delta Playground at the Untia Fisherman's Settlement is rated "medium", that is, not too good and not too bad. This is because there are several variables whose assessments are in very low to very high category, so the GPSI value is in the medium category.
b. Based on the results of the GPSI assessment analysis and interviews with local communities and village officials, there are several factors that affect the GPSI value of this Non-Green Public Space including the moderate category, among others: (a) accessibility in terms of quality and quantity is inadequate. Facilities for disabled visitors are not available. (b) The vegetation factor as a comfort factor is one of the most influencing factors in people's reluctance to use this Non-Green Public Space, especially during hot weather. (c) Supporting elements are still lacking, such as toilets and trash cans that are not available in this public space. Similarly, lods of food/beverage sellers do not exist at all. (d) Public space management factors that do not yet exist so that the existence of many public facilities is neglected/unmaintained.

*6.2. Suggestion*

Recommendations that can be given in this study are the effectiveness of the reuse of functions and the essence of the existence of the Non-Green Public Space Delta Playground in the Untia Makassar Fishermen's Settlement for better cooperation from various parties. Not only from the disciplines of architecture and urban planner, but also from managers, government and society.

*6.2.1. Study Advice*

a. Advanced Studies
   There is a need for further studies on Non-Green Public Space that are both able to see the changes that occur and are able to adapt or be flexible by themselves. Many designs of public spaces fail because they do not have a vision of the changes that may occur.
b. Atraction and destination
   Activities Programmed programs and various attractions will revive the Non-Green Public Space Delta Playground, thus making it a destination for community members to have activities and socialize in the area.

*6.2.2. Operational Advice*

a. Good management
   No matter how good a design is, without being managed and programmed properly, the public space will not be able to survive and develop properly. An understanding of the character of the institutions, institutions and communities involved in determining how the Non-Green Public Space management process can run well.
b. Source of Income
   Basically, the Non-Green Public Space can be used as a source of funds for the city government by collaborating with companies to participate in the management and use of the city's public spaces in a proportion that benefits all parties, including residents who use the Non-Green Public Space Delta Playground.

## References

[1] S. Carr, M. Francis, L. G. Rivlin, and A. M. Stone, *Public Space*. New York: Cambridge University Press, 1992.
[2] P. M. Sherer, "The Benefits of Parks; Why America Needs More City Parks and Public Space," 2003. [Online]. Available: http://conservationtools.org/libararies/1/library_items/729/The-Benefits-of-Parks-Why-America-Needs-More-City-Parks-and-Open- Space. [Accessed: 30-May-2021].
[3] M. Carmona *et al.*, *Public Places Urban Spaces: The Dimensions of Urban Design*. Oxford: Architectural Press, 2003.
[4] J. Parlindungan, "Good Public Space Index:Theory and Method. Research Center of Public Space," University of Brawijaya, 2013.
[5] P. S. Sondang, *Tips to Increase Work Productivity*. Jakarta: PT. Rineka Cipta, 2002.
[6] Komaruddin, *Management Encyclopedia*, 2nd Ed. Jakarta: Literacy Development, 1994.
[7] M. R. Soetrisno, "Effectiveness of Utilization of Non-Green Public Space at Perumnas Toddopuli Panakkukang Permai Makassar City," Diponegoro University, 2010.
[8] F. Webster, *Theories of the Information Society*, Third edit. New York Roy, 2006.
[9] E. Budiharjo and D. Sujarto, *Sustainable Cities*. Bandung: Alumni, 1999.
[10] N. Dewang and Leonardo, "Accessibility of Public Public Spaces for Certain Community Groups: A Study of Public Facilities for People with Disabilities in the Taman Suropati Menteng area, Central Jakarta," *PLANESA J. Plan. Eng. Dep.*, vol. 1, no. 1, p. 8, 2010.
[11] S. F. S. Burhanuddin, "Assessment of Park Comfort in Public Public Spaces in the Pankajene Riverside Tourism Area," Hasanuddin University, Makassar, 2018.
[12] "Minister of Public Works Regulation No. 12 of 2009 concerning Guidelines for Provision and Utilization of Non-Green Public Spaces in Cities/Urban Areas."
[13] S. Meira, "Analysis of the Effectiveness of City Parks through an Approach to Site Conditions and Visitor Behavior," Bogor

Agricultural University, 2002.

[14] E. F. Porajouw *et al.*, "Effectiveness of Public Public Space in Tomohon City," *Unsrat E-Journal*, vol. 4, no. 17, 2017.

[15] J. Gehl, *Life Between Buildings: Using Public Space*. Washington: Island Press, 2011.

[16] J. Parkinson, *Democracy and Public Space*. Oxford: University Press, 2012.

[17] H. Shaftoe, *Convivial Urban Space*. Earth scan, 2008.

[18] W. H. Whyte, *The Social Life of Small Urban Spaces*. Washington: Conservation Foundation, 1979.

[19] Wardhani *et al.*, "Identification of the Quality of Use of Public Public Space in Housing in the City of Bandung," Bandung Institute of Technology, 2015.

# Analysis of the Floodlight Lighting Effect on the Visual Quality of the Phinisi Tower Building Facade

Mahsun Wahid[a,*], Nurul Jamala[b]

[a]Department of Architecture, Faculty of Engineering, Hasanuddin University, Makassar. Indonesia. Email: mahsunwahid@gmail.com
[b]Department of Architecture, Faculty of Engineering, Hasanuddin University, Makassar. Indonesia. Email: nuruljamala@yahoo.co.id

**Abstract**

Lighting is one of the important factors to recognize the environmental situation. Lighting is needed by humans, with good lighting we can visually recognize objects clearly. The suitability of lighting with recommended light standards and the arrangement of building facades in accordance with the distribution of lighting will have an impact on the visual quality of a building. Along with the development of technology and information, people's lifestyles are increasingly advanced and developing. Likewise, the function of artificial lighting, which used to only function as lighting at night, has now developed into an important part of the aesthetic forming factor of a building. So there is a need for a survey to see how big the difference in perception of the visual quality of lighting using floodlights on the Phinsi Tower. The survey method of data collection used quantitative and qualitative research methods. Mixed methods are divided into quantitative methods (research using questionnaires and SPSS data processing) and qualitative (respondent perception, interview and observation). Based on the results of surveys and tests conducted on 17 simulation models, different results were obtained in each test model. This explains that the use of floodlights greatly influences the visual quality of the Phinsi Tower facade. Of the 17 lighting simulation models that have been made, Model 17 has the highest average score of 5.08 and the lowest is Model 10 of 2.53 (a rating scale of 1 to 7).

*Keywords: Lighting; lighting simulation; visual quality*

## 1. Introduction

Exterior lighting of buildings and their appearance at night is an important issue in architectural design. While the effect of natural daylight on the appearance of a building during the day is not completely under the control of the designer, exterior lighting at night is a design choice that can strongly effects the beauty of a building. The current research Delft University of Technology examined the effect of exterior lighting on the appearance of buildings at night using a questionnaire-based research methodology accompanied by in-depth statistical analysis of the results [1].

To get the desired impression and character, a flexible lighting system is needed. The use of spotlights is considered the most appropriate because spotlights have high flexibility in terms of lighting levels (lux) to lighting angles (angle). Not only that, spotlights also have a wide beam angle that can be adjusted as needed.

The lighting quality of a building is largely determined by the feelings that arise in someone who visually accesses it. The perception of lighting is the result of the brain's interpretation and physiological reactions to the lighting regulation. The psychological perception of lighting depends not only on the intensity of light, the pattern of light and the color of the light, but also on the experience, culture, and mood of the person who observes it. Thus, the quality of building lighting is not something that can be measured quantitatively, but must go through a direct approach to everyone who visually accesses it.

To optimize the lighting, all relevant aspects that together make lighting quality need to be considered. It is not straightforward to determine all these aspects, as this research is extensive and complex; therefore, this kind of research is limited. The first step in optimizing the lighting quality is measuring all relevant photometric aspects, related to the understanding of lighting quality [2].

Therefore, in maintaining the information and visual quality of a building, it is necessary to conduct research to see the quality of its lighting. To know this, it takes a perception from the community's point of view to assess so that the results obtained are objective.

By considering the philosophy, the shape of the building and the lighting applied to the Phinisi Tower, this building is very interesting to be used as research material for a visual quality of the building facade, to study the factors and the phenomena that exist in shaping the pattern of lighting arrangements on the unique Phinisi tower facade.

*Corresponding author. Tel.: +6281343853433
*Jalan Tanjubulu, 23B*
*Palu, Central Sulawesi, 94221*

## 2. Literature Review

### 2.1. Facade

The word facade is taken from the Latin word "facies" which is a synonym for the words *face* and *appearance* Therefore, the facade is translated as the front part facing the street [3]. The facade of this building is also often called the appearance, the outer skin or the appearance of the building, because the facade of a building is the one that is most often given an assessment by observers without firstly checking the entire building, both on the outside and on the inside of the building.

In rural areas of Europe, however, facade lighting is often the brightest and most conspicuous source of lighting in a region. For example, Jechow et al. recently reported that 9% of the public light sources in a Spanish town of about 16,000 were for ornamental lighting, and that switching these lamps off reduced the artificial sky brightness overhead on a clear night by 20% at a location 1 km from the town center [4].

The appearance of the building facade in an area has an important role to build a visual character of the area that can describe the image of the area itself. A character will make it easier for people to recognize the area itself [5].

### 2.2. Floodlight lighting

Spotlights are lights that shine their rays in one direction. This tool projects light which is usually sourced from a high-pressure sodium lamp or LED lamp, with a parabolic reflector mirror.

Figure 1 describes light scattering patterns in floodlights lighting. Spotlights and floodlights are two types of light scattering patterns, the term refers to how the light is projected. Floodlights are generally used to illuminate a large area. On the contrary, spotlights are designed to travel a longer distance but in a much narrower beam [6].

### 2.3. Outdoor lighting

Good exterior lighting with decorative luminaires also underlines the stylistic statement made by the building's architect and adds to the appeal of the complex as a whole [7].

The following aspects should be taken into account for outdoor lighting (squares, gardens, buildings and facades) [8]:

a. The illumination according to the target area to be visualized, both horizontally and vertically.
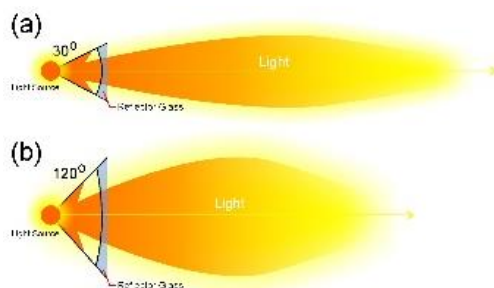


Figure 1. Light scattering patterns: (a) Spotlight; (b) Floodlight

b. The creation of a three-dimensional perception of a room through different levels of brightness and nuance.
c. A balanced brightness distribution.
d. The avoidance of strong dark-light contrast.
e. The limitation of glare effect for occupants and passersby
f. Choosing a suitable light color and color rendering.
g. No "unused" light.
h. When lighting a horizontal area there is no light emission at the top of the room.

### 2.4. Visual quality

Some experts say that 80% of information is received by humans visually through the senses of sight or eyes. While on the other hand, the eyes will be able to see an object if there is light with adequate intensity [9]. According to Lam, our judgment of space depends on how it meets our expectations. We base our judgment on whether a room is bright or dark not actually because of the level of lighting, but the state of whether environmental lighting can meet expectations and satisfy visual information needs or not [10].

There are 3 important things that support visual quality: a series of views (optic), the reaction of the observer with the place (place), and the elements of space in it (content) [11].

Different light sources have their own spectral characteristics and we might therefore be able to characterize the chromaticity and pollution performance of some of these sources. Hale's work showed that some traditional light sources, low pressure sodium, high pressure sodium, metal halide and mercury vapor lamps, could be classified from aerial night photograph using color information with a good accuracy [12].

Those things are also found in the design of outdoor lighting (building facades). Where by considering the arrangement of lights, the perception or assessment of respondents, and the influence of the elements forming the facade, we can obtain a good visual quality assessment of the building. The approach is based on photographic method to measure the luminance of the facade. Using qualitative assessment, pictures will be indexed with a qualitative criterion (aggressive or attractive), but most important, with a quantitative criterion (measured luminance). The approach is based on photographic method to measure the luminance of the facade. Using qualitative assessment, pictures will be indexed with a qualitative criterion (aggressive or attractive), but most important, with a quantitative criterion (measured luminance) [13].

## 3. Research Methods

This research uses mixed method. Mixed research method basically emerge from problems that arise when researchers cannot obtain complete data using quantitative or qualitative methods [14]. The focus of mixed method is to collect, analyze and combine quantitative and qualitative data in one study or one research session.
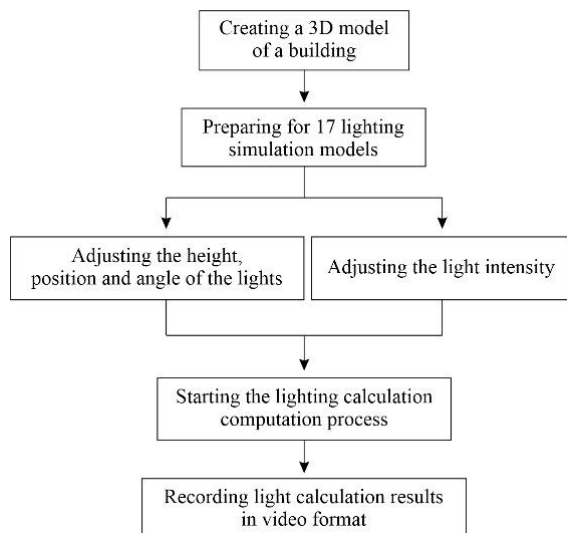
Figure 2. Light simulation setup using the dialux evo application



Figure 4. Buliding detail: (a) Phinsi tower; (b) Folding material (ACP); (c) Sun shading

### 3.2. Visual quality assessment variables

This study aims to see and analyze the effect of lighting on the visual quality of the Phinisi Tower facade at night. Figures 6 to 14 is a visualization simulation of lighting used to assess respondents' perceptions of the visual quality of the buildings.

In the design of illumination, it is expected that some of the light rays emitted from the floodlights towards the upper facade parts after reflection could be directed towards observers, ensuring the proper level of luminance of the facade [16].

Table 1 shows researchers use 14 variables of assessment. Respondents can give a value to each variable to finally be used as an assessment of the visual quality of the building facade.

Observations were made on the facade of the Phinisi tower from the left side, front side and right side of the building. The height of the phinisi tower is 97.5 meter (including lightning rod elements) with a base length of 25 meter at the front and 45 meter from the side. The front facade that faces to Andi Pangeran Pettarani street gets more highlights or lights than the side of the building.

In this study, what was observed was the visual quality of the facade lighting of the Phinisi Tower. In the case of research on the visual quality of artificial lighting, especially at the Phinisi Tower, experimental research is used. In the experimental method, researchers must carry out three requirements, namely controlling, manipulating, and observing activities.

Figure 2 describes the setup of simulation. After conducting a field analysis and collecting all the necessary data, the researcher then made a simulation using the DIALux evo application to calculate the light scattering pattern and then presented it to the respondents in the form of a video simulation to be assessed.

### 3.1. Research Location

Figure 3 is the research location. The research is located on Jalan Andi Pangeran Pettarani, Rappocini District, Makassar City, South Sulawesi and the object of research is the iconic Makassar City building, the Phinisi Tower.

Phinisi Tower was chosen because the building is considered full of meaning and full of philosophy in each of its parts. The Phinisi Tower building consists of 17 floors and has openings in the building envelope on each floor with the same area and shape, except for the front left and right sides of the building. the shape of the Phinisi Tower building with a Paraboloid hyperbolic facade model [15]. On the front and back sides of the tower, there are 3-dimensional folding materials formed from a series of triangular and trapezoidal planes made of aluminum composite panels shown in Fig. 4.

Table 1. Visual quality assessment variables

| No. | Variable (X) |
|---|---|
| 1 | Brightness (Dark – Light) |
| 2 | Texture (Blur - Clear) |
| 3 | Shadow (Irregular shading pattern - Regular) |
| 4 | Lighting (Not Applicable - Applicable) |
| 5 | Harmony (Harmony - Contrast) |
| 6 | Symmetrical (Asymmetric - Symmetrical) |
| 7 | Attractiveness (Monotone – Varied) |
| 8 | Lighting effect (Not dominant – Dominant) |
| 9 | Ambience (Not Inviting – Inviting) |
| 10 | Arts (Not Interesting - Interersting) |
| 11 | Proportionality (Disproportionate - Proportionate ) |
| 12 | Visual comfort (Boring – Fun) |
| 13 | Basic form (Simple - Complex) |
| 14 | Effect (Dislike - Like) |



Figure 3. Research location: (a) Map of Sulawesi; (b) Map of Makassar; (c) Map of Phinisi Tower Building Location



Figure 5. Lighting angle and height information

By adjusting the angle, height and intensity of the light used, different facade lighting patterns are found, especially in the front facade lighting shown in figure 5.

### 3.3. Population and sample

Determination of population and sample using purposive sampling technique. The purposive sampling technique, also called judgment sampling, is the deliberate choice of a participant due to the qualities the participant possesses. It is a nonrandom technique that does not need underlying theories or a set number of participants. Simply put, the researcher decides what needs to be known and sets out to find people who can and are willing to provide the information by virtue of knowledge or experience [17].

A total of 60 respondents are active students or architectural scholars who come from outside and within the city of Makassar.

### 3.4. Data collection

The data collected are divided into primary and secondary data. Primary data includes observations and questionnaires. Through observation techniques, researchers can obtain data on the pattern of lighting arrangements, types of lamps, the level of illumination in the building and the visual impact felt by the community around the Phinisi Tower. The researcher used a semi-open questionnaire in this study, which was supported by interviews to crosscheck the answers to the questions in the questionnaire that were not understood by the respondents.

In terms of data collection techniques, this research is quantitative, namely prioritizing the use of questionnaires, while qualitative research is used during interviews and observations [18].

The measurement scale used is a semantic differential scale type. The differential scale is a scale to measure attitudes and perceptions, but the form is not multiple choice or checklist, but is arranged in a continuum line where the most positive answer is located on the rightmost and vice versa [19].

Secondary data are obtained by taking documentation or information that has been collected by other parties or related agencies. This documentation function is used as a support and a complement to the primary data obtained through observation and questionnaires.

### 3.5. Data analysis

Data analysis in mixed method research refers to a research methodology that emphasizes the systematic integration or "mixing" of qualitative and quantitative data in single research or continuous programs. This integration allows for a more complete and synergistic use of data than the separate collection and analysis of quantitative and qualitative data. The use of this mixed method is needed to achieve results in form of values or percentages, visual quality, and respondents' perceptions of the Phinisi Tower facade lighting.

In comparing the visual quality of each building facade lighting model, the results of the questionnaire were formulated into a table and then processed using the SPSS 16 analysis program using the Multiple Linear Regression analysis method to obtain the average value and the percentage of assessment, in order to determine the aspects that affect respondents' perceptions of a lighting quality. Linear regression is used to determine the effect of one or several independent variables on one dependent variable. In general, linear regression is divided into two, namely simple linear regression with one independent variable and one dependent variable, and multiple linear regression with several independent variables and one dependent variable [20].

## 4. Results and Discussion

### 4.1. Model characteristics and lighting simulation results

In this study, researchers used 17 models of lighting patterns. Table 2 shows a description of the detail specifications and the pattern of laying the lights in the simulation.

Table 2. Specifications and patterns of laying lights on the simulation

| Model | Light Type | Number of Lamps | Height (Ev) | Angle | Light intensity (lm) | Power (w) |
|---|---|---|---|---|---|---|
| Existing | *SVHPL* | 3 | ± 0,00 | 45∘ | - | 250 |
| Model 1 | *SVHPL* | 1 | ± 0,00 | 45∘ | 500878 | 250 |
| Model 2 | *SVHPL* | 2 | ± 0,00 | 45∘ | 500878 | 250 |
| Model 3 | *SVHPL* | 1 | ± 0,00 | 45∘ | 500878 | 250 |
| Model 4 | *SVHPL* | 1 | ± 0,00 | 45∘ | 500878 | 250 |
| Model 5 | *SVHPL* | 3 | ± 0,00 | 45∘ | 500878 | 250 |
| Model 6 | *SVHPL* | 3 | ± 0,00 + 12,00 | 45∘, 0º | 500878 | 250 |
| Model 7 | *SVHPL* | 2 | ± 0,00 + 12,00 | 45∘, 0º | 500878 | 250 |
| Model 8 | *SVHPL* | 2 | ± 0,00 + 79,00 | 45∘, -40º | 500878 | 250 |
| Model 9 | *SVHPL* | 2 | ± 0,00, +79,00 | 45∘, -65∘ | 500878 | 250 |
| Model 10 | *SVHPL* | 2 | ± 0,00, ± 0,00 | 45∘ | 500878 | 250 |
| Model 11 | *SVHPL* | 4 | ± 0,00 | 45∘ | 300878 | 250 |
| Model 12 | *SVHPL* | 2 | + 12,00 | 0∘ | 300878 | 250 |
| Model 13 | *SVHPL* | 1 | +79,00 | -78∘ | 300878 | 250 |
| Model 14 | *SVHPL* | 6 | ± 0,00, +12,00 | 45∘, 0∘ | 300878 | 250 |
| Model 15 | *SVHPL* | 4 | ± 0,00, +79,00 | 45∘, -78∘ | 300878 | 250 |
| Model 16 | *SVHPL* | 3 | + 12,00 +79,00 | 0∘, -78∘ | 300878 | 250 |
| Model 17 | *SVHPL* | 7 | ± 0,00, +12,00, +79,00 | 45∘, 0∘, -78∘ | 300878 | 250 |
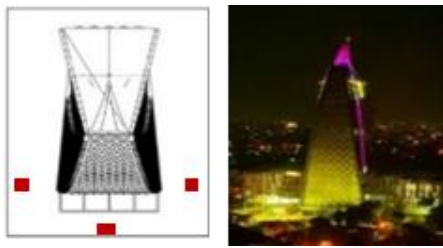
Figure 6. Existing condition

Table 3. Average luminance value of the phinisi tower existing conditions

| Average Value | |
|---|---|
| Existing | 4.48 |
| X < 4 = negative value;   X > 4 = positive value | |

Figure 6 shows the position and height of the phinisi tower lights. Lighting in the existing Phinisi Tower currently uses a Sodium Vapor High-Pressure Lamp (SVHPL) type, floodlight which is located in the middle-front of the building and on the left and right side of the building.

Table 3 shows the average value of the visual quality of lighting in the existing condition of the Phinisi Tower given by the respondent of 4.48 and has a positive value (X>4), which means it has good lighting. Figure 7 shows the position and height of the phinisi tower lights. Table 4 shows the average value of the visual quality of the lighting of the Phinisi Tower between model 1 and model 2 given by respondents ranging from 4-5 with an average of 4.32 for model 1 and 4.55 for model 2. the visual quality of lighting on model 1 and model 2 is positive (X>4) which means it has good lighting.
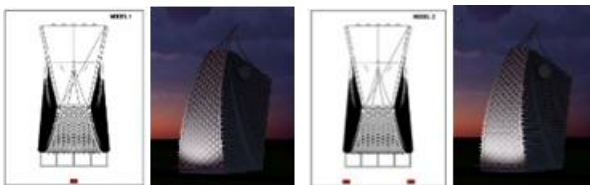


Figure 7. Model 1 and Model 2

Table 4. Average luminance value of the Model 1 and Model 2

| Average Value | |
|---|---|
| Model 1 | 4.32 |
| Model 2 | 4.55 |
| X < 4 = negative value;   X > 4 = positive value | |
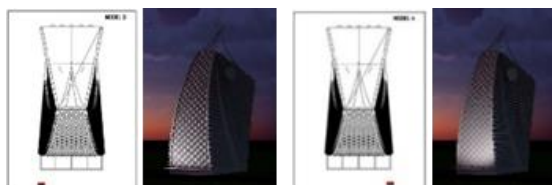


Figure 8. Model 3 and Model 4

Table 5. Average luminance value of the Model 3 and Model 4

| Average Value | |
|---|---|
| Model 3 | 4.53 |
| Model 4 | 4.05 |
| X < 4 = negative value;   X > 4 = positive value | |
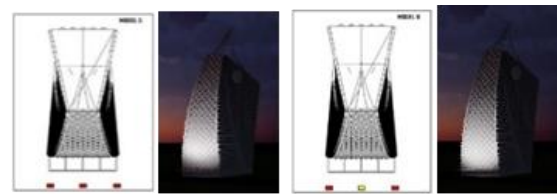


Figure 9. Model 5 and Model 6

Table 6. Average luminance value of the Model 5 and Model 6

| Average Value | |
|---|---|
| Model 5 | 4.50 |
| Model 6 | 4.25 |
| X < 4 = negative value;   X > 4 = positive value | |

Figure 8 shows the position and height of the phinisi tower lights. Table 5 shows the average value of the visual quality of the lighting of the Phinisi Tower between model 3 and model 4 given by respondents ranging from 4-5 with an average of 4.53 for model 3 and 4.05 for model 4. These results indicate that the assessment the visual quality of lighting on model 3 and model 4 is positive (X>4) which means it has good lighting.

Figure 9 shows the position and height of the phinisi tower lights. Table 6 shows the average value of the visual quality of the lighting of the Phinisi Tower between model 5 and model 6 given by respondents ranging from 4-5 with an average of 4.50 for model 5 and 4.25 for model 6. the visual quality of lighting on model 5 and model 6 is positive (X>4) which means it has good lighting.

Figure 10 shows the position and height of the phinisi tower lights. Table 7 shows the average value of the visual quality of the Phinisi Tower lighting between model 7 and model 8 given by respondents ranging from 4-5 with an average of 4.34 for model 7 and 4.30 for model 8. the visual quality of lighting on model 7 and model 8 is positive (X>4) which means it has good lighting.
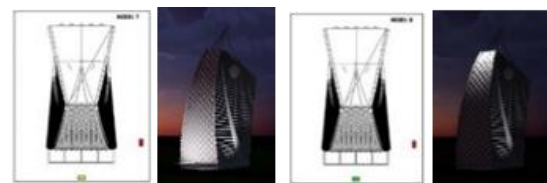


Figure 10. Model 7 and Model 8

Table 7. Average luminance value of the Model 7 and Model 8

| Average Value | |
|---|---|
| Model 7 | 4.34 |
| Model 8 | 4.30 |
| X < 4 = negative value;   X > 4 = positive value | |
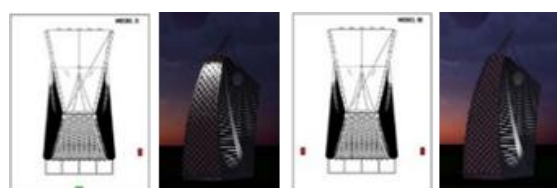


Figure 11. Model 9 and Model 10

Table 8. Average luminance value of the Model 9 and Model 10

| Average Value | |
|---|---|
| Model 9 | 4.82 |
| Model 10 | 2.53 |
| X < 4 = negative value;   X > 4 = positive value | |
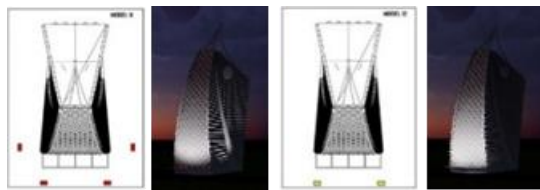


Figure 12. Model 11 and Model 12

Table 9. Average luminance value of the Model 11 and Model 12

| Average Value | |
|---|---|
| Model 11 | 4.18 |
| Model 12 | 4.11 |
| X < 4 = negative value;   X > 4 = positive value | |

Figure 11 shows the position and height of the phinisi tower lights. Table 8 shows the average value of the visual quality of the lighting of the Phinisi Tower between model 9 and model 10 given by respondents ranging from 2-5 with an average of 4.82 for model 9 and 2.53 for model 10.

These results indicate that the assessment the visual quality of lighting on model 9 is positive (X>4) and model 10 is negative (X<4), which means that the value of visual quality of lighting for model 9 is quite good while model 10 has poor lighting.

Figure 12 shows the position and height of the phinisi tower lights. Table 9 shows the average value of the visual quality of the lighting of the Phinisi Tower between model 11 and model 12 given by respondents ranging from 4-5 with an average of 4.18 for model 11 and 4.11 for model 12. These results indicate that the assessment the visual quality of lighting on model 11 and model 12 is positive (X>4) which means it has good lighting.

Figure 13 shows the position and height of the phinisi tower lights. Table 10 shows the average value of the visual quality of the Phinisi Tower lighting between model 13 and model 14 given by respondents ranging from 2-5 with an average of 2.65 for model 13 and 4.95 for model 14.



Figure 13. Model 13 and Model 14

Table 10. Average luminance value of the Model 13 and Model 14

| Average Value | |
|---|---|
| Model 13 | 2.65 |
| Model 14 | 4.95 |
| X < 4 = negative value;   X > 4 = positive value | |
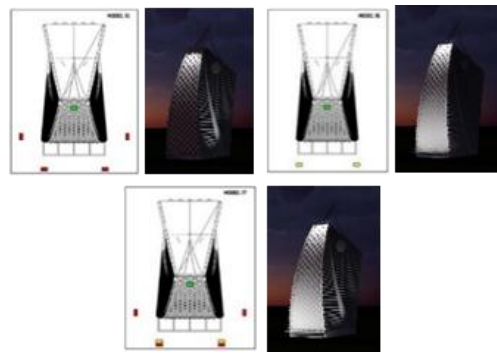


Figure 14. Model 15, Model 16 and Model 17

Table 11. Average luminance value of the Model 15, Model 16 and Model 10

| Average Value | |
|---|---|
| Model 15 | 3.94 |
| Model 16 | 4.47 |
| Model 17 | 5.08 |
| X < 4 = negative value;   X > 4 = positive value | |

These results indicate that the assessment the visual quality of lighting in model 13 is negative (X<4) and model 14 is positive (X>4), which means that the visual quality of lighting for model 13 is not good while model 14 has good lighting.

Figure 14 shows the position and height of the phinisi tower lights. Table 11 shows the average value of the visual quality of the Phinisi Tower lighting between models 15, 16 and model 17 given by respondents ranging from 3-6 with an average of 3.94 for models 15, 4.47 for models 16 and 5.08 for model 17. These results indicate that the assessment of the visual quality of lighting on model 15 is negative (X<4) and model 16, 17 is positive (X>4), which means that the value of the visual quality of lighting for model 15 is slightly less good, while models 16 and 17 have good lighting.

### 4.2. Analysis of the visual quality perception results

Previously, a visualization simulation test was carried out using the DIALux evo application and it was also known the average value of each lighting model. Then the data is compiled and arranged into a graph table to see the comparison of each simulation model.

From the graph (Fig. 15), it can be seen that the lighting simulation models 10 and 13 are simulation models that have poor lighting quality and are inversely proportional to the simulation model 17 which gets the highest rating from almost all respondents.
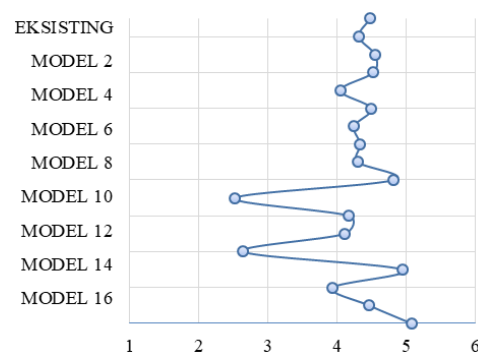


Figure 15. Average rating of each lighting model

Table 12. the percentage of respondents voted

| Respondent Rating | % | EKS | % | Model 1 | % | Model 2 |
|---|---|---|---|---|---|---|
| X < 4 (Negative Value) | 13 | 8 | 30 | 18 | 13 | 8 |
| X > 4 (Positive Value) | 87 | 52 | 70 | 42 | 87 | 52 |
| Respondent Rating | % | Model 3 | % | Model 4 | % | Model 5 |
| X < 4 (Negative Value) | 12 | 7 | 43 | 26 | 27 | 16 |
| X > 4 (Positive Value) | 88 | 53 | 57 | 34 | 73 | 44 |
| Respondent Rating | % | Model 6 | % | Model 7 | % | Model 8 |
| X < 4 (Negative Value) | 40 | 24 | 27 | 16 | 33 | 20 |
| X > 4 (Positive Value) | 60 | 36 | 73 | 44 | 67 | 40 |
| Respondent Rating | % | Model 9 | % | Model 10 | % | Model 11 |
| X < 4 (Negative Value) | 10 | 6 | 87 | 52 | 37 | 22 |
| X > 4 (Positive Value) | 90 | 54 | 13 | 8 | 63 | 38 |
| Respondent Rating | % | Model 12 | % | Model 13 | % | Model 14 |
| X < 4 (Negative Value) | 37 | 22 | 87 | 52 | 17 | 10 |
| X > 4 (Positive Value) | 63 | 38 | 13 | 8 | 83 | 50 |
| Respondent Rating | % | Model 15 | % | Model 16 | % | Model 17 |
| X < 4 (Negative Value) | 53 | 32 | 30 | 18 | 10 | 6 |
| X > 4 (Positive Value) | 47 | 28 | 70 | 42 | 90 | 54 |

Table 12 is the detail of respondents' percentage choices for each simulation model. as many as 60 respondents participated in this study

*4.2.1. Classic assumption test results*

a. Normality test

Normality test in Table 13 was done by Kolmogorov Smirnov test. The results of the analysis showed that the significance of the Kolmogorov Smirnov test was 0.318 > 0.05 ($\alpha$=5%). These results conclude that the assumption of normality has been met.

Table 13. Normality test result

**One-Sample Kolmogorov-Smirnov Test[a]**

| | | Unstandardized Residual |
|---|---|---|
| N | | 60 |
| Normal Parameters[a] | Mean | .0000000 |
| | Std. Deviation | .20969359 |
| Most Extreme Differences | Absolute | .124 |
| | Positive | .065 |
| | Negative | -.124 |
| Kolmogorov-Smirnov Z | | .958 |
| Asymp. Sig. (2-tailed) | | .318 |

a) Test distribution is normal

Table 14. Multicollinearity test result

| Variable | VIF |
|---|---|
| X1 (Brightness) | 6.033 |
| X2 (Texture) | 4.246 |
| X3 (Shadow) | 5.265 |
| X4 (Lighting) | 4.340 |
| X5 (Harmony) | 5.265 |
| X6 (Symmetrical) | 7.912 |
| X7 (Attractiveness) | 2.296 |
| X8 (Lighting effect) | 3.715 |
| X9 (Ambience) | 4.125 |
| X10 (Arts) | 7.260 |
| X11 (Proportionality) | 5.262 |
| X12 (Visual comfort) | 4.767 |
| X13 (Basic form) | 2.548 |
| X14 (Effect) | 4.513 |

Table 15. Coefficient of determination

**Model Summary[b]**

| Model | R | R Square | Adjusted R Square | Std. Error of the Estimate |
|---|---|---|---|---|
| 1 | .571[a] | .326 | .116 | .11818 |

a) Predictors: (Constant), X14, X2, X13, X5, X7, X4, X8, X9, X12, X11, X3, X1, X10, X6
b) Dependent Variable: Y

b. Multicollinearity test

Multicollinearity test in Table 14 was carried out by looking at the variance inflation factor (VIF) value. The results of the analysis show that the VIF value is < 10.

c. Autocorrelation test

The autocorrelation test was carried out using the Runs Test, where the value of Asym. Sig. obtained is 0.118 > 0.05. So it can be concluded that there is no autocorrelation in the regression model or in other words the non-autocorrelation assumption has been fulfilled.

*4.2.2. Coefficient of determination*

Table 15 is the value of the coefficient of determination generated in the regression model in this study. The value of the correlation coefficient (R) shows how closely the relationship between the independent variable (X) and the dependent variable (Y), the value of the correlation coefficient is 0.571. This value indicates that the relationship between variable X and variable Y is 57.1%. The results of the SPSS calculation obtained the value of R2 = 0.326, which means that 32.6% of the lighting quality can be explained by the X variable. While the remaining 67.4% is influenced by other variables outside the model studied.

*4.2.3. F test results*

F test is a test that is carried out to see simultaneously (overall) the relationship between the Xn variable and the Y variable. Table 16 summarizes the results of the F test generated in the regression model in the study.

Table 16. F test results

**ANOVA**[b)]

| Model | | Sum of Squares | df | Mean Square | F | Sig. |
|---|---|---|---|---|---|---|
| 1 | Regression | 53.406 | 14 | 3.815 | 66.168 | .000[a)] |
| | Residual | 2.594 | 45 | .058 | | |
| | Total | 56.000 | 59 | | | |

a) Predictors: (Constant), X14, X2, X13, X5, X7, X4, X8, X9, X12, X11, X3, X1, X10, X6
b) Dependent Variable: Y

Table 17. t test results

| Variable | Sig. |
|---|---|
| X1 (Brightness) | 0.06 |
| X2 (Texture) | 0.285 |
| X3 (Shadow) | 0.514 |
| X4 (Lighting) | 0.031 |
| X5 (Harmony) | 0.057 |
| X6 (Symmetrical) | 0.004 |
| X7 (Attractiveness) | 0.588 |
| X8 (Lighting effect) | 0.131 |
| X9 (Ambience) | 0.495 |
| X10 (Arts) | 0.005 |
| X11 (Proportionality) | 0.055 |
| X12 (Visual comfort) | 0.088 |
| X13 (Basic form) | 0.087 |
| X14 (Effect) | 0.200 |

Based on the Table 16, it can be seen that the F test produces a calculated F of 66.168 with a significance value of 0.000 <0.05 ($\alpha$=5%). From these results it can be concluded that the variable Xn simultaneously affects the quality of lighting.

### 4.2.4 t test result

t test is a test that is carried out to see partially (respectively) the relationship between the X variable and the Y variable. Table 17 are the results of the t test generated in the regression model in the study. Based on the Table 17, the significance value of the independent variable < 0.05 ($\alpha$=5%) which has a partially significant effect on lighting quality is X1 (Brightness), X4 (Lighting), X6 (Symmetrical), and X10 (Arts).

From the comparison of visual perceptions above, it is clear that there are differences in perceptions that arise due to the variety of lighting designs. The reason is, lighting is not just dark or light, but rather to realize the desires that arise from the observers of the existing visual conditions related to the architecture of the building. A poor lighting approach to a building that has strong characteristics will actually give a negative perception when choosing or using an inappropriate lighting method.

### 5. Conclusion

The results of the assessment of respondents' perceptions of the visual quality of the Phinsi Tower facade lighting can be concluded several things, namely,

the current lighting of the Phinisi Tower building (existing) is considered to be quite good and in accorandce with its designation as an iconic building in Makassar City. With an average rating of 4.48 (the highest rating is 7), it can be concluded that the Phinisi Tower currently has the right facade lighting.

The visual quality of lighting on the facade of the Phinisi tower can be further improved by using the lighting arrangement pattern of model 17. The visual quality of lighting that is very influential on the facade of the phinisi tower is in terms of "Brightness", "Lighting", "Symmetrical" and "Arts". With appropriate artificial lighting, it can improve the visual quality of the building so that it presents a positive impression.

### Acknowledgements

### References

[1] F. Nikoudel, M. Mahdavinejad, and J. Vazifehdan, "Nocturnal Architecture of Buildings: Interaction of Exterior Lighting and Visual Beauty," *Light Eng.*, vol. 26, no. 1, 2018.

[2] T. Kruisselbrink, R. Dangol, and A. Rosemann, "Hotometric Measurements of Lighting Quality: An Overview," *Build. Environ.*, vol. 138, pp. 42–52, 2018.

[3] R. Krier, *Architectural Composition*. Jakarta: Erlangga, 2001.[in Bahasa]

[4] C. Kyba, A. Mohar, G. Pintar, and J. Stare, "Reducing the Environmental Footprint of Church Lighting: Matching Facade Shape and Lowering Luminance with the EcoSky LED," *Int. J. Sustain. Light.*, vol. 20, no. 1, 2018.

[5] A. R. Harani. and K. Motic, "The Effect of Building Facades on the Visual Character of the Area (case studies: Semarang Chinatown, Malaysia and Singapore)," *J. Pengemb. Kota*, vol. 5, no. 1, pp. 1–8, 2017. [in Bahasa]

[6] O. S. M. De, "Spotlights Vs. Floodlights: What's the Difference?" www.superbrightleds.com/blog/spotlights-vs-floodlights-whats-difference/3282/.

[7] Fördergemeinschaft Gutes Licht, *Good Lighting for Schools and Educational Establishments 2*. Frankfurt, 2015.

[8] Zumtobel, *The Lighting Handbook*. Austria, 2018.

[9] P. Manurung, "Historical Building Facade Lighting Design Approach," in *Simposium Nasional RAPI XIV – FT UMS*, 2015, p. 9. [in Bahasa]

[10] P. Manurung, "Lighting Quality in Historic Buildings," *J. Dimens. Tek. Arsit.*, vol. 36, no. 1, pp. 28–34, 2008. [in Bahasa]

[11] S. Nurmasari, "Relation of Outdoor Media (Using Artificial Lighting) with Visual Quality of Corridor at Night according to Public Perception (Case Study of Jalan Pahlawan Semarang Corridor)," Universitas Diponegoro, Semarang, 2008. [in Bahasa]

[12] Q. Yao, H. Wang, Q. Dai, and F. Shi, "Quantification Assessment Of Light Pollution Of Façade Lighting Display in Shenzhen, China," *Opt. Express*, vol. 28, no. 9, pp. 14100–14108, 2020.

[13] C. D. Gălăţanu, I. Gherasim, D. Beu, and D. D. Lucache, "Luminance Field of the Façades: From Aggressive to Attractive Lighting," in *2018 IEEE International Conference on Environment and Electrical Engineering and 2018 IEEE Industrial and Commercial Power Systems Europe (EEEIC/I&CPS Europe)*, 2018, pp. 1–5.

[14] Iskandar, Nehru, and C. Riantoni, *Mixed Methods Research (Concepts, Procedures and Application Examples)*. Penerbit NEM – Anggota IKAP, 2021. [in Bahasa]

[15] N. Jamala, "The Effect of Building Facade Model on Light Distribution (Case Study: Phinisi Tower Building of UNM)," *Dimens. − J. Archit. Built Environ.*, vol. 44, no. 2, pp. 149–154, 2017.

[16] H. Wachta, K. Baran, and M. Leśko, "The Meaning of Qualitative Reflective Features of the Facade in the Design of

Illumination of Architectural Objects," in *AIP Conference Proceedings, 2078(1)*, 2019, p. 20102.

[17] I. Etikan, S. A. Musa, and R. S. Alkassim, "Comparison of Convenience Sampling and Purposive Sampling," *Am. J. Theor. Appl. Stat.*, vol. 4, no. 1, pp. 1–4, 2016.

[18] Hamidi, *Qualitative Research Method: Practical Applications for Making Research Proposals and Reports*. Malang: Malang UMM Press, 2004. [in Bahasa]

[19] F. Nurlan, *Quantitative Research Methods*. Parepare: CV. Pilar Nusantara, 2019. [in Bahasa]

[20] E. P. Kusumah, *Processing Thesis Data with SPSS 22*. Bangka Belitung: Lab. Kom Manajemen FE UBB, 2016. [in Bahasa]

# Evaluation of Achievement of Overburden Production Target Using Fishbone Diagram Method at Pit A Site B PT XYZ, South Sumatera Province

Aurah Masyitha Ayu Namira[a,*], Aryanti Virtanti Anas[b], Rizki Amalia[c], Rini Novrianti Sutardjo Tui[d]

[a]Department of Mining Engineering, Engineering Faculty. Hasanuddin University.  Email: aurahmasyithaayu@gmail.com
[b]Department of Mining Engineering, Engineering Faculty. Hasanuddin University.  Email: aryantiv@unhas.ac.id
[c]Department of Mining Engineering, Engineering Faculty. Hasanuddin University.  Email: rizkiamalia@unhas.ac.id
[d]Department of Mining Engineering, Engineering Faculty. Hasanuddin University.  Email: rini@unhas.ac.id

## Abstract

PT XYZ is the companies engaged in the coal mining and energy. Mining activities at the Pit A Site B are still focused on stripping overburden using the Komatsu PC-3000E power shovel. The company has established a 513,333 BCM production target of overburden stripping in November 2020. The existence of factors that affect the productivity of the equipment will determine the achievement of production targets. One of the methods that can be used to determine the factors causing problems in achievement production target is a fishbone diagram. The purpose of this research is to calculate overburden production in November 2020, identify factors that influence the achievement of overburden production targets using a fishbone diagram, and make recommendations for improvement plans based on factors that affect the achievement of overburden production targets. Based on the results of the fishbone diagram analysis, there are four factors that influence the achievement of overburden production targets, which is manpower, material, machine and methods. The problems that affect the achievement of production targets on the machine factor is equipment failure, the manpower factor is time discipline, the method factor is not maximum material pick up and the material factor is material type. The recommended improvement plan for each factor causing the problem are four recommendations for improvement plans on manpower factors, three recommendations on improvement plans on machine factors, three recommendations on improvement plans on material factors and three recommendations on improvement plans on method factors.

*Keywords: Coal; excavator; fishbone diagram; overburden*

## 1. Introduction

PT XYZ is a company engaged in coal mining and energy in South Sumatra Province. Since December 2016, mining activities at Site B, which consist of Pit A and Pit C East, have been electrified (self-managed) or carried out and managed by the company itself. Mining activities at the Pit A mine site are still focused on overburden stripping. The equipment used is a Komatsu PC-3000E power shovel with three units.

Several factors can affect the equipment productivity, including equipment cycle time are caused by the difficulty of loading material, queues occur on hauler, long hauling distances, operator performance that is not optimal at work, machine conditions, excavation height, equipment rotation angle, loading factor for equipment [1]–[3].

Mining companies calculate cycle times to determine equipment performance and operator work efficiency [4]. The calculation of the equipment cycle time is carried out by monitoring the movement pattern of mechanical equipment during activities [5]. The cycle time for equipment is the total time it takes the equipment to complete one cycle [6]. The better of level use the equipment, the greater the productivity produced by the equipment [7].

One of parameters that can be used to determine the results of the work (success) of a mechanical earthmoving equipment are good or bad is the total production that can be achieved by the heavy equipment used [8]. The company has assign a production target of overburden stripping in November 2020 of 513,333 BCM. The existence of factors that affect the equipment productivity will determine the achievement of production targets, so it is necessary to evaluate production by identifying the factors causing the problem. These factors can be classified based on the cause of the problem including man power factors, machine factors, method factors and material factors [1].

One of method that can be used to determine the root cause of the problem can be determined using a fishbone diagram. The fishbone diagram or also known as the cause and effect diagram or ishikawa diagram was first introduced by its originator, Kaoru Ishikawa (1915-

*Corresponding author. Tel.: +62-813-5487-2847
 Poros Malino Street KM. 6 Bontomarannu
 Gowa, South Sulawesi
 Indonesia, 92171

1989), a professor at the University of Tokyo [9]. Fishbone diagram is a method used to identify the root cause of a quality problem [10].

Fishbone diagrams which are shaped like a fish bone are a common tool used for cause and effect analysis to identify causal relationships in a particular problem or event [11]. The benefit of a fishbone diagram is that it focuses individuals or organizations on the main problem [12]. The parts of the fishbone diagram consist of fish heads used to state the main problem that needs to be solved, fins are used to write down problem groups and fish bone are used to state the cause of the problem [13].

Based on the results of the fishbone diagram analysis, recommendations for improvement plans can be designed for each factor causing the problem, so the overburden production target can be achieved. Therefore, this study was conducted to identify the root cause of the problem using a fishbone diagram to arrange recommendations for improvement plans, so the overburden production target at Pit A Site B PT XYZ can be achieved.

## 2. Research Methods

The research activity was carried out in PT XYZ department unit which is responsible for managing production activities at Pit A Site B. The overburden production target assigned by in November 2020 at the Pit A Site B is 513,333 BCM/month. Equipment productivity is very influential on whether or not the production target is achieved. Equipment productivity is influenced by several factors, therefore it is necessary to evaluate the factors that affect the overburden production target.

### 2.1. Data Collection

Data collection in this study consisted of:

- Cycle time

Cycle time data of two units of the Komatsu PC-3000E power shovel were gathered by direct observation in the mining area of Pit A Site B. The data collection period was on November 30, 2020 for 32 cycles for the Komatsu PC-3002 power shovel and 29 cycles for the Komatsu PC-3003 power shovel with a bucket capacity of 16 m$^3$.

- Productive working time

The data obtained in the form of the amount of productive working time in one month consisting of an effective working time of 660 hours and loss time data of the Komatsu PC-3000E power shovel.

- Swell Factor

Swell factor used is determined by the company at 0.72.

- Equipment correction factor

The correction factor for the Komatsu PC-3000E power shovel tool is shown in Table 1.

- Equipment specifications

The required specification of the Komatsu PC-3000E power shovel is a bucket capacity of 16 m$^3$.

Table 1. Correction factor of the Komatsu PC-3000E power shovel

| Correction Factor | Unit PC | |
|---|---|---|
| | 3002 | 3003 |
| | Cycle Time | |
| | 27.31 seconds | 28.29 seconds |
| Bucket fill factor | 1.04 | 1.04 |
| Time efficiency | 0.52 | 0.59 |
| Machine Condition | 0.97 | 1.00 |
| Operator Skill | 0.95 | 0.95 |
| Material Properties | 0.95 | 0.95 |
| Field Condition | 1.00 | 1.00 |
| Weather | 0.90 | 0.90 |
| Total | 0.43 | 0.50 |

- Cause of problem factors

The research questionnaires was conducted to determine the factors that effect the failure to achieve the overburden production target using purposive sampling method. Simply put, the researcher decides what needs to be known and sets out to find people who can and are willing to provide the information by virtue of knowledge or experience [14].

Respondents in this study were determined based on the results of discussions with the company, therefore it resulted in the people most responsible for the production of overburden. There are 14 respondents of the questionnaire, which consist of one self-managed Mining Manager, two Supervisors and 11 Dispatchers.

### 2.2. Data Processing

Data processing is carried out at the Mine Planning and Valuation Laboratory with the following stages:
- Calculating power shovel productivity

The productivity of the Komatsu PC-3000E power shovel is calculated using Equation 1 (company's formula).

$$Q = ql \times fk \times \frac{3600}{Ct} \times SF \qquad (1)$$

- Making diagram fishbone

The steps of fishbone diagram analysis are:
a. Determine the root cause of the problem based on the results of the questionnaire.

Determine the possible causes of the main factors that become the basis of the problem of achieving the overburden production target based on the results of the questionnaire. The possible causes of each factor are described as small bones in the main bone. Each possible cause is also searched for the root cause and can be described as a branch in the outline of the previous possible cause.

b. Making fishbone diagram outline

The fishbone diagram outline includes the fish head which is placed on the right side of the diagram. This fish head is used to state the main problem, namely the achievement of the overburden production target. The second part is

the fin used to write down the group of causes of the problem and the third part is the thorn used to state the possible causes of the problem.

c. Grouping the cause of problem factors

Factors that influence the achievement of overburden production targets are grouped into four categories namely, man power factors, machine factors, method factors and material factors. These factors are assigned to the fish fins on the fishbone diagram.

d. Analyzing fishbone diagrams

After making a fishbone diagram, it can be seen all the root causes of the problem of achieving the overburden production target. The root causes that have been found are further analyzed for the priority and significance of the causes. Solutions are given to solve the existing problem by solving the root of the problem.

e. Arrange recommendations for improvement plans

The 5W + 1H technique is used to arrange recommendations for improvement plans after knowing the factors and sources of problems so that production targets can be achieved.

## 3. Research Results

### 3.1. Overburden production

Overburden production is calculated from the productivity of the Komatsu PC-3000E power shovel with total of two unit, which are PC-3002 and PC-3003. The data used to calculate the productivity of power shovel (Q) are cycle time (Ct), swell factor (Sf), correction factor (Fk) (Table 1), and bucket capacity (Ql). The cycle time of the power shovel (Ct) is calculated by adding up each component of the time required to perform one cycle, namely the digging time, fill swing time, loading time, and empty swing time.

The average cycle time (Ct) of the PC-3002 and PC-3003 power shovel obtained were 27.31 seconds and 28.29 seconds, respectively. Swell factor (Sf) obtained from the company is 0.72. Correction factor (Fk) obtained from the company is 0.43 for PC-3002 and 0.50 for PC-3003. The bucket capacity (Ql) of the PC-3000 power shovel is $16m^3$. The results of the calculation of the power shovel productivity using Eq. 1 can be seen in Table 2.

The productivity of the Komatsu PC-3002 power shovel was obtained at 652.98 BCM/hour and PC-3003 at 732.98 BCM/hour. The production of overburden in November 2020 is calculated by multiplying the productivity value of power shovel per hour (Table 3.1) by the productive working time in November 2020 which is shown in Table 3.

Table 2. Productivity of Power Shovel Komatsu PC-3002 and PC-3003

| Unit | Ql ($m^3$) | Sf | Fk | Ct (Seconds) | Q (BCM/Hour) |
|---|---|---|---|---|---|
| PC-3002 | 16 | 0.72 | 0.43 | 27.31 | 652.98 |
| PC-3003 | 16 | 0.72 | 0.50 | 28.29 | 732.98 |

Table 3. Overburden production in November 2020

| Unit | Q (BCM/ Hour) | Productive Working Time (Hour/ Month) | Q (BCM/ Month) | Total Production (BCM/ Month) |
|---|---|---|---|---|
| PC-3002 | 652.98 | 306.98 | 200,138,37 | 488,162 |
| PC-3003 | 732.98 | 392.95 | 287,024.49 | |

Total overburden production at Pit A Site B in November 2020 is 488,162 BCM while the overburden production target obtained was 513,333 BCM. The production of overburden indicates that the production target is not achieved or the production achieved is only 95% of the production target that has been assign. Factors that influence the achievement of overburden production targets are analyzed for cause and effect using a fishbone diagram based on the results of the questionnaire.

### 3.2. Fishbone diagram

The fishbone diagram is used to identify the cause and effect of problems regarding the achievement of PT XYZ's overburden production target in November 2020. The pattern used to make the fishbone diagram is the 4M pattern consisting of machines, methods, materials and manpower.

### 3.2.1. Root cause of the problem

The root cause of the problem of achieving the overburden production target can be identified based on the results of the questionnaire. The results of the questionnaire show the root cause of the problem in each factor, namely the machine factor, man power factor, method factor and material factor. Determination of the root cause of the problem based on the problem with the highest frequency for each factor.

- Machines Factor

The problems affecting the achievement of overburden production targets on the machines factor consist of:

a. Equipment failure

There are three units of Komatsu PC-3000E power shovel used in Pit A Site B, namely PC-3002 and PC-3003. During data collection, the Komatsu PC-3002 power shovel was failure because it was used more than the working time of the equipment.

b. Loss time

The increase in the value of working time constraints affects the productivity of the Komatsu PC-3000E power shovel because the productive working time of the equipment is limited.

c. Equipment maintenance

Proper management and maintenance of equipment is very influential in accelerating overburden stripping activities, so that the work is completed on time and production targets can be achieved [15].
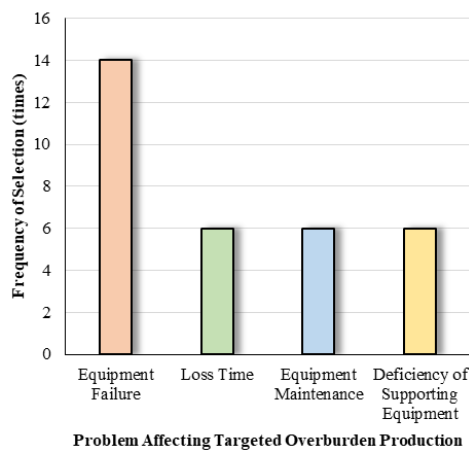
Figure 1. Machine factor
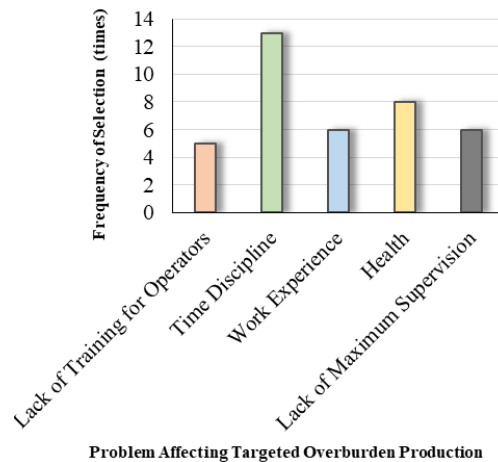


Figure 2. Manpower factor

d. Deficiency supporting equipment

Mining support equipment has an important role in the process of overburden stripping activities. Mining support equipment such as dozers function as equipment can clear the land if that land still has shrubs or trees and is also used for the formation of a flat surface [3].

A bar chart of problems affecting the achievement of the machines factor overburden production target is shown in Fig. 1.

Equipment failure has a selection frequency of 14 times, while the loss time, equipment maintenance and deficiency supporting equipment have a frequency of 6 times. The problem with machines factor that has the highest influence on the production target is equipment failure.

- Manpower factor

  The problems affecting the achievement of overburden production targets on man power factors consist of:

  a. Lack of training for operators

  Operators who lack of training have an effect on their skills, so that technical errors often occur due to operators themselves, such as too long a time needed to move the equipment from one location to another and too many maneuvers on the hauler.

  b. Time discipline

  The operator's time discipline affects the start time of the overburden stripping operation. Operators are usually ±30-60 minutes late from the scheduled time to start overburden removal operations.

  c. Work experience

  The average operators work experience of operating equipment is ±2 years at the research site, this affects the achievement of overburden production targets.

  d. Health

  The operator's working time is divided into two shifts, one shift consists of 11 hours and is only given a break of about one hour for each shift. The working time affects the operator's health such as eye fatigue and decreased concentration power.

e. Lack of maximum supervision

Supervision of the overburden stripping activity process is not optimal due to a shortage of manpower in the field of supervision at Site B, especially Pit A.

A bar chart of problems affecting the achievement of man power factor overburden production targets is shown in Fig. 2.

Lack of training for operators has a selection frequency of 5 times, time discipline has a frequency of 13 times, work experience and health has a frequency of 8 times, and lack of maximum supervison has a frequency of 6 times. The problem with man power factor that has the highest influence on the production target is time discipline.

- Method Factor

  The problems affecting the achievement of overburden production targets on method factors consist of:

  a. Non-maximum material pick-up

  The overburden material was taken using a bottom loading technique with a slope height that was not in accordance with the standard so that the material was not taken optimally. Taking of material that is not optimal causes too many buckets needed for material loading on the hauler, this can affect a large value of the cycle time on the Komatsu PC-3000E power shovel and affect the achievement of production targets.

  b. Hauler maneuvers excessively

  Hauler maneuvers excessively causing an increase in the value of the hauler cycle time and causing the Komatsu PC-3000E power shovel to wait, thus affecting the achievement of production targets.

A bar chart of the problems affecting the achievement of the overburden production target by the method factor is shown in Fig. 3.

Non-maximum material pick up has a selection frequency of 6 times and hauler maneuvers excessively has a selection frequency of 9 times. The problem with the method factor that has the highest influence on the production target is non-maximum material pick up.
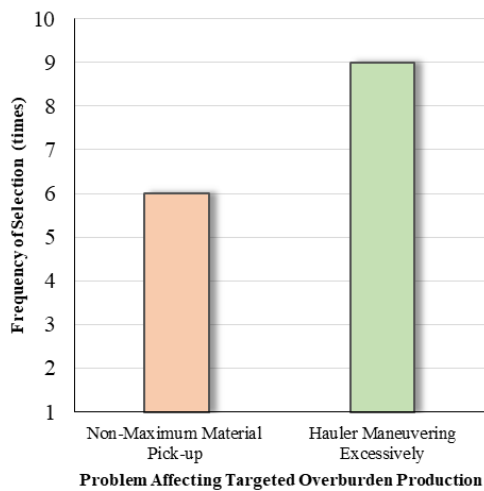
Figure 3. Method factor
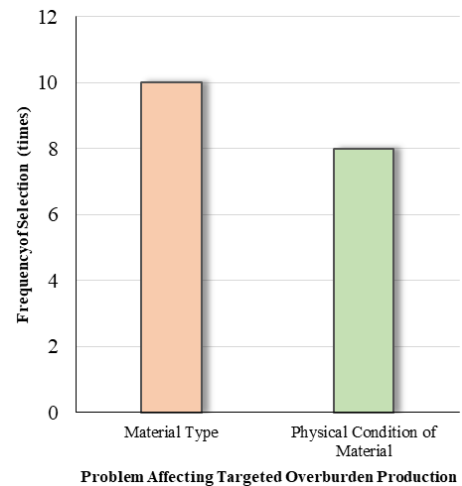


Figure 4. Material factor

- Material Factor

The problems affecting the achievement of overburden production targets on material factors consist of:

a. Material type

The road building material is in the form of clay and sand that easily sinks and breaks down quickly causes obstruction for the hauler.

b. Physical condition of material

The overburden material consists of hard clay which then affects the productivity of the Komatsu PC-3000E power shovel.

A bar chart of the problems affecting the achievement of the overburden production target by the material factor is shown in Fig. 4.

Material type has a selection frequency of 10 times and physical condition of material has a selection frequency of 8 times. The problem with the material factor that has the highest influence on the production target is the type of material.

The root causes of the problems that most influence the achievement of overburden production targets are equipment failure with a selection frequency of 14 times, time discipline with a frequency of selection of 13 times, hauler maneuvering with a frequency of selection of 9 times and the material type with a frequency of selection of 10 times.

### 3.2.2. Fishbone diagram outline

The fishbone diagram outline for problems affecting the achievement of overburden production targets consists of:

- Fish head

Fish head represent the main problem, which is achieving the overburden production target. The head is placed on the right side of the fishbone diagram (Fig. 5).

- Fish fin

Fish fins are used to write groups that cause problems. The groups of problems in achieving the overburden production target are man power factors, machine factors, method factors, and material factors (Fig. 6).
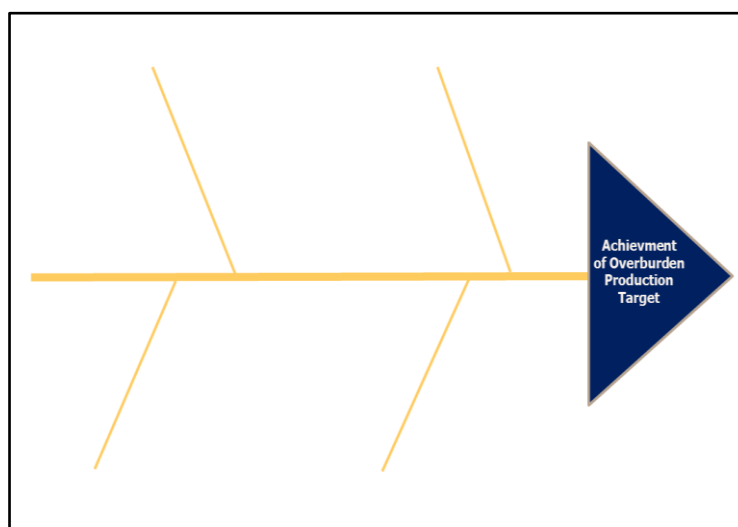


Figure 5. Fish head of fishbone diagram
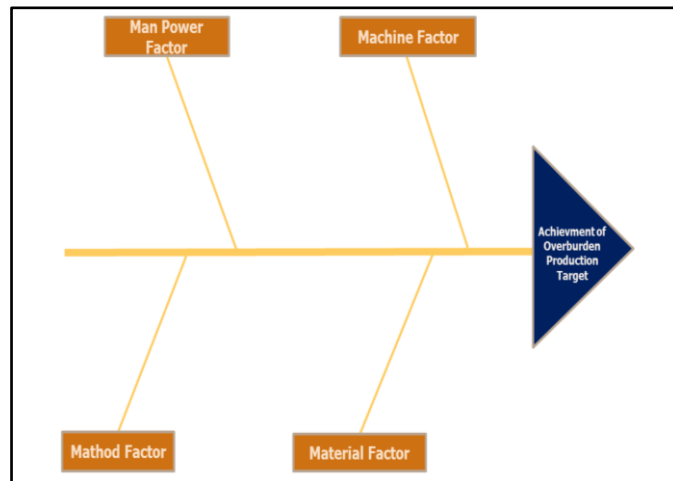
Figure 6. Fish fin of fishbone diagram
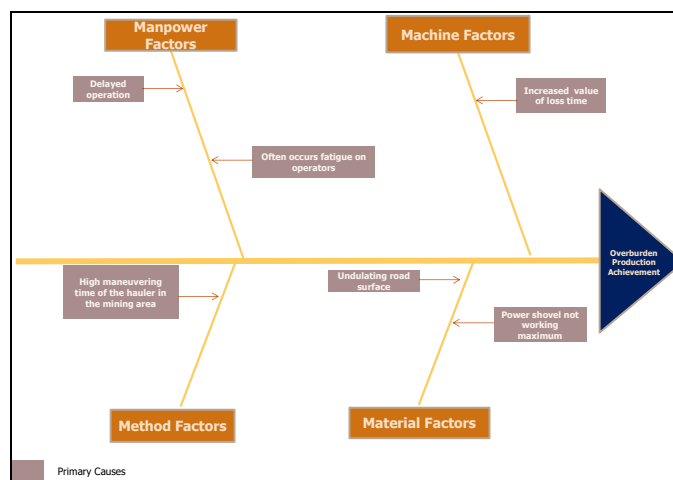


Figure 7. The primary causes on the fishbone diagram

- Fish bone

Fish bone are used to state the possible causes of problems for each group. Fish bones consist of primary causes, secondary causes and tertiary causes which are determined based on the results of questionnaires, direct observations and interviews. Primary causes consist of:

a. Man power factors are delayed operation and often occurs fatigue on operators.
b. Machine factors is the increase in the value of loss time.
c. Method factors is high maneuvering time of hauler in the mining area.
d. The material factors are the undulating road surface and the power shovel not working maximum.
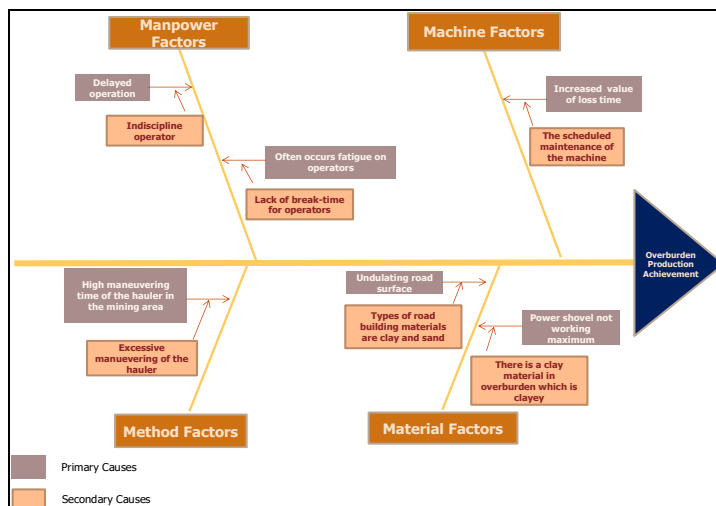


Figure 8. The secondary causes on the fishbone diagram

163
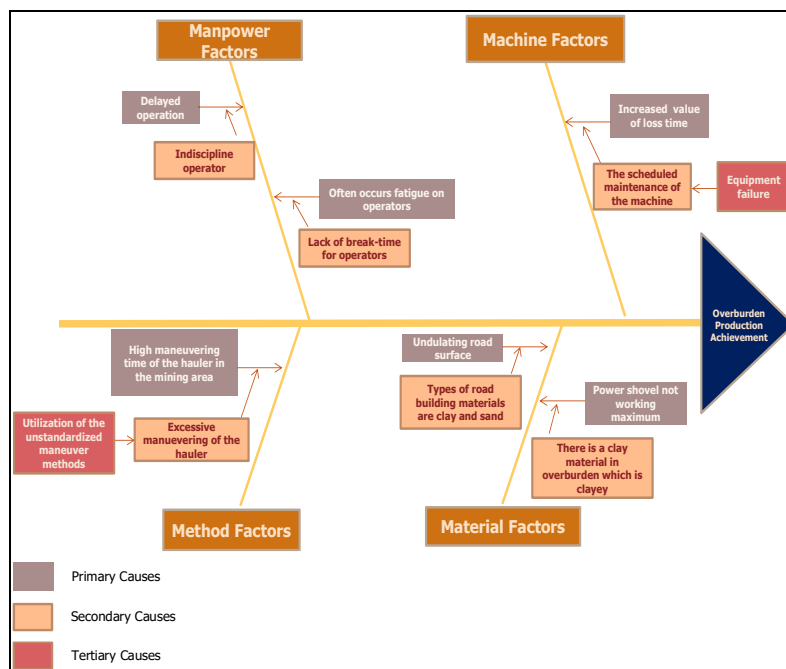
Figure 9. The tertiary causes on the fishbone diagram

Figure 7 shows the primary causes on the fishbone diagram. Secondary causes consist of:
a. Man power factors are indiscipline operator and lack of breaktime for operators.
b. Machine factors is the scheduled maintenance of the machine.
c. Method factors is excessive maneuvering of the hauler.
d. Material factors there is a clay material in overburden which is clayey.

Figure 8 shows secondary causes on a fishbone diagram.
Tertiary causes consist of:
a. Machine factor is equipment failure.
b. Method factor is utilization of the unstandardizied maneuver methods.
Figure 9 shows the tertiary causes on the fishbone diagram.

### 3.2.3. Group of factors causing problem

Factors that affect the achievement of overburden production targets are grouped into four categories, which are man power factors, machines factors, method factors and material factors. These factors are assigned to the fish fins on the fishbone diagram.

Man power factor are delayed operation and often occurs fatigue on operators. Machine factor is increase value of loss time. Method factors is high maneuvering time of hauler in the mining area. The material factors are the undulating road surface and the power shovel can't work to the maximum.

### 3.3. Fishbone Diagram Analysis

Fishbone diagram analysis was carried out to identify the root cause of the problem of achieving PT XYZ's overburden production target in November 2020. The analysis was carried out based on four causal factors,

which are man power factors, machine factors, method factors and material factors. These causative factors are:

- Manpower factor
  The causes that affect the achievement of overburden production targets from man power factors are:
  a. Indiscipline operators cause delays in starting overburden stripping operations.
  b. Lack of breaktime for operators which causes often occurs fatigue on operators.

- Material factor
  The causes that affect the achievement of overburden production targets from material factors are:
  a. There is an overburden material in the form of clay that is clayey or sticky when the material is dry it will become a hard lump, so that the power shovel not working maximum.
  b. The type of road building material in the form of clay and sand causes the road surface to be undulating.

- Machine factor
  The causes that affect the achievement of overburden production targets from machine factors is equipment failure causes the equipment need maintenance which results in an increase in the value of the loss time.

- Method factor
  The causes that affect the achievement of overburden production targets from method factors are is utilizing unstandardized maneuver methods causes hauler maneuvers excessively, resulting in a high maneuvering time for the hauler to adjust its position with the loader in the mining area.

The causes that affect the achievement of overburden production targets from each factor can be classified in tabular form based on data and facts that occur in the field. The classification of the problem of achieving the overburden production target can be seen in Table 4.

164

Table 4. Classification of problems for achievement of overburden production targets

| No. | Data and Facts | Problem Statements | Stratification Factor |
|---|---|---|---|
| 1. | a. The increase value of the loss time. <br> b. Indiscipline operators. | Delayed operation | Manpower |
| 2. | Lack of breaktime for operators | Often occurs fatigue on operators | Manpower |
| 3. | Equipment failure | The increase value of the loss time. | Machine |
| 4. | Utilizing unstandardized maneuver methods on hauler | The hauler maneuvers excessively, resulting in a high maneuvering time for the hauler to adjust its position with the loader in the mining area. | Method |
| 5. | Types of road construction in the form of clay and sand | Undulating road surface | Material |
| 6. | There is a clay material in overburden which is clayey | Power shovel can not work maximum | Material |

### 3.4. Recommended improvement plan

Recommendations for improvement plans are prepared after the root cause of the problem is determined so that the overburden production target can be achieved using the 5W+1H technique. The 5W+1H technique is an analytical method that is used as the basis for determining corrective action against each root of the problem and consists of what shows the problem, why shows the reason for recommending a repair plan for each problem, where indicates the location of the repair plan, when shows the time of the problem, who indicates the person in charge answer of each problem and how to show recommendations for improvement plans for each problem.

Recommendations for improvement plans are carried out in two stages, the first stage is the determination of the improvement plan (how) is carried out by the interview process and the second stage is the determination of the improvement plan recommendations based on the results of discussions conducted three times, namely on 21, 23, 25 December 2020 with other parties companies in the office.

### 3.4.1. Manpower factor

The causes of the unachieved overburden production target on the man power factor are indiscipline operator lack of breaktime for operators. The operator's work schedule is divided into two shifts, one shift consisting of 12 hours each working day starting Monday-Sunday. Shift one starts from 06.00-18.00 and shift two starts from 18.00 06.00. However, indiscipline operators

resulted in a delay in the start of the operation by about ±30-60 minutes, resulting in a mismatch of the predetermined work schedule. The improvement plans are:

- Updating initial standard of the operation.
- Providing penalty against operators who commit an infringement and perform real time attendance.

Lack of break time for operators resulted in frequent fatigue on the operator. The improvement plan are:

- Identify, evaluate and controlling factors that may cause operator fatigue.
- Assess and manage operator fatigue levels before working shifts and during work.

Recommendations for improvement plans using the 5W+1H technique for man power factors can be seen in Table 5.

### 3.4.2. Material factor

The cause of the non-achievement of the overburden production target is the material factor, namely road construction in the form of clay and sand as well as hard materials. Hard materials make it difficult during overburden excavation activities which result in the power shovel not working optimally. If the power shovel is operated not in accordance with its capabilities, it will cause equipment failure. The improvement plans are:

- Undertake overburden blasting activities on dry material.
- Undertake ripping and dozing activities on wet materials.

Table 5. Recommendations for improvement plans on manpower factors

| No | *What* | *Why* | *Where* | *When* | *Who* | *How* |
|---|---|---|---|---|---|---|
| 1. | Indiscipline operators | Increased of effective working hours | Pit A | November period | Self-managed mining | 1. Updating initial standart of the operation. <br> 2. Providing penalty against operators who commit an infringement and perform real time attendance. |
| 2. | Lack of break time for operators | Minimizing Work Accidents | Pit A | November period | Self-managed mining | 2. Identify, evaluate and controlling factors that may cause operator fatigue. <br> 3. Assess and manage operator fatigue levels before working shifts and during work. |

Table 6. Recommendations for improvement plans on material factors

| No | What | Why | Where | When | Who | How |
|---|---|---|---|---|---|---|
| 1. | There is a clay material in overburden which is clayey | Efficient material loading activities | Pit A | November period | Self-managed mining | 1. Undertake overburden blasting activities on dry material. <br> 2. Undertake ripping and dozing activities on wet materials. |
| 2. | The types of road building materials are clay and sand | Undulating road surface | Pit A | November period | Self-managed mining | 1. Aggrandize the use a motor grader on mine roads to compact the road building materials |

The types of materials that compose the mining road are clay and sand which basically have pores, so that if they are under pressure they will be compacted and cause the road surface to be undulating or failure quickly and result in obstruction of hauler to the mining site. The improvement plan is to aggrandize the use a motor grader on mine roads to compact the road building materials. Recommendations for improvement plans using the 5W+1H technique for material factors can be seen in Table 6.

### 3.4.3. Machine factor

The causes of not achieving the overburden production target on the machine factor is equipment failure. Equipment failure factor on the PC-3002 unit occurs because the use of the equipment exceeds the maximum working time, the breakdown of equipment, so the equipment must get maintenance. Types of equipment failure consist of breakdown schedule and breakdown unschedule. Breakdown schedule is equipment maintenance that is carried out every month while breakdown unschedule is equipment failure when the process of stripping the overburden is in progress. Breakdown schedule and breakdown unschedule can cause an increase in the value of the working time of the PC-3002 and PC 3003 units to 11 hours and 6 hours, respectively. The improvement plan is managing the utilization of equipment by checking before and after the equipment to avoid major failure.

Recommendations for improvement plans using the 5W+1H technique for the machine factor can be seen in Table 7.

### 3.4.4. Method factor

The cause of not achieving the overburden production target on the method factor does not use standard maneuvering methods on transportation equipment. The factor of the method of maneuvering the hauler used in the field is the 1.5 side loading maneuver method but the maneuver method used several times at the research location is often not in accordance with the standard maneuver method, causing hauler to maneuver too much and result in a high average the maneuvering time of hauler in the mining area is 41.87 seconds. The improvement plan is to improve supervision and controlling operators as performing maneuvers. Recommendations for improvement plans using the 5W+1H technique for method factors can be seen in Table 8.

Based on the results of the fishbone diagram analysis, there are four factors that affect the achievement of overburden production targets, namely man power, materials, machine and methods. The problems in the man power factor caused by the operator with four recommendations for improvement. The problem with the machine factor is caused by equipment failure which is given one recommendation for improvement. The problem with the material factor is caused by the type of road building material and there is a clay material in overburden which is clayey with three recommendations for improvement plans. The problem with the method factor is caused by utilizing unstandardizied maneuver methods given one recommendation for improvement plan.

### 4. Conclusion

The conclusions obtained from this research are the overburden production target at Pit A Site B in November 2020 is 513,333 BCM while the total overburden production obtained is 488,162 BCM which shows the production target was not achieved. Factors influencing the achievement of overburden production targets are machine factor that has the highest influence is equipment failure with a frequency of 14 times, man power factor that has the highest influence is time discipline with a frequency of 13 times, method factor that has the highest influence is hauler maneuvers excessively with a frequency of 9 times and material factor that has the highest influence is material type with a frequency of 10 times.

Table 7. Recommendations for improvement plans on machine factors

| No | What | Why | Where | When | Who | How |
|---|---|---|---|---|---|---|
| 1. | Equipment failure | Increasing loss time | Pit A | November period | Self-managed mining | 1. Managing the utilization of equipment by checking before and after the equipment to avoid major failure. |

Table 8. Recommendations for Improvement Plans on Method Factors

| No | What | Why | Where | When | Who | How |
|---|---|---|---|---|---|---|
| 1. | Unstandardized maneuvering methods | The cycle time of the hauler is relatively small | Pit A | November period | Self-managed mining | 1. Improve supervision and controlling operators as performing maneuvers |

## References

[1] A. E. Purwandanu, M. T. Toha, and Bochori, "Parameters Affecting Drilling, Blasting, and Shovel-Dump Truck Systems in Andesite Mines," *J. Min.*, vol. 4, no. 2, pp. 81–89, 2020. [in Bahasa]

[2] Y. P. Parissing *et al.*, "Analysis of Decline in Achievement of Nickel Ore Production Targets Using the Fault Tree Analysis Method at PT Ifishdeco, Southeast Sulawesi Province," *JPE J.*, vol. 24, no. 1, pp. 46–51, 2020. [in Bahasa]

[3] S. F. Rostiyanti, *Heavy Equipment For Construction Projects*. Jakarta: Rineka Cipta, 2008. [in Bahasa]

[4] S. V. Manyele, "Investigation of Excavator Performance Factors in an Open-Pit Mine Using Loading Cycle Time," *Eng. J.*, vol. 9, no. 7, pp. 599–624, 2017.

[5] S. Hidayat, T. Iskandar, and M. Kudiantoro, F. F. Wijayaningtyas, "Heavy Equipment Efficiency, Productivity and Compatibility of Coal Mine Overburden Work in East Kalimantan," *Int. J. Mech. Eng. Technol.*, vol. 10, no. 6, pp. 194–202, 2019.

[6] M. Fisonga and V. Mutambo, "Optimization of the Fleet Per Shovel Productivity in Surface Mining: Case Study of Chilanga Cement, Lusaka Zambia," *Cogent Eng.*, vol. 4, no. 1, pp. 1–16, 2017.

[7] I. Idham, S. Sumarya, and A. Octova, "Making Production Count Program Using Visual Basic Net Programming Language To Evaluate Productivity Of Loading Equipment And Transport Equipment In Limestone Mining Activities PT. Padang Cement," *J. Bina Tambang*, vol. 3, no. 1, pp. 379–389, 2018.

[8] M. R. Yusuf, Y. M. Anarta, and R. Malyudi, "Optimization of Loading Equipment Production in Overburden Stripping Using the 2018 Overall Equipment Effectiveness (OEE) Method at Block B PT. Minemax Indonesia, Mandi Angin Regency, Jambi Province," *J. Bina Tambang*, vol. 4, no. 3, pp. 98–108, 2018.

[9] C. W. Kang and P. Kvam, *Basic Statistical Tools for Improving Quality*. New Jersey: Hoboken, 2011.

[10] J. M. Juran and A. B. Godfrey, *Juran's Quality Handbook Fifth Edition*. New York: McGraw-Hill, 1999.

[11] H. M. Mustofa, "Work Productivity Planning from Productivity Evaluation Results with Fishbone Method at PT X . Packaging Printing Company," *J. Heuristic Ind. Tech.*, vol. 11, no. 1, pp. 28–46, 2014.

[12] A. E. Ilori, B. A. Sawa, and A. A. Gobir, "Application of Cause-and-Effect-Analysis for Evaluating Causes of Fire Disasters in Public and Private Secondary Schools in Ilorin Metropolis, Nigeria," *Arch. Curr. Res. Int.*, vol. 19, no. 2, pp. 1–11, 2019.

[13] H. R. Bernard, *Research methods in anthropology: Qualitative and quantitative approaches 3rd ed.* New York: Alta Mira Press, 2002.

[14] M. Coccia, "The Fishbone Diagram to Identify, Systematize and Analyze the Sources of General Purpose Technologies," *J. Soc. Adm. Sci.*, vol. 4, no. 4, pp. 291–303, 2018.

[15] Pratama and Pratiwi, "Productivity of the Sumitomo SH 210 Excavator Heavy Equipment in the Construction of the Sultan Agung Bandar Lampung Fly Over," *SENDI J.*, vol. 1, no. 1, pp. 48–53, 2020. [in Bahasa]

# Feasibility Analysis of Runway, Taxiway and Apron Dimensions of Torea Airport in Fakfak Regency, West Papua Province

Muhammad Yunus[a,*], Ratna Septa Sari Tuhepaly[b], Ahmad Fitriadhy[c]

[a]Department of Civil Engineering, Polytechnic State of Fakfak. Email: muhammadyunus@polinef.id
[b]Department of Civil Engineering, Polytechnic State of Fakfak. Email: ratnasarituhepaly@gmail.com
[c]Programme of Maritime Technology, School of Ocean Engineering, University Malaysia Terengganu. Email: naoe.afit@gmail.com

## Abstract

The development of transportation sector modes, especially air transportation modes, is currently experiencing very significant development. This is because the mode of air transportation in the form of aircraft can make people move very quickly, unlike land and sea transportation modes which require a longer time. In this regard, an airport that meets the requirements in terms of flight security and safety is needed. The study aimed was to analyze the dimensions of the runway, taxiway, apron and evaluate the feasibility of the runway, taxiway, apron dimensions at Torea Airport in Fakfak Regency, West Papua Province. From the results of the research conducted, it was found that the dimensions of the runway length of Torea Airport have met the minimum requirements set by the International Civil Aviation Organization (ICAO) in 2016 with a runway length of 1201.8 m Torea Airport but in terms of requirements for the type of aircraft ATR 72-600 does not meet the requirements. While for the standard dimensions of the runway width and the width of the runway shoulder of Torea Airport according to the Regulation of the Ministry of Transportation of the Directorate-General of Civil Aviation Number: KP 39 of 2015 concerning Technical and Operational Standards of Civil Aviation Safety Regulations.

*Keywords: Airport; International Civil Aviation Organization (ICAO); modes of transportation; runway*

## 1. Introduction

An airport is an area or area on land and or waters with certain boundaries that is used as a place for aircraft, in addition to landing and taking off, as well as a place for passengers to get on and off, loading and unloading goods, and a place for intra and intermodal transportation equipped with transportation facilities. aviation safety and security, as well as basic facilities and other supporting facilities [1, 2].

Along with flight fares in Indonesia that are increasingly affordable for the public, the increasing interest of the Indonesian people in using air transportation [1]. This is also what makes Indonesia experience very rapid development in the aviation industry [3].

Torea Airport is an airport that serves flights in the Fakfak Regency, West Papua Province. Not many flights depart from this airport, there is only one airline with one aircraft serving at the airport, namely Wings Air with ATR 72-600 aircraft [4].

Civil Aviation Safety Regulations – Part 139 (Manual Of Standard CASR - Part 139) Volume I, airports (aerodromes) are guidelines for airport operators so that every construction and operation of airports (aerodromes) can meet the technical and operational standards of airports that have been set determined by the Directorate General of Civil Aviation and as an effort to realize aviation security and safety [5, 6].

According to the Regulation of the Director-General of Civil Aviation No. KP 39 of 2015, airport safety is a vital link in aviation safety [6]. Airport safety is achieved by providing airport facilities and maintaining an airport environment that ensures the safety of aircraft operations [7-9]. By adhering to established standards and procedures and adopting a proactive safety management approach, airport operators can demonstrate that they have fulfilled their safety obligations to their passengers who are essentially a travelling public [10–12].

Torea airport facilities are currently far from good because the airport looks small and obstacles in the form of tall trees across the runway make it difficult for pilots to make the landing process [4]. Not to mention, to both ends of the runway and one side of the runway there are ravines. With such obstacles and gaps, the true aspect of flight safety is at stake. However, this aircraft continues to operate with several requirements, namely the cargo in the form of passengers and goods must not be optimal. However, this transportation restriction still has potential safety risks. The study aimed to analyze the dimensions of the runway, taxiway, apron and evaluate the feasibility of the runway, taxiway, apron dimensions at Torea Airport in Fakfak Regency, West Papua Province.

---

*Corresponding author. Tel.: +62-811-4212-748
*Jalan TPA Imam Bonjol Atas Air Merah, Kelurahan Wagom Fakfak, Papua Barat, Indonesia, 98611*

## 2. Literature Review

### 2.1. Airport definition

An airport is an area on land and/or waters with certain limits that are used as a place for aeroplanes to land and take off, boarding passengers, loading and unloading goods, and places for intra and inter-mode transportation, which are equipped with aviation safety and security facilities, as well as other facilities shops and other supporting facilities [13].

### 2.2. Airport facilities

Airport facilities have two types, namely basic facilities and supporting facilities. Both of these facilities are useful for organizing flight service activities. The following are the facilities at the airport:

a. Basic Airport Facilities

According to the Regulation of the Directorate-General of Civil Aviation through SKEP/77/VI/2005, the main airport facilities are as follows [14] :

1) Airside facilities
    a) Runway and runway markings
    b) Runway strip/runway end safety area
    c) Taxiway
    d) Apron
    e) Obstruction restriction facilities
    f) Drainage facilities
2) Landside facilities
    a) Passenger terminal building
    b) Cargo terminal building
    c) Operational building facilities
    d) Roads and vehicle parking

b. Airport Support Facilities

The following are facilities that support the needs for other activities at the airport :

1) Hotel
2) Restaurant
3) Motor vehicle parking facilities
4) General treatment facilities
5) Warehousing facilities
6) Aircraft repair facilities
7) Hangar facilities
8) Waste treatment facilities

### 2.3. Runway

a. Runway definition

According to SKEP – 161 IX (Runway, Taxiway, and Apron Planning Instructions, 2003), a runway is a pavement used by aircraft to land (landing) or take off (take off) [14]. According to Horonjeff, the runway at an airport consists of structural pavement, shoulder, blast pad and runway end safety area [15].

b. Runway classification

International Civil Aviation Organization divides the classification of airports based on the runway geometry available at an airport and the type of aeroplanes operating at the airport. ICAO classifies airports based on the Airplane Reference Field Length (ARFL) and the size of the aircraft (distance outside the main gear and wingspan) operating at the airport [9, 10] as shown in Table 1.

Table 1. Airport reference code

| Reference Code Aerodrome | | | |
|---|---|---|---|
| Element Code 1 | | Element Code 2 | |
| Code No. | Runway Length Reference for Aircraft use | Letter Code | Wingspan | Width of the distance between main wheels Outermost |
| 1 | < 800 m | A | < 15 m | < 4.5 m |
| 2 | 800 m - 1.200 m | B | 15 m - 24 m | 4.5- 6 m |
| 3 | 1.200 m - 1.800 m | C | 24 m - 36 m | 6 m - 9 m |
| | | D | 36 m - 52 m | 9 m - 14 m |
| 4 | > 1.800 m | E | 52 m - 65 m | 9 m - 14 m |
| | | F | 65 m - 80 m | 14 m - 16 m |

Table 2. Wide taxiway standards by ICAO

| Code Letter | Aircraft Classification | Wide Taxiway (m) | Minimum Clearance from Outer Side of Main Wheel with Taxiway Edge (m) |
|---|---|---|---|
| A | I | 7.5 | 1.5 |
| B | II | 10.5 | 2.25 |
| C | III | 15[A] 18[B] | 3[A] 4.5[B] |
| D | IV | 18[C] 23[D] | 4.5 |
| E | V | 25 | 4.5 |
| F | VI | 30 | 4.5 |

### 2.4. Taxiway

a. Taxiway definition

According to Basuki, the taxiway serves as a way in and out of the aircraft from the runway to the apron and vice versa, or from the runway to the maintenance hangar [13]. Taxiways are arranged so that a plane that has just landed does not interfere with another plane that is taxiing, ready to head to the end of take-off. At many airports, the taxiway makes a right angle with the runway so that landing aircraft must be slowed to a very low speed before turning onto the taxiway. However, a taxiway designed for aircraft to turn at high speed off the runway, will reduce runway usage time.

b. Wide Taxiway

Some of the requirements issued by ICAO in the geometric design of taxiways are as follows [8, 9] as shown in Table 2.

### 2.5. Apron

According to SKEP - 161 - IX Runway Planning Instructions, Taxiway and Apron, an apron is a certain part of an airport that is used to load/unload passengers to/from aircraft, loading and unloading goods or posts, refuelling, parking and maintenance aircraft. The apron is on the airside which is directly in contact with the terminal building, and is also connected to the taxiway leading to the runway [12]. The geometry of the apron is determined by the parking layout, the number and size of the gates and the geometry of the aircraft being served. The regulatory capacity in the apron is determined through the following parameters:

a) Fasteners on underground transport (parking lots, main roads).
b) Passenger management (number of check-in counters).
c) Management of goods (number of shelters and capacity of support systems).

Table 3. Wings clearance

| Code (letter) | Free Distance |
|---|---|
| A | 3.0 m |
| B | 3.0 m |
| C | 4.5 m |
| D | 7.5 m |
| E | 7.5 m |
| F | 7.5 m |

d) Passport check, security check, check before boarding (size of waiting room and the number of shelters).

As analysis for the apron, ICAO issued the following requirements for wing clearances as shown in Table 3.

### 2.6. Aircraft dimensions and size

The dimensions of the aircraft that need to be known include (Fig. 1):

1) Wingspan, is the distance or wingspan that is used to determine the width of the taxiway, the distance between taxiways, the size of the apron, the size of the hangar.
2) Length, is the length of the fuselage used to determine the width of the taxiway (bend), the width of the exit R/W, T/W, the size of the apron, the size of the hangar.
3) Height, is the height of the aircraft used to determine the height of the hangar door, as well as installation in the hangar.
4) Wheel/Gear Tread, is the distance between the main wheels from axle to axle which is used to determine the turning radius of the aircraft.
5) Wheel Base, is the distance between the main wheel (main gear) and the front wheel of the aircraft (nose gear) which is used to determine the T/W exit radius.
6) Outer Main Gear Wheel Span (OMGWS), is the distance between the outermost main wheels, where this value determines the Reference Code Letter.
7) Tail Width, is the rear wing width used to determine the area of the appron.

## 3. Research Methodology

### 3.1. Time and place of research

This research was conducted at Torea Fakfak Airport, Jl. Yos Sudarso Fakfak, Pariwari District, Fakfak Regency, West Papua Province. The research time is carried out from March-May 2021. The existing conditions at Torea Fakfak Airport can be seen in Fig. 2.
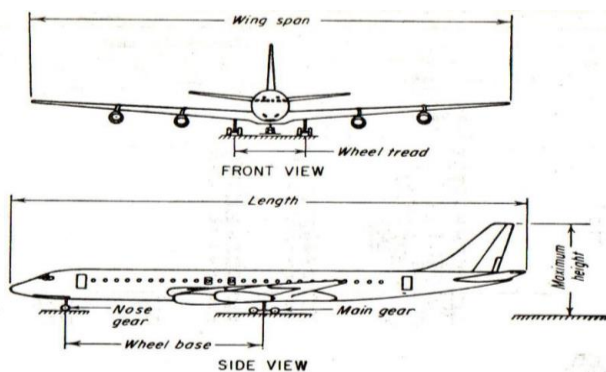


Figure 1. Aircraft characteristics components



Figure 2. General view from the Torea Fakfak airport

### 3.2. Data collection technique

The data collection carried out in this study used the direct observation method in the field. The data was obtained in the form of primary data and secondary data.

a. Primary Data

Primary data is data taken directly in the field, using the direct observation method which will obtain data on the existing condition of Torea Airport, Fakfak Regency. The data obtained is survey data conducted for 1 week with the following survey steps:

1) Prepare the tools used, namely preparing stationery, roll meter and push meter.
2) Requesting permission from Torea Fakfak UPBU (Airport Implementing Unit) for data collection.
3) The survey was conducted on the airside (runway, taxiway, and apron) of Torea Airport, Fakfak Regency during weekdays.
4) The survey was conducted by measuring the dimensions of the runway, taxiway, and apron at Torea Airport, Fakfak Regency. The data collection is carried out as follows:
   a) Length of runway, taxiway and apron
   b) Width of runway, taxiway and apron
5) Direct field observations are carried out carefully by taking into account the existing condition.

b. Secondary Data

Secondary data is data obtained from related parties, while secondary data needed include:

1) Data on temperature, the surface slope at the Torea. Airport location.
2) Data on the dimensions of the existing runway, taxiway, and apron at Torea Fakfak Airport.
3) Collecting secondary data in the UPBU office of Torea Fakfak Airport.

### 3.3. Data analysis techniques

Data analysis techniques used in this study with the following stages:

a) Sketching drawings and dimensions of Torea airport conditions according to the results of measurements and observations in the field.
b) Analyze the dimensions of the existing runway, taxiway, and apron at Torea Fakfak airport according to the results of the sketch drawing.
c) Evaluating the feasibility of the dimensions of the existing runway, taxiway, and apron at Torea Fakfak airport using ICAO (International Civil Aviation Organization) standards.

d) Provide recommendations for the feasibility of the dimensions of the existing runway, taxiway, and apron at Torea Fakfak airport using ICAO (International Civil Aviation Organization) standards.

## 4. Results and Discussion

### 4.1. Results

#### 4.1.1. The existing condition of measurement results

Data on the existing condition of Torea Fakfak Airport obtained from the results of direct measurements carried out at Torea Fakfak Airport obtained the data in Table 4.

#### 4.1.2. Airport existing condition

The data on the existing condition of Torea Fakfak Airport obtained from the Torea Fakfak Airport Operator Unit includes general airport data and data on the existing condition of the airport. These data can be seen in Table 5 and Table 6.

Table 4. Measurement data at Torea airport

| No. | Air Facilities | Results |
|-----|----------------|---------|
| | *Runway Dimension* | |
| 1. | - Length | 1201.8 m |
| | - Wide | 30 m |
| | *Taxiway Dimension* | |
| 2. | - Length | 53 m |
| | - Wide | 18 m |
| | *Appron Dimension* | |
| 3. | - Length | 110 m |
| | - Wide | 63 |

Table 5. Technical data of aircraft type ATR 72-600

| No. | Description | Aircraft Technical Characteristics Data |
|-----|-------------|------------------------------------------|
| 1. | Referensi Kode | 3C |
| 2. | Aeroplane references field length (ARFL) | 1290 m |
| 3. | Wingspan | 27.05 m |
| 4. | Outer Main Gear Wheel Span (OMGWS) | 4.10 m |
| 5. | Length | 27.16 m |
| 6. | Maximum Take-Off Weight (MTOW) | 22800 Kg |

Aircraft ATR 72-600 characteristics data

For data on the characteristics of the ATR 72-600 type aircraft serving flights at Torea Airport, Fakfak Regency, obtained from the 2015 General Air Transportation Regulation which can be seen in Table 5.

As for the grouping of airports and aircraft classes according to the 2015 General Regulation of Air Transportation, it is shown in Table 6.

### 4.2. Discussion

#### 4.2.1. Runway

- *Runway Length*

Torea Airport in Fakfak Regency is grouped into 3C group (ADC) with a runway length of between 1200 m – 1800 m and a wingspan of aircraft that can operate at Torea Airport (Table 7-8), Fakfak Regency between 24 m – 36 m. From the results of the research that has been carried out, a comparison of the runway length data obtained from measurements and data obtained from the Torea Airport Implementation Unit (UPBU) can be seen in Table 9 and Fig. 3.

Table 6. Airport grouping and aircraft class

| Airport Group | No. Code | *Aeroplane Reference Field Length* (ARFL) | Letter Code | Wingspan |
|---------------|----------|-------------------------------------------|-------------|----------|
| A (*Unattended*) | 1 | $\leq 800$ m | A | $\leq 15$ m |
| B (AFIS) | 2 | 800 m $\leq$ p $\leq$ 1200 m | B | 15 m $\leq$ \| $\leq$ 24 m |
| | 3 | 1200 m $\leq$ p $\leq$ 1800 m | C | 24 m $\leq$ \| $\leq$ 36 m |
| C (ADC) | | | D | 36 m $\leq$ \| $\leq$ 52 m |
| | 4 | $\leq 1800$ m | E | 52 m $\leq$ \| $\leq$ 65 m |
| | | | F | 64 $\leq$ \| $\leq$ 80 m |

Table 7. Torea airport general data

| No. | Description | Airport General Data |
|-----|-------------|----------------------|
| 1. | Airport Names | Torea |
| 2. | City / Regency | Fakfak |
| 3. | Manager Name | Directorate General Air Transportation |
| 4. | Airport Status | Class III (UPT) |
| 5. | Distance and Directions to Nearest City/Airport | ± 7 km |
| 6. | Airport Reference Coordinates | 02˚ 55' 11.5" S / 132˚ 15' 42" E |
| 7. | Elevation | 446 feet Msl |
| 8. | Temperature | 32˚ C |
| 9. | Types of Air Traffic Services | AFIS |
| 10. | Operating Hours | H/S 06.00 - 16.30 WIT |

Table 8. Torea airport existing condition data

| No. | Air Facilities | Existing Data |
|---|---|---|
| 1. | Dimension Strip | |
| | - Length | 1260 m |
| | - Wide | 60 m |
| 2. | Runway | |
| | a. Runway | 10 – 28 |
| | b. Designation/Number/Azimuth | 02° 55' 11.5" S |
| | | 132° 15' 42.2" E |
| | c. Dimension | |
| | - Length | 1200 m |
| | - Wide | 30 m |
| | d. Turning Area | Exist |
| | e. Long Slope | 1 % |
| | f. Transverse Slope | 1 % |
| | g. Surface Type | Asphalt Hotmix |
| | h. Strenght | Dsh 8 |
| | i. Pavement Clasification Ind (PCI) | - |
| | j. Flatness (Profil) | - |
| | k. Skid Resistance (Violence) | - |
| | l. Marking | |
| | - Runway Designation Marking | Exist |
| | - Runway Center Line Marking | Exist |
| | - Runway Edge Marking | Exist |
| | - Threshold Marking | Exist |
| | - Touchdown Marking | Exist |
| | - Aiming Point Marking | Exist |
| | - Exit Guidance Line Marking | Exist |
| 3. | Taxiway | Exist |
| | a. Dimension | |
| | - Length | 60 m |
| | - Wide | 19 m |
| | b. Long Slope | 0.8 % |
| | c. Transverse Slope | 1 % |
| | d. Surface Type | Asphalt Hotmix |
| | e. Strenght | Dsh 8 |
| | f. Rapid Exit Taxiway | |
| | - Minimum turning radius | R 15 |
| | - The angle of intersection between the rapid exit and the runway | R 15 |
| | g. Marking | |
| | - Taxiway Center Line Marking | Ada |
| | - Runway Holding Position Marking | Ada |
| | - Taxiway Guidance Marking | Ada |
| | - Taxiway Edge Marking | Ada |
| 4. | Apron | |
| | a. Dimension | |
| | - Length | 73 m |
| | - Wide | 64 m |
| | b. Long Slope | 0.50 % |
| | c. Transverse Slope | 0.50 % |
| | d. Surface Type | Asphalt Hotmix |
| | e. Strenght | Dsh 8 |
| | f. Marking | |
| | - Apron Edge Marking | Exist |
| | - Apron Guidance Marking | Not Exist |
| | - Parking Stan Position Marking | Not Exist |
| 5. | Fillet : (Round/Radius) R: | |
| | a. Runway with Taxiway | Exist |
| | b. Taxiway with Appron | Exist |
| 6. | Overrun (Stopway) | Exist |
| | a. Dimension | |
| | - Length | 60 m |
| | - Wide | 30 m |
| | b. Long Slope | - |
| | c. Transverse Slope | - |
| | d. Surface Type | - |
| | e. Strenght | - |

| 7. | Runway Strip | | 1260 m |
|---|---|---|---|
| | a. | Dimension | |
| | | - Length | 1260 m |
| | | - Wide | 60 m |
| | b. | Long Slope | - |
| | c. | Transverse Slope | - |
| | d. | The First 3m outward from the runway | Grass |
| 8. | Runway and Safety Area (RESA) | | Not Exist |
| | a. | Dimension | |
| | | - Long | 45 m |
| | | - Wide | 85 m |
| | b. | Long Slope | - |
| | c. | Transverse Slope | - |
| 9. | Obstacle Limitation Surface | | |
| | a. | Take off Runway 10 and Approach area 28 | |
| | b. | Take off Runway 28 and Approach area 10 | |
| | c. | Obstacle transitional surface | 30% |

Tablel 9. Runway length comparison based on research results

| No. | Description | Results |
|---|---|---|
| 1. | Torea Airport Implementation Unit (UPBU) | 1200.0 m |
| 2. | Existing Measurement | 1201.8 m |

Tabel 10. Standard runway length comparison of Torea airport

| Torea Airport Runway Length | ICAO Standard | Aircraft ATR 72-600 Standard |
|---|---|---|
| 1201.8 m | 1200 – 1800 m | 1290 m |
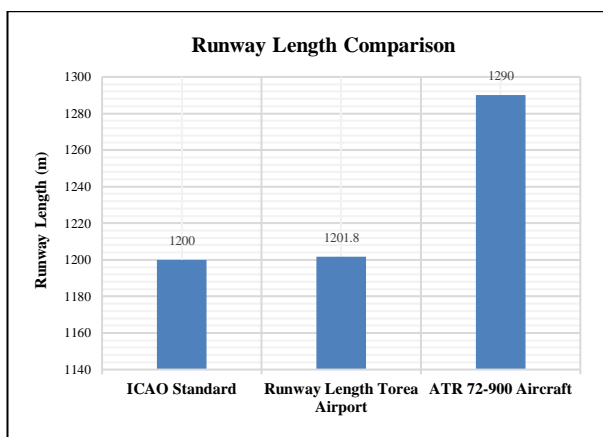


Figure 3. Runway length comparison of Torea airport

From Table 10 and Fig. 3, it can be seen that the length of the runway at Torea Airport in Fakfak Regency has met the minimum standard requirements set by the International Civil Aviation Organization (ICAO) in 2016 which is 1200 m. Meanwhile, according to the Regulation of the Ministry of Transportation of the Directorate General of Civil Aviation Number: KP 39 of 2015 concerning Technical Standards and Operations of Civil Aviation Safety Regulations which regulates the minimum standard limit for the length of the runway for the type of aircraft ATR 72-600 is 1290 m, so that if we analyze that the length of the Torea airport runway does not meet the minimum standard requirements and poses a risk to flight safety and security factors, especially for ATR 72-600 aircraft.

- *Runway Wide*

For data on the comparison of runway wide obtained from the results of measurements in the field and from the Torea Airport Implementation Unit (UPBU), which can be seen in Table 11 and Fig. 4.

From Table 11 and Fig. 4, it can be seen that the width of the runway at Torea Airport in Fakfak Regency has met the minimum standard requirements set by the International Civil Aviation Organization (ICAO) in 2016 which is 30.0 m (Table 12).

Table 11. Comparison of runway wide

| No. | Description | Result |
|---|---|---|
| 1. | Torea Airport Implementation Unit (UPBU) | 30.0 m |
| 2. | Existing Measurement | 30.0 m |
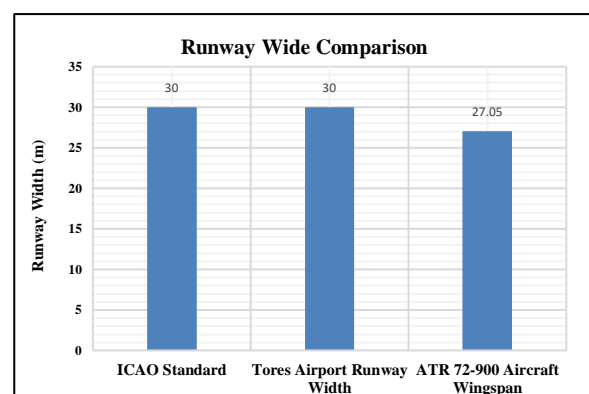


Figure 4. Runway wide comparison of Torea airport

173

Table 12. Standard runway shoulder dimensions according to ICAO

| Code Letter | Aircraft Classification | Runway Shoulder Wide |
|---|---|---|
| A | I | 3 m |
| B | II | 3 m |
| C | III | 6 m |
| D | IV | 7.5 m |
| E | V | 10.5 m |
| F | VI | 12 m |

Meanwhile, according to the Regulation of the Ministry of Transportation of the Directorate General of Civil Aviation Number: KP 39 of 2015 concerning Technical Standards and Operations of Civil Aviation Safety Regulations where it is regulated regarding the wingspan for the type of aircraft ATR 72-600 is 27.05 m (Ministry of Transportation, 2015), so that If we analyze it, the runway width of Torea Airport meets the minimum standard requirements for flights, especially for ATR 72-600 type aircraft operating at Torea Airport in Fakfak Regency. When the upper structure load is not working.

- *Runway Shoulder*

For the feasibility analysis of the runway shoulder at Torea Airport in Fakfak Regency, refer to the International Civil Aviation Organization (ICAO) standard in Annex 14 Vol I (2016) as seen in Table 9, where the dimensions of the runway shoulder are for the ATR 72-600 aircraft type. which has a 3C reference code is 6.0 m.

From the results of research conducted for the condition of the runway shoulder width of Torea Airport, it is obtained a comparison of the runway shoulder width according to ICAO standards and the existing condition of the runway shoulder width of Torea Fakfak Airport which can be seen in Table 13 and Fig. 5.

*4.2.2. Taxiway*

- *Taxiway Dimension*

The taxiway wide of Torea Fakfak Airport is 18 m, based on the ICAO standard in Annex 14 Vol I (2016), the taxiway width for the ATR 72-600 aircraft type which has a reference code 3C is 18 m. So, it meets the standards for use by ATR 72-600 aircraft as shown in Table 14 and Table 15.
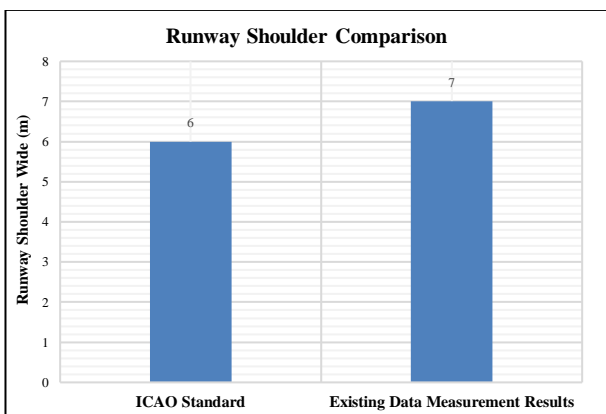


Figure 5. Runway shoulder wide comparison of Torea airport

Tabel 13. Runway shoulder-width comparison

| No. | Description | Results |
|---|---|---|
| 1. | Existing Measurement | 7.0 m |
| 2. | Standard ICAO | 6.0 m |

Table 14. Taxiway dimensión of ICAO Standard

| Code Letter | Aircraft Classification | Taxiway Wide (m) |
|---|---|---|
| A | I | 7.5 |
| B | II | 10.5 |
| C | III | 15[A] 18[B] |
| D | IV | 18[C] 23[D] |
| E | V | 25 |
| F | VI | 30 |

Table 15. Taxiway dimensión comparison of Torea airport

| No. | Description | Result |
|---|---|---|
| 1. | ICAO Standard | 18.0 m |
| 2. | Existing Measurement | 18.0 m |
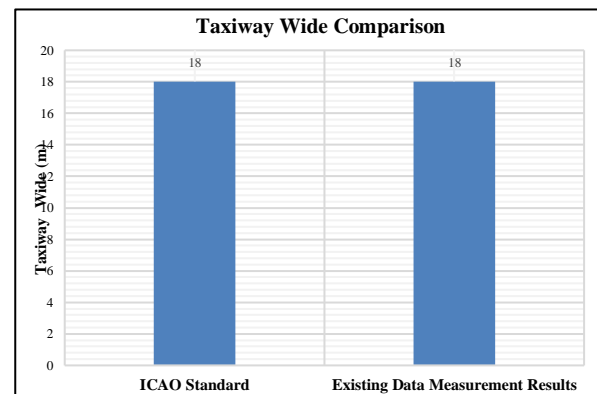


Figure 6. Taxiway dimensión comparison of Torea airport

From the results of the above analysis, a comparison of stopway dimensions according to ICAO standards and the existing condition of the runway width of Torea Fakfak Airport can be seen which can be seen in Fig. 6.

- *Taxiway Shoulder*

The taxiway shoulder width of Torea Fakfak Airport is 7 m, based on the ICAO standard in Annex 14 Vol I (2016), the runway width for the ATR 72-600 aircraft type which has a 3C reference code is 25 m. So, it does not meet the standards for use by ATR 72-600 aircraft as shown in Table 16 and Table 17.

Table 16. Taxiway shoulder of ICAO Standard

| Code Letter | Aircraft Classification | Minimum Width of Taxiway Shoulder on Straight Section |
|---|---|---|
| A | I | 25 m |
| B | II | 25 m |
| C | III | 25 m |
| D | IV | 38 m |
| E | V | 44 m |
| F | VI | 60 m |

Table 17. Taxiway shoulders comparison of Torea airport

| No. | Description | Result |
|---|---|---|
| 1. | ICAO Standard | 25.0 m |
| 2. | Existing Measurement | 7.0 m |
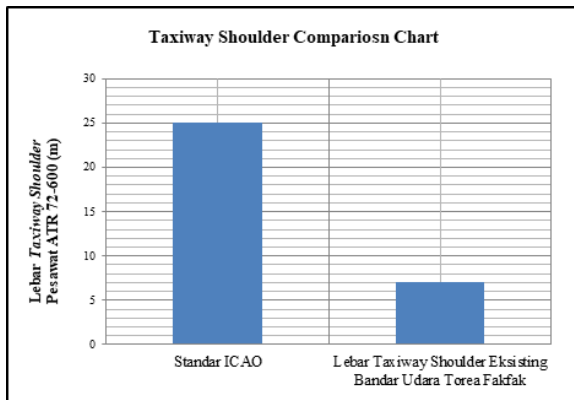


Figure 7. Taxiway shoulder wide comparison of Torea airport

From the results of the above analysis, a comparison of the width of the taxiway shoulder according to ICAO standards and the existing condition of the runway width of Torea Fakfak Airport which can be seen in Fig. 7.

### 4.2.3. Appron

The length of the apron at Torea Fakfak Airport which has a nose-in parking type of aircraft parking is 110 m and the width is 66 m, based on the ICAO standard in Annex 14 (2016), the length of the apron for the type of aircraft ATR 72-600 which has a reference code 3C is 95 m and the width is 45 m. So, it meets the standards for use by ATR 72-600 aircraft as shown in Table 18, Table 19 and Fig. 8.

Table 18. Apron dimensión of Torea airport

| No. | Description | Result Measurement |
|---|---|---|
| 1. | Apron Length | 110.0 m |
| 2. | Apron Wide | 66.0 m |

Table 19. Apron dimension comparison of Torea airport

| No. | Description | ICAO Standard | Existing Measurement |
|---|---|---|---|
| 1. | Length Apron | 95 m | 110 m |
| 2. | Wide Apron | 45 m | 66 m |
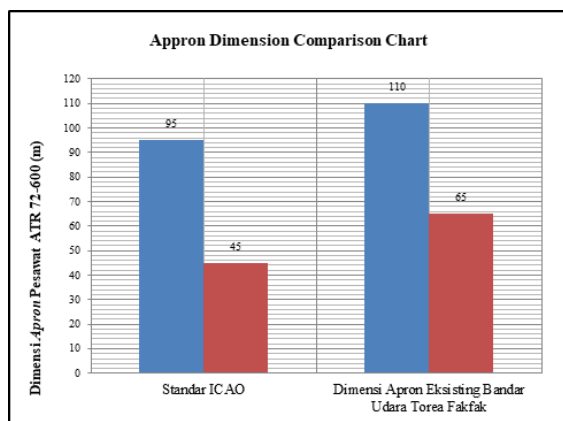


Figure 8. Apron dimension comparison of Torea airport

## 5. Conclusion

From the research results, it can be concluded that the length of the runway at Torea Fakfak Airport has not met the eligibility requirements for dimensions for ATR 72-600 aircraft because ATR 72-600 aircraft must land and take off at an airport whose type of air traffic service is C (ADC) with ARFL 1290 m, while Torea Fakfak Airport has a type of air traffic service that is B (AFIS) with a runway length (ARFL) of 1201.8 m and a runway width of Torea. The Torea Fakfak Airport Taxiway which has a width of 18 meters meets the standard for use by the ATR 72-600 aircraft type, the ICAO standard for the width of the taxiway which has a 3C reference code is 18 meters. The length of the apron at Torea Fakfak Airport which has a nose-in parking type of aircraft parking is 110 m and the width is 66 m, based on the ICAO standard in Annex 14, the length of the apron for the ATR 72-600 aircraft type which has a 3C reference code is 95 m and width is 45 m.

## References

[1]  H. Purwanto and S. Agung, "Runway, Taxiway, and Apron Planning Analysist at Sultan Mahmud Badaruddin II Airport Palembang Using FAA Method," *Deform. J.*, vol. 4, no. 1, pp. 21–30, 2019.

[2]  D. Warsito, *Airport Management : Runway, Taxiway and Apron.* Jakarta: Erlangga, 2017.

[3]  W. Sartono, Dewanti, and T. Rahman, *Airports: Introduction and Geometric Design of Runway, Taxiway, and Apron.* Yogyakarta: Gadjah Mada University Press, 2016.

[4]  T. R. S. Sari and H. Widyastuti, "Probability Analysis of Aircraft and Seaship Mode Selection on Fakfak-Sorong Route with Revealed Preference Method," *J. Civ. Eng. Appl.*, vol. 17, no. 1.

[5]  Directorate-General of Air Transportation Ministry of Transportation, "Regulation of the Director General of Civil Aviation," 2016.

[6]  Ministry of Transportation, "Regulation of the Director-General of Civil Aviation Number: KP 93 of 2015 concerning Technical and Operational Standards of Civil Aviation Safety Regulations - Section 139 Volume I Airport. I, 125.," 2015.

[7]  Federal Aviation Association (FAA), "Airport Capacity a Delay," United States, 2010.

[8]  International Civil Aviation Organization (ICAO), "Aerodromes- Annex 14 International," 1999.

[9]  International Civil Aviation Organization (ICAO), "Volume I Aerodrome Design and Operations," 2009.

[10]  P. J. Mapeda, S. V. Pandey, and L. G. J. Lalamentik, "Analysis of Runway Capacity at Sam Ratulangi International Airport Manado," *J. Civ. Static*, vol. 8, no. 1, pp. 83–90.

[11]  A. Mutaqin, "Geometric Analysis of Airside Facilities at Lombok International Airport," 2009.

[12]  A. Sandhyavitri and H. Taufik, *Airport Engineering 1 (Basic Theory).* Civil Engineering Department Riau University, 2005.

[13]  H. Basuki, *Designing and Planning Airport.* Bandung: P.T. Alumni, 1986.

[14]  Regulation of the Director-General of Civil Aviation Number: SKEP/161/IX/03, "Instructions for Implementing Runway, Taxiway, and Airport Design."

[15]  R. Horonjeff and F. Mckelvey, *Airport Planning and Design.* Jakarta: Erlangga, 1993.

# The Function, Space, Form and Meaning of the Traditional House of *Tolaki* Tribe in Konawe, Southeast Sulawesi

Nidia Islamiah[a,*], Ria Wikantari[b], Asniawaty Kusno[c]

[a]Department of Architecture, Faculty of Engineering, Hasanuddin University. Email: nidiaislamiah94@gmail.com
[b]Department of Architecture, Faculty of Engineering, Hasanuddin University. Email: rwikantaria@gmail.com
[c]Department of Architecture, Faculty of Engineering, Hasanuddin University. Email: asniawaty@unhas.ac.id

## Abstract

The architecture of traditional house of the *Tolaki* tribe has characteristics that indicate the activities, identity and socio-cultural values of the community. This study aimed to examine the function, space, form, and meaning of the traditional house of the *Tolaki* tribe. Field surveys were conducted at Meluhu Village in Meluhu District and Asambu Village in Unaaha District of Konawe Regency. This research is qualitative with phenomenological method. Data were collected through field observations, in-depth interviews, and document studies. The objects of research were is *Laika Mbuu* (main house) and *Laika Aha* (big house) houses which were selected from nine forms of *Laika* in Konawe Regency using purposive-criteria sampling technique. Data were analyzed descriptively, then the results were discussed and associated with relevant theories. The result revealed that the function of *Laika Mbuu* and *Laika Aha* was formerly the residence a *Mokole* (King) and a place to hold traditional ceremonies. However nowadays *Laika Mbuu* has become a communal gathering place and other public purposes, whereas *Laika Aha* become a customary house for ceremonial events. The spatial arrangement *of Laika Mbuu* has no partition hence the local community can carry out all activities in one open space, whereas *Laika Aha* still remains with partitions that divide the space into several rooms. Both the *Laika Mbuu* and *Laika Aha* have a rectangular building shape. The square shape on the building facade has a bottom container called *Kalo Sara*, which is a set of objects perceived as symbol of social class and has a meaning as customary law in the *Tolaki* community. This research concludes that both the *Laika Mbuu* and *Laika Aha* are similar in function and form but different in spatial arrangement. Both the *Laika*s express many symbolic meanings, among others that the house as symbol of a human body, and the residents symbolize organs of the human body, so that once the house is built and filled, it must try to protect itself from all obstacles and calamities.

*Keywords: Customary house; Laika Aha; Laika Mbuu; symbolic meaning; traditional architecture; Tolaki tribe*

## 1. Introduction

Traditional houses were commonly built in the same way by previous generations without undergoing any changes so that the houses were formed based on the traditions that existed in the community. Traditional houses are also called customary houses or original houses or folk houses [1].

A house is the result of culture, the product of the hands and the human minds guided by their cultures which are manifested in the form of physical buildings and which have certain functions and values [2]. On the other hand, in a traditional society where the house represents a microcosm of the whole universe. Every element of the house may symbolizes a particular element of the universe.

In the architecture of the *Tolaki* community in Konawe, a house is called *Laika* which has several forms, namely *Laika Aha* (large house or palace), *Komali* (palace) or *Laika Mbinapati* (carved palace house), *Laika Mbu'u* (main house), *Laika Landa* (garden house), *Laika Kataba* (board house), *Patende* (rest area), and *Laika Mborasa'a* (guard house). The differences between these seven buildings are the size of the building's height, the type of stairs, the carvings, the function, and the meaning of the building [3]. Considering the physical condition of the existing buildings and the state of their habitability, this study discussed two of the most intact ones that are *Laika Mbuu* and *Laika Aha*.

A number of previous studies have discussed the *Tolaki* tribe, including the concept of religion, system of government, to the traditional customs [4-8]. However, the discussions about *Laika*, particularly regarding the function, space, form and meaning not been carried out more rigorously by previous researchers.

Studies on the relationship between the *Laika*s and the socio-cultural activities as well as the community values of

*Corresponding author. Tel.: +6285249936621
*Kompleks Villa Racing Center, Blok. A, No.18*
*Makassar, Sulawesi Selatan, 90231*

176

the *Tolaki* tribe are still lacking. In this regard, this study intended to raise the uniqueness of the architecture of *Laika Mbuu* and *Laika Aha* as the objects of research. Accordingly, this research aimed to examine the traditional houses of the *Tolaki* Tribe in Konawe Regency, focusing on the function, space, form and meaning of both the *Laika Mbuu* and *Laika Aha*.

## 2. Literature Review

### 2.1. Functions in architecture

Function is a group of activities belonging to the same type based on its nature, implementation, or other considerations. Broadbent [9] asserted six functions that can be carried out by architecture, namely:

a. Environmental filter
b. Container of activities
c. Capital investment
d. Symbolic function
e. Behavior modifier
f. Aesthetic function

Moreover, according to Norberg-Schulz [10] there are four functions in architecture, namely:

a. Physical control
b. Functional frame
c. Social milieu
d. Cultural symbolization

So according to Christian Noberg Schulzt [10] function is a task and work that must be carried out by an environment.

### 2.2. Space in architecture

According to Prijotomo [11] space is a part of the building in the form of cavity, between two objects and the open nature that surrounds and encloses us. Space is not a visible object that tangible, it can only be felt by hearing, smelling and touching.

Rapoport [12] stated that there are five aspects that can affect the formation of dwellings, these are:

a. Some basic need, which is a basic human need.
b. Family, namely the existence of a lifestyle that adheres to the understanding of polygamy or monogamy and the existence of planning for house expansion because one family with relatives living together.
c. Position of women, the position and role of women that create different perceptions and interpretations of space in the social system of a particular society.
d. The need for privacy, namely the role of having self-esteem in the space that is its territory and personal places that can influence a person's attitude which refers to self-liberation.
e. Social intercourse, where humans need the opportunity to meet or gather with other people.

According to Surasetja [13] space is formed by three elements that make up space, namely:

a. The base plane
b. The vertical space divider
c. The overhead plane

### 2.3. Forms in architecture

Shape is the result of a certain configuration of the surfaces and sides of the shape [14]. Shapes can also be recognized because they have visual characteristics, namely:

a. Form, is the result of a certain configuration of the surface and sides of the form.
b. Dimensions, a shape is length, width and height. This dimension determines the proportion, while the scale is determined by the ratio of its size relative to the shape around it.
c. Color, is the pattern, intensity and tone on the surface of a form. Color is also the most striking attribute that distinguishes a form from its environment.
d. Texture is the surface character of a shape. Texture affects how we feel when we touch it, as well as when the quality of the reflection of light hits the surface of the shape.
e. Position, the relative location of a shape to an environment or visual field.
f. Orientation, the relative position of a shape to the base plane, the cardinal directions or to the viewer's view.
g. Inertia visual, is the degree of concentration and availability of a form

With appreciation of the form we can get satisfaction. Being can captivate our attention, invite curiosity, give a pleasant or unpleasant sensation in various ways.

### 2.4. Meaning in architecture

Meaning is intersubjective because it is grown and developed individually. However, meaning is shared, accepted and approved by the community, to comprehensively interpret the meanings that are interwoven in various wide and complex networks of social relations. Thus, a system of meaning becomes a cultural unit for the phenomena described [15]. Art is a sensory phenomenon that supports implicit meaning, the meaning of art and culture cannot be separated from the form of its symbols even though it is theoretically separated from it.

Phenomenology uses the word meaning in terms of the essence or nature of something, psychoanalysis uses it to explain will and desire, aesthetics uses it to describe a certain level of emotion involved in a work, hermeneutics sees meaning as the product and interpretation of a text, symbolic is concerned with the unique relations between an object and the world and semiotics uses the term meaning to explain the concept behind a sign.

According to Sumarjo [16] what is meant by referent is everything, object, fact, quality, experience, idea, thought, response, psychological, and so on. While symbols in the

form of words or images that must be interpreted, when a symbol is expressed, meaning appears. Symbols in premodern Indonesian culture do not simply refer to concepts but something absolute, something transcendent, the immanence of God, something supreme. The symbol is a sign of absolute presence. The symbols in modern civilization refer to meanings, concepts and experiences.

Referring to the description above, this research on *Laika Mbuu* and *Laika Aha* examines the cultural and social meanings. The purpose of the study is to find out the cultural meanings such as customs and cultural beliefs of the *Tolaki* tribe as well as the social meanings contained in the *Laika Mbuu* and *Laika Aha* buildings, such as social strata and socio-cultural interactions in the *Tolaki* tribe.

## 2.5. A brief history of the Tolaki tribe

Regarding the historical background, it can be stated that before the *Tolaki* tribe inhabited this area it is suspected that the indigenous people who inhabited the coastal area of the Konawe Eha River were *To Laiwoi*. They lived in rock caves and subsisted on farming and hunting. They were very small in number and lived in remote places, before the coming of a group of people from the North who to be called the *Tolaki* people afterwards. The existence of the *Tolaki* tribe historically cannot be separated from *Kalo Sara,* an object or a set of objects considered sacred by the tribe.

*Kalo Sara* for the *Tolaki* people is something that can integrate the elements that exist in *Tolaki* culture which has four functions [17], namely:

a. Idea in culture and as a reality in the life of the *Tolaki* people.
b. Focus and integration of elements of *Tolaki* culture.
c. Way of life for the creation of social and moral order in the life of the *Tolaki* society.
d. Unifier and solution to socio-cultural conflicts in the life of the *Tolaki* people.

The *Tolaki* people generally live by farming, fishing, hunting, trading, carpentry, civil servants, and others. The *Tolaki* tribe is called *rapu* which means clump, someone who marries is called *merapu* which means to form a new clump or household. Each nuclear family has its own house and takes care of its own household economy as well.

Before embracing Islam and Christianity, the *Tolaki* people believed in gods who controlled nature and life. Besides, there is belief in spirits, supernatural powers, metaphysical powers, and so on. Among the *Tolaki* tribe, the God is known as *Sangia*. There are three main *sangia*, namely:1) *Sangia Mbuu* (god of tree) as the creator of nature; 2) *Sangia Wonua* (land god) who takes care of nature; and 3) *Sangia Mokora* (god of destruction).

## 2.6. Traditional Tolaki architecture

The house is one of several shelters in the architectural civilization of *Tolaki*, namely as: 1) Temporary shelter (*Pineworoko*); 2) Moveable shelter (*Payu*); 3) Lake (*Patande*); and 4) Barn (*O'ala*).

Based on the function, the *Tolaki* people recognize several types of houses, those are:

a. Palace or Big House (*Laika Aha*), a building that has a wide, large, and rectangular shape made of wood which is raised about 20 feet above the ground, and is located in the forest.
b. House in the Garden (*Laika Landa*), namely the type of house built in the middle or on the edge of the garden and inhabited by a family.
c. *Patande*, namely the type of house built in the middle of the garden as a place of resting. The shape of the building is smaller than *Laika Landa*.
d. Burial House (*Laika Soronga* or *Laika Nggoburu*), that serves as the burial house for the king (*Mokole/ Sangia*).
e. Board House (*Laika Kataba*), a board type building that was built using a certain password or code.
f. Headhunting House (*Laika Mborasaa*), a type of house that was built in a place of guard, and as a place of resting for people who have carried out the task of headhunting.
g. King's Residence (*Komali*), a type of *Laika Owose* or a big house, a strong and tall building.
h. Land House (*Laika Wuta*), a smaller building than *Laika Landa*, which shape of roof is like a *jengki* house.
i. Rice Storage (*O'ala*), a type of storage house, small in shape with high pillars, its wall material consists of thick barks, arranged tightly with four or six pillars.
j. Dutch Architectural Style Long House (*Laika Walanda*), a type of long house, also known as a Dutch house which is used as a place to relax and party.
k. Roast House (*Laika Mbondapoa*), a type of building on stilts where copra is roasted.
l. Main House (*Laika Mbuu*), a type of building that is larger than an ordinary house, also often referred to as the main house or prime house and is erected on the outskirts of fields or gardens.

The house where the *Tolaki* tribe lives consists of the following parts: 1) Pole (*Otusa*); 2) Floor (*Ohoro*); 3) Wall (*Orini*); 4) Door (*Otambo*); 5) Ladder (*Lausa*); 6) Rafter (*Olaho*); 7) Roof (*O'ata*); 8) Insert house (*Powire*); 9) Window (*Lomba-lomba*); 10) House ridge shape (*Pemumu*); 11) Attic (*Lembe-Lembe, Owaha* and *Para-para*); 12) Additional space (*Tinumba, Kinesa, Galamba*); and 13) Connection room (*Pineworoko*).

Prior to the construction of a *Tolaki* traditional house, a ceremony is conducted called *mombaka owuta* which means feeding the land, while during the construction process another ceremony is also carried out called *molisa* which means restoring. The purpose of all these ceremonies is as a repellent for reinforcements, so that the residents of

the house can live healthy and peaceful lives, lots of good luck, and away from all diseases and calamities.

## 3. Research Method

This research is qualitative with phenomenological methods. The researcher collects data about the traditional houses of the *Tolaki* tribal community, especially regarding the function, space, form and meaning, including facts, aspirations, and idea, which are obtained through field observations and direct interactions with informants in the community, and analyzes the phenomena that occur.

### 3.1. Research sites

The research is located in Konawe Regency, South Sulawesi Province. *Laika Mbuu* is in Meluhu Village, Meluhu District, while *Laika Aha* in Arombu Village, Unaaha District (Figs. 1 and 2).
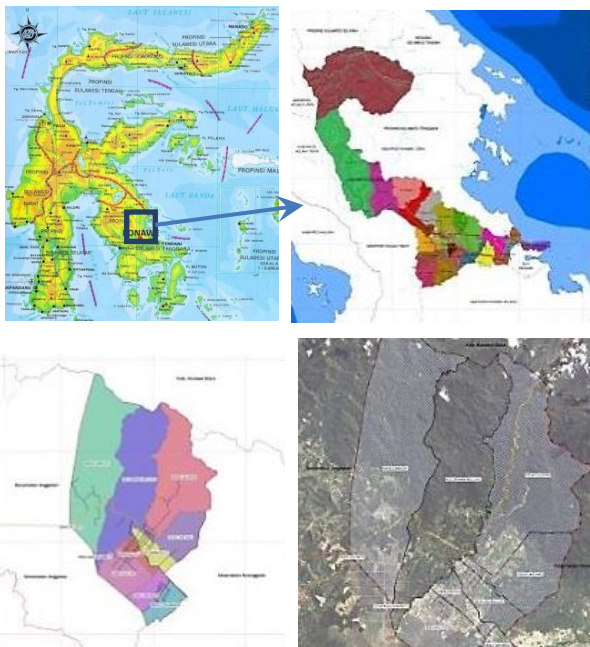


Figure 1. (a) Map of Sulawesi Island (b) Map of Konawe Regency; (c) Meluhu District; (d) Meluhu Kelurahan Village



Figure 2. (a) Unaaha District Map; (b) Arombu Village Map

### 3.2. Research object

The object of research is a scientific goal to obtain data with a certain purpose and use about something objective, valid and reliable about a thing or a certain variable [18]. The objects examined in this research are: a*) Laika Mbuu*, the former palace or the king's residence of *Mokole* More Wekoila (circa 1150), however at present this building has been rebuilt and become the home of the indigenous community of *Wonua Ndinudu Meluhu* which is a *Tolaki* community located in the administrative area of Meluhu District; b) *Laika Aha* which used to be the palace or the king's residence of *Mokole* Lakidende II (circa 1701). For the purpose to maintain and preserve the customs and culture of the ancestors, the local government has rebuilt the *Laika Aha* in order to bring back the wheels of the past and the local wisdom of the *Tolaki* people.

### 3.3. Data collection

Data were collected using 3 techniques: 1) Field observation; 2) In-depth interviews with informants who were selected using purposive-criteria sampling and snowball sampling; and 3) Archive and document studies. The informants comprised of: (1) Ajemain Suruambo who was *Puutobu Ndinuhu* Meluhu; (2) Gusli Topan Sabara, H. Ujung Lasandara and Bachrudin Lakoreasa who are traditional leaders for the *Tolaki* community; (3) Basrin Melamba who is a historian and writer about *Tolaki* tribal culture; (4) Lasmudin Pagala who is an ordinary people.

### 3.4. Data analysis

Qualitative data analysis is an effort made by working with data, organizing data, sorting it into manageable units, synthesizing it, looking for and finding patterns, discovering what is important and what is learned, and deciding what to tell others [19]. The data analysis process is carried out with the following stages:

- Data reduction: as the process of selecting, focusing on simplifying, abstracting, and transforming rough data that emerges from written notes in the field.
- Display (data presentation): limited as a set of structured information that is adjusted and clarified to make it easier for researchers to master the data and not be immersed in a pile of data.
- Verification (conclusion): during the research, the meanings that emerged from the data that were tested for their validity, robustness and compatibility were then linked to theoretical insights that served as background knowledge.

## 4. Discussion

### 4.1. The function, space and meaning of the Tolaki tribe traditional house

*Laika Mbuu* has the meaning of main house and *Laika Aha* has the meaning of big house. Although with different names both the two buildings have the same function as the

residence of the king, the center of government, and a place to hold customary events or traditional ceremonies. At the reigning time of the *Mokole More Wekoila* kingdom, cultural influences were very strong. The development of traditional architectural values was very important as a reflection of symbolical performance of social strata. The king's house was called *Laika Mbuu*, the house which at that time had the largest size and was domiciled in Unaaha as the center of government.

At the time *Mokole Lakidende* II came to power, he built his house as *Laika Aha* or the big house, before he moved the government from Unaaha to Anggaberi. *Laika Aha* was built very large with the extra large to accommodate many people when an important meeting was held by the village leaders. Another reason was that the large size was made so that the house was built as a respect for *Mokole*.

The form of *Tolaki* tribal house reflects two meanings, namely: 1) A house as traditional customary space; and 2) A house as devided spaces, where the house symbolizes application of a human body, and the occupant as fillers symbolize organs of the human body. Accordingly, once the house is built and filled, it must try to protect itself from all obstacles. When the house does not have interior elements and details then it is considered as a house that is functioned not for its occupants but for everyone, so that it expresses openness and keeps no secrecy.

Spatial arrangement of the house vertically and horizontally can be described as the followings:

a. Vertical

Vertically, *Laika Mbuu* and *Laika Aha* are divided into three parts, namely, *Wawo Laika* (top of the house), *Tonga Laika* (middle of the house), and *Lolo Laika* (bottom of the house) as shown in Fig. 3.

- *Wawo Laika*

*Wawo Laika* is called the upper house, which has the meaning of life above human consciousness, related to beliefs that are not visible (holy, goodness, suggestion, sacred). As in the understanding of *Tolaki* society, the world above is the abode of the Goddess of Rice (*Sanggoleo Mbae*). With this understanding and belief, many *Tolaki* people use the top of the house as a storage place for rice or other agricultural products, also as a hiding place for girls who are being secluded.
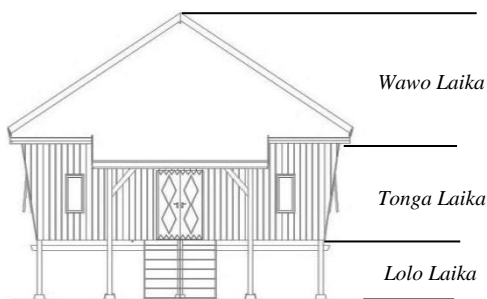
- *Tonga Laika*

*Tonga Laika* which is called the middle of the house, contains the meaning of life in the human consciousness which is related to daily activities. *Tonga Laika* or the body of the house is also divided into three parts, consisting of the front which is used for receiving relatives or family and a place for traditional activities, the middle part which is used for bedrooms, and the back which is used for the kitchen.

- *Lolo Laika*

*Lolo Laika* which is called the bottom of the house, constitute the part of the house that is between the floor and the ground. This section is usually used as a place to store agricultural tools, also to raise livestock, and other activities related earning a living.

The meaning of the vertical spatial arrangement of the interior spaces is manifestation of the human body. The top of the building or the attic space of the roof is identified as the sky or the human head, the middle space of the building is identified as the surface of the earth or the human body trunk, and the bottom of the house or space under the house is identified as the human foot of the underworld.

b. Horizontal

Horizontally, the *Laika Mbuu* building is divided into four parts, namely (Fig. 4):

- Front part: *Tinumba Hohu.*
- Middle part: *Butono Laika.*
- Attic part: *Lembe-lembe.*
- Rear part: *Dongge.*

The *Laika Mbuu* is a unique building since it does not have partitions between one room and the others. *Butono Laika* is a room that serves as a meeting place, a place for reception of guests, a place to eat, a place to sleep and even this place can be a multipurpose room, while the kitchen or *dongge* is on the back side as shown in Fig. 5.

In *Laika Mbuu* there is *lembe-lembe* which means the attic of the house which functions as a place for storing valuable objects, a place for ancestor worship, a place for storing crops, and a place for seclusion for girls as shown in Fig. 6.



Figure 3. *Laika* vertical shape
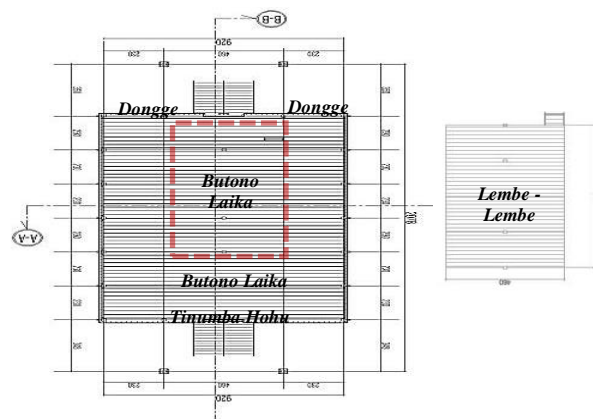


Figure 4. Floor plan *Laika Mbuu*

Figure 5. (a) *Butono Laika Mbuu*; (b) *Dongge Laika Mbuu*



Figure 6. *Lembe-lembe Laika Mbuu*



Figure 7. *Tinumba Hohu Laika Mbuu*
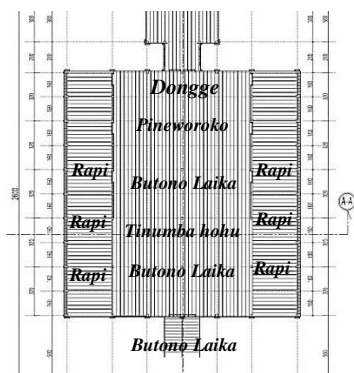


Figure 8. Floor plan *Laika Aha*

*Tinumba Hohu* shown in Fig. 7 means the terrace of the house that serves as a place to pound rice and a place to wait for guests before entering the house.

The *Laika Aha* consists of three parts, namely: 1) The *Tinumba Hohu* and *Butono Laika*, 2) *Rapi*, the middle part, and 3) *Pineworoko* and *Donggae* the, rear part.

Figure 8 shows that there is a space *tinumba hohu* which means the terrace of the house that serves as a transitional space from the outside area to the inside of the house or vice versa. The location of the terrace is in front of the house, and the function is as a waiting place for guests until the host comes out to entertain. This is because at *Laika Aha* shown in Fig. 9 every new guest or ordinary people must firstly get permission before entering the house, and not to behave carelessly in entering the house.



Figure 9. *Tinumba Hohu Laika Aha*



Figure 10. *Butono  Laika Aha*

*Butono Laika* shown in Fig. 10 means the living room or the guest room that serves as a room to receive ang entertain guests. In *butono laika* there are no chairs and tables for guests. Instead, the owner of the house only uses mats as a seat to be set on a raised floor that has a different floor height with a size of about twenty-five centimeters, also sloping wall that functions as a place to lean on for guests.

*Rapi* shown in Fig. 11 means a room as an insulated space, used as a resting place for the owner of the house. *Laika Aha* has a total of six *rapi* which are also commonly occupied by the nobles when visiting. *Rapi* is also a place for discussion, yet ordinary people are forbidden to enter. All *rapi* rooms have the same size so that there is no differences between one aristocrat and the others.

*Pineworoko* is the connection between the main house and the kitchen, also a place to put the water basin or water well of the home owner. *Dongge,* which is also a separate building, is kitchen that serves as cooking and dining place.

When the construction is completed and the owner of the house will enter the house, a ceremony is held with the aim that all residents of the house can live safely and peacefully. In order to carry out the ceremony, the owner of the house will call *mbusehe* as the leader and performer of the ceremonies.
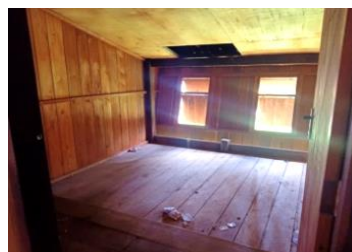


Figurue 11. *Rapi  Laika Aha*

### 4.2. The shape and meaning of the Tolaki tribe traditional house

• *O'tusa* (Pole)

In every house on stilts, the first thing that is erected is the pillar of the house shown in Fig. 12. The pole is the part of the house that functions as a support for the house to carry the burden of the body of the house such as the floor, walls and roof. The buildings of *Laika Mbuu* and *Laika Aha* have the shape of a rectangular house pole, and the pole material must be especially selected wood, namely iron wood (*nona*). Moreover, the wood must be selected first consideraing that the tree trunk to be used should not have branches.

In addition, the meaning of the rectangular pillar is a hope that everything given by the ancestors will reach their successors as inheritance that remains intact. The concept of intactness is in the sense that everything given by their ancestors can be maintained and continuously implemented such as traditional rules, customary laws, ceremonial events, festivities, and rituals.

In pole construction, as shown in Fig. 13, in order to protect the base of the pole from being eaten by termites and other insects also fungus, the tip must be firstly burned to become charcoal. The charcoal naturally will not rotten in the soil, and will be safe from termites (called *anai-anai* in the *Tolaki* language) attacks.

The nowadays existing *Laika Mbuu* and *Laika Aha* use a pedestal made of trapezoidal concrete. The pedestal is installed under each support post as shown Fig. 14. All poles are interconnected each other with wooden beams that are installed at the bottom of the pole, which also serves as a support for the floorboards. The top of the pole is then attached to the roof frame. In order to maintain durability of the wood, the pedestal is constructed protruding from the ground surface as high as 20 cm.


Figure 12. (a) *O'tusa Laika Mbuu*; (b) *O'tusa Laika Aha*
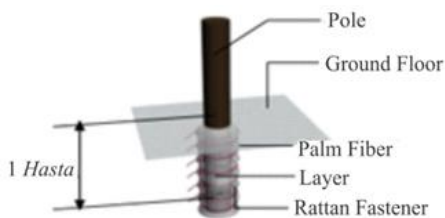

Figure 13. *Laika* foundation system


Figure 14. (a) Home baseboard *Laika Mbuu*; (b) Baseboard *Laika Aha*


Figure 15. (a) *O'tusa Laika Mbuu*; (b) *O'tusa Laika Aha*

After the installation of *Otusa Petumbu*, the eight pillars are installed surrounding it and continue to the installation of other *Otusa*s aferwards shown in Fig. 15. Furthermore, there are four pillars at the corners of the house called *tusa huno* which are the main pillars of the house. The main poles must not have interconnecting parts, they must be whole poles fro the base to the upper cover of the pole. Other poles that are located between the main poles are called *totoro* or supporting pole.

In the interior space of *Laika Mbuu* and *Laika Aha*, there are four pillars that symbolize the Konawe kingdom's territory and their meanings, namely: 1) *Bara Tahihara* which is called the right side wing or the north side, 2) *Bara Tahi'iwohei*, the left wing or the south side; 3) *Tambo Loso Alo Oleo,* the east gate, and 4) *Tambo Tepui Alo Oleo*, the west gate.

The number of poles in *Laika Aha* as many as ninety pillars and *Laika Mbuu* has seventy-seven pillars. In *Tolaki* society, odd numbers relate to leadership in the sense that odd numbers are equated with the structure of Konawe kingdom called *tolu eto lausa* and *sio sowu ananiawo* which mean three hundred steps or three hundred household heads and nine hundred commoners.

Material for *otusa* is sepecially selected wood which is usually called spinach wood (*upi*), iron wood (*nona*), and bitti tree. The height of the ground floor space under the main floor is based on consideration to the extent of being unreachable by buffalo horns when tied under the house.

• *Ohoro* (Floor)

The floor is the basic part of a space, which has an important role to strengthen the existence of objects in the space. The function of the floor in general is to support activities in space. The floor of the house is used to put furniture and household appliances such as chairs, tables, cabinets, and so on and supports various activities such as walking.

Figure 16. (a) *Ohoro Laika Mbuu*; (b) *Ohoro Laika Aha*
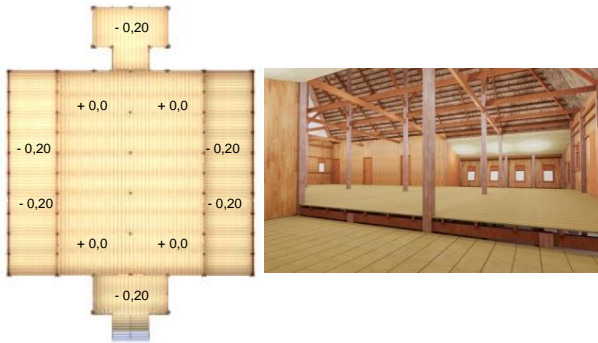


Figure 17. Height *Ohoro Laika Aha*

The floors of *Laika Mbuu* and *Laika Aha* shown in Fig. 16 are made of board construction which is positioned longitudinally called *porambuhi*, and arranged rather rarely called *sumaki* or *polandangi* which aims as gaps for the wind to enter from the groundfloor underneath.

There is a different in floor height in *Laika Aha* which is located on the front, the right and left sides of the building, the terrace, also the neck of the building to the kitchen, where the floor height is meant to differentiate the seating of *Mokole* with the people as shown in. Fig. 17.

- *Orini* (Wall)

The wooden wall is space divider which is generally built vertically as shown in Fig. 18. The essence of the wall lies in its capacity as a separator of two areas that cannot be penetrated, even if it is manifested in a transparent or non-solid form. Board walls that are arranged vertically produce the shape of a building facade that has elements of vertical lines. Board walls with a vertical type are directly attached to wooden posts and beams. Installation only uses nails that are used at every connection of the board walls and the beam. The board are installed tightly to avoid opening gaps in the walls. The vertical line is also a measuring tool for the occupants.



Figure 18. (a) *Orini Laika Mbuu*; (b) *Orini Laika Aha*



Figure 19. *Lembe-lembe Laika Mbuu*

*Orini* or the walls are shaped like rectangular pillars following the shape of the house. *Orini* limits a building and supports other structures, restricts space in a building into a room, or protects or limits a space in the open nature. *Orini Laika Mbuu* and *Laika Aha* are installed vertically and the wall is tilted about 15 degrees, this wall serves as a replacement backrest *kadera*.

- *Lembe-lembe* dan *O'waha* (Attic)

*Lembe-lembe* or an attic is located at the top of the building as shown below.

*Lembe-lembe* in *Laika Mbuu* functions as a place for protecting girls, a place to store heirlooms, a place to store agricultural products, also a place to present offerings to the ancestors as seen in box notation in Fig. 19.

*Lembe-lembe* It has a width of three meters and a length of five meters at a height of two meters and a half from the ground floor of the building and there is a circular slit measuring twenty centimeters to see outside the building walls.

*Owaha* shown in Fig. 20 is also a building attic which is located above the kitchen door and serves as a place to store food and other kitchen utensils. *Lembe-lembe* and *owaha* are only found in the *Laika Mbuu* building and not in *Laika Aha*.
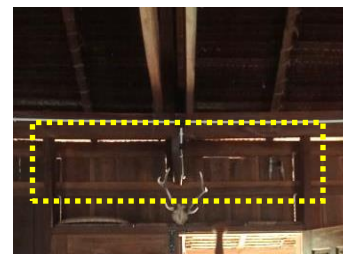


Figure 20. *Owaha Laika Mbuu*



Figure 21. (a) *Lausa Laika Mbuu*; (b) *Lausa Laika Aha*

● *Lausa* (Ladder)

*Lausa* or the stairs shown in Fig. 21 is a construction link between the ground floor and the upper floor. *Lausa* in the *Laika Mbuu* and *Laika Aha* have an odd rung of seven steps which means the seven power structures of the Konawe kingdom, namely: 1) *Sulemandara I Pu'osu,* who is in charge of political affairs or the prime minister, is in the kingdom of *Puosu*; 2) *Tusawuta I Kasipute* who is in charge of agricultural affairs is in *Kasipute*; 3) *Kotubitara I Wonggeduku* who is in charge of justice matters, is in *Wongeduku*; 4) *Kapita Ana Molepo I Uepai* who is in charge of security and land affairs, is in *Uepai*; 5) *Kapita Lau I Sambara* who is in charge of maritime security and defense in Sambara; 6) *Tamalaki Tutuwi Motaha I Anggaberi* who is in charge of war matter and enemy attacks is in Anggaberi; and 7) *Pombeota'eahako I Toriki* who is in charge of logistics matter is in Toriki. According to the *Tolaki* tribe, the number of steps must be odd because according to their belief even numbers associated with possible misfortune, otherwise odd numbers are called *konanggoa* to be believed that the owner will continuously get fortune.

In the *lausa* there is a neck of the ladder which is in the middle or called *woroko lausa* which has the meaning of a mother's love for her child. The head of the ladder that leans on the door step to the left and right has the meaning of responsible and reliable head of the household who always maintains the dignity and safety of his family.

● *O'ata* (Roof)

The roof is the main part as a distinguishing feature for the existing types of the traditional houses. The roof covering materials are generally relatively light, *O'ata* is the roof of a house that made of thatch leaves woven using a layer of *poambisi* or bamboo tongs as shown in Fig. 22.

The triangle shape is a formation that is commonly used as roof shape. A triangle is considered a form that has a solid structure so that it is stable applied for roof sructure. The triangle applied for roof shape resulting in pointed shape at the top of the triangle pointing upwards. According to Basrin Melamba, this symbolizes the existence of the great above (God), then the closest thing to God is the thoughts that come from the head. So the triangular shape of the roof means the human head.
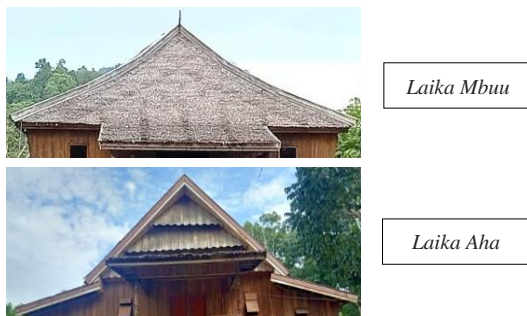


Figure 22. (a) *O'ata Laika Mbuu*; (b) *O'ata Laika Aha*



Figure 23. (a) *Lomba-lomba Laika Mbuu*; (b) *Lomba-lomba Laika Aha*

The roof of *Laika Mbuu* and *Laika Aha* have the same shape but are different in form when they are built. There are two tips that protrude above the front and the back of the roofs. The tips are symbols of human desires in realizing higher achievements such as the sun and the moon as the highest objects in this universe. This means that the owner of the house has high aspirations as high as the sun and the moon.

● *Lomba-lomba* (Window)

Windows of houses for the *Tolaki* people are made for the lighting purposes and surveillance of the enemy. There is no standard regarding the number of windows to be used for houses. Windows are made according to the needs of home owners. According to H. Ujung Lasandara, the number of windows or *lomba-lomba* are six to seven window holes in *Laika Mbuu*. He added that the *Tolaki* house has four holes which are analogous to two elements of *obiri* (ears) and two elements of *totopa* (armpits). However, empirically regarding the number of *lomba-lomba* can be made as needed, because in each *kataba* there are *lomba-lomba* in each room as shown in Fig. 23.

*Laika Mbuu* and *Laika Aha* has the shape of window with up-swing model, thus a type of window that open by tilting it outward. This window mechanism prevents the narrowing of the room. Up-swing windows provide good air insulation, and prevent rain from entering the room. The size of the *lomba-lomba* in *Laika Mbuu* is 60 centimeters wide and 120 centimeters high and for the *Laika Aha* is 80 centimeters wide and 60 centimeters high.

*Lomba-lomba Laika Mbuu* has a window hole of 12 holes while for buildings *Laika Aha* as many as 24 holes. There is a believe in *Tolaki community* that putting *lomba-lomba* should be in the direction where the sun rises and sets. This is related to a belief about the flow of upstream and downstream rivers that flow like a fortune coming from downstream to upstream under the river current. In order to get fortune, windows are the place where the fortune enters.

● *Otambo* (Door)

*Otambo* uses a rectangular shape as shown in Fig. 24. This shape is the basic form of wood used as the main material for making doors, so using the basic shape is considered to save time and costs. The entrance to the house has two doors, which contain the meaning that all happiness can be opened with the hope of goodness that enters *Laika*. *Otambo Laika Aha* has only one entrance and that door must face the road and must not turn its back, while *Laika Mbuu* has two doors in front and back.

Figure 24. (a) *Otambo Laika Mbuu*; (b) *Otambo Laika Aha*

Based on the results of the discussion above, the function of the building is divided into four [10], namely:

- Physical control (controlling factors), the role of physical control on the function and role of the building includes climate control (air, humidity, temperature, wind, rainfall, light, sound, smell, dust, smoke, insects, animals and humans as well as radioactivity). Most of the factors mentioned above are geographical in nature and it can be understood that all aspects of physical control are related to the relationship between the building and its environment.
- Functional frame, discussion of the physical aspects of human behavior. Basically, humans always carry out activities, so they need an architectural container to accommodate these activities.
- Social millieu (social environment), can be a static expression, roles, groups, associations, institutions and groups of buildings that can represent the social system as a whole.
- Cultural symbolization (cultural symbol), architecture can symbolize cultural objects that reap empirical facts, because the history of architecture shows that this aspect has formed an important part of the role of the building.

What was found in the field was that *Laika Mbuu* and *Laika Aha* functioned to protect their residents from exposure to weather changes, protect them from natural disasters, attacks by wild animals and criminals. Even *Laika Mbuu* and *Laika Aha* also function as a place to accommodate variuous activities, including traditional ceremony and customary events. *Laika Mbuu* and *Laika Aha* are social and cultural symbols of the *Tolaki* people in Konawe Regency.

The atmosphere can change with history, while the function remains. Functions will change when there is a fundamental change in lifestyle. The fact is that every activity requires a certain space, and every space can have a size. According to Rapoport [12], space is not only physical environment where there is an organizational relationship between various kinds of objects and humans who are separated in certain spaces. A space becomes meaningful when social intercourses occurs, where people need the opportunity to meet or gather, a space is formed by sosial and cultural ideas occuring within.

*Laika Mbuu* is a building that does not have a room divider so that objects and humans are inseparable, *Laika Mbuu* and *Laika Aha* have interconnected spaces and there is also a space that has a role as a personal place that can affect a person's attitude, namely the space contained *otusa*

*petumbu* or king's pole which is a sign that the pole is the seat of a Mokole the pole is right in the middle of the building which also signifies that other people other than family members cannot cross the boundary and sit in that place.

From the results of the configuration of the space can produce a form with visual characteristics. According to Ching [14] a form has visual characteristics, namely: 1) Form; 2) Dimensions; 3) Color; 4) Texture; 5) Position; 6) Orientation; 7) Inersia visual. It is known that *Laika Mbuu* and *Laika Aha* have the visual characteristics described and the building forms of *Laika Mbuu* and *Laika Aha* have the same building shape. According to Santosa [15] a system of meaning becomes an integrated cultural setting for the phenomena described. The phenomena found in the *Laika Mbuu* and *Laika Aha* buildings are the cultural meanings and beliefs of the *Tolaki* people.

### 4.3. Concluding remarks

This research has clarified 3 (three) important findings as the followings:

- The function of both the *Laika Mbuu* and *Laika Aha* traditional houses is as a residence for a *Mokole* (King). *Laika Mbuu* which means the main house is also a place to carry out social life of the royal family with the community, also as a place of worship to the spirits of their ancestors and grandmothers. Meanwhile *Laika Aha* means a big house whose function is not only as a place for *Mokole* to live in, but also as a gathering place for large families from one tribe and a place for ceremonies and other customary activities.
- The space of both *Laika Mbuu* and *Laika Aha* are vertically divided into three parts, namely: 1) *Wawo Laika* (above the house); 2) *Tonga Laika* (middle of the house); and 3) *Lolo Laika* (under the house) which means identification of the human body. *Lolo laika* is the foot, *tonga laika* is the body and *wawo laika* is the head. Horizontally, the *Laika Mbuu* space has four zones, namely: 1) The front consists of *tinumba hohu*; 2) The middle part is *butono laika*; 3) The back consists of *dongge* and 4) The upper part consists of *lembe-lembe*. *Laika Aha* has three zones, namely: 1) The front consists of *tinumba hohu* and *butono laika*; 2) The middle part consists of *rapi*; and 3) The back consists of *pineworoko* and *dongge*.
- The building form of both *Laika Mbuu* and *Laika Aha* is stilt house like *Tolaki* houses in general and is rectangular in shapes, indicating social status of the occupants. The square shape in the building facade shows the lower part, so that the square is considered the underworld (earth), yet it can also be seen as a container called *Kalo Sara*, which is a set of objects as symbols of social class and has a meaning as customary law in the *Tolaki* tribe community. The sloping shape of wall in *Laika Mbuu* and *Laika Aha* reflect and symbolize a boat from, from wich the *Tolaki* community believe to have come to Konawe

using boats. On the roof there are two tips that protrude towards the front and back that symbolize, human desire in realizing or achieving wishes in life.

- The house symbolizes a human body, and the residents simbolize organs of the human body, so that once the house is built and filled, it must try to protect itself from all obstacles and calamities. The concept of intactness of the four main pillars symbolizes that everything given by their ancestors can be maintained and continuously implemented including traditional rules, customary laws, and ceremonial events. The triangle roof shape pointing upward symbolizes the human head look up towards the existence of God. The protruding tips of roof form to the sky are symbols of human desires and aspirations in realizing higher achievements as high as the sun and the moon. Position of windows to the direction where the sun rises and sets, symbolises the flow of upstream and downstream rivers like a fortune flow coming coming through and entering the house. The middle neck of the ladder symbolizes a mother's love for her child, while the strong and balancing head of the ladder symbolizes a responsible and reliable head of the household to keep the dignity and safety of his family.

## 5. Conclusions and Suggestions

### 5.1. Conclusions

This research concluded that both the *Laika Mbuu* and *Laika Aha* have similar function and form, however differ spatial arrangement. Both the *Laikas* were formerly residences of a king, however nowadays *Laika Mbuu* has become an ordinary communal home whereas *Laika Aha* become a customary house for public purposes. *Laika Mbuu* has no partition so that the local community carries out all activities in one openspace, whereas *Laika Aha* contains partitions that device the space into several rooms. The form of both *Laika Mbuu* and *Laika Aha* building is rectangular in shape, in which the square shape in the building facade shows the lower part, as a form of container called the *Kalo Sara*, which is a set of objects as symbol of social class and has a meaning as customary law. Moreover, both *Laikas* express many symbolic meanings, among others that the house symbolizes a human body and the residents simbolize organs of the human body, the concept of four main pillars symbolizes that everything given by thr ancestors should be conserved.

Thus, this research has strengthened Rapoposrt's theory [12] that socio-cultural aspect are utmost important in shaping the traditional architecture of tribal communities. This research has also developed Ching's theory [14] that architecture concerns not only form, space, and order, but also sosio-cultural meanings in individual and communal life. Moreover, this research has also verified Broadbent's theory [9], [20] that symbol is an indispensable characteristics in the architecture of human settlement.

### 5.2. Suggestions

Based on the above coclusion, the proposed suggestions are as follows:

- The architecture of the *Tolaki* traditional houses, especially the *Laika Mbuu* and *Laika Aha* buildings, is the product of the thoughts of the *Tolaki* people, in Konawe Regency, which must be preserved as part of the regional culture as well as one of the diversity and richness of the Indonesian culture.
- The values implied in the traditional houses built by *Laika Mbuu* and *Laika Aha* should be used as guidelines to maintain and strengthen solidarity for the *Tolaki* community.
- The government would be better restore the *Laika Mbuu* and *Laika Aha* buildings based on originality referring to relevant archive and historical document, considering that the current buildings appear to hardly resemble the original.
- Future researchers should continue this research by adding other objects of *Laika* with the topic of the *Tolaki* tribal architecture.

## References

[1] A. A. Said, *Symbolism of Visual Elements of Traditional Toraja Houses and Changes in Its Application to Modern Design*. Tegalrejo, Yogyakarta: Ombak, 2004. [in Bahasa]

[2] Triyanto, "The Meaning of Space and Its Arrangement in The Architecture Of The Kudus House." Mekar kerja Study Group in Collaboration with Yayasan Adikarya IKAPI dan Ford Foundation, Semarang, 2001. [in Bahasa]

[3] B. Melamba *et al.*, *Traditional Architecture of the Tolaki Tribe in Southeast Sulawesi*. Denpasar; Lembaga Pengembangan Sejarah dan Kebudayaan Sultra: Pustaka Larasan; Program Pendidikan Sejarah, FKIP Universitas Haluoleo, 2011. [in Bahasa]

[4] B. Franciska and L. K. Wardani, "The Form, Function, and Interior Meaning of the Traditional Houses of the Tolaki and Wolio Tribes in Southeast Sulawesi," *J. INTRA*, vol. 2, no. 2, pp. 688–701, 2014. [in Bahasa]

[5] A. A. H. Balo, "Tolaki Vernacular Architecture," *Semin. Nas. Teknol. Terap. Berbas. Kearifan Lokal*, vol. 1, pp. 79–88, 2010. [in Bahasa]

[6] A. Faslih, "Philosophy and Placement of Pedestal Poles as a Characteristic of the Houses of the Indigenous People of Abuki Village, Konawe Regency 1," pp. 9–15, 2018. [in Bahasa]

[7] S. Ramadan, "Interpretation of Kalosara in a Tolaki Traditional House," *NALARs*, vol. 17, no. 2, p. 145, 2018. [in Bahasa]

[8] Z. M. Husba, "Tutu Ran Me K: Ethnic Marking System in Social Interaction of the Tolaki Tribe in Uku, Southeast Sulawesi," *Patanjala J. Penelit. Sej. dan Budaya*, vol. 7, no. 2, pp. 327–344, 2015. [in Bahasa]

[9] G. Broadbent, R. Bunt, and C. Jencks, *Signs, Symbols and Architecture*. Chichester: John Wiley & Sons, 1980.

[10] N. Pratiwi *et al.*, "Overview of the Surabaya Culinary Academy Building in the Theory of Christian Norberg-Schulz Functions," vol. 2, no. 2, 2013.

[11] J. Prijotomo, *Space in Javanese architecture: a Discourse*. Surabaya: Wastu Lanas Grafika, 2009. [in Bahasa]

[12] A. Rapoport, "Rapoport-Amos-House-Form-and-Culture.Pdf." pp. 15, 179, 24, 96, 1969.

[13] R. I. Surasetja, "Function, Space, Form and Expression in Architecture," *Bahan Kuliah*, pp. 1–13, 2007. [in Bahasa]

[14] F. D. K. Ching, "Architecture Form, Space, & Order." John Wiley & Sons, 2007.

[15] R. B. Santosa, *Omah: Read the Meaning of Javanese House*. 2019. [in Bahasa]

[16] J. Sumardjo, *Paradoxical Aesthetics*. Bandung; STSI: Sunan Ambu Press, 2010. [in Bahasa]

[17] Amiruddin, I. K. Suardika, and Anwar, "Kalosara in the Tolaki Community in Southeast Sulawesi," *Mudra J. Seni Budaya*, vol. 32, no. 2, pp. 209–219, 2017. [in Bahasa]

[18] Sugiyono, "Quantitative, Qualitative and R&D Research Methods" Bandung: Alfabeta, 2013. [in Bahasa]

[19] L. J. Moleong, "Qualitative Research Methodology" Bandung : Remaja Rosdakarya, 1990, 2005. [in Bahasa]

[20] P. F. Erahman, A. M. Nugroho, and N. Sujudwijono, "Rent Office with Natural Lighting Approach in Malang City," *J. Mhs. Jur. Arsit. Univ. Brawijaya*, vol. 3, no. 4, 2015. [in Bahasa]

# The Impact of Local Wisdom on the Coastal Settlement Spatial Configuration in the City of Parepare

Hasniar Baharuddin[a,*], Idawarni Asmal[b], Edward Syarif[c]

[a]Department of Architecture, Faculty of Engineering, Hasanuddin University, Makassar, Indonesia. Email: hasniarbaharuddin@gmail.com
[b]Department of Architecture, Faculty of Engineering, Hasanuddin University, Makassar, Indonesia. Email: idawarniasmal@yahoo.com
[c]Department of Architecture, Faculty of Engineering, Hasanuddin University, Makassar, Indonesia. Email: edosyarif@yahoo.com

**Abstract**

Soreang Settlement is located on the waterfront of Parepare City in South Sulawesi, Indonesia. Initially, it was inhabited by the Soreang kingdom community and then developed due to by local culture. This research was to explain the influence of local culture on the spatial configuration of the Soreang settlement. The research method used is a synchronic reading analysis technique, which is supported by ArcGIS and the space syntax methods. The results of the research are: the first, the spatial configuration of Soreang settlements is influenced by three local cultures, namely *Sipakatau* cultural meaning is sense mutual respect, *Sipakalebbi* cultural meaning is sense of equity and *Simasemaseang* cultural meaning is sense of family. The second, the *Simasemaseang* culture, infact to a clustered settlement pattern formed. *Sipakalebbi* culture in fact to settles into a linear and spreading pattern formed, whereas *Sipakatau* culture in fact to a settles into an elongated and centered pattern formed. Third, *Simasemaseang* culture forms the most integrated spatial configuration. This research might well be utilized to generate a design for waterfront settlement based on local wisdom.

*Keywords: Local wisdom; settlements; spatial configuration; waterfront*

## 1. Introduction

Soreang settlement is the first settlement formed since the beginning of the formation of the City of Parepare known as the Kingdom of Soreang [1]. According to *Lontara*, in the XIV century, a son of King Suppa left the palace and went south to establish his settlement area on the waterfront because it has a hobby of fishing, initially consisting of several plots of houses, as the population grew and was influenced by the activities that occurred now developing to form groups of settlements that are bound to each other with various settlement patterns.

The aspect that develops the settlement group is the activity of local wisdom, which is part of a society's culture and should be used as a principle/guide to life. Local wisdom is made up of three principles: *Sipakatau*, *Sipakalebbi* and *Simasemaseang* cultures, which are still followed as a basic of community life and are firmly maintained by the people of Parepare [2].

In Buginese philosophy about people, *Sipakatau* is the essential component that maintains all of our human ways [3], humanizing one another regardless of origin. *Sipakalebbi* means "to complement one another", meaning that both humans and nature need to comprehend one another. This includes seeing one's own characteristics in others and appreciating one's own inherent abilities by experiencing and living in harmony with nature. Love, care for, aid, collaborate, give, and have a deep sense of kinship with one another is what *Simasemaseang* implies.

Local wisdom's three principles are essentially concepts of connectedness that serve as guidance for social interaction and relationships. Claims that a community's social interaction, namely its sense of oneness, has a substantial influence on the urban space arrangement [4]. In his book "Human Aspect of Urban Form"[5], he proposes three aspects that determine the space and structure of the built environment, including culture, physicality, and mechanism. This characteristic of culture is used to assess its influence on the space formed in coastal settlements [6] and [7].

A study is needed to interpret the textual form of local wisdom into the distribution pattern of coastal settlements, explain its influence on the configuration of the space formed by measuring the connectivity and integrity of space using space syntax analysis, and use it as a reference in structuring coastal settlement areas by looking at the conditions of settlements that carry local wisdom. The conclusions of this study are critical for the growth of architectural science, particularly in terms of understanding the form of coastal areas while taking into consideration the effect of local wisdom.

*Corresponding author. Tel.: +62-813-552-225-33
*Address Kompleks BLK D5/90 Jl. Keterampilan No.63*
*Parepare, Indonesia, 91122*

## 2. Research Method

A mixed methods approach describes the impact of local wisdom on the spatial configuration of coastal settlements [8]. In this study, mapping methods using Arcgis software and space syntax analysis methods were used to enhance synchronic reading analysis approaches [9] in [10]. Researchers utilized synchronic reading analysis approaches based on field observation data [11], as well as settlement mapping with Arcgis software, to translate literary forms of culture into settlement distribution patterns. Meanwhile, the space syntax approach [12], is used to investigate and describe the culture of *sipakatau*, *sipakalebbi*, and *Simasemaseang's* influence on space configuration.

The space syntax analysis approach is used to determine axiality, convexity, and isovist. Convexity is used to examine interactions in space (interior), whereas Isovist is used to test how far the eye can see when moving in one direction [13]. Axiality is the ability to determine the longest line of a road segment by drawing it through the axial line using the idea of the longest line that can be seen and to monitor movement. In order to assess the space's connectivity and integrity, only the axiality of coastal towns is measured in this study.

Based on their administrative territories along the seaside areas of the Makassar Strait in Parepare City, South Sulawesi Province, Ujung Sabbang Village, Kampung Pisang Village, Lakessi Village, and Wattang Soreang Village were separated into four zones. The research location is shown in Fig. 1.
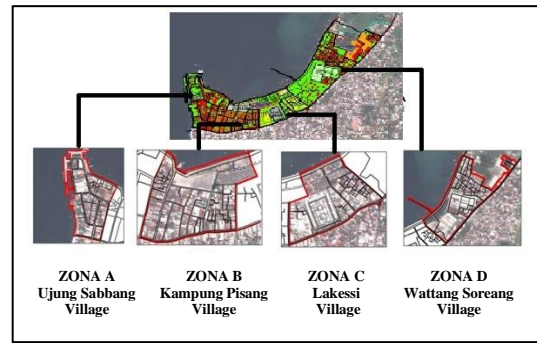


Figure 1. The research site is in Parepare City's Coastal Settlement

## 3. Results and Discussion

### 3.1. The Parepare seaside communities' arrangement has evolved in response to cultural influences

The distribution of settlement patterns carrying cultural principles is mapped using a sample system at two or three delineations in each village, exhibiting the interpretation of the literary form of local wisdom in the shape of a map of Parepare City's seaside region. Figure 2 displays the culture of four village's: Ujung Sabbang Village's *Simasemaseang* Culture and *Sipakatau* Culture; Kampung Pisang Village's *Simasemaseang* Culture and *Sipakatau* Culture; Lakessi Village's *Simasemaseang* Culture and *Sipakatau* Culture; and Lakessi Village's *Sipakatau* Culture. Wattang Soreang is a settlement where the cultures of *Simasemaseang* and *Sipakalebbi* interact.
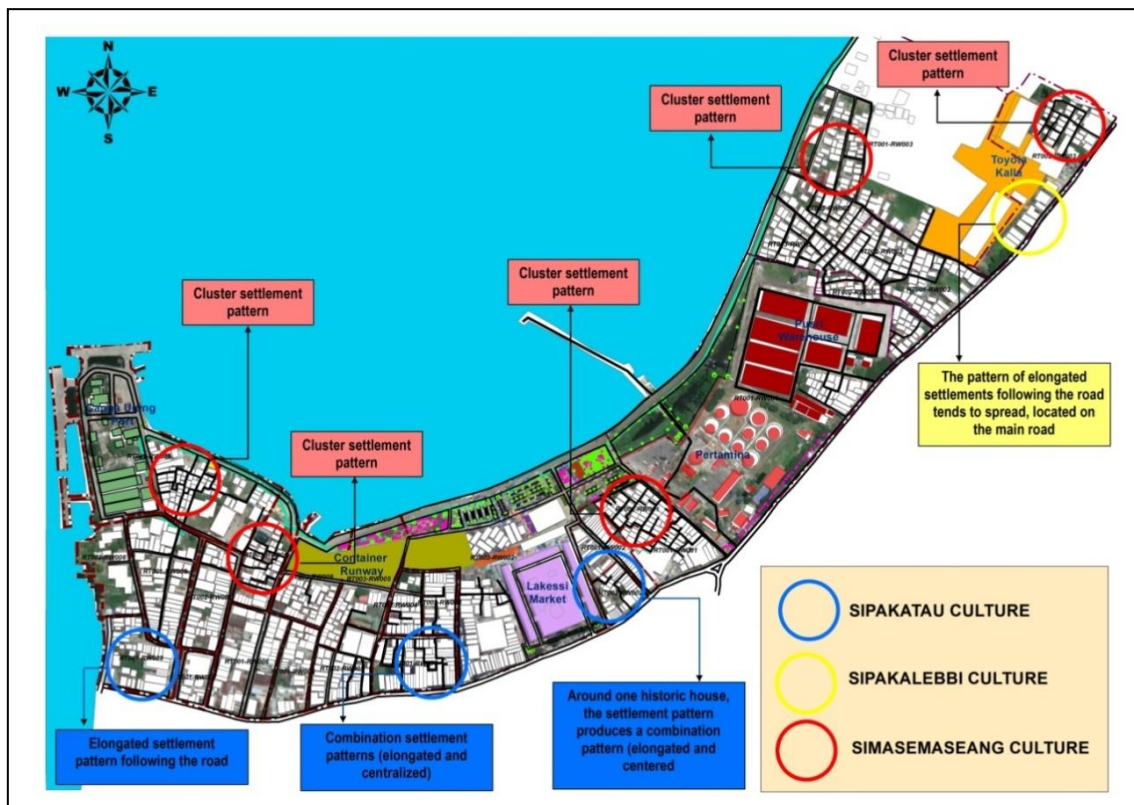


Figure 2. Map of cultural representation based on the layout of settlements created in Parepare City's Seaside Area

### 3.2. The three cultures of the city of Parepare have created a unique configuration of coastal settlement space

In measuring the interactions/relationships between road networks in a spatial configuration, apart from using the RA (integration result) calculation to see the depth of space, we also use the Depthmap x-0.50 software. The use of simulations with UCL Depthmap x-0.50 can produce differences in depth analysis by providing a spectrum display to blue where the red color indicates the area that receives the most movement and is most integrated with other spaces or roads [14]. While the blue color indicates the area that receives the least movement and is also the least integrated with other spaces or roads. The results of the spatial configuration are as follows:

#### a. Ujung Sabbang village's coastline settlement space configuration

The spatial configuration indicated in Figs. 3 and 4, the settlements in Ujung Sabbang Village bear the *Simasemaseang* and *Sipakatau* culture.

The influence of *Simasemaseang* Culture on the Spatial Configuration of the Ujung Sabbang Settlement is shown in Fig. 3. (a) Shows that the location of Ujung Sabbang via google earth image 2019, (b) show in the *Simasemaseang* civilization, the spatial structure of the clustered settlemen pattern is positioned on the edge of the sea, (c) draw an axial map with the observation point at Lontangnge harbor street so that the steps to the deepest section, (d) as shown in the access diagram, may be counted it takes 6 steps (step depth) with a total of 110 steps to reach the deepest side, the RA value is 0.109, showing that the spatial arrangement is integrated. (e) Road section 0 (Lontangnge Harbor street), roads 5 and 3, highlighted in red and orange, have the highest connectedness, suggesting that the road network is most directly connected to other roads. Meanwhile, the road network with limited connection is designated in teal and dark blue on roads 24, 17, 27, 18, 25, 26, 22, 13, 32, suggesting that the road network is at least connected to other road networks. (f) The road segment 0 (Lontangnge Harbor street), roads 5 and 3, shown in red, has the highest integration, suggesting that the route is the most accessible to users, is busy with varied activities, and is easy to access. While sections 24, 18, 25, 32, and 27 are marked with a dark blue color, indicating that the road is accessed by the fewest people, is quiet from activities, is difficult to access, is not connected (dead end), and has the potential to be ignored, sections 24, 18, 25, 32, and 27 are marked with a light blue color, indicating that the road is accessed by the fewest people, is quiet from activities, is difficult to access, and has the potential to be ignored.



Figure 3. *Simasemaseang* Culture analysis map of Ujung Sabbang (a) Location map, (b) Map of Sipakatau culture Settlement pattern, (c) Axial maps, (d) Access graph and computation of RA values, (e) Maps of connectivity analysis, (f) Maps of integration analysis



Figure 4. *Sipakatau* Culture analysis map of Ujung Sabbang (a) Location map, (b) Map of Sipakatau culture Settlement pattern, (c) Axial maps, (d) Access graph and computation of RA values, (e) Maps of connectivity analysis, (f) Maps of integration analysis

190

Figure 4 shows in the influence of *Sipakatau* Culture on the Spatial Configuration of the Ujung Sabbang Settlement. (a) Shows that the location of Ujung Sabbang via google earth image 2019, (b) show in the *Sipakatau* civilization, the spatial results in an elongated settlement pattern that follows the road, (c) illustrates an axial map with observation points from section 0 so that steps can be computed to reach the deepest part, as shown in the access diagram (d) It takes 3 steps to reach the deepest side, for a total of 21 steps, a RA of 0.268 indicates that the spatial arrangement is integrated. (e) Road sections 1 (Zasilia street) and 5 (Zasilia street) have high connectivity, suggesting that the road network is most directly connected to other roads. Meanwhile, roads 8 and 2, which are shown in teal and dark blue, respectively, have minimal connectivity, indicating that the road network is at least connected to other road networks. (f) The highest levels of integration are seen on road sections 1 (Zasilia street) and 5, which are highlighted in red. Shows that the route is the most frequently used by users, that it is bustling with diverse activities, and that it is easy to reach. Meanwhile, the least integrated parts are 8 and 2, which are indicated with a dark blue color to indicate that the road is used by the fewest people, is quiet from activities, is difficult to access, and is not connected (dead end).

### b. Kampung Pisang village's coastline settlement space configuration

The spatial configuration indicated in Figs. 5 and 6, the settlements in Kampung Pisang Village bear the *Simasemaseang* and *Sipakatau* culture

The influence of *Simasemaseang* Culture on the Spatial Configuration of the Kampung Pisang settlement is shown in Fig. 5. (a) Shows that the location of Kampung Pisang via google earth image 2019, (b) show in the *Simasemaseang* civilization, the spatial layout results in a clustered settlement pattern near the sea. (c) illustrates an axial map with observation sites from Abdul Hamid Saleh street so that the steps to reach the deepest segment may be estimated, (d) as shown in the access diagram, it takes 6 steps (step depth) to reach the deepest side, for a total of 91 steps, the RA value of 0.182 suggests that the integrated spatial arrangement is good (e) Road 2 (Abdul Hamid Saleh street), roads 0 and 3 (shown in red and orange) have the highest connectivity, indicating that the road network is most directly connected to other roads. While the road network with poor connectivity is shown in teal and dark blue on roads 16, 15, 12, 11, 13, 27, 19, 9, 6, 7, 25, 24, and 23, suggesting that the road network is the least connected to other road networks. (f) The highest level of integration is seen on road section 2 (Abdul Hamid Saleh street), which includes roads 0, 20, 5, and 3, all of which are marked in red. Shows that the route is the most frequently used by users, that it is bustling with diverse activities, and that it is easy to reach. Meanwhile, the lowest integration occurs on sections 16, 15, 12, 11, 13, 27, 19, 9, 6, 7, 25, 24, and 23, which are marked with a dark blue color to indicate that the road is accessed by the fewest people, is quiet from activities, is difficult to access, is not connected (deadlocked), and has the potential to be used as a garbage disposal site.



Figure 5. *Simasemaseang* Culture analysis map of Kampung Pisang (a) Location map, (b) Map of Simasemaseang culture Settlement pattern, (c) Axial maps, (d) Access graph and computation of RA values, (e) Maps of connectivity analysis, (f) Maps of integration analysis
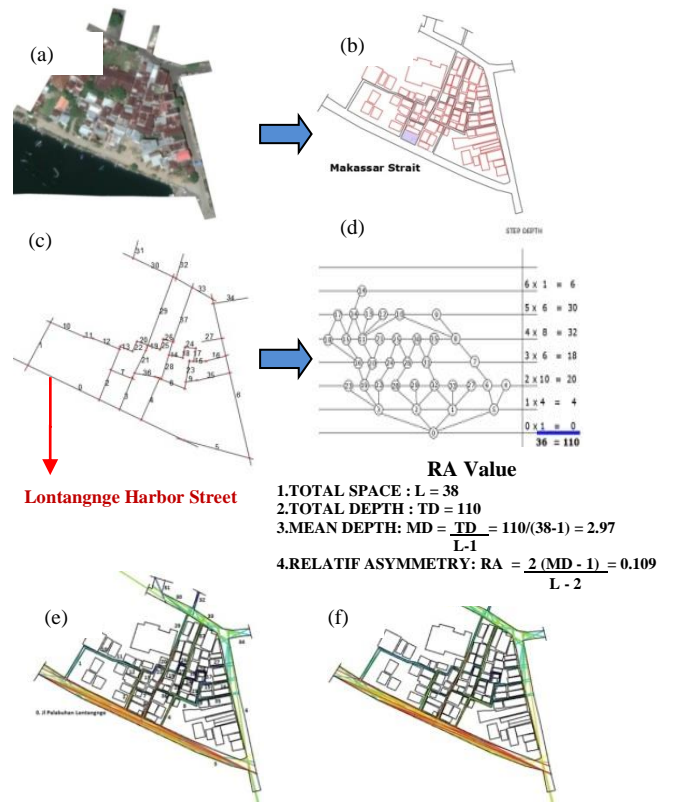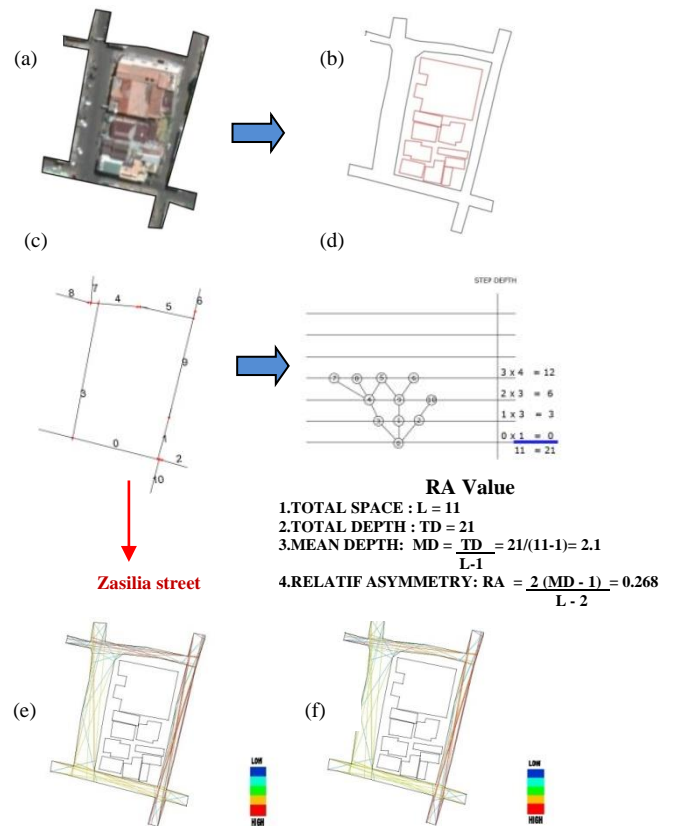


Figure 6. *Sipakatau* Culture analysis map of Kampung Pisang (a) Location map, (b) Map of *Sipakatau* culture Settlement pattern, (c) Axial maps, (d) Access graph and computation of RA values, (e) Maps of connectivity analysis, and (f) Maps of integration analysis

Figure 6 shows in the influence of *Sipakatau* Culture on the Spatial Configuration of the Kampung Pisang Settlement. (a) Shows that the location of Kampung Pisang via google earth image 2019, (b) show the spatial configuration in *sipakatau* culture forms a combination settlement pattern (elongated and centered). (c) The *Sipakatau* culture's spatial configuration depicts an axial map with observation points from Lasinrang street with circular routes and connected to each other to move from one place to another so that steps can be counted to arrive at the deepest segment, (d) Illustrated in the access diagram, it takes 5 steps (step depth) to reach the deepest side, for a total of 62 steps, and the RA value of 0.195 indicates that the spatial arrangement is integrated. (e) The road network is most directly connected to other roads on road section 0 (Lasinrang street), road sections 3, 4, 6, and 20, which are all marked in red and orange. Meanwhile, the road network with limited connection is designated in teal and dark blue on roads 5, 10, 11, 14, 16, 17, 18, 19, and 21, suggesting that the road network is at least connected to other road networks. (f) The road portion 0 (Lasinrang street) has the most integration, while roads 3 and 4 are highlighted in red. Shows that the route is the most frequently used by users, that it is bustling with diverse activities, and that it is easy to reach. Sections 5, 9, 10, 11, 14, 15, 16, 17, 18, 19, and 21 are highlighted in dark blue, suggesting that the road has the least access to people, is silent from activities, is difficult to access, is not connected (dead end), and might be used as a dumping ground.

### c. Residential space along the coast at Lakessi village

With the spatial structure shown in Figs. 7 and 8, the settlements in Lakessi Village bear the *Simasemaseang* and *Sipakatau* culture.

**RA Value**

1. TOTAL SPACE : L = 36
2. TOTAL DEPTH : TD = 110
3. MEAN DEPTH : $MD = \dfrac{TD}{L-1} = 110/(36-1) = 3.14$
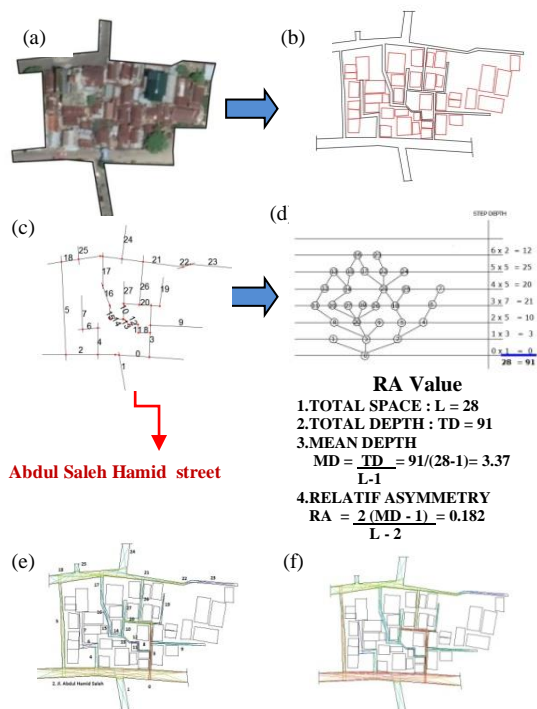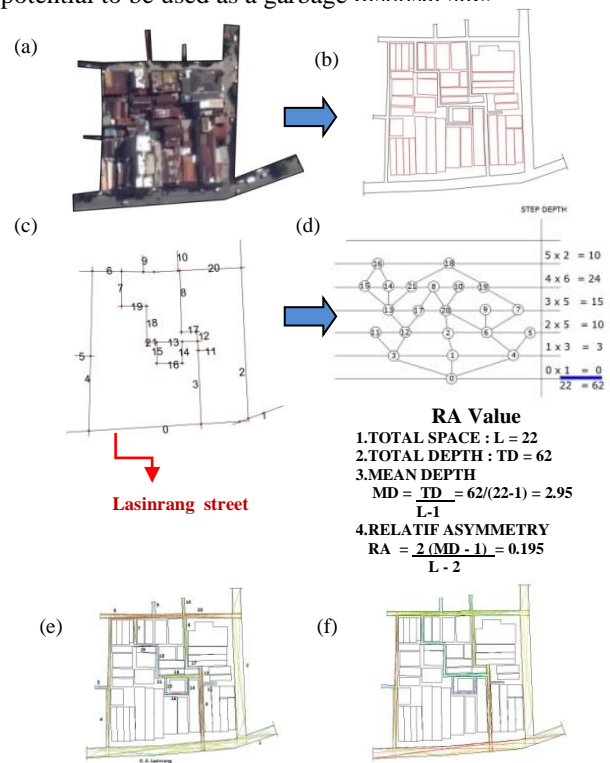4. RELATIF ASYMMETRY ( RA ) $= \dfrac{2 (MD - 1)}{L - 2} = 0.125$

Figure 7. *Simasemaseang* Culture analysis map of Lakessi (a) Location map, (b) Map of *Simasemaseang* culture Settlement pattern, (c) Axial maps, (d) Access graph and computation of RA values, (e) Maps of connectivity analysis, (f) Maps of integration analysis

The influence of *Simasemaseang* Culture on the Spatial Configuration of the Lakessi settlement is shown in Fig. 7. (a) Shows that the location of Lakessi via google earth image 2019, (b) Show the *Simasemaseang* culture has a clustered settlement pattern near the sea. (c) Depicting an axial map with observation points from Pertamina street so that the steps to reach the deepest segment can be calculated, (d) As shown in the access diagram, it takes 6 steps (step depth) to reach the deepest side, for a total of 110 steps, and the RA value is 0.125. (e) Road segments 0 (Pertamina street) and 5 (marked with red and orange colors) have high connectivity, suggesting that the road network is most directly connected to other roads. Meanwhile, the road network with low connectivity is designated in teal and dark blue on roads 31, 37, 33, 28, 24, 18, 21, 7, 4, 29, 14, 13, 12 and 9, indicating that it is the least connected to other road networks. (f) On road sections 0 (Pertamina street) and 5, highlighted in red, the highest integration occurs. Shows that the route is the most frequently used by users, that it is bustling with diverse activities, and that it is easy to reach. Meanwhile, the lowest integration occurs on sections 26, 30, 31, 37, 21, 18, 17, 14, 13, 12, 9, 4, 23, 29, and 25, which are marked in dark blue and indicate that the road is accessed by the fewest number of people, quiet from activities, difficult to access, roads are not connected (deadlocked), and have the potential to be used as a garbage dump.

Figure 8 shows in the influence of *Sipakatau* Culture on the Spatial Configuration of the Lakessi Settlement. (a) Shows that the location of Lakessi via google earth image 2019, (b) Show The spatial configuration in *sipakatau* culture forms a combination settlement pattern (elongated and centered), which extends along the road and is centered around 1 house with a circular route and is connected to each other to move from one place to another. (c) Describes an axial map with observation points from lasinrang street so that steps can be counted to arrive at the deepest segment. (d) As shown in the access diagram, it takes 5 steps (step depth) to reach the deepest side, for a total of 41 steps, and the RA value is 0.208. (e) Road section 0 (Lasinrang street), roads 3 and 7, highlighted in red and orange, have the highest connectivity, suggesting that the road network is most directly connected to other roads. While roads 10, 12, 13, 8, 9, 5 and 15 are highlighted in teal and dark blue, suggesting that they are at least connected to other road networks, the road network with minimal connection is found on roads 10, 12, 13, 8, 9, 5 and 15. (f) The road portion (Lasinrang street), roads 3 and 7, indicated in red, has the maximum integration. Shows that the route is the most frequently used by users, that it is bustling with diverse activities, and that it is easy to reach. While sections 10, 12, 13, 8, 9, 5 and 15 are marked in dark blue, indicating that the road is accessed by the fewest people, is quiet from activities, is difficult to access, is not connected (dead end), and has the potential to be ignored, sections 10, 12, 13, 8, 9, 5 and 15 are marked in light blue.
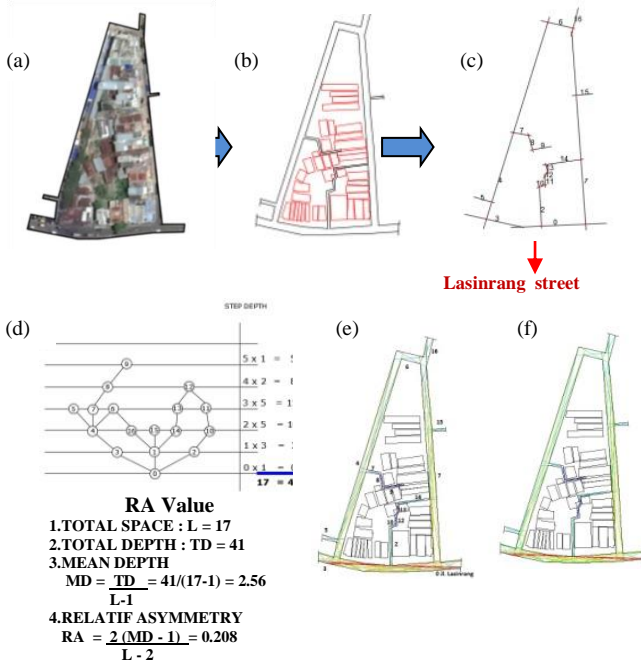
Figure 8. *Sipakatau* Culture analysis map of Lakessi (a) Location map, (b) Map of *Sipakatau* culture Settlement pattern, (c) Axial maps, (d) Access graph and computation of RA values, (e) Maps of connectivity analysis, (f) Maps of integration analysis

### d. Wattang Soreang village's coastline settlement space configuration

The *Simasemaseang* and *sipakalebbi* cultures are carried by the settlements in the Wattang Soreang Village, as shown in Figs. 9, 10 and 11.
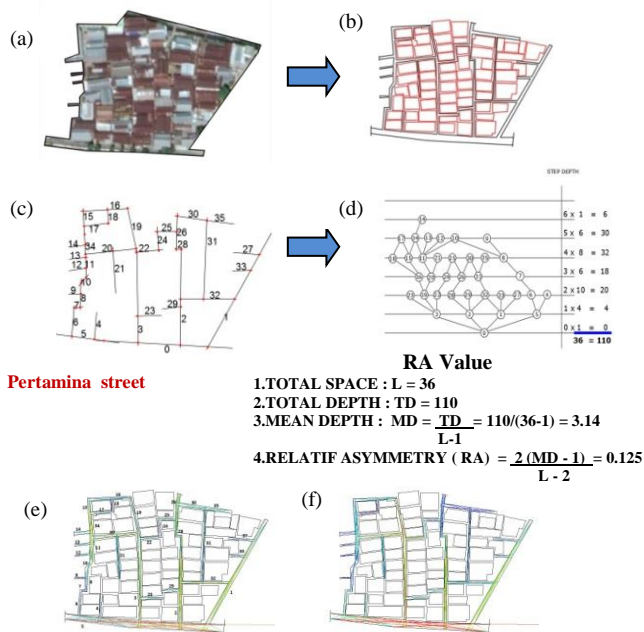


Figure 9. *Simasemaseang* Culture analysis map of Wattang Soreang 1, (a) Location map, (b) Map of *Simasemaseang* culture Settlement pattern 1, (c) Axial maps, (d) Access graph and computation of RA values, (e) Maps of connectivity analysis, (f) Maps of integration analysis

The influence of *Simasemaseang* Culture on the Spatial Configuration of the Wattang Soreang settlement is shown in Fig. 9. (a) Shows that the location of Wattang Soreang via google earth image 2019, (b) Show the *Simasemaseang* 1 culture's spatial configuration is a clustered settlement pattern near the sea with interconnected routes but connected by passageways to move from one place to another. (c) Depicting an axial map with observation points from Pertamina street so that the steps to reach the deepest segment can be calculated. (d) As shown in the access diagram, it takes 4 steps (step depth) to reach the deepest side, for a total of 25 steps, and the RA value is 0.12. (e) Road sections 0 (Pusri street) and 4 (marked with red and orange colors) have high connectivity, suggesting that the road network is most directly connected to other roads. While roads 2, 3, 5, 6, and 12 are indicated in teal and dark blue, suggesting that they are at least connected to other road networks, the road network with minimal connection is found on roads 2, 3, 5, 6, and 12. (f) The road sections 0 (Pusri street) and 4 (marked in red) have the highest integration. Shows that the route is the most frequently used by users, that it is bustling with diverse activities, and that it is easy to reach. Meanwhile, sections 2, 3, 5, 6, and 12 are indicated in dark blue, suggesting that the road is used by the fewest number of people, is quiet from activities, is difficult to reach, is not connected, and has the potential to be neglected.



Figure 10. *Simasemaseang* Culture analysis map of Wattang Soreang 2, (a) Location map, (b) Map of *Simasemaseang* culture settlement pattern 2, (c) Axial maps, (d) Access graph and computation of RA values, (e) Maps of connectivity analysis, (f) Maps of integration analysis

193

Figure 10 shows in the influence of *Simasemaseang* Culture on the Spatial Configuration of the Lakessi Settlement 2 (a) Shows that the location of Lakessi via google earth image 2019, (b) Show the spatial configuration in the *Simasemaseang* 2 culture forms a clustered settlement pattern near Toyota with interconnected routes but not connected to the main road. (c) Depicting an axial map with observation point from M. Arsyad street so that steps can be counted to arrive at the deepest segment. (d) Illustrated in the access diagram, it takes 7 steps (step depth) to reach the deepest side, for a total of 80 steps, and the RA value is 0.28. (e) Roads 1, 4, and 7, which are colored red and orange, have high connectivity, suggesting that the road network is most directly connected to other roads. Meanwhile, the road network with minimal connectivity is marked in teal and dark blue on roads 8, 14, 15, 18, and 3, showing that it is at least connected to other road networks. (f) The red-colored roadways 1, 4, 5, and 6 have the highest level of integration. Shows that the route is the most frequently used by users, that it is bustling with diverse activities, and that it is easy to reach. Sections 6, 17, 15, 14, 8, 11, and 3 have the lowest integration, indicating that the road is visited by the fewest people, is quiet from activities, is difficult to reach, is not connected, and has the potential to be utilized as a location to reside. removing rubbish.
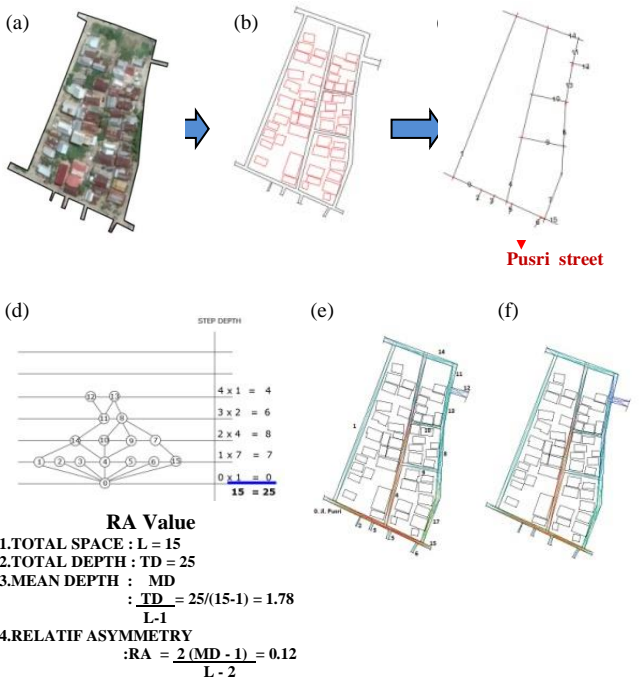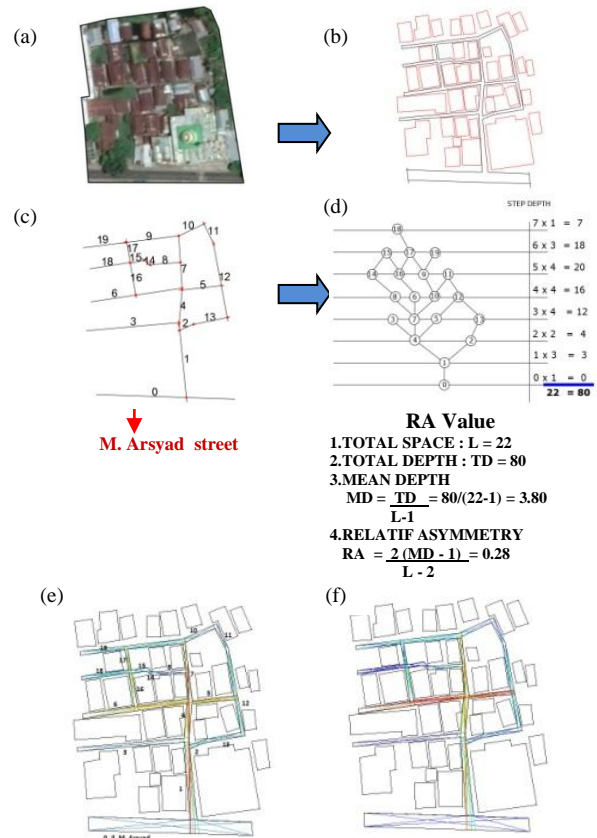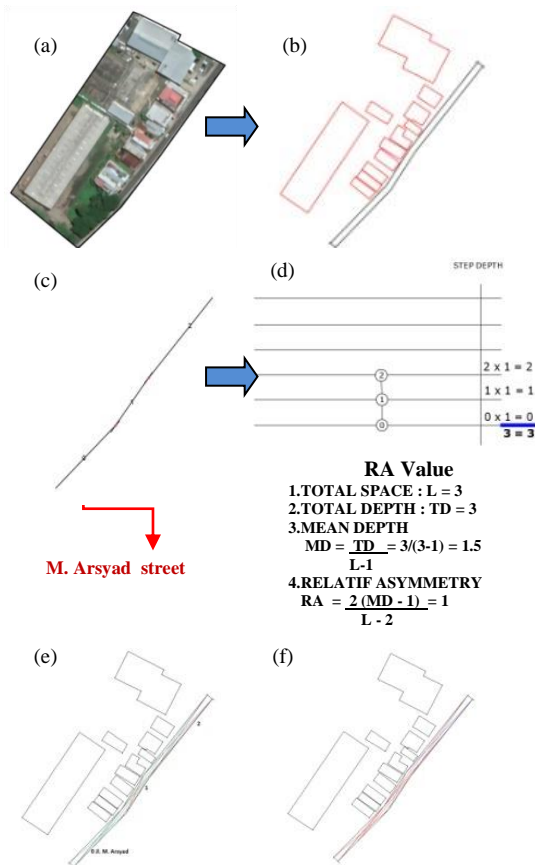


Figure 11. *Sipakalebbi* Culture analysis map of Wattang Soreang (a) Location map, (b) Map of *Sipakalebbi* culture Settlement pattern, (c) Axial maps, (d) Access graph and computation of RA values, (e) Maps of connectivity analysis, (f) Maps of integration analysis

Table 1. The results of the room configuration analysis

| Village | The culture that is formed | The pattern and layout of settlements | RA Value |
|---|---|---|---|
| Ujung Sabbang | *Simasemaseang* | Cluster settlement pattern | 0,109 |
| | *Sipakatau* | Elongated settlement pattern following the road | 0,268 |
| Kampung Pisang | *Simasemaseang* | Cluster settlement pattern | 0,182 |
| | *Sipakatau* | Combination settlement patterns (elongated and centralized) | 0,195 |
| Lakessi | *Simasemaseang* | Cluster settlement pattern | 0,125 |
| | *Sipakatau* | Around one historic house, the settlement pattern produces a combination pattern (elongated and centered). | 0,208 |
| Wattang Soreang | *Simasemaseang* 1 | Cluster settlement pattern | 0,12 |
| | *Simasemaseang* 2 | Cluster settlement pattern | 0,28 |
| | *Sipakalebbi* | The pattern of elongated settlements following the road tends to spread, located on the main road | 1 |

The influence of *Simasemaseang* Culture on the Spatial Configuration of the Wattang Soreang settlement is shown in Fig. 11. (a) Shows that the location of Wattang Soreang via google earth image 2019, (b) Show The *Sipakalebbi* culture's spatial configuration forms a pattern of elongated settlements that follow the road and tend to spread, located on the primary collector road with one route connecting the settlements.(c) Depicting an axial map with observation points from M. Aryad street so that steps can be counted to arrive at the deepest segment. (d) As shown in the access diagram, the RA value of 1 also shows that the spatial arrangement is integrated but has low integrity, as it takes 2 steps (step depth) to reach the deepest side with a total of 3 steps (e) Roads 0, 1 and 2 (M. Arsyad street), highlighted in red and orange, have the highest connectedness, suggesting that the road network is most directly connected to other roads. And there isn't a single road network that isn't connected. (f) The maximum level of integration is found on routes 0, 1, and 2 (M. Arsyad street), which are highlighted in red. Shows that the route is the most frequently used by users, that it is bustling with diverse activities, and that it is easy to reach. There is also no road network with a poor level of integration.

### 3.3. The comparison of the findings of the spatial configuration study in each culture.

Table 1 shows comparison of findings of spatial configuration studies in each culture in line with, that spatial patterns of coastal settlements have different shapes according to ecological characteristics and growth processes (Kostof dan Darjosanjoto, 2007) in [15]. Spatial patterns of coastal settlements generally form elongated patterns, group patterns, and spread patterns.

### 4. Conclusion

There are three cultures that influence the development of the spatial configuration of slums in the Commercial area of Parepare City, namely *Sipakatau* culture which means mutual respect, forming a combined settlement pattern (elongated and centralized) with moderate integration, *Sipakalebbi* culture meaning mutual respect, forming a linear settlement pattern

(elongated) and tends to spread. with low integration and *Simasemaseang* Culture means loving each other, forming a clustered settlement pattern with high integration. *Simasemaseang* culture has a spatial arrangement that is mutually integrated/high integration (low depth) with other rooms in the layout or is well connected to the observation room, because it has a smaller RA value, where RA produces a number between 0 and 1, the smaller the RA value indicates integrity is getting higher.

## REFERENCES

[1]  Regional Planning Agency (Bappeda), "History of Parepare," 2013. [Online]. Available: https://bappeda.pareparekota.go.id/?page_id=315. [in Bahasa]

[2]  Regional Regulation of the Regional Medium Term Development Plan (RPJMD) for the city of Parepare, 2009. [in Bahasa]

[3]  A. Safitri and S. Suharno, "Siri' na pacce and Sipakatau Cultures in the South Sulawesi Community Social Interaction," *J. Anthropol. Cult. Issues*, vol. 22, no. 1, p. 102, 2020. [in Bahasa]

[4]  I. Can, "In-Between Space and Social Interaction: a Case Study of Three Neighbourhoods in Izmir (Issue July)," University of Nottingham, 2012.

[5]  A. Rapoport, *Human Aspects of Urban Form*. 1977.

[6]  E. Syarif, "Local Wisdom in Formation of Mariso Seaside Settlement Spatial Configuration," 2018. [in Bahasa]

[7]  E. Syarif, "Mariso and Tallo Waterfront Settlement Space Configuration From a Sustainability Aspect," *Indones. J. Built Environ.*, vol. 7, no. 1, pp. 1–8, 2018. [in Bahasa]

[8]  J. W. Creswell and A. Tashakkori, "Differing Perspectives on Mixed Research Methods," *J. Mix. Res. Methods*, vol. 1, no. 4, pp. 303–308, 2007.

[9]  B. Hillier, *Space is the Machine: a Configurational Theory of Architecture*. London, UK: Space Syntax, 2007.

[10] J. P. Siregar, "Basic Methodology of Space Syntax in the Spatial Configuration Analysis," University of Brawijaya, Malang, 2014.

[11] A. B. Darjosanjoto, S. Rachmawati, Murni. Tribhuwaneswari and E. Titi, "The Spatial Consequences of High-Rise Building of The Public Space of Basuki Rahmat Corridor, Surabaya," *IPTEK J. Proc. Ser.*, vol. 2, no. 1, pp. 55–56, 2016.

[12] J. Hillier, Bill, Hanson, J., Peponis, "What do We Mean by Building? Habitat International," vol. 5, no. 3–4, pp. 271–288, 1980.

[13] M. Batty, K. Axhausen, and G. Fosca, "Reformulating Space Syntax: The Automatic Definition and Generation of Axial Lines and Axial Maps," 2008.

[14] M. F. Romdhoni, "Analysis of City Open Space Configuration Patterns Using the Space Syntax Method as Spatial Logic and Space Use," *NALARs*, vol. 17, no. 2, 2018. [in Bahasa]

[15] E. Syarif and N. Amri, "Green Architecture in the Morphology of the Tallo Riverside Settlement," *Indones. J. Built Environ.*, vol. 6, no. 2, pp. 82–87, 2017. [in Bahasa]

# Free Vibration Characteristics of Thin Spherical Shells

Koji Sekine [a,*]

[a]Field of Mechanical Engineering, Department of Creative Engineering, National Institute of Technology, Kushiro College.
Email:sekine@kushiro-ct.ac.jp

## Abstract

Free vibration characteristics of thin spherical shells having freely boundary conditions are analyzed. In this study, the fundamental properties of natural vibration for the spherical shells are investigated. The power function is employed as the admissible function, displacement functions satisfying the geometric boundary conditions are expressed in the form of single series. The eigenvalue problem for free vibration of the shells derived by using the Lagrange's equation of motion, is processed numerically to acquire the natural frequencies and mode shapes. The reliability and accuracy of the present results are verified by convergence tendencies of the present solutions and comparisons of the data between the current analysis, FEM (finite element method) and published literatures. In numerical results, the variations of natural vibration characteristics of the shells due to the circumferential wavenumber and various shell geometries are illustrated.

*Keywords: Free vibration; vibration of structural element; solid of revolution; spherical shell*

## 1. Introduction

Spherical shells have a very broad range of application in industrial products as a structural element on the fields of mechanical, aerospace and civil engineering. In structural design, it is particularly significant that the natural vibration characteristics of the shells are comprehended as a valuable countermeasure against the resonance phenomenon.

Consequently, free vibration of the spherical shells has been widely and actively studied until recently. Niordson [1] presented the complete solution for axisymmetric and non-axisymmetric vibration of thin elastic spherical shell with two boundaries. Tornabene and Viola [2] dealt with the dynamical behaviour of hemispherical domes and spherical shell panels by using Generalized Differential Quadrature (GDQ) method. Lee [3] investigated the axisymmetric and asymmetric free vibration analysis of spherical caps, which have displacements and the rotations expressed by Chebyshev polynomials. Qu et al. [4] indicated a general formulation for vibration analyses of functionally graded shells of revolution subjected to arbitrary boundary conditions. Shi et al. [5] treated the free vibration analysis of open and closed shells with arbitrary boundary conditions. Xie et al. [6] presented an approach to analyze free vibrations of thin spherical shells with arbitrary boundary conditions and non-uniform thickness. Li et al. [7] described the free vibration of uniform and stepped annular-spherical shells with general boundary conditions by using a semi-analytical approach. Du et al. [8] showed the free vibration of spherical caps with uniform and stepped thickness subjected to various boundary conditions. Hu et al. [9] mentioned the free vibration characteristics of moderately thick annular spherical shell structure with general boundary conditions. In addition, Du et al. [10] proposed the free vibration characteristic of truncated spherical shell subjected to classical and elastic edge constraints. In the study introduced avobe, the governing equation of motion (the partial differential equations) is analyzed, and Chebyshev, Legendre and Jacobi polynomials are employed as the displacement admissible functions. Also, the analysis using artificial springs to give elastic boundary conditions has been solved by the Ritz method. On the other hand, the spherical shells deeper than the hemispherical shell and the sphere are rarely found, and there are few examples of variations in the natural vibration characteristics by the difference of the shell geometries.

Therefore, in this paper, the free vibration characteristics of the spherical shells is analyzed by using energy method and a commercial FEM (finite element method) software, SolidWorks simulation. Specifically, the power function is applied as the admissible function, and the energy functional of the shells consisting of the elastic strain energy and the kinetic energy are established. Furthermore, the eigenvalue problem for free vibration of the shells is derived by using the Lagrange's equation of motion. In numerical results, the

---

*Corresponding author. Tel.: +81-154-57-7294
*Otanoshike-Nishi 2-32-1, Kushiro, Hokkaido*
*Japan, 084-0916*

reliability and accuracy of the present solutions are showed from the point of view of the convergence for solutions and the comparisons with the data from published literatures and FEM software. Moreover, the variations of natural vibration characteristics such as natural frequencies and vibration modes of the shells by various shell geometries and the circumferential wavenumber are discussed.

## 2. Theory and Formulation

### 2.1. Geometry and displacement field of the spherical shell

The geometry and the coordinate system of the spherical shell are shown in Fig. 1. The coordinate system o-$\varphi$-$\theta$-$z$ is taken and the displacements in $\varphi$, $\theta$ and $z$ directions at arbitrary points on the shell are represented by $\hat{u}$, $\hat{v}$ and $\hat{w}$, respectively. The shell has the hole at upper and lower poles, and the radius and thickness of the shell are denoted by $R$ and $h$. Also, open angles at the poles are indicated by $\Phi_1$ and $\Phi_2$. As shown in Fig. 2, the shell has four types of geometry: with open angle $\Phi_2$, with open angles $\Phi_1$ and $\Phi_2$ (symmetric or asymmetric to the equator) and sphere.
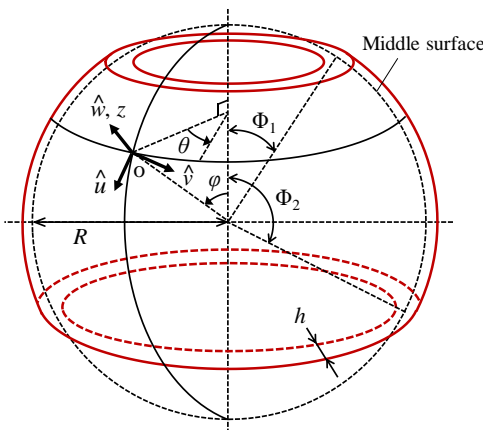


Figure 1. Geometry and the coordinate system of a spherical shell
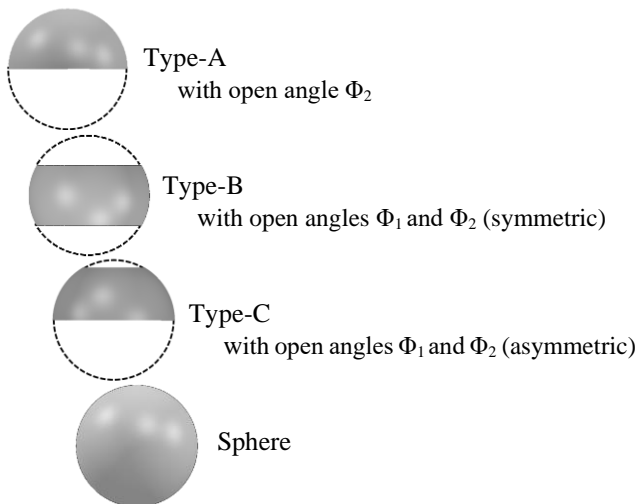


Figure 2. Geometry types of the spherical shell

On the bending deformation of the shell, the hypothesis of Kirchhoff-Love (Line elements perpendicular to the middle surface of the shell remain straight and perpendicular to the middle surface during deformation) is applied. Therefore, the displacements $\hat{u}$, $\hat{v}$ and $\hat{w}$ at arbitrary points of the shell can be written in Eq. (1). In this equation, $u$, $v$ and $w$ are the displacements on the middle surface of the shell and "$t$" denotes the time.

$$\hat{u}(\varphi,\theta,z,t)=\left(1+\frac{z}{R}\right)u(\varphi,\theta,t)-\frac{z}{R}\frac{\partial w(\varphi,\theta,t)}{\partial \varphi}$$

$$\hat{v}(\varphi,\theta,z,t)=\left(1+\frac{z}{R}\right)v(\varphi,\theta,t)-\frac{z}{R\sin\varphi}\frac{\partial w(\varphi,\theta,t)}{\partial \theta} \quad (1)$$

$$\hat{w}(\varphi,\theta,z,t)=w(\varphi,\theta,t)$$

### 2.2. Elastic strain and kinetic energies

Considering that the spherical shell consists of a linear elastic body, the strain-displacement relations are expressed as Eq. (2).

$$\varepsilon_\varphi = \frac{1}{R}\left(\frac{\partial \hat{u}}{\partial \varphi}+\hat{w}\right)$$

$$\varepsilon_\theta = \frac{1}{R}\left(\frac{1}{\sin\varphi}\frac{\partial \hat{v}}{\partial \theta}+\frac{\hat{u}}{\tan\varphi}+\hat{w}\right) \quad (2)$$

$$\gamma_{\varphi\theta} = \frac{1}{R}\left(\frac{\partial \hat{v}}{\partial \varphi}+\frac{1}{\sin\varphi}\frac{\partial \hat{u}}{\partial \theta}-\frac{\hat{v}}{\tan\varphi}\right)$$

Also, the stress-strain relations are expressed as Eq. (3). In this equation, $Q_{ij}$ ($i,j$ =1, 2, 6) are the stiffness coefficients composed of Young's modulus $E$ and Poisson's ratio $v$, respectively.

$$\begin{Bmatrix}\sigma_\varphi\\\sigma_\theta\\\tau_{\varphi\theta}\end{Bmatrix}=\begin{bmatrix}Q_{11}&Q_{12}&0\\Q_{12}&Q_{22}&0\\0&0&Q_{66}\end{bmatrix}\begin{Bmatrix}\varepsilon_\varphi\\\varepsilon_\theta\\\gamma_{\varphi\theta}\end{Bmatrix}$$

$$(3)$$

$$Q_{11}=Q_{22}=\frac{E}{1-v^2}, \quad Q_{12}=\frac{vE}{1-v^2}, \quad Q_{66}=\frac{E}{2(1+v)}$$

Applying the elasticity theory, the elastic strain energy $U$ stored in the shell due to elastic deformation is expressed by Eq. (4). In this equation, [A] and [D] are stretching and bending stiffness matrix, $\{\varepsilon\}$ and $\{\kappa\}$ are strain and curvature vectors on the middle surface of the shell. Also, the components of the matrices and the vectors are written by Eqs. (5) and (6).

$$U=\frac{R^2}{2}\int_{-\frac{h}{2}}^{\frac{h}{2}}\int_0^{2\pi}\int_{\Phi_1}^{\Phi_2}(\sigma_\varphi\varepsilon_\varphi+\sigma_\theta\varepsilon_\theta+\tau_{\varphi\theta}\gamma_{\varphi\theta})\sin\varphi\,d\varphi\,d\theta\,dz$$

$$=\frac{R^2}{2}\int_0^{2\pi}\int_{\Phi_1}^{\Phi_2}\left[\{\varepsilon\}^T[A]\{\varepsilon\}+\{\kappa\}^T[D]\{\kappa\}\right]\sin\varphi\,d\varphi\,d\theta \quad (4)$$

$$[A] = \begin{bmatrix} A_{11} & A_{12} & 0 \\ A_{12} & A_{22} & 0 \\ 0 & 0 & A_{66} \end{bmatrix}, \quad [D] = \begin{bmatrix} D_{11} & D_{12} & 0 \\ D_{12} & D_{22} & 0 \\ 0 & 0 & D_{66} \end{bmatrix}$$

$$A_{ij} = hQ_{ij}, \quad D_{ij} = \frac{h^3}{12}Q_{ij} \quad (i, j = 1, 2, 6) \tag{5}$$

From now on, $p_s$ and $p_{rs}$ ( $p \to u, v, w$ and $r, s \to \varphi, \theta$ ) denote the differentiation for $\partial p /\partial s$ and $\partial^2 p /\partial r \partial s$.

$$\{\varepsilon\} = \frac{1}{R} \left\{ u_\varphi + w, \quad \frac{u}{\tan\varphi} + \frac{v_\theta}{\sin\varphi} + w, \quad v_\varphi - \frac{v}{\tan\varphi} + \frac{u_\theta}{\sin\varphi} \right\}^{\mathrm{T}}$$

$$\{\kappa\} = \frac{1}{R^2} \left\{ u_\varphi - w_{\varphi\varphi}, \quad \frac{v_\theta}{\sin\varphi} - \frac{w_{\theta\theta}}{\sin^2\varphi} + \frac{u}{\tan\varphi} - \frac{w_\varphi}{\tan\varphi}, \right.$$

$$\left. v_\varphi - \frac{v}{\tan\varphi} - \frac{2w_{\varphi\theta}}{\sin\varphi} + \frac{\cos\varphi \, w_\theta}{\sin^2\varphi} + \frac{u_\theta}{\sin\varphi} \right\}^{\mathrm{T}} \tag{6}$$

On the other hand, the kinetic energy $T$ of the shell is evaluated by Eq. (7), where $\rho$ is corresponding to the mass density of the material per unit volume.

$$T = \frac{R^2\rho}{2} \int_{-\frac{h}{2}}^{\frac{h}{2}} \int_0^{2\pi} \int_{\Phi_1}^{\Phi_2} \left\{ \left(\frac{d\hat{u}}{dt}\right)^2 + \left(\frac{d\hat{v}}{dt}\right)^2 + \left(\frac{d\hat{w}}{dt}\right)^2 \right\} \sin\varphi \, d\varphi d\theta dz$$

$$= \frac{R^2}{2} \int_0^{2\pi} \int_{\Phi_1}^{\Phi_2} \left[ I_t (\dot{u}^2 + \dot{v}^2 + \dot{w}^2) + I_r (\dot{u}^2 + \dot{v}^2) \right.$$

$$\left. - 2I_r \left( \dot{u}\dot{w}_\varphi + \frac{\dot{v}\dot{w}_\theta}{\sin\varphi} \right) + I_r \left( \dot{w}_\varphi^2 + \frac{\dot{w}_\theta^2}{\sin^2\varphi} \right) \right] \sin\varphi \, d\varphi d\theta \tag{7}$$

where the dot represents the derivative with respect to time, and the inertia terms can be written as follows:

$$I_t = \rho h, \quad I_r = \frac{\rho h^3}{12R^2} \tag{8}$$

### 2.3. Derivation of the eigenvalue problem

Assuming that the shell maintains a harmonic vibrating at the angular frequency $\omega$[rad/s], each displacement on the middle surface can be expressed as follows:

$$u(\varphi, \theta, t) = \sum_{i=0}^{I-1} u_i(t) X_{ui}(\varphi) Y_u(\theta) = \sin\omega t \sum_{i=0}^{I-1} U_i \, \varphi^i \cos N\theta$$

$$v(\varphi, \theta, t) = \sum_{i=0}^{I-1} v_i(t) X_{vi}(\varphi) Y_v(\theta) = \sin\omega t \sum_{i=0}^{I-1} V_i \, \varphi^i \sin N\theta \tag{9}$$

$$w(\varphi, \theta, t) = \sum_{i=0}^{I-1} w_i(t) X_{wi}(\varphi) Y_w(\theta) = \sin\omega t \sum_{i=0}^{I-1} W_i \, \varphi^i \cos N\theta$$

where $N$ denotes the circumferential wave number, and the power function $\varphi^i$ is employed as the admissible function $X_{pi}(\varphi)$ ( $p \to u, v, w$) so that freely boundary conditions described in Eq. (10) are satisfied at the hole edges of the shell.

Displacements : $\left. \hat{u} \right|_{\varphi = \Phi_{1,2}}, \left. \hat{v} \right|_{\varphi = \Phi_{1,2}}, \left. \hat{w} \right|_{\varphi = \Phi_{1,2}} \neq 0$

Slopes : $\left. \dfrac{\partial \hat{w}}{\partial \varphi} \right|_{\varphi = \Phi_{1,2}}, \left. \dfrac{\partial \hat{w}}{\partial \theta} \right|_{\varphi = \Phi_{1,2}} \neq 0$ (10)

Furthermore, the displacement functions given by Eq. (9) are substituted into the elastic strain and the kinetic energy described by Eqs. (4) and (7). Also, applying the Lagrangian ( $L=T-U$ ) to the Lagrange's equation of motion written as Eq.(11), the generalized eigenvalue problem can be summed up by Eq. (12).

$$\frac{\partial}{\partial t}\left(\frac{\partial L}{\partial \dot{q}_i(t)}\right) - \frac{\partial L}{\partial q_i(t)} = 0 \quad (L = T - U) \tag{11}$$

where $q_i(t)$ ( $q \to u, v, w$ ) are the generalized coordinates, which have been described in Eq. (9).

$$[K]\{a\} = \omega^2 [M]\{a\}$$

$$\{a\} = \{ U_i, V_i, W_i \}^{\mathrm{T}} \tag{12}$$

In Eq. (12), $[K]$ and $[M]$ represent the stiffness and the mass matrices, respectively. Natural frequencies $\omega$ and the corresponding eigenvectors $\{a\}$ are obtain by solving Eq. (12). Substituting the eigenvector $\{a\}$ including unknown coefficients $U_i$, $V_i$ and $W_i$ into the displacement functions given by Eq. (9), the natural vibration mode of the shells can be calculated. In numerical results, the natural frequencies $\omega$ are handled by the nondimensional frequency $\Omega$ expressed as follows:

$$\Omega = \omega R \sqrt{\frac{\rho}{E}} \tag{13}$$

### 3. Numerical Applications and Discussions

In this section, the accuracy and reliability of the present solutions are verified, and numerical study will be discussed on the free vibration characteristics of the spherical shells. In present numerical studies, Young's modulus $E$=190GPa, Poisson's ratio $v$=0.3 and the volume density $\rho$=8000kg/m³ are employed for the material constant of the spherical shells.

Within each tables and figures, the solutions by SolidWorks simulation as a commercial FEM (finite element method) software are indicated with present results. Also, in example results, $m$ denotes mode number in the meridional direction.

Table 1 presents the convergence characteristics of nondimensional frequencies $\Omega$ with respect to variations of the number of terms $I$ in displacement functions shown by Eq. (9). It is seen that nondimensional frequencies $\Omega$ converge with two or more significant figures, and the present solutions show good agreement with the results given by FEM simulation. Therefore, the number of terms $I$ =10 is employed for *Type-A* and *Sphere*, and $I$ =8 is applied to *Type-B* and *Type-C* in Eq. (9). In the case of *Type-A* and

198

*Sphere*, the shells have small open angles $\Phi_1 = 0.01°$ and $\Phi_2 = 179.99°$ due to avoid errors.

Table 2 demonstrates the comparisons of nondimensional frequency $\Omega$ of the spherical shell specified as *Type-A*. In the list, Niordson [1] shows the complete solution for natural vibration of the spherical shells, and Lee [3] presents the analytical solutions by using Chebyshev polynomials.

Table 3 shows the comparisons of nondimensional frequency $\Omega$ of the spherical shell specified as *Type-B*. Xie et al. [6] present an approach to analyze the free vibrations of thin spherical shells with various boundary conditions.

Table 4 gives the comparisons of nondimensional frequency $\Omega$ of the spherical shell specified as *Type-C*. Ref. [1] and [6] present the complete solution and an approach for the free vibration analysis of thin spherical shells, respectively.

Table 1. Convergence study of nondimensional frequencies $\Omega$  [ $R/h$=100 ]

| $\Phi_1$ [deg] | $\Phi_2$ [deg] | $N$ | Num. of terms $I$ | Mode No. $m$ 1 | 2 | 3 |
|---|---|---|---|---|---|---|
| 0.01 | 90 | 0 | 7 | 0.8705 | 0.9530 | 0.9874 |
| | | | 8 | 0.8705 | 0.9526 | 0.9843 |
| | | | 9 | 0.8705 | 0.9525 | 0.9834 |
| | | | 10 | 0.8705 | 0.9525 | 0.9830 |
| | | | FEM | 0.8709 | 0.9528 | 0.9850 |
| | | 7 | 7 | 0.2146 | 1.011 | 1.079 |
| | | | 8 | 0.2104 | 1.011 | 1.062 |
| | | | 9 | 0.2081 | 1.010 | 1.058 |
| | | | 10 | 0.2074 | 1.010 | 1.054 |
| | | | FEM | 0.2069 | 1.010 | 1.053 |
| 0.01 | 179.99 | 0 | 7 | 0.7349 | 0.8712 | 0.9527 |
| | | | 8 | 0.7349 | 0.8710 | 0.9265 |
| | | | 9 | 0.7349 | 0.8705 | 0.9261 |
| | | | 10 | 0.7349 | 0.8705 | 0.9246 |
| | | | FEM | 0.7360 | 0.8709 | 0.9245 |
| | | 7 | 7 | 0.9908 | 1.048 | 1.188 |
| | | | 8 | 0.9884 | 1.019 | 1.151 |
| | | | 9 | 0.9873 | 1.011 | 1.063 |
| | | | 10 | 0.9867 | 1.006 | 1.046 |
| | | | FEM | 0.9858 | 1.002 | 1.019 |
| 30 | 90 | 0 | 5 | 0.9200 | 0.9824 | 1.018 |
| | | | 6 | 0.9197 | 0.9809 | 1.007 |
| | | | 7 | 0.9195 | 0.9796 | 1.002 |
| | | | 8 | 0.9195 | 0.9793 | 1.001 |
| | | | FEM | 0.9184 | 0.9792 | 1.002 |
| | | 7 | 5 | 0.2253 | 0.6846 | 1.014 |
| | | | 6 | 0.2122 | 0.6664 | 1.013 |
| | | | 7 | 0.2088 | 0.6567 | 1.012 |
| | | | 8 | 0.2075 | 0.6510 | 1.012 |
| | | | FEM | 0.2067 | 0.6657 | 1.012 |

Table 2. Comparisons of nondimensional frequencies $\Omega$  [ $R/h$=100,  *Type-A* ]

| $\Phi_2$ [deg] | $N$ | $m$ | Present | FEM | Ref. [1] | Ref. [3] |
|---|---|---|---|---|---|---|
| 90 | 0 | 1 | 0.8705 | 0.8709 | 0.8705 | 0.8707 |
| | | 2 | 0.9525 | 0.9528 | - | 0.9531 |
| | 2 | 1 | 0.0138 | 0.0130 | 0.0129 | 0.0138 |
| | | 2 | 0.9174 | 0.9188 | 0.9174 | 0.9174 |
| 150 | 0 | 1 | 0.7648 | 0.7665 | 0.7648 | - |
| | 2 | 1 | 0.0429 | 0.0484 | 0.0461 | - |
| | | 2 | 0.7916 | 0.7934 | 0.7917 | - |

Table 3. Comparisons of nondimensional frequencies $\Omega$  [ $R/h$=100, $N$=2,  *Type-B* ]

| $\Phi_1$ [deg] | $\Phi_2$ [deg] | $m$ | Present | FEM | Ref. [1] | Ref. [6] |
|---|---|---|---|---|---|---|
| 30 | 150 | 1 | 0.0408 | 0.0435 | 0.0432 | 0.0421 |
| | | 2 | 0.0464 | 0.0500 | 0.0495 | - |
| 45 | 135 | 1 | 0.0189 | 0.0203 | 0.0201 | 0.0196 |
| | | 2 | 0.0250 | 0.0268 | 0.0265 | - |
| 60 | 120 | 1 | 0.0122 | 0.0128 | 0.0127 | 0.0124 |
| | | 2 | 0.0196 | 0.0206 | 0.0204 | - |

Table 4. Comparisons of nondimensional frequencies $\Omega$  [ $R/h$=100, $N$=2,  *Type-C* ]

| $\Phi_1$ [deg] | $\Phi_2$ [deg] | $m$ | Present | FEM | Ref. [1] | Ref. [6] |
|---|---|---|---|---|---|---|
| 30 | 90 | 1 | 0.0133 | 0.0126 | 0.0126 | 0.0123 |
| | | 2 | 0.0471 | 0.0515 | 0.0510 | - |
| | 120 | 1 | 0.0149 | 0.0155 | 0.0153 | 0.0151 |
| | | 2 | 0.0445 | 0.0492 | 0.0478 | - |
| 60 | 90 | 1 | 0.0104 | 0.0104 | 0.0103 | 0.0100 |
| | | 2 | 0.0223 | 0.0230 | 0.0226 | - |

In Tables 2−4, it's observed that the present solutions agree well with the ones obtained by the commercial FEM software and the references. As can be seen, the accuracy, validity and the verification of the present solutions can be confirmed in the view point of these comparisons. In the following, the present and FEM solutions are illustrated with respect to the shell geometries of *Type-A*, *B* and *C*.

Fig. 3 shows the variations of the nondimensional frequency $\Omega$ with respect to the circumferential wave number $N$ for the spherical shell specified as *Type-A*. In the figure, the solid and broken lines indicate the present solutions, and the small circles show FEM solutions. For any of the open angle $\Phi_2$, the fundamental frequency has been obtained at $N$=1, and so a significantly low frequency can be illustrated because the spherical shells behave like a rigid body motion at $N$=1. At axisymmetric mode with $N$=0, the nondimensional frequency of *Sphere* is the lowest, and at

$\Phi_2$=30°(shallow cap), high nondimensional frequency can be achieved. Whereas, when *N* is larger than 1, the hemispherical shell(dome) with $\Phi_2$=90° has the lowest nondimensional frequency, and the shell geometry of *Sphere* gives high one.

Fig. 4 gives the variations of the nondimensional frequency $\Omega$ with respect to the open angle $\Phi_2$ for the spherical shell characterized as *Type-A*. In this figure, the lowest nondimensional frequency is given at $\Phi_2$ =90° for each *N* except *N*=0, and it is effective to set the open angle $\Phi_2$ greater than 150° in order to increase the natural frequency of the shells.

Fig. 5 shows the vibration modes with respect to the open angle $\Phi_2$ for the spherical shell specified as *Type-A*. In the figure, nondimensional frequency $\Omega$ and $\Omega_{FEM}$ by the present and FEM solution are indicated under each vibration modes. At *N*=0, the axisymmetric mode shapes are illustrated for

each open angle $\Phi_2$ , and the node exists on the circumferential direction for the meridional direction mode number *m*=2. On the other hand, *N*=7 as the non-axisymmetric mode, it's recognized that multiple waves appear at the circumferential direction of the shell. Also, the waves exist clearly at the hole edge except *Sphere*.

Fig. 6 shows the variations of the nondimensional frequency $\Omega$ with respect to the circumferential wave number *N* for the spherical shell specified as *Type-B*. In this figure, the lines and the small circles indicate the present solutions and FEM ones, respectively. For any of the open angle $\Phi_1$ , the fundamental frequency has been given at *N*=1.



Figure 3. Variations of nondimensional frequencies $\Omega$
versus the circumferential wave number *N*
[ *R/h*=100, *m*=1, *Type-A* ]



Figure 5. Vibration modes of the spherical shells
[ *R/h*=100, *Type-A* ]



Figure 4. Variations of nondimensional frequencies $\Omega$
versus the open angle $\Phi_2$
[ *R/h*=100, *m*=1, *Type-A* ]



Figure 6. Variations of nondimensional frequencies $\Omega$
versus the circumferential wave number *N*
[ *R/h*=100, *m*=1, $\Phi_2$ =180°−$\Phi_1$ , *Type-B* ]

For $N$=0 as an axisymmetric mode, it turns out that the nondimensional frequency of *Sphere* is the lowest, and high nondimensional frequency can be obtained at $\Phi_1$=60°. When $N$ is larger than 1, the opposite tendency can be seen. That is, the shell geometry of *Type-B* with $\Phi_1$=60° gives the lowest nondimensional frequency, and *Sphere* shows high one.

Fig. 7 gives the variations of the nondimensional frequency $\Omega$ with respect to the open angle $\Phi_1$ for the spherical shell characterized as *Type-B*. In the figure, the lowest nondimensional frequency is given at $\Phi_1$ =60° for each $N$ except $N$=0. If the design of a high natural frequency for the shells is required, it's desirable to set the open angle $\Phi_1$ less than 10°.

Fig. 8 shows the vibration modes with respect to the open angle $\Phi_1$ for the spherical shell specified as *Type-B*. As $\Phi_1$ increases, the geometry of the shell becomes closer to a ring. At $N$=0 as an axisymmetric vibration, mode shapes of the

torus type are indicated for each open angle $\Phi_1$. Also, it is seen that according as the circumferential wave number $N$ becomes larger, the waves increase on the circumferential direction of the shells. In addition, a vertically symmetrical vibration modes appear except for $N$=7 with $\Phi_1$=30°.

Fig. 9(a)-(c) show the variations of the nondimensional frequency $\Omega$ versus the circumferential wave number $N$ for the spherical shell characterized as *Type-C* having the open angle $\Phi_1$ =10°, 30° and 60°, respectively. Where, the lines and the small circles denote the present and FEM solutions. As shown in these figures, when $N$ is larger than 1, the shells having $\Phi_2$ =90° give the lowest nondimensional frequency for each the open angle $\Phi_1$. Also, for the shells with the open angles $\Phi_2$=60°, 90° and 120°, it can be seen that the nondimensional frequencies are hardly affected by the change of the open angles $\Phi_1$. Furthermore, Fig.9(a) presents that the shallow shells with $\Phi_2$ =30° or the deep shells with $\Phi_2$ =150° give high nondimensional frequency while in $N$ larger than 1.



Figure 7. Variations of nondimensional frequencies $\Omega$ versus the open angle $\Phi_1$
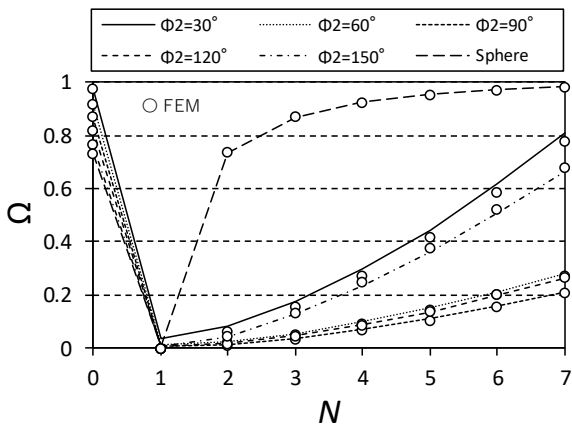[ $R/h$=100, $m$=1, $\Phi_2$ =180°−$\Phi_1$, *Type-B* ]



Figure 9(a). Variations of nondimensional frequencies $\Omega$ versus the circumferential wave number $N$
[ $R/h$=100, $m$=1, $\Phi_1$ =10°, *Type-C* ]
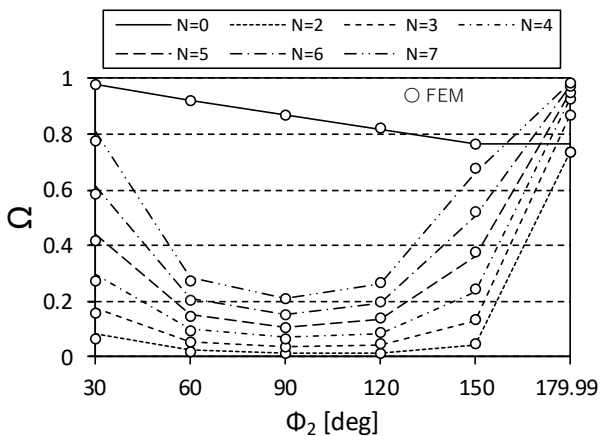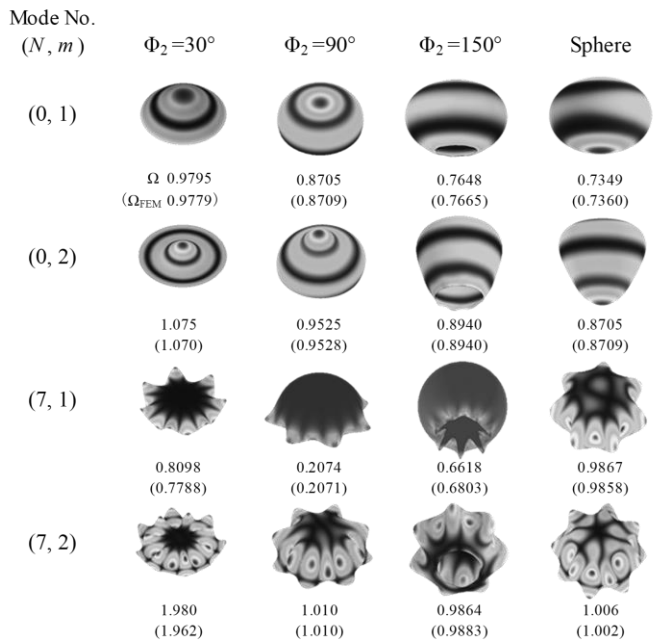


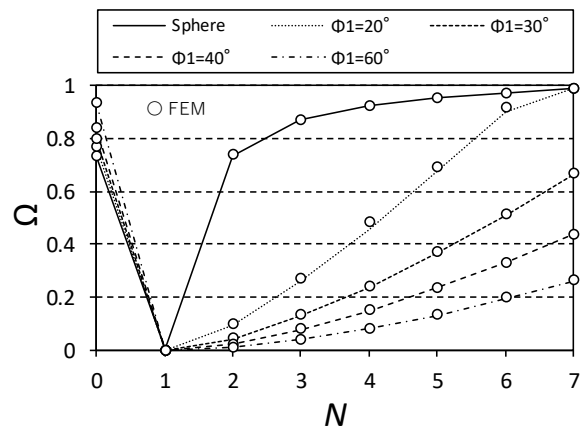Figure 8. Vibration modes of the spherical shells
[ $R/h$=100, *Type-B* ]



Figure 9(b). Variations of nondimensional frequencies $\Omega$ versus the circumferential wave number $N$
[ $R/h$=100, $m$=1, $\Phi_1$ =30°, *Type-C* ]

Fig. 10(a), (b) give the variations of the nondimensional frequency $\Omega$ versus the open angle $\Phi_2$ for the spherical shell specified as *Type-C* having the open angle $\Phi_1 =10°$, $30°$ and $60°$, respectively.

In these figures, for each open angles $\Phi_1$, the lowest nondimesional frequency can be obtained by the shells with $\Phi_2 =90°$. When high natural frequency of the shells is required in the structural design due to avoid the resonance, it is effective to adapt the shells to be shallow($\Phi_2 =30°$) or deep($\Phi_2 =150°$). Also, when $\Phi_2$ increase as the shells becomes deep, the nondimensional frequency decreases linearly for $N=0$ as an axisymmetric mode.

Fig. 11 indicates the vibration modes with respect to the open angles $\Phi_1$ and $\Phi_2$ for the spherical shell specified as *Type-C*. It is worth noting that the influences on the nondimensional frequency due to the changes in $\Phi_1$ are weak for each the open angle $\Phi_2$. In particular, when the circumferential wave number $N=7$, the mode shapes indicate local wavy deformations at lower hole edge. Therefore, the effects due to the changes of $\Phi_1$ on the nondimensional

frequencies are very small, and the nondimensional ones decrease slightly. On the contrary, when $N=0$, it is recognized that nondimensional ones increase as $\Phi_1$ increase.
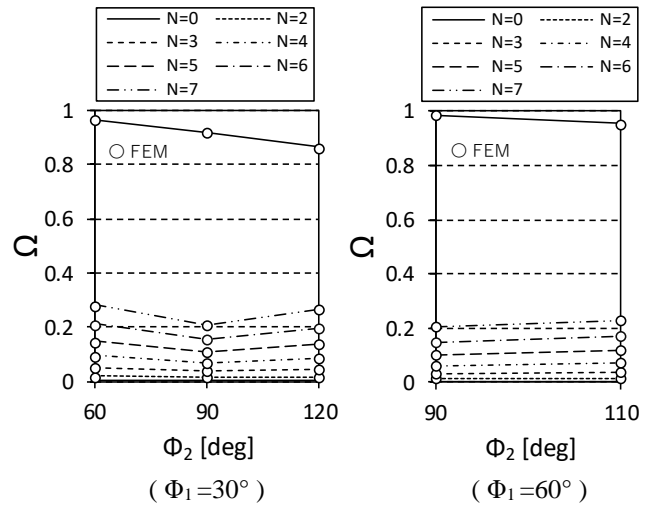


Figure 10(b). Variations of nondimensional frequencies $\Omega$ versus the open angle $\Phi_2$  [ $R/h=100$, $m=1$, *Type-C* ]
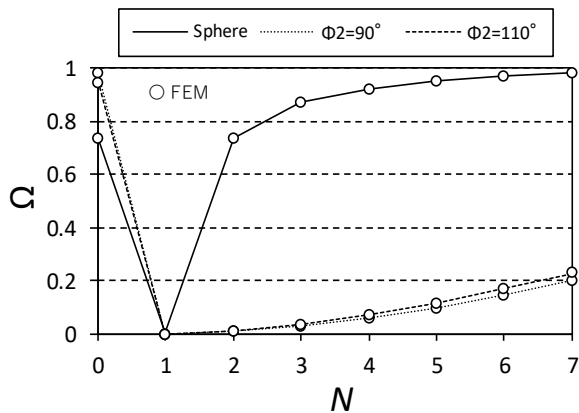


Figure 9(c). Variations of nondimensional frequencies $\Omega$ versus the circumferential wave number $N$
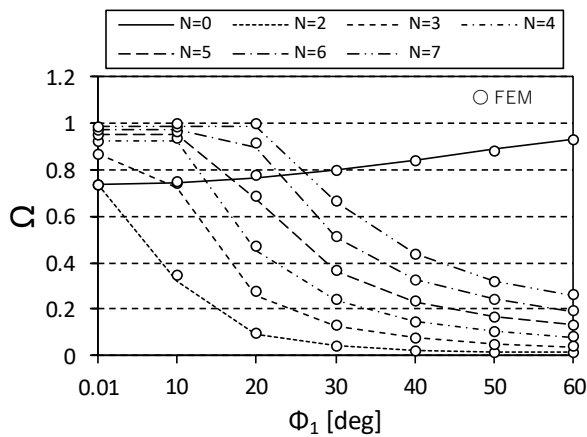[ $R/h=100$, $m=1$, $\Phi_1 =60°$, *Type-C* ]
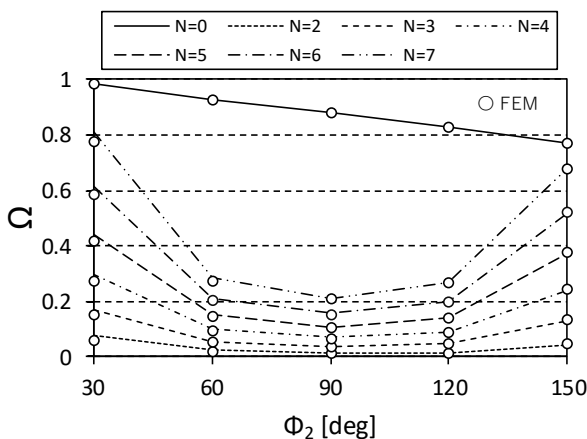


Figure 10(a). Variations of nondimensional frequencies $\Omega$ versus the open angle $\Phi_2$
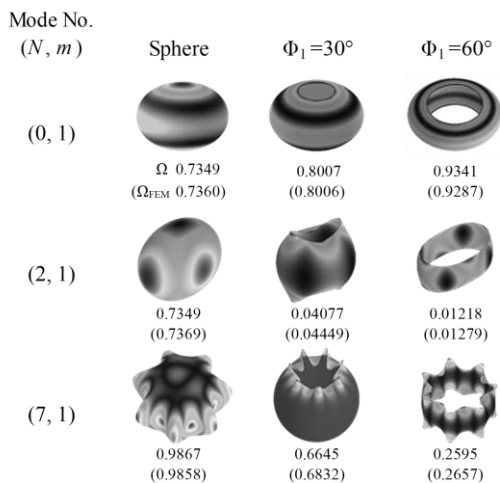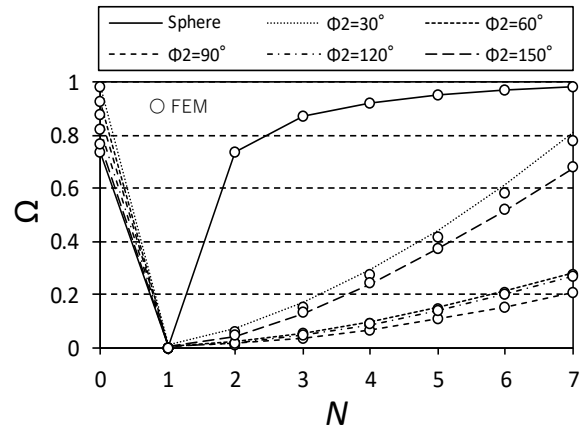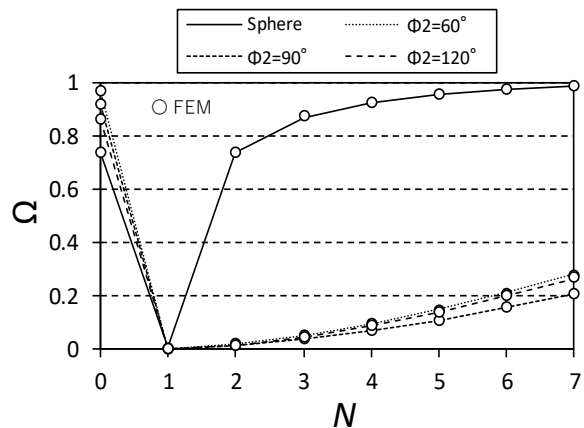[ $R/h=100$, $m=1$, $\Phi_1 =10°$, *Type-C* ]
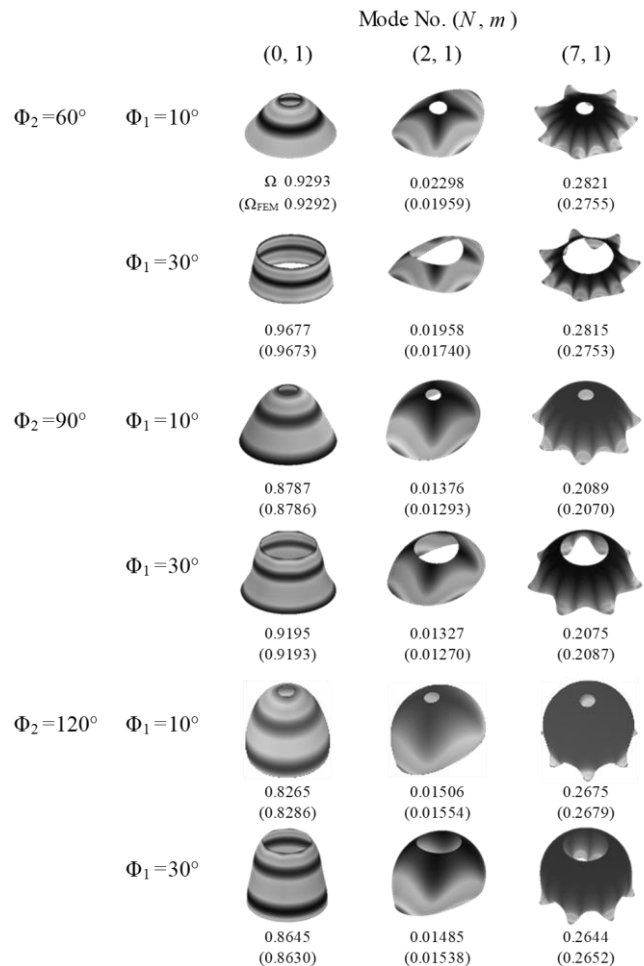


Figure 11. Vibration modes of the spherical shells
[ $R/h=100$, *Type-C* ]

## 4. Conclusions

This paper has dealt with the free vibration characteristics of thin spherical shells having freely boundary conditions.

First of all, the formulation of natural vibration analysis of the spherical shell has been expanded by applying the energy method. Also, the convergence study of the present solutions with respect to the number of terms in displacement functions has been indicated. Furthermore, the accuracy, validity and the verification of the present solutions have been confirmed through the comparisons with the solutions given by the commercial FEM software and the references.

In several numerical example, the present and FEM solutions for the free vibration characteristics of the shells have been illustrated with respect to the shell geometries specified by *Type-A*, *B* and *C*. Practically, the variations of natural frequencies and vibration modes of the shells due to the circumferential wavenumber, various shell geometries and the open angles have been illustrated in the figures.

It is expected that the present solution obtained in this study be able to suggest the fundamental properties of the spherical shells. Also, the present solution will give a reference data in similar studies of the solids of revolution. In addition, taking into account the problem due to avoid the resonance of the structures, the present results can be referred for the optimization design of the spherical shells.

## References

[1] Niordson F I. Free vibrations of thin elastic spherical shells. Int J Solids Struct 1984;20(7):667-678.

[2] Tornabene F, Viola E. Vibration analysis of spherical structural elements using the GDQ method. Comput Math Appl 2007;53:1538-60.

[3] Lee J. Free vibration analysis of spherical caps by the pseudospectral method. J Mech Sci Technol 2009;23:221-8.

[4] Qu Y, Long X, Yuan G, Meng G. A unified formulation for vibration analysis of functionally graded shells of revolution with arbitrary boundary conditions. Compos B Eng 2013;50:381-402.

[5] Shi D, Zhao Y, Wang Q, Teng X, Pang F. A unified spectro-geometric-Ritz method for vibration analysis of open and closed shells with arbitrary boundary conditions. Shock Vib 2016; Article ID 4097123: 30pages.

[6] Xie K, Chen M, Li Z. A semi-analytical method for vibration analysis of thin spherical shells with elastic boundary conditions. J Vibroeng 2017;19(4):2312-30.

[7] Li H, Pang F, Chen H. A semi-analytical approach to analyze vibration characteristics of uniform and stepped annular-spherical shells with general boundary conditions. Europe J Mech / A Solids 2019;74:48–65.

[8] Du Y, Huo R, Pang F, Li S, Huang Y, Zhang H. Free vibration of spherical cap subjected to various boundary conditions. Adv Mech Eng 2019;11(9):1-12.

[9] Hu B, Gao C, Zhang H, Li H, Pang F, Lang J. Free vibration characteristics of moderately thick spherical shell with general boundary conditions based on Ritz method. Shock Vib 2020; Article ID 4130103:20pages.

[10] Du Y, Sun L, Li S, Li S. Vibration analysis of truncated spherical shells under various edge constraints. Thin-Walled Struct 2020;147:106544.

# Accurate Results for Free Vibration of Doubly Curved Shallow Shells of Rectangular Planform (Part. 2 Thickness effect)

Yoshihiro Narita[a,*]

[a]Yamato University, Katayama, Suita, Osaka. (Professor Emeritus, Hokkaido University). Email: ynarita@eng.hokudai.ac.jp

**Abstract**

This paper presents a follow-up study of a previous work that deals with the free vibration of moderately thin isotropic shallow shells under general edge conditions. The same semi-analytical method is used in this study for identical shape and degree of curvature in doubly curved geometry, and accurate natural frequencies are tabulated for a wide range of the shell edge conditions. Emphasis is made, however, to present the frequency parameters for the shallow shells with very thin thickness (representative length/shell thickness=100). In numerical experiments, convergence test is made against series terms in the case of very thin shallow shells. Twenty-one sets of frequency parameters are tabulated for three shell shapes (spherical, cylindrical and hyperbolic paraboloidal shells) and two curvature ratios. These two papers (Part. 1 and 2) will constitute the accurate standard in the area of shallow shell vibration of rectangular planform and serve for future comparison and practical design purpose.

*Keywords: Accuracy; free vibration; natural frequency; shallow shell; small thickness*

## 1. Introduction

There has been active and increasing usage of shallow shell structures in mechanical and structural engineering. A growth in the literature on shallow shell vibration has reflected this technical trend [1]. This author has, however, noticed in the published literature a significant lack of comprehensive sets of accurate natural frequencies to cover a wide range of shallow shell geometries and boundary conditions.

In a previous work [2], an attempt was made to present a semi-analytical method and to provide comprehensive lists of natural frequencies of open shallow shells of rectangular planform. As distinctive feature, not found in other types of closed shells, open shallow shell can take wide variations of geometric form, such as spherical shell, cylindrical shell and parabolic hyperbolic shell, each with different degree of curvature. In other words, there are a large number of combinations in the shape parameters.

For shallow shell vibration, relevant previous works are summarized in Ref. [2]. Practically the first landmark paper on this topic is one [3] published by Leissa and Kadi that formulates the exact solution of shallow shells of rectangular planform supported along four edges by shear diaphragm. This paper is followed by other works [4-7] in the 1980's, and by many works [8-18] up to the present. From the viewpoint of providing comprehensive lists of natural frequencies for general boundary conditions, it is noted that two papers [19, 20] present methods and numerical results under various combinations of in-plane and out-of-plane boundary conditions. In Ref. [19], Mochida and his co-workers use a superposition method and present natural frequencies of various shallow shells, but shallow shells with free edges are not included. Qatu and Asadi [20] present frequencies of the shells with twenty-one different sets of boundary conditions, but it seems to the present author that the numerical results are not well converged.

The objective of this work (Part. 2) is to present comprehensive lists of accurate frequency parameters of very thin shallow shells for twenty-one sets of the boundary conditions. With the two studies, reasonably sufficient free vibration information can be summarized to cover shallow shells with relatively thick case (representative edge length/shell thickness=20) in Part. 1 [2] and very thin case in Part. 2 (thickness ratio=100). The convergence of the solution and comparison with other methods are severely checked, and effect of thickness is discussed by comparing these sets of results.
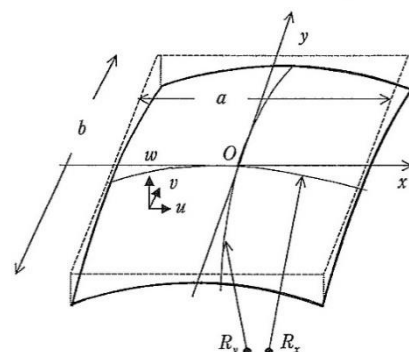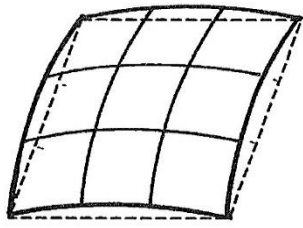


Figure 1. Shallow shell in the coordinate system

---

*Corresponding author.
Yamato University, Katayama, Suita, Osaka, Japan.

(a) Spherical shallow shell
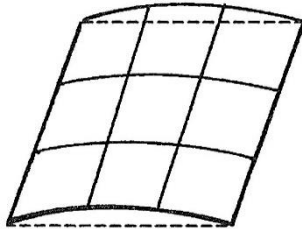


(b) Cylindrical shallow shell
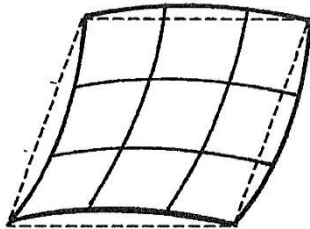


(c) Hyperbolic paraboloidal shallow shell

Figure 2. Shallow shells of rectangular planform

## 2. Outline of Analytical Method

The geometry of quadratic mid-surface can be expressed for a doubly curved shallow shell in a rectangular coordinate system (see Fig. 1) by

$$\phi(x,y) = -\frac{1}{2}\left(\frac{x^2}{R_x} + \frac{y^2}{R_y}\right) \qquad (1)$$

where $R_x$ and $R_y$ are the radii of curvature in the $x$ and $y$ directions, respectively. The dimension of its planform is given by $a \times b$ and the thickness is $h$. The four sides are subjected to uniform in-plane (i.e., stretching) and out-of-plane (bending) boundary conditions.

This shell takes geometric form of a spherical shell for $1/R_x = 1/R_y = $ (finite) in Fig. 2(a), and takes form of a cylindrical shell for "$1/R_x = $ (finite) and $1/R_y = 0$ ($R_y = \infty$)" or "$1/R_y = $ (finite) and $1/R_x = 0$ ($R_x = \infty$)" in Fig. 2(b). When positive curvature exists in $x$ direction and negative curvature in $y$ direction, or vice versa, it takes form of a hyperbolic paraboloidal shell for $1/R_x = -1/R_y = $ (finite) in Fig. 2(c).

In the previous study [2], details of extended Ritz method are presented based on Donnell-type shallow shell theory. The same method is used here. The stretching, stretching-bending coupling and bending stiffness matrices are given, respectively, by

$$[A] = \begin{bmatrix} A_{11} & A_{12} & A_{16} \\ A_{12} & A_{22} & A_{26} \\ A_{16} & A_{26} & A_{66} \end{bmatrix} \qquad (2a)$$

$$[B] = \begin{bmatrix} B_{11} & B_{12} & B_{16} \\ B_{12} & B_{22} & B_{26} \\ B_{16} & B_{26} & B_{66} \end{bmatrix} \qquad (2b)$$

$$[D] = \begin{bmatrix} D_{11} & D_{12} & D_{16} \\ D_{12} & D_{22} & D_{26} \\ D_{16} & D_{26} & D_{66} \end{bmatrix} \qquad (2c)$$

For isotropic material, they are simply reduced to

$$A_{ij} = hQ_{ij} \ , \ B_{ij} = 0 \ , \ D_{ij} = \left(\frac{h^3}{12}\right)Q_{ij} \qquad (3)$$

$(i,j=1,2,6)$, where the coefficients are elastic constants

$$Q_{11} = Q_{22} = \frac{E}{1-v^2}, \ Q_{12} = vQ_{11}, \ Q_{66} = G \quad (4)$$

Here, $E$ is the modulus of elasticity, $G=E/2(1+v)$ is the shear modulus and $v$ is Poisson's ratio.

This semi-analytical method requires the evaluation of energy functional

$$L = T_{max} - \left(V_{s,max} + V_{bs,max} + V_{b,max}\right) \qquad (5)$$

where $V_s$, $V_{bs}$ and $V_b$ are the parts of the total strain energy due to stretching, bending- stretching coupling and bending, respectively, and $T$ is translational kinetic energy. The stationary value is determined in the functional by

$$\frac{\partial L}{\partial P_{ij}} = 0, \ \frac{\partial L}{\partial Q_{kl}} = 0, \ \frac{\partial L}{\partial R_{mn}} = 0 \qquad (6)$$

$(i,k,m = 0,1,2,..,(M-1); \ j,l,n = 0,1,2,...,(N-1)$

where $P_{ij}$, $Q_{kl}$ and $R_{mn}$ are unknown coefficients in the displacement functions. The displacement functions are formulated to satisfy at least the kinematical boundary conditions along the edges. Use of boundary index makes it possible to accommodate any combination of in-plane and out-of-plane boundary conditions [2].

After applying the process in Eq. (6), frequency equation is derived as

$$det\left([K] - \Omega^2[M]\right) = 0 \qquad (7)$$

where $[K]$ and $[M]$ are global stiffness and mass (inertia) matrices, respectively. The $\Omega$ is a frequency parameter

$$\Omega = \omega a^2 \sqrt{\frac{\rho h}{D}} \text{ (dimensionless frequency)} \qquad (8)$$

$$D = Eh^3 / 12\left(1-v^2\right) \text{ (reference plate stiffness)} \qquad (9)$$

The lowest six eigenvalues from Eq.(7) are frequency parameters to be listed in the following tables. It should be noted again that arbitrary sets of boundary conditions can be specified, and details are given in previous study [2]. For edge condition, "F" and ""C" indicate all four displacements are unconstrained and constrained, respectively, and "S" does simply support with in-plane displacement parallel to the edge is zero but one perpendicular to the edge is unconstrained [2].

## 3. Numerical Examples and Accuracy of Solution

### 3.1. Convergence and comparison of the solution

In the present numerical examples, very thin thickness ($a/h$=100) is assumed to study the thickness effect by comparing the results with those in previous study [2] for relatively thick case ($a/h$=20). Square planform ($a/b$=1), except in Table.2, and Poisson's ratio =0.3 are used.

Table 1 presents convergence study of frequency parameters of spherical ($R_x/R_y$=1), cylindrical ($R_x/R_y$=0, i.e., $R_y=\infty$) and hyperbolic paraboloidal ($R_x/R_y$= -1) shells of square planform. The shells (SSSS) in this table are supported by shear diaphragm along four edges, and the exact solution is available [3]. For each shell configuration, two degrees of curvature $a/R_x$=0.2 and 0.5 are used. The present results are calculated for the number of terms 8×8, 10×10 and 12×12 for each of $u, v$ and $w$, and as in the

relatively thick shell [2], the present parameters similarly converge well within five significant figures, and are in very good agreement with the exact values. A pair of half wave number of out-of-plane displacement $w$ is given by ($m,n$) in the table.

Table 2 is a comparison study with values of Ref. [19] by Mochida and his co-workers. They use the method of superposition that is known as a method to provide numerical solutions in good accuracy. They provide frequency parameters only for combinations of two types of in-plane constraints, where displacement normal to the edge is zero and displacement parallel to the edge is zero, and two type of out-of-plane displacement, i.e., simple support and clamped edge. In their work, no results are presented for cases involving free edges.

In a previous study [2], comparison is made also with their values, but for avoiding duplication in this work, different sets of boundary conditions are used. Also result for CCCC is given for a rectangle ($a/b$=0.5). It is found in the table that the present values exactly agree with their values, when the present ones are rounded with four significant figures. Accuracy of the present solution is

Table 1 Convergence and comparison of frequency parameters $\Omega$ of simply supported shallow shells (SSSS), $a/b$ =1, $a/h$ =100, $v$ =0.3.

|  | $\Omega_1$ | $\Omega_2$ | $\Omega_3$ | $\Omega_4$ | $\Omega_5$ | $\Omega_6$ |
|---|---|---|---|---|---|---|
| **Spherical shell ($R_x/R_y$=1, $a/R_x$=0.2)** | | | | | | |
| 8 × 8 | 68.858 | 82.426 | 82.426 | 102.92 | 118.77 | 118.77 |
| 10 × 10 | 68.857 | 82.425 | 82.425 | 102.92 | 118.74 | 118.74 |
| 12 × 12 | 68.857 | 82.425 | 82.425 | 102.92 | 118.74 | 118.74 |
| Exact | 68.858 | 82.425 | 82.425 | 102.92 | 118.74 | 118.74 |
| (m,n) | (1,1) | (1,2) | (2,1) | (2,2) | (1,3) | (3,1) |
| **Spherical shell ($R_x/R_y$=1, $a/R_x$=0.5)** | | | | | | |
| 8 × 8 | 164.63 | 171.70 | 171.70 | 182.64 | 192.09 | 192.09 |
| 10 × 10 | 164.63 | 171.70 | 171.70 | 182.63 | 192.05 | 192.05 |
| 12 × 12 | 164.63 | 171.70 | 171.70 | 182.63 | 192.05 | 192.05 |
| Exact | 164.63 | 171.70 | 171.70 | 182.63 | 192.05 | 192.05 |
| (m,n) | (1,1) | (1,2) | (2,1) | (2,2) | (1,3) | (3,1) |
| **Cylindrical shell ($R_x/R_y$=0, $a/R_x$=0.2)** | | | | | | |
| 8 × 8 | 38.437 | 51.061 | 72.299 | 85.563 | 98.921 | 115.24 |
| 10 × 10 | 38.437 | 51.059 | 72.299 | 85.562 | 98.893 | 115.22 |
| 12 × 12 | 38.437 | 51.059 | 72.299 | 85.562 | 98.892 | 115.22 |
| Exact | 38.437 | 51.059 | 72.299 | 85.562 | 98.893 | 115.22 |
| (m,n) | (1,1) | (1,2) | (2,1) | (2,2) | (3,1) | (1,3) |
| **Cylindrical shell ($R_x/R_y$=0, $a/R_x$=0.5)** | | | | | | |
| 8 × 8 | 59.191 | 84.179 | 99.987 | 114.02 | 137.86 | 140.79 |
| 10 × 10 | 59.184 | 84.179 | 99.915 | 114.02 | 137.81 | 140.79 |
| 12 × 12 | 59.184 | 84.179 | 99.914 | 114.02 | 137.81 | 140.79 |
| Exact | 59.184 | 84.179 | 99.914 | 114.02 | 137.81 | 140.79 |
| (m,n) | (2,1) | (1,1) | (3,1) | (2,2) | (3,2) | (1,2) |
| **Hyperbolic paraboloidal shell ($R_x/R_y$=-1, $a/R_x$=0.2)** | | | | | | |
| 8 × 8 | 19.660 | 63.238 | 63.238 | 78.879 | 111.95 | 111.95 |
| 10 × 10 | 19.659 | 63.236 | 63.236 | 78.877 | 111.93 | 111.93 |
| 12 × 12 | 19.660 | 63.236 | 63.236 | 78.877 | 111.93 | 111.93 |
| Exact | 19.660 | 63.236 | 63.236 | 78.877 | 111.93 | 111.93 |
| (m,n) | (1,1) | (1,2) | (2,1) | (2,2) | (1,3) | (3,1) |
| **Hyperbolic paraboloidal shell ($R_x/R_y$=-1, $a/R_x$=0.5)** | | | | | | |
| 8 × 8 | 19.257 | 78.472 | 109.98 | 109.98 | 142.75 | 142.75 |
| 10 × 10 | 19.257 | 78.461 | 109.98 | 109.98 | 142.70 | 142.70 |
| 12 × 12 | 19.258 | 78.461 | 109.98 | 109.98 | 142.70 | 142.70 |
| Exact | 19.257 | 78.461 | 109.98 | 109.98 | 142.70 | 142.70 |
| (m,n) | (1,1) | (2,2) | (1,2) | (2,1) | (1,3) | (3,1) |

Table 2 Comparison of frequency parameters $\Omega$ of shallow shells, $a/R_x$ =0.5, $a/h$ =100, $v$ =0.3.

|  | $\Omega_1$ | $\Omega_2$ | $\Omega_3$ | $\Omega_4$ | $\Omega_5$ | $\Omega_6$ |
|---|---|---|---|---|---|---|
| **SCSS ($a/b$=1)** | | | | | | |
| Spherical shell ($R_x/R_y$=1) | | | | | | |
| Present | 168.71 | 173.78 | 181.43 | 188.92 | 193.37 | 204.54 |
| Ref.[19] | 168.7 | 173.8 | 181.4 | 188.9 | 193.4 | 204.6 |
| Cylindrical shell ($R_x/R_y$=0) | | | | | | |
| Present | 64.987 | 87.899 | 102.51 | 120.76 | 144.25 | 144.86 |
| Ref.[19] | 64.98 | 87.90 | 102.5 | 120.8 | 144.2 | 144.9 |
| Hyperbolic paraboloidal shell ($R_x/R_y$=-1) | | | | | | |
| Present | 82.623 | 90.895 | 130.08 | 131.01 | 150.55 | 169.19 |
| Ref.[19] | 82.62 | 90.90 | 130.1 | 131.0 | 150.5 | 169.2 |
| **SCSC ($a/b$=1)** | | | | | | |
| Spherical shell ($R_x/R_y$=1) | | | | | | |
| Present | 177.61 | 182.78 | 185.75 | 195.19 | 196.05 | 219.24 |
| Ref.[19] | 177.6 | 182.8 | 185.8 | 195.2 | 196.1 | 219.2 |
| Cylindrical shell ($R_x/R_y$=0) | | | | | | |
| Present | 71.325 | 92.637 | 105.67 | 127.94 | 149.84 | 151.31 |
| Ref.[19] | 71.32 | 92.63 | 105.7 | 127.9 | 149.8 | 151.3 |
| Hyperbolic paraboloidal shell ($R_x/R_y$=-1) | | | | | | |
| Present | 127.84 | 133.29 | 135.91 | 142.72 | 170.73 | 171.02 |
| Ref.[19] | 127.9 | 133.3 | 135.9 | 142.7 | 170.7 | 171.0 |
| **CCCC ($a/b$=0.5)** | | | | | | |
| Spherical shell ($R_x/R_y$=1) | | | | | | |
| Present | 179.41 | 179.90 | 180.47 | 187.88 | 189.62 | 192.52 |
| Ref.[19] | 179.4 | 179.9 | 180.5 | 187.9 | 189.6 | 192.5 |
| Cylindrical shell ($R_x/R_y$=0) | | | | | | |
| Present | 72.277 | 95.799 | 106.45 | 116.43 | 120.96 | 132.05 |
| Ref.[19] | 72.27 | 95.78 | 106.4 | 116.4 | 120.9 | 132.0 |
| Hyperbolic paraboloidal shell ($R_x/R_y$=-1) | | | | | | |
| Present | 131.04 | 131.20 | 139.19 | 139.90 | 154.35 | 155.52 |
| Ref.[19] | 131.0 | 131.2 | 139.2 | 139.9 | 154.4 | 155.5 |

thus established, and the following results are obtained in using the 12×12 solution that are presented in five significant figures.

*3.2. Comprehensive results of shallow shells*

Table 3(a) presents the lowest six frequency parameters $\Omega$ of shallow spherical shell ($R_x/R_y=1$) of square planform ($a/b=1$) with very small thickness ($a/h=100$) for twenty-one sets of boundary conditions. The degree of curvature is taken as $a/R_x=a/R_y=0.2$. Table 3(b) has the same format as Table 3(a), except that the curvature is larger in $a/R_x/=a/R_y=0.5$. Addition of curvature causes frequencies to be increased. In Table 3(a), the average increase from flat plates for the fundamental frequencies in $\Omega_1$ is 105.5 percent, including the highest increase 20 percent of CSSS shell. These increases are much larger than the case of relatively thin shell ($a/h=20$) in [2], and roughly speaking, are almost ten times larger. One should note, however, that the frequency parameter defined in Eqs. (8) and (9) include the thickness $h$ explicitly, and direct comparison between two sets of the parameters with different thickness ratios ($a/h=20$ and 100) may not be appropriate. This will be discussed later in this paper.

In Table 3(b), the deeper curvature $a/R=0.5$ causes the average increase of 252 percent in $\Omega_1$ with the maximum 734 percent of SSSS shell, when they are compared to the flat plate frequencies.

Table 4(a) and (b) tabulate the lowest six frequency parameters of shallow cylindrical shells with $R_x=$(infinity) and $a/R_y=0.2$ and $a/R_y=0.5$, respectively. This shell takes straight edges of the shell along the $x$ axis, and curvature

is given only along $y$ direction. When these tables are compared with those of spherical shell in Tab. 3(a) and (b), the effect of unidirectional curvature is a half of the spherical shells, and generally the effect of curvature increase in one direction is a half of curvatures in two directions of spherical shells.

Table 5(a) and (b) also tabulate the lowest six frequency parameters of shallow cylindrical shells, but with $R_y=$(infinity) and $a/R_x=0.2$ and $a/R_x=0.5$, respectively. Straight edges of the shell exist along the $y$ axis, and curvature exists only along $x$ direction. Likewise in results in [2], For cylindrical shells with FFFF, SSSS and CCCC, the frequency values are the identical as in Table 4(a) and (b) due to uniform boundary condition along four edges. Similarly, cylindrical shells with SSFF, CCFF and CCSS give the identical results as in Table 4(a) and (b) since the 90 degree rotation of the shell gives essentially the same boundary conditions. The same results in six cases are underlined.

Table 6(a) and (b) list up the lowest six parameters of shallow hyperbolic paraboloidal shells with $a/R_y=0.2$ and $a/R_y=0.5$, respectively. Just like in [2], the negative curvature ratio ($R_x/R_y=-1$) gives rise unusual response in frequency. Namely, for shell of hyperbolic paraboloidal shell, negative curvature causes decrease of frequencies, when shell has free edges. Four cases among twenty-one, the shell gives lower frequencies than frequencies of flat plate given in Table 7. As the constrained is increased along the edges, this tendency disappears.

Table 3(a) Frequency parameters $\Omega$ of shallow spherical shells, $R_x/R_y=1$, $a/R_x=a/R_y=0.2$, $a/b=1$, $a/h=100$, $v=0.3$.

| B.C. | $\Omega_1$ | $\Omega_2$ | $\Omega_3$ | $\Omega_4$ | $\Omega_5$ | $\Omega_6$ |
|------|------|------|------|------|------|------|
| FFFF | 13.521 | 19.753 | 35.878 | 35.878 | 42.331 | 69.570 |
| SFFF | 6.6712 | 17.335 | 26.490 | 35.783 | 61.072 | 61.267 |
| CFFF | 6.5822 | 8.8500 | 24.876 | 32.141 | 38.908 | 68.677 |
| SSFF | 3.4094 | 18.027 | 28.038 | 57.296 | 66.252 | 74.143 |
| CSFF | 8.4529 | 21.169 | 33.288 | 60.520 | 74.132 | 78.481 |
| CCFF | 16.271 | 26.213 | 43.803 | 68.672 | 79.180 | 83.149 |
| SFSF | 12.424 | 16.938 | 47.450 | 49.994 | 75.167 | 93.448 |
| CFSF | 21.671 | 37.610 | 58.211 | 64.713 | 77.247 | 100.30 |
| SSSF | 14.395 | 48.653 | 71.242 | 86.457 | 90.390 | 98.601 |
| CSSF | 31.481 | 61.465 | 74.028 | 92.204 | 93.843 | 113.78 |
| CCSF | 31.773 | 61.515 | 79.182 | 97.294 | 101.32 | 113.82 |
| CFCF | 61.320 | 61.437 | 69.751 | 74.382 | 82.536 | 103.95 |
| SCSF | 15.689 | 48.666 | 76.431 | 90.101 | 98.635 | 99.237 |
| CSCF | 61.391 | 71.924 | 80.512 | 94.731 | 102.02 | 127.78 |
| CCCF | 61.426 | 71.952 | 87.036 | 104.06 | 105.42 | 132.40 |
| SSSS | 68.857 | 82.425 | 82.425 | 102.92 | 118.74 | 118.74 |
| CSSS | 72.522 | 84.443 | 90.352 | 109.41 | 120.20 | 131.99 |
| CCSS | 76.255 | 91.412 | 93.796 | 115.75 | 133.02 | 133.89 |
| CSCS | 80.177 | 87.332 | 98.107 | 117.07 | 122.04 | 147.14 |
| CCCS | 84.183 | 96.662 | 100.01 | 123.14 | 135.28 | 148.86 |
| CCCC | 96.717 | 102.74 | 102.74 | 130.31 | 148.49 | 154.07 |

Table3(b) Frequency parameters $\Omega$ of shallow spherical shells, $R_x/R_y=1$, $a/R_x=a/R_y=0.5$, $a/b=1$, $a/h=100$, $v=0.3$.

| B.C. | $\Omega_1$ | $\Omega_2$ | $\Omega_3$ | $\Omega_4$ | $\Omega_5$ | $\Omega_6$ |
|------|------|------|------|------|------|------|
| FFFF | 13.574 | 19.983 | 36.858 | 36.858 | 49.526 | 70.625 |
| SFFF | 6.6235 | 17.914 | 27.470 | 38.759 | 64.412 | 71.594 |
| CFFF | 9.0041 | 9.7546 | 30.402 | 33.937 | 49.019 | 71.839 |
| SSFF | 3.3656 | 18.488 | 30.212 | 61.617 | 78.160 | 123.22 |
| CSFF | 12.169 | 23.168 | 42.208 | 67.551 | 88.251 | 128.57 |
| CCFF | 21.593 | 32.629 | 68.321 | 78.368 | 110.04 | 140.52 |
| SFSF | 13.116 | 17.328 | 53.474 | 54.929 | 110.64 | 110.95 |
| CFSF | 31.378 | 53.208 | 73.001 | 98.427 | 127.89 | 138.31 |
| SSSF | 14.987 | 54.190 | 110.80 | 166.05 | 173.40 | 175.80 |
| CSSF | 48.905 | 87.488 | 132.54 | 169.13 | 177.43 | 180.71 |
| CCSF | 49.647 | 87.592 | 132.58 | 174.10 | 182.71 | 188.86 |
| CFCF | 89.330 | 98.185 | 114.66 | 114.86 | 172.38 | 173.84 |
| SCSF | 20.617 | 54.193 | 110.80 | 172.06 | 176.98 | 182.58 |
| CSCF | 93.828 | 114.76 | 173.01 | 180.06 | 184.06 | 186.22 |
| CCCF | 93.835 | 114.77 | 173.26 | 184.38 | 189.33 | 195.28 |
| SSSS | 164.63 | 171.70 | 171.70 | 182.63 | 192.05 | 192.05 |
| CSSS | 168.71 | 173.78 | 181.43 | 188.92 | 193.37 | 204.54 |
| CCSS | 171.60 | 180.27 | 186.99 | 195.32 | 204.04 | 210.09 |
| CSCS | 177.61 | 182.78 | 185.75 | 195.19 | 196.05 | 219.24 |
| CCCS | 179.90 | 187.88 | 192.50 | 202.47 | 208.02 | 228.73 |
| CCCC | 191.99 | 191.99 | 196.93 | 209.96 | 216.19 | 242.22 |

Table 4(a) Frequency parameters Ω of shallow cylindrical shells, $R_x$ =(infinity), $a/R_y$ =0.2, $a/b$ =1, $a/h$ =100, $v$ =0.3.

| B.C. | $\Omega_1$ | $\Omega_2$ | $\Omega_3$ | $\Omega_4$ | $\Omega_5$ | $\Omega_6$ |
|------|------|------|------|------|------|------|
| FFFF | 13.483 | 21.903 | 34.850 | 37.642 | 38.468 | 61.117 |
| SFFF | 6.6792 | 25.137 | 27.266 | 29.361 | 53.625 | 62.120 |
| CFFF | 8.3592 | 8.9008 | 26.822 | 33.231 | 35.102 | 58.709 |
| SSFF | 3.3876 | 18.187 | 28.597 | 49.805 | 52.146 | 63.917 |
| CSFF | 9.5159 | 21.294 | 34.312 | 52.845 | 54.308 | 73.867 |
| CCFF | 11.007 | 29.916 | 35.356 | 62.297 | 65.099 | 74.651 |
| SFSF | 17.370 | 19.560 | 39.632 | 50.600 | 52.218 | 75.590 |
| CFSF | 22.359 | 25.244 | 43.750 | 60.101 | 61.232 | 77.857 |
| SSSF | 19.168 | 36.550 | 51.489 | 62.571 | 73.691 | 97.950 |
| CSSF | 24.151 | 40.977 | 60.740 | 65.130 | 80.745 | 104.66 |
| CCSF | 24.529 | 50.278 | 60.808 | 77.810 | 85.915 | 113.99 |
| CFCF | 28.583 | 31.660 | 48.648 | 70.829 | 71.612 | 80.604 |
| SCSF | 19.697 | 46.614 | 51.545 | 75.749 | 79.201 | 99.759 |
| CSCF | 30.225 | 45.975 | 68.284 | 71.291 | 89.195 | 112.37 |
| CCCF | 30.533 | 54.804 | 71.342 | 80.478 | 94.018 | 121.44 |
| SSSS | 38.437 | 51.059 | 72.299 | 85.562 | 98.892 | 115.22 |
| CSSS | 41.773 | 54.061 | 79.051 | 92.603 | 100.63 | 127.85 |
| CCSS | 48.570 | 67.079 | 81.803 | 100.93 | 116.03 | 129.48 |
| CSCS | 45.944 | 57.772 | 87.426 | 100.72 | 102.78 | 142.05 |
| CCCS | 51.987 | 69.788 | 90.013 | 108.44 | 117.90 | 143.61 |
| CCCC | 67.681 | 78.294 | 94.610 | 116.46 | 135.00 | 145.76 |

Table 5(a) Frequency parameters Ω of shallow cylindrical shells, $R_y$ =(infinity), $a/R_x$ =0.2, $a/b$ =1, $a/h$ =100, $v$ =0.3.

| B.C. | $\Omega_1$ | $\Omega_2$ | $\Omega_3$ | $\Omega_4$ | $\Omega_5$ | $\Omega_6$ |
|------|------|------|------|------|------|------|
| FFFF | 13.483 | 21.903 | 34.850 | 37.642 | 38.468 | 61.117 |
| SFFF | 6.6303 | 15.153 | 25.367 | 38.286 | 49.549 | 59.200 |
| CFFF | 3.4740 | 8.4730 | 21.673 | 30.718 | 38.552 | 61.123 |
| SSFF | 3.3876 | 18.187 | 28.597 | 49.805 | 52.146 | 63.917 |
| CSFF | 5.3711 | 23.986 | 29.189 | 58.193 | 62.305 | 65.517 |
| CCFF | 11.007 | 29.916 | 35.356 | 62.297 | 65.099 | 74.651 |
| SFSF | 9.7012 | 16.074 | 38.965 | 46.722 | 62.804 | 75.604 |
| CFSF | 15.183 | 36.307 | 49.399 | 61.353 | 66.142 | 86.169 |
| SSSF | 11.672 | 41.185 | 51.040 | 62.204 | 83.750 | 90.277 |
| CSSF | 26.655 | 53.502 | 56.075 | 74.830 | 86.146 | 105.96 |
| CCSF | 30.034 | 54.215 | 59.721 | 78.205 | 94.146 | 106.29 |
| CFCF | 58.315 | 60.258 | 61.144 | 70.589 | 73.150 | 96.003 |
| SCSF | 19.980 | 42.029 | 54.733 | 66.491 | 90.640 | 91.840 |
| CSCF | 58.926 | 63.964 | 67.510 | 84.225 | 89.974 | 118.23 |
| CCCF | 59.122 | 64.590 | 70.454 | 87.422 | 97.705 | 125.27 |
| SSSS | 38.437 | 51.059 | 72.299 | 85.562 | 98.892 | 115.22 |
| CSSS | 45.859 | 64.956 | 75.151 | 94.571 | 114.52 | 116.94 |
| CCSS | 48.570 | 67.079 | 81.803 | 100.93 | 116.03 | 129.48 |
| CSCS | 63.541 | 73.706 | 80.634 | 103.59 | 119.33 | 131.90 |
| CCCS | 65.171 | 75.764 | 86.896 | 109.46 | 131.64 | 133.36 |
| CCCC | 67.681 | 78.294 | 94.610 | 116.46 | 135.00 | 145.76 |

Table 4(b) Frequency parameters Ω of shallow cylindrical shells, $R_x$ =(infinity), $a/R_y$ =0.5, $a/b$ =1, $a/h$ =100, $v$ =0.3.

| B.C. | $\Omega_1$ | $\Omega_2$ | $\Omega_3$ | $\Omega_4$ | $\Omega_5$ | $\Omega_6$ |
|------|------|------|------|------|------|------|
| FFFF | 13.507 | 22.073 | 34.868 | 48.702 | 54.308 | 61.193 |
| SFFF | 6.7626 | 25.729 | 34.960 | 41.383 | 64.227 | 79.883 |
| CFFF | 10.588 | 16.980 | 30.638 | 42.203 | 47.659 | 65.439 |
| SSFF | 3.3702 | 18.226 | 37.799 | 52.273 | 79.338 | 83.783 |
| CSFF | 14.358 | 32.691 | 44.477 | 54.022 | 86.787 | 91.932 |
| CCFF | 14.983 | 42.872 | 49.155 | 73.302 | 89.760 | 96.679 |
| SFSF | 22.529 | 29.269 | 61.011 | 64.354 | 65.594 | 77.232 |
| CFSF | 29.383 | 34.058 | 71.553 | 73.837 | 74.882 | 80.774 |
| SSSF | 25.569 | 65.016 | 66.151 | 71.716 | 116.30 | 116.48 |
| CSSF | 31.551 | 70.922 | 74.274 | 79.607 | 118.44 | 123.64 |
| CCSF | 31.933 | 74.264 | 76.427 | 108.31 | 131.26 | 132.00 |
| CFCF | 36.942 | 39.735 | 82.233 | 84.268 | 84.971 | 85.003 |
| SCSF | 26.099 | 65.100 | 70.344 | 104.38 | 118.41 | 124.46 |
| CSCF | 38.287 | 76.311 | 84.646 | 87.429 | 121.03 | 131.22 |
| CCCF | 38.528 | 82.521 | 84.699 | 113.45 | 138.63 | 143.98 |
| SSSS | 59.184 | 84.179 | 99.914 | 114.02 | 137.81 | 140.79 |
| CSSS | 64.986 | 87.899 | 102.51 | 120.76 | 144.25 | 144.86 |
| CCSS | 72.375 | 105.48 | 127.24 | 133.02 | 147.49 | 168.62 |
| CSCS | 71.325 | 92.637 | 105.67 | 127.94 | 149.84 | 151.31 |
| CCCS | 78.068 | 108.33 | 134.01 | 134.72 | 153.32 | 173.98 |
| CCCC | 99.263 | 119.00 | 151.13 | 156.35 | 172.52 | 192.43 |

Table 5(b) Frequency parameters Ω of shallow cylindrical shells, $R_y$ =(infinity), $a/R_x$ =0.5, $a/b$ =1, $a/h$ =100, $v$ =0.3.

| B.C. | $\Omega_1$ | $\Omega_2$ | $\Omega_3$ | $\Omega_4$ | $\Omega_5$ | $\Omega_6$ |
|------|------|------|------|------|------|------|
| FFFF | 13.507 | 22.073 | 34.868 | 48.702 | 54.308 | 61.193 |
| SFFF | 6.5659 | 15.172 | 25.255 | 48.942 | 51.902 | 59.303 |
| CFFF | 3.4483 | 8.2887 | 21.400 | 29.527 | 51.692 | 60.834 |
| SSFF | 3.3702 | 18.226 | 37.799 | 52.273 | 79.338 | 83.783 |
| CSFF | 5.3196 | 23.755 | 38.350 | 62.825 | 80.388 | 89.447 |
| CCFF | 14.983 | 42.872 | 49.155 | 73.302 | 89.760 | 96.679 |
| SFSF | 9.6518 | 15.726 | 38.968 | 46.600 | 87.930 | 95.924 |
| CFSF | 14.858 | 46.682 | 49.066 | 90.447 | 102.91 | 106.34 |
| SSSF | 11.528 | 41.099 | 76.463 | 90.188 | 109.96 | 111.74 |
| CSSF | 39.866 | 69.777 | 85.768 | 109.29 | 117.32 | 140.36 |
| CCSF | 46.746 | 74.034 | 90.546 | 109.96 | 120.78 | 147.64 |
| CFCF | 60.841 | 85.618 | 101.77 | 106.69 | 129.75 | 137.60 |
| SCSF | 39.743 | 43.622 | 82.174 | 90.776 | 112.50 | 115.78 |
| CSCF | 69.222 | 103.23 | 112.13 | 124.49 | 156.98 | 158.29 |
| CCCF | 71.051 | 104.02 | 115.45 | 127.91 | 163.30 | 163.49 |
| SSSS | 59.184 | 84.179 | 99.914 | 114.02 | 137.81 | 140.79 |
| CSSS | 67.289 | 103.11 | 120.99 | 131.59 | 142.40 | 164.20 |
| CCSS | 72.375 | 105.48 | 127.24 | 133.02 | 147.49 | 168.62 |
| CSCS | 92.641 | 114.28 | 140.12 | 145.75 | 168.92 | 182.49 |
| CCCS | 95.798 | 116.43 | 145.24 | 150.67 | 170.30 | 187.31 |
| CCCC | 99.263 | 119.00 | 151.13 | 156.35 | 172.52 | 192.43 |

Table 6(a) Frequency parameters $\Omega$ of shallow hyperbolic paraboloidal shells, $R_x/R_y = -1$, $a/R_y = 0.2$, $a/b = 1$, $a/h = 100$, $v = 0.3$.

| B.C. | $\Omega_1$ | $\Omega_2$ | $\Omega_3$ | $\Omega_4$ | $\Omega_5$ | $\Omega_6$ |
|------|------|------|------|------|------|------|
| FFFF | 13.462 | 24.738 | 36.955 | 36.955 | 52.563 | 63.898 |
| SFFF | 6.6380 | 21.641 | 26.605 | 43.730 | 55.348 | 63.658 |
| CFFF | 6.4996 | 8.7953 | 29.914 | 32.664 | 46.110 | 64.991 |
| SSFF | 3.3656 | 20.411 | 38.508 | 39.592 | 63.965 | 66.883 |
| CSFF | 7.6241 | 28.830 | 42.288 | 52.961 | 65.428 | 75.539 |
| CCFF | 8.6992 | 33.048 | 50.320 | 63.530 | 74.322 | 78.713 |
| SFSF | 16.528 | 16.753 | 50.102 | 54.907 | 56.478 | 70.884 |
| CFSF | 26.302 | 37.366 | 59.804 | 64.066 | 64.665 | 84.047 |
| SSSF | 17.199 | 38.042 | 54.112 | 63.519 | 77.934 | 95.426 |
| CSSF | 33.152 | 48.479 | 64.771 | 76.666 | 81.357 | 105.33 |
| CCSF | 41.686 | 56.645 | 65.357 | 83.766 | 92.208 | 115.14 |
| CFCF | 61.217 | 63.091 | 70.497 | 73.361 | 74.448 | 94.428 |
| SCSF | 34.797 | 46.701 | 54.358 | 72.630 | 89.198 | 100.62 |
| CSCF | 62.678 | 66.374 | 74.210 | 86.152 | 87.457 | 114.99 |
| CCCF | 63.201 | 71.908 | 74.659 | 92.908 | 97.131 | 124.50 |
| SSSS | 19.660 | 63.236 | 63.236 | 78.877 | 111.93 | 111.93 |
| CSSS | 41.441 | 68.114 | 74.443 | 91.002 | 114.11 | 125.71 |
| CCSS | 52.386 | 77.989 | 79.478 | 100.61 | 127.67 | 127.81 |
| CSCS | 65.750 | 77.903 | 83.122 | 100.84 | 117.48 | 141.59 |
| CCCS | 69.936 | 86.409 | 87.335 | 109.50 | 130.71 | 143.33 |
| CCCC | 79.599 | 94.110 | 94.110 | 117.77 | 145.72 | 145.92 |

Table 6(b) Frequency parameters $\Omega$ of shallow hyperbolic paraboloidal shells, $R_x/R_y = -1$, $a/R_y = 0.5$, $a/b = 1$, $a/h = 100$, $v = 0.3$.

| B.C. | $\Omega_1$ | $\Omega_2$ | $\Omega_3$ | $\Omega_4$ | $\Omega_5$ | $\Omega_6$ |
|------|------|------|------|------|------|------|
| FFFF | 13.424 | 25.664 | 38.909 | 38.909 | 64.227 | 79.301 |
| SFFF | 6.5797 | 23.152 | 28.121 | 48.293 | 72.323 | 88.044 |
| CFFF | 8.2199 | 9.4072 | 36.242 | 36.427 | 72.068 | 81.721 |
| SSFF | 3.3264 | 21.403 | 38.639 | 72.319 | 82.019 | 94.838 |
| CSFF | 8.9011 | 34.299 | 75.355 | 80.171 | 88.219 | 112.27 |
| CCFF | 9.8110 | 38.144 | 85.107 | 95.412 | 110.78 | 127.38 |
| SFSF | 17.348 | 18.533 | 60.794 | 71.367 | 107.19 | 111.31 |
| CFSF | 43.390 | 58.519 | 89.161 | 102.31 | 113.00 | 123.96 |
| SSSF | 18.753 | 64.362 | 73.281 | 96.120 | 111.74 | 122.48 |
| CSSF | 66.052 | 71.660 | 107.99 | 112.92 | 125.04 | 141.99 |
| CCSF | 77.735 | 94.160 | 109.74 | 126.07 | 145.85 | 151.05 |
| CFCF | 98.601 | 116.10 | 121.74 | 127.34 | 128.31 | 140.44 |
| SCSF | 73.294 | 74.852 | 88.379 | 98.575 | 123.21 | 146.89 |
| CSCF | 105.30 | 124.20 | 130.30 | 140.39 | 141.58 | 146.16 |
| CCCF | 106.46 | 126.11 | 137.44 | 143.08 | 165.67 | 166.80 |
| SSSS | 19.258 | 78.461 | 109.98 | 109.98 | 142.70 | 142.70 |
| CSSS | 82.623 | 90.895 | 130.08 | 131.01 | 150.55 | 169.19 |
| CCSS | 94.181 | 122.38 | 136.98 | 149.24 | 173.01 | 173.62 |
| CSCS | 127.84 | 133.29 | 135.91 | 142.72 | 170.73 | 171.02 |
| CCCS | 131.20 | 139.90 | 154.35 | 158.42 | 186.02 | 189.83 |
| CCCC | 157.35 | 157.35 | 157.41 | 166.52 | 204.03 | 208.69 |

Table 7 Frequency parameters $\Omega$ of flat square plates, $a/b = 1$, $v = 0.3$.

| B.C. | $\Omega_1$ | $\Omega_2$ | $\Omega_3$ | $\Omega_4$ | $\Omega_5$ | $\Omega_6$ |
|------|------|------|------|------|------|------|
| FFFF | 13.468 | 19.596 | 24.270 | 34.801 | 34.801 | 61.093 |
| SFFF | 6.6433 | 14.902 | 25.376 | 26.001 | 48.449 | 50.579 |
| CFFF | 3.4711 | 8.5065 | 21.286 | 27.199 | 30.958 | 54.189 |
| SSFF | 3.3674 | 17.316 | 19.293 | 38.211 | 51.035 | 53.487 |
| CSFF | 5.3512 | 19.076 | 24.671 | 43.089 | 52.707 | 63.762 |
| CCFF | 6.9200 | 23.907 | 26.586 | 47.655 | 62.709 | 65.537 |
| SFSF | 9.6313 | 16.135 | 36.726 | 38.945 | 46.738 | 70.740 |
| CFSF | 15.192 | 20.584 | 39.736 | 49.449 | 56.280 | 77.324 |
| SSSF | 11.685 | 27.756 | 41.197 | 59.065 | 61.861 | 90.294 |
| CSSF | 16.792 | 31.114 | 51.397 | 64.021 | 67.540 | 101.12 |
| CCSF | 17.537 | 36.023 | 51.812 | 71.077 | 74.326 | 105.79 |
| CFCF | 22.168 | 26.407 | 43.597 | 61.176 | 67.176 | 79.817 |
| SCSF | 12.687 | 33.065 | 41.702 | 63.015 | 72.398 | 90.611 |
| CSCF | 23.371 | 35.571 | 62.875 | 66.762 | 77.374 | 108.87 |
| CCCF | 23.921 | 39.998 | 63.221 | 76.710 | 80.572 | 116.66 |
| SSSS | 19.739 | 49.348 | 49.348 | 78.957 | 98.696 | 98.696 |
| CSSS | 23.646 | 51.674 | 58.646 | 86.134 | 100.27 | 113.23 |
| CCSS | 27.054 | 60.538 | 60.786 | 92.836 | 114.56 | 114.70 |
| CSCS | 28.951 | 54.743 | 69.327 | 94.585 | 102.22 | 129.10 |
| CCCS | 31.826 | 63.331 | 71.076 | 100.79 | 116.36 | 130.35 |
| CCCC | 35.985 | 73.394 | 73.394 | 108.22 | 131.58 | 132.20 |

### 3.3. Discussion on thickness effect

Although the frequency parameter $\Omega$ defined in Eqs. (8) and (9) has been used for shallow shell vibration in the past literature, it turns out in this study that direct comparison is not appropriate because thickness $h$ is included in the parameter $\Omega$. A new frequency parameter is therefore proposed here as

$$\Omega^* = \Omega\left(\frac{h}{a}\right) = \omega a \sqrt{\frac{12\rho\left(1-v^2\right)}{E}} \qquad (10)$$

that is still nondimensional and proportional to $\omega$, but excludes thickness ratio ($a/h$) in the parameter. In other words, comparison of $\Omega^*$ is more reasonable between two cases with different thickness.

Figure 3 illustrates variations of new frequency parameter $\Omega^*$ for three lowest modes of spherical shell versus four different thickness ratios of $a/h=10$ (thick shell), 20, 100 and 1000 (extremely thin shell). Theoretically, $a/h=10$ might be almost limit of applicable range of the thin shell theory. Figure 3(a) represents small curvature of $a/R_x=a/R_y=0.2$, and lower figure (b) does large curvature $a/R_x=a/R_y=0.5$. Values of $\Omega^*$ are inserted for $a/h=10$ and 20 in each figure, but omitted for $a/h=100$ and 1000 due to lack of space. It is clearly seen in both figures that all frequency parameters $\Omega^*$ monotonically decrease with decreasing bending stiffness, but interestingly the difference due to curvature increase from $a/R_x=a/R_y=0.2$ to $a/R_x=a/R_y=0.5$ is not significant.
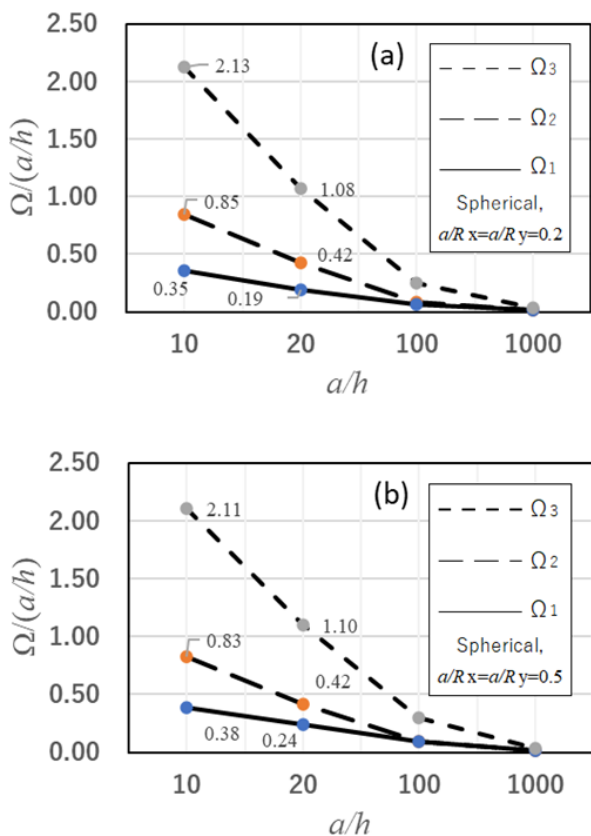
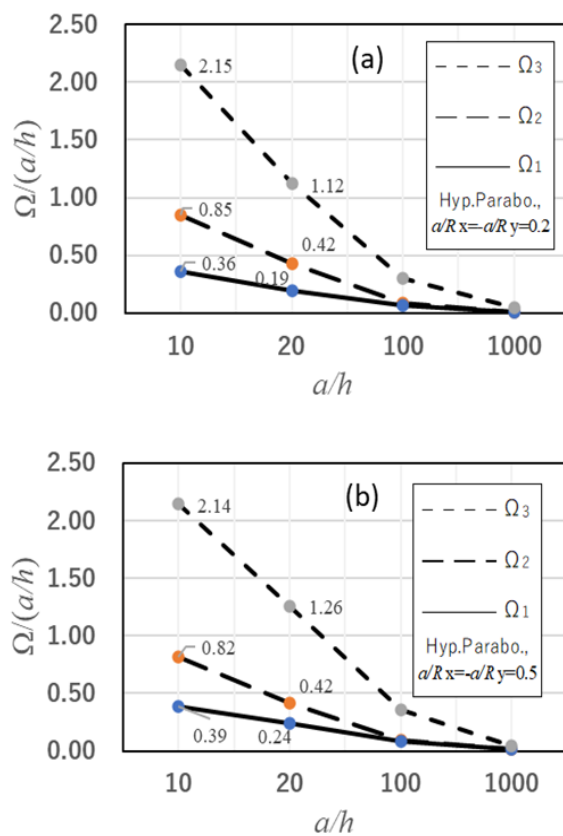Figure 3. Thickness effect (Spherical shell, CFFF)



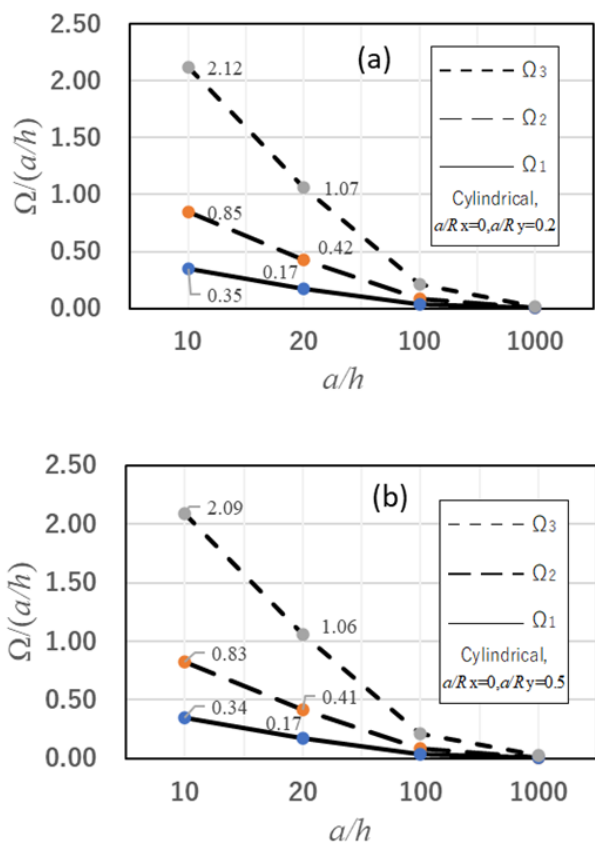Figure 5. Thickness effect (Hyp.Para. shell, CFFF)



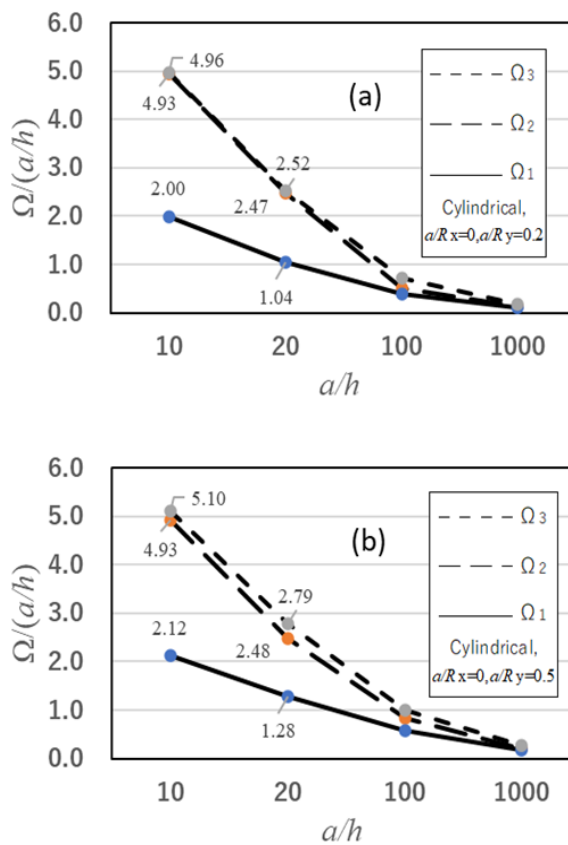Figure 4. Thickness effect (Cylindrical shell, CFFF)



Figure 6. Thickness effect (Cylindrical shell, SSSS)

Figures 4 and 5 present in the same format the results of frequency $\Omega^* = \Omega(h/a)$ for cylindrical shell and hyperbolic paraboloidal shell, respectively. When these six sets of variations in $\Omega^*$ in Fig.3-5 are compared, the difference in frequencies stays within a small range of parameter, for example, the first frequency parameter changes between $\Omega_1^* = 0.34$ and 0.39 for $a/h = 10$, and does between $\Omega_1^* = 0.17$ and 0.24 for $a/h = 20$. Generally speaking, these six figures present quite similar forms of variation.

Figure 6 illustrates the variation of $\Omega_1^*$ for cylindrical shell with totally simply supported edges (SSSS). Figures 6(a) and (b) show that frequency behavior and values of the parameters differ from shell with cantilever type boundary condition (CFFF) in in Fig.3-5, but the frequency decrease takes similar tendency.

## 4. Conclusions

As Part. 2 with a previous study (Part. 1) [2], this paper tabulated accurate natural frequencies for free vibration of doubly curved, isotropic shallow shells of rectangular (square) planform, when the shell thickness is small (representative length/shell thickness=100). Twenty-one different sets of boundary conditions are included. The same mathematical procedure was used and was briefly outlined.

In the process of this study, it was found that the traditional representation in frequency parameter may not be appropriate to evaluate the effect of changing shell thickness on free vibration of the shells. Based on this finding, a new frequency parameter was proposed by excluding thickness in the parameter. With this new parameter, rather unified behavior was identified, and more effective use of this parameter will be studied.

## References

[1] Leissa AW, Vibration of Shells, NASA-SP-288, 1973.
[2] Narita D, Narita Y, Accurate results for free vibration of doubly curved shallow shells of rectangular planform (Part.1), EPI Intl. J. Eng., 4 (2021), 29-36.
[3] Leissa AW, Kadi AS, Curvature effects on shallow shell vibrations, J. Sound Vibr., 16 (1971), 173–187.
[4] Leissa, AW, Lee, JK, Wang, AJ. Vibrations of cantilevered shallow cylindrical shells of rectangular planform, J. Sound Vib., 78 (1981), 311-228.
[5] Leissa AW, Lee JK, Wang AJ., Vibrations of cantilevered doubly curved shallow shells., Int. J. Solids Struct., 19 (1983), 411–424.
[6] Leissa AW, Narita Y, Vibrations of completely free shallow shells of rectangular planform, J. Sound Vibr., 96 (1984), 207–218.
[7] Narita Y, Leissa AW, Vibrations of corner point supported shallow shells of rectangular planform. Earthq. Eng. Struct. Dynam., 12 (1984), 651–661.
[8] Qatu MS, Leissa AW. Effects of edge constraints upon shallow shell frequencies, Thin. Wall. Struct., 14 (1992), 347–379.
[9] Qatu MS, Review of shallow shell vibration research, Shock and Vibration Digest, 24 (1992), 3–15.
[10] Yu SD, Cleghorn WL, Fenton RG, On the accurate analysis of free vibration of open circular cylindrical shells, J. Sound Vibr., 188 (1995), 315–336.
[11] Liew KM, Lim CW, Vibratory behavior of doubly curved shallow shells of curvilinear planform, J. Eng. Mech., 121 (1995), 1277–1284.
[12] Liew KM, Lim CW, Vibration of doubly-curved shallow shells, Acta Mech., 114 (1996), 95–119.
[13] Lim CW, Liew KM, A pb-2 Ritz formulation for flexural vibration of shallow cylindrical shells of rectangular planform, J. Sound Vibr., 173 (1994), 343–375.
[14] Liew KM, Lim CW, Kitipornchai S, Vibration of shallow shells: a review with bibliography, Appl. Mech. Rev., 50 (1997), 431–444.
[15] Qatu MS, Recent research advances in the dynamic behavior of shells. Part 2: Homogeneous shells, Appl. Mech. Rev., 55 (2002), 415–434.
[16] Narita Y, Robinson P, Maximizing the fundamental frequency of laminated cylindrical panels using layerwise optimization, Intl. J. Mech. Sci., 48 (2006), 1516–1524.
[17] Monterrubio LE, Free vibration of shallow shells using the Rayleigh–Ritz method and penalty parameters, Proc. Inst. Mech. Engr., Part C: J. Mech. Eng. Sci., 23 (2009), 2263–2272.
[18] Qatu MS, Effect of inplane edge constraints on natural frequencies of simply supported doubly curved shallow shells. Thin Walled Struct., 49 (2011), 797–803.
[19] Mochida Y, Ilanko S, Duke M, Narita Y, Free vibration analysis of doubly curved shallow shells using the Superposition-Galerkin method, J. Sound Vibr., 331 (2012), 1413–1425.
[20] Qatu MS, Asadi E, Vibration of doubly curved shallow shells with arbitrary boundaries, Applied Acous., 73 (2012), 21-27.